The long-term effect of sex-biased dispersal on the population demographic history of the brown bear *Ursus arctos* in Hokkaido, Japan, and around areas based on genome sequencing analysis

ゲノム解析に基づく北海道を中心としたヒグマ個体群における

雌雄の分散様式の違いが長期にわたって集団史に与えた影響

Yu Endo

Department of Natural History Sciences

Graduate School of Science

Hokkaido University

Doctoral Dissertation

March 2024

Contents

Abstract

Sex-biased dispersal, the difference in dispersal distance between sexes, is a universal trait observed in many mammalian species. Previous studies utilizing population genetic analysis have demonstrated its reflection in genetic structure, predicting that it is a result of the long-term effect of sex-biased dispersal on population demography. However, accurately evaluating the effect of sex-biased dispersal faces challenges, primarily due to two reasons. One challenge is the influence of other factors, such as differences between sexes in ratio, lifespan, and reproductive success, which can also affect the outcomes of population genetics analyses. The other lies in the difficulty of detecting slight differences in gene flow between different inheritable regions using limited genetic data, such as haploid genome data like mitochondrial and Y chromosomal data, which have the potential to miss the nuanced effect of sex-biased dispersal.

The brown bear, *Ursus arctos*, is a large solitary Carnivoran and has been observed with extreme male-biased dispersal and no significant differences in ratio, lifespan, and reproductive success between sexes. In addition, genomic data across different inheritable genetic regions such as mitochondrial DNA, X chromosome, autosome, and Y chromosome is relatively abundant compared with other wildlife. Thus, it is suitable to examine the process by which sex-biased dispersal affects the population demography. This dissertation aims to reveal the process and evaluate the sex-biased dispersal through the population demographic history of the brown bear.

In Chapter 2, I focused on the brown bear on Hokkaido Island, Japan, which consists of three geographically distinct subpopulations representing different mitochondrial lineages, and gene flow between subpopulations due to male-biased dispersal. I determined whole-genomic

sequences for six Hokkaido brown bears and analyzed the data along with previously published genomic sequences of 17 brown bears from other parts of the world. A phylogenetic analysis of the autosomal data revealed that the Hokkaido population was genetically distinct from the other populations, such as North American and European populations. The genetic diversity was higher than the endangered populations in Western Europe while it was lower than most populations on the continents. A reconstruction of historical demography showed no increase in population size for the Hokkaido bear population during the Eemian interglacial period (130,000–114,000 years ago). A little autosomal genetic difference between different mitochondrial DNA lineages was observed in the Hokkaido population. This autosomal genetic similarity within Hokkaido contrasts with the geographically separate mitochondrial lineages, indicating the occurrence of male-driven gene flow between subpopulations.

In Chapter 3, I analyzed a reduced-representation genome sequencing (ddRAD-seq) of the Hokkaido population and whole-genome resequencing data of both Hokkaido and foreign populations to investigate how such a characteristic genetic structure has been shaped and to evaluate the influence of male-biased dispersal on the process. Despite ongoing admixture within the population due to male-biased dispersal, a slight difference was detected between subpopulations. Population demographic analysis indicated a historical population decline around the Last Glacial Maximum (ca. 21,000 years ago), followed by a recent rapid expansion. Additionally, a comparison of the genetic differentiation between autosomes and the X chromosome revealed a significant influence of male-biased dispersal during migration from the continent. This study also explored the correlation between these findings and environmental factors, such as landforms and climate changes. Landscape genetic analysis suggested that the observed differentiation could be attributed to restricted gene flow due to lowlands. Furthermore,

the species distribution modeling showed a historical trend of the brown bear's relatively suitable habitat decreasing significantly during the Last Glacial Maximum. The results indicate that the Hokkaido bear population had contracted due to global climate change despite the appearance of the land bridge between the Eurasian Continent and that it has expanded rapidly while being influenced by the lowlands. Thus, this study emphasizes the importance of considering multiple factors in phylogeography and male-biased dispersal contributing to migration into new habitats and rapid population colonization.

In Chapter 4, whole-genome resequencing was employed on the local populations of the brown bear around or on the Eurasian Continent. Through population genetic analysis using the genome data combined with previous datasets, I solved the sampling bias and verified the hypothesis that the brown bear’s nuclear genome reflects both the ancestral genetic traits and the replacement of old genetic characteristics with new ones resulting from the recent expansion, and the scale of this replacement driven by male-biased dispersal. The ancestral genetic characteristics have persisted in Western Asia and Central Asia, particularly in Kazakhstan and Tibet. Recent ancestors of these populations have experienced a rapid expansion slightly, as indicated by the calculation of the number of alleles shared with individuals speculated to possess many alleles from recent dispersal, based on mitochondrial DNA haplotypes. The Hokkaido and Etorofu Island populations were found to have more alleles from gene flow from the polar bear *Ursus maritimus*, akin to the North American brown bear population previously reported to have hybridized with the polar bear. This phenomenon may be attributed to the lesser influence of recent expansion compared to continental populations. The results support the hypothesis and suggest the multi-layers from different time migrations in the genetic structure of

the brown bear. This study contributes to understanding the local genetic variation and the effect of the male-biased dispersal of not only brown bears but also animals.

In conclusion, male-biased dispersal has played a substantial role in admixture between different lineages, migration into new habitats, rapid colonization, and the formation of the multi-layer genetic structure. The long-term effects on population demography due to male-biased dispersal could have resulted in genetic differences between local populations and a mismatch in genetic structure patterns between maternally inherited mitochondrial DNA and paternally inherited Y-chromosomal DNA.

On the other hand, environmental factors, such as climate changes, have also exerted an influence on population demography. Climate changes and landform dynamics, such as the formation of land bridges during glacial periods, are influential factors that either promote or restrict male-biased dispersal. In the population demographic history of the brown bear, encompassing events like the extinction of local populations and hybridization with closely related species, the environmental factors hold significance parallel to male-biased dispersal. Considering multiple factors and placing emphasis on local genetic traits and environmental influences could enable an investigation into the overlooked population demographic history.

Acknowledgments

I express my sincere gratitude to Professor Ryuichi Masuda (Hokkaido University) for providing the opportunity to initiate and develop this project. I also extend my thanks to Associate Professor Toru Katoh, Professor Hiroshi Kajihara, and Professor Masaoki Takagi (Hokkaido University) for their insightful review of the manuscript. I highly appreciate Associate Professor Naoki Osada (Hokkaido University) for introducing me to population genetics and bioinformatics, engaging in scientific discussions, and offering valuable advice. Special thanks are due to Professor Matthew H. Dick (Hokkaido University) for his assistance in scientific writing.

I am deeply grateful to Dr. Tsutomu Mano (Hokkaido Research Organization) and Dr. Alexei V. Abramov (Zoological Institute Russian Academy of Sciences) for providing invaluable samples. My thanks also go to Professor Atsushi J. Nagano (Ryukoku University) for his contributions to sequencing. I extend my appreciation to the past and present members of the Laboratory of Genetic Diversity and Laboratory of Information Biology for discussion.

This project received support from the Japan Society for the Promotion of Science for Scientific Research (KAKENHI grant nos. 18H05508 and 22KJ0055), the establishment of university fellowships towards the creation of science technology innovation (grant no. JPMJFS2101), the Sasakawa Scientific Research Grant from The Japan Science Society, and the Alumni Association of the Faculty of Science, Hokkaido University.

Finally, this dissertation is dedicated to all brown bears worldwide.

Chapter 1. General introduction

Sex-biased dispersal of animals

The difference between sexes is observed naturally in polyploidy wildlife. The differences in morphology, like sexual dimorphism (McPherson & Chenoweth 2012), social structure (Holekamp & Sawdy 2019), and life history (Lemaître et al. 2020), are well known. Although the reason why these differentiations have occurred has still been argued because of multiple factors, the phenomenon itself is known in a wide range of taxa.

The rate and pattern of dispersal frequently differ between sexes, which is called sex-biased dispersal. The sex-biased dispersal occurs due to many reasons, such as resource availability like food and mating opportunities (Greenwood 1980), inbreeding avoidance (Packer 1979), sexual conflict (Kuijper & Johnstone 2017), and human activities (de Oliveira et al. 2022), and is evident across many taxa (Li & Kokko 2019; Trochet et al. 2016). For example, in plants, pollen carrying paternal genes disperses over longer distances compared to seeds containing genes from both the paternal and maternal sides (Ghazoul 2005; Li & Kokko 2019). Animals such as insects, fish, amphibians, and birds have also been confirmed sex-biased dispersal, even though the specific sex that disperses over longer distances may vary (Trochet et al. 2016). In most mammals, particularly carnivores, males disperse more widely, while females exhibit philopatry (Greenwood, 1980).

Long-term effect of sex-biased dispersal

The sex-biased dispersal has a long-term influence on the population demographic history and the genetic structure formed by the history (e.g., de Jong et al. 2023), so it is important to investigate the scale and pattern of sex-biased dispersal for understanding the population

demographic history. The scale of the sex-biased dispersal has been revealed by individual tracking (e.g. Zedrosser et al. 2007; Shirane et al. 2019), but this method is not suitable to evaluate its long-term influence on population demographic history (Lawson Handley & Perrin 2007). Genetic analysis solves this issue and proves effective in assessing the influence. Numerous studies using genetic analysis have detected the mismatch of genetic patterns between maternally inherited mitochondrial DNA (mtDNA) and the paternally inherited nonrecombining region of the Y chromosome (e.g., Andrews et al. 2013; Coia et al. 2013; Matsudaira et al. 2018; Seielstad et al. 1998).

However, the process underlying this mismatch needs further investigation because of some reasons. When employing a genetic approach, determining sex-biased dispersal is complicated by various factors beyond just dispersal, including societal differences, lifespan, and sex ratio, all of which influence the sex-biased demography (Webster & Wilson Sayres 2016). Only haploid genome data, commonly used in previous studies, made it challenging to accurately identify differences in sex-biased dispersal because it could not narrow down the reason from various factors such as gene flow between groups, balancing selection on markers, and the limited resolution of markers (Bossart & Pashley Prowell 1998). Although some studies solve it using nuclear markers (e.g., Schregel et al. 2018; Tucker et al. 2017), most studies evaluate sex-biased dispersal in the single generation by categorizing individuals based on sex and comparing the results between different sexes. This method cannot evaluate the long-term difference of sex-biased dispersal in gene flow.

Recently, estimating population demography based on genome data has become relatively straightforward for various species, even non-model wild species, thanks to the acquisition of massive sequence data using next-generation sequencers. The innovation makes us reveal

population divergence (Novembre et al. 2008; Ragsdale et al. 2023), hybridization with the related species (Green et al. 2010; Reich et al. 2010), and natural selection (Mathieson et al. 2015). The sex bias on the population demography, such as effective population size and migration, could also also detected by comparing the genetic diversity and differentiation of the different inheritable regions (Keinan et al. 2009; Musharof et al. 2019). However, studies for even non-model wild species are still limited.

Extreme male-biased dispersal of the brown bear

The brown bear, *Ursus arctos*, is a member of the order Carnivora for studying sex-biased dispersal in population demographic history since dispersal is the only confirmed sex-biased trait that affects population demography. Males typically disperse widely from their birthplace, while females exhibit philopatry (McLellan & Hovey 2001; Sato 2015; Zedrosser et al. 2007). This difference was reflected in their home range size (adult females: 13.4–43.0 km^2, adult males: 199–496 km^2; Sato 2015). This species is solitary except during child-rearing. In addition, there is no confirmed significant bias in the sex ratio in the population (Swenson et al. 1994) and difference in reproductive success between sexes (Shimozuru et al. 2019).

The previous studies reported the genetic mismatch patterns between mtDNA and Y-chromosomal DNA (Figure 1). Studies based on the analysis of mitochondrial cytochrome *b* and control region sequences (Davison et al. 2011) and that of a complete mitogenome (Hirata et al. 2013) have shown several lineages were found across the northern hemisphere, while the analyses of Y-chromosomal sequences showed no phylogeographic correlation with the mtDNA lineages (Bidon et al. 2014; Hirata et al. 2017).

Recently, some studies reported the available genomic data of the brown bear (Barlow et

al. 2018; Cahill et al. 2013, 2015, 2018; de Jong et al. 2023; Liu et al. 2014; Miller et al. 2012; Tumendemberel et al. 2023), which makes us possible to assess the long-term effect of the sex-biased dispersal to the population demographic history. While de Jong et al. (2023) demonstrated the effect of recent male-biased dispersal on population demography and the potential to erase the former genetic structure, it is still crucial to investigate the often-overlooked population demographic history and the long-term effects of male-biased dispersal. It is because this investigation could be achieved by focusing on the genetic differences of local populations. Tumendemberel et al. (2023), for example, showed that the isolated Central Asian populations were clearly different from European and North American populations. In addition, some local exhibit endemic traits whose genetic basis is unknown have been reported (Colangelo et al. 2012; Sato et al. 2011b).

Aims of this study

This dissertation focuses on the population demography of the brown bear and discusses its history in Chapters 2, 3, and 4 (Figure 1) to evaluate the long-term effect of sex-biased dispersal on the population demographic history. Chapter 2 focuses on the Hokkaido brown bear population containing three mtDNA haplotypes whose divergence times are distributed separately. I applied whole-genome resequencing and then conducted population genetic analysis to investigate the differences between the populations on the continents based on their population demographic history. Chapter 3 evaluates the long-term effect of male-biased dispersal and environmental factors on the colonization of the Hokkaido population by population genetic analysis and landscape genetic analysis using a reduced representation sequencing, ddRAD-seq (double digest restriction-site associated DNA sequencing), and species distribution modeling.

Chapter 4 investigates the genetic diversity of the local population in Eurasia (Hokkaido, Etorofu Island, Sakhalin, Far East area, Kazakhstan, Tibet, Central Russia, and the Caucasus). By population genetic analysis based on whole-genome resequencing for both modern and ancient samples, I discuss the hypothesis that the brown bear genome reflects both ancestral genetic traits and the recent expansion, with the extent of the expansion playing a crucial role.

Chapter 2

Demographic history of the brown bear *Ursus arctos* on Hokkaido Island, Japan, based on whole-genomic sequence analysis

The content of this chapter is based on the following published paper: Endo Y, Osada N, Mano T. Masuda R. 2021. Demographic history of the brown bear (*Ursus arctos*) on Hokkaido Island, Japan, based on whole-genomic sequence analysis. *Genome Biology and Evolution*. 13: evab195.

Introduction

The Wallacean shortfall, defined as a lack of or poor information about the geographical distribution of species, presents a critical challenge in phylogeography (Lomolino et al. 2016). Due to this shortfall, there is a risk of overlooking biodiversity, including species diversity and genetic diversity, and these crises are exacerbated by human activities, climate change, etc. Therefore, addressing the Wallacean shortfall is crucial for the comprehensive investigation of biodiversity.

The brown bear *Ursus arctos* is widely distributed in the northern hemisphere (McLellan et al. 2017) and has become a model for studying mammalian evolution at the population level system (Davison et al. 2011). Brown bear populations show complex demographic histories that reflect geographical isolation (Randi et al. 1994), bottlenecks caused by human activity (Waits et al. 2000), hybridization between related species (Pongracz et al. 2017), and local phenotypic adaptation to a variety of environments (Sato et al. 2011b; Colangelo et al. 2012). Various previous studies have shed light on these processes by nuclear genetic analysis, but almost all these studies focused on Europe or North America (Hailer et al. 2012; Miller et al. 2012; Cahill et al. 2013, 2015, 2018; Liu et al. 2014; Barlow et al. 2018).

Three different mitochondrial DNA lineages, clades 4, 3a2, and 3b, appear to have migrated from the Eurasian Continent to Hokkaido Island, Japan, at different times (Hirata et al.

2013) and distributed separately in Southern, Central, and Eastern Hokkaido, respectively (Matsuhashi et al. 1999; Hirata et al. 2013). Some gene flow, however, occurs between subpopulations within Hokkaido due to males dispersing more widely than females (Hirata et al. 2017). Both separated distribution and admixture between subpopulations have thus been reflected in the brown bear genome of the Hokkaido population. However, the genetic characteristics of the parentally inherited regions in comparison to continental populations and the processes involved in their formation remain unclear. These limitations arise from the reliance on maternal or paternal haplotype data and a lack of genomic information in Hokkaido.

The goal of this study was to clarify further the demographic history of brown bears, especially those in Hokkaido, by analyses of whole-genomic sequences obtained by next-generation sequencing (NGS) technology. Here, I report the basic genetic traits of the Hokkaido brown bear on the genetic diversity, genetic structure, genealogy, and demographic dynamics based on whole-genomic sequences; compare my results with those from previous studies on other populations; and discuss the demographic history between the Hokkaido bears and continental populations.

Materials and methods

Samples and genome sequencing

This study utilized muscle tissue samples from six Hokkaido brown bears, one individual per sex per mitochondrial DNA lineage (Figure 2 and Table 1) that had been collected in previous studies (Matsuhashi et al. 1999; Hirata et al. 2017). Total genomic DNA was extracted with the DNeasy Blood & Tissue Kit (Qiagen, Hilden, Germany) and stored at 4°C or –20°C until use.

Paired-end libraries were prepared by using the TruSeq DNA Nano Sample Prep Kit (Illumina, San Diego, USA), and whole-genome shotgun sequences were generated by Macrogen Japan (Tokyo, Japan), using an Illumina HiSeq X sequencer. Samples were sequenced to an average depth of 30×. FastQC ver. 0.11.8 (Babraham Bioinformatics 2011) and trimomatic ver.0.39 (Bolger et al. 2014) were used to check the quality of the sequences and remove Illumina adapters.

Mapping and variant calling

Whole-genomic sequence data from 17 brown bears (Miller et al. 2012; Cahill et al. 2013, 2015; Benazzo et al. 2017; Barlow et al. 2018; Taylor et al. 2018) were downloaded for analysis. Figure 2 and Table 1 indicate the sampling locations of these bears. One individual from Alaska (sample name: Alaska) is not shown in Figure 2 because no information on the sampling location was available. The reads from 23 brown bears and one Asiatic black bear (Kumar et al. 2017, Table 1) were mapped to the polar bear reference genome (Liu et al. 2014; UrsMar_1.0, accession number: GCF_000687225.1) by using the BWA-MEM algorithm implemented in the BWA package ver. 0.7.17 (Li & Durbin 2009) with the '-M' command option. The number of reads aligned to the reference genome and the proportion of the genome covered was summarized by using CollectAlignmentSummaryMetrics in GATK ver. 4. 1. 2. 0 (McKenna et al. 2010). Single nucleotide variants (SNVs) were called by using HaplotypeCaller in GATK, and then further hard-filtered under the following parameters: significant fisher strand test (FS) > 60.0; variant confidence/quality by depth (QD) < 2.0; RMS mapping quality (MQ) < 40.0; strand odds ratio (SOR) > 9.0; MQRankSum < −12.5, and significant read position bias (ReadPosRankSum) < −8.0.

The reference polar bear genome included thousands of short fragments (< 200 bp), which are not suitable for many population genetic analyses, and so only single nucleotide polymorphisms (SNPs) on 356 scaffolds longer than 100 kb and excluding sex chromosome-linked scaffolds (Cahill et al. 2013; Bidon et al. 2014), and one mitochondrial DNA (mtDNA) scaffold, were analyzed. Genmap ver. 1.3.0 (Pockrandt et al. 2020) was used to calculate genome mappability and exclude SNPs with (30, 2)-mappability < 1 (i.e., the 30-mer starting from the site is unique in the genome even allowing for 2 mismatches). To assess the reliability of sequence data, the mean depth of SNPs per individual was calculated by using vcftools ver. 0. 1. 17 (Danecek et al. 2011).

Phylogenetic tree based on the mitogenome

A phylogenetic tree based on the whole mitogenome was reconstructed with the maximum likelihood method implemented in MEGA X (Kumar et al. 2018). To construct the tree, consensus sequence files per individual were created using bcftools (Danecek et al. 2021). The optimal substitution model determined under the Bayesian information criterion (BIC) was HKY + G (gamma-distributed rate variation). The Asiatic black bear (Table 1) was included as an outgroup taxon because previous studies (Talbot & Shields 1996; Hirata et al. 2013) have found that polar bears group within clade 2, which includes brown bears from the Admiralty, Baranof, and Chichagof islands (ABC islands).

Genetic diversity and genetic structure and genealogy

To assess genetic diversity, heterozygosity was calculated using PLINK ver. 1.9 (Purcell et al. 2007) under the options “--het”.

A principal component analysis (PCA) and Bayesian clustering analyses were performed by using EIGENSOFT ver. 7.2.1 (Patterson et al. 2006) and ADMIXTURE ver. 1.3.0 (Alexander et al. 2009), respectively. SNPs under linkage disequilibrium (LD) were excluded before analyses by using PLINK options "--indep-pairwise 50 5 0.5".

To construct a neighbor-joining tree (Saitou & Nei 1987), a distance matrix was calculated based on the identity-by-state PLINK option "--distance". The tree was plotted by using the R package phangorn ver. 2. 5. 5 (Schliep 2011), with the Asiatic black bear (Table 1) as an outgroup. TreeMix ver. 1.13 (Pickrell & Pritchard 2012) was run to estimate patterns of population splits and mixtures in brown bear populations, with the polar bear reference genome (Liu et al. 2014) as the outgroup.

To infer which individuals were closely related to the Hokkaido individuals, f_3 statistics were calculated with the AdmixTools software package (Patterson et al. 2012). F_{st} values (Hudson et al. 1992; Keinan et al. 2007) were calculated by using EIGENSOFT.

To estimate the relationship among populations, f_4 statistics were calculated with the AdmixTools software package. The smaller the value of f_4(A, B; C, D) calculated using the allele frequencies of A, B, C, and D, the more alleles are shared between B and C (Patterson et al. 2012). Because polar bears admixed with brown bears in the past (Miller et al. 2012; Cahill et al. 2013; Liu et al. 2014), I used the sequence of the Asiatic black bear as the outgroup.

I tested three situations, f_4(Asiatic black bear, Denali, Kenai, and Russia; other Europe or North America, Hokkaido), f_4(Asiatic black bear, Europe; North America, Hokkaido), f_4(Asiatic black bear, North America; Russia, Hokkaido), and f_4(Asiatic black bear, X; Hokkaido 1, Hokkaido 2), where X indicates brown bears other than those from Hokkaido, to detect the genetic relationship between bears from Europe and North America, and allele sharing

bias between other brown bears on the continent and Hokkaido.

Demographic dynamics

The pairwise sequentially Markovian coalescent methods (PSMC; Li & Durbin 2011) were applied to estimate past demography. The diploid consensus sequence for each sample was created from a bam file by using SAMtools ver. 1.9 (Li et al. 2009), with the “mpileup” command set to the “-C50” option. Each consensus sequence was transformed into the required format by using the fq2psmcfa tool in the PSMC package, and was analyzed with PSMC under the option “-N25 -t15 -r5 -p "4+25*2+4+6"”. The mutation rate and generation time were set at $1.82*10^{-8}$ mutations per site per generation and 11 years, respectively, as indicated by previous studies (Liu et al. 2014; Benazzo et al. 2017).

Results

Whole-genome sequencing and genetic diversity

This study included the whole-genomic sequences I obtained from six brown bears from Hokkaido (Accession number: DRR276774–DRR276779) and previously reported sequences of 17 individuals from other areas (Figure 2 and Table 1). The proportion of the genome covered was 96.6–99.4% (Table 1). The number of SNPs found per individual ranged from 3,726,121 to 4,748,290, with a depth range of 8.61 to 54.87 (Table 1). Figure 3 shows the heterozygosity. The values were lower for the Hokkaido individuals than for most individuals from other populations but higher than in endangered populations in Western Europe.

Phylogenetic tree based on the mitogenome

A phylogenetic tree (Figure 4a) reconstructed using complete mtDNA sequences shows two major clades, one comprising bears from western Europe, a polar bear, and bears from southeastern Alaska, the ABC islands, and the other comprising bears from Alaska (Kenai and Denali), Hokkaido, and eastern Europe. Within the latter clade, the Hokkaido individuals comprise three distinct lineages, clade 4, 3b, and 3a2, from southern, eastern, and central Hokkaido, respectively, and an European individual from Georgia was included in neither clades 3a1 nor 3a2.

Genetic structure and genealogy

PCA for all brown bears examined (Figure 5) showed separation among Hokkaido, European, and North American individuals. In particular, the first principal component (horizontal axis) indicated strong separation between the Hokkaido population and other populations. In a PCA for only the Hokkaido individuals (Figure 6), the first principal component (horizontal axis) showed separation of the three known subpopulations. The second principal component (vertical axis) separated Southern Hokkaido 1 from Southern Hokkaido 2, whereas in each case the two individuals from Central Hokkaido and those from Eastern Hokkaido were closely related to one another.

Figure 7 shows the genetic structure of the bears analyzed, based on ADMIXTURE. At $K = 3$, which was the most likely number of clusters (Figure 7a), three clusters, Hokkaido, Europe, and North America are evident. At $K = 2$ (Figure 7b), which was the second most likely number of clusters, the Hokkaido individuals are separate from the others. Figures 7a and 7b both show the probability that the individual from Russia belongs to both the European population and other populations.

The F_{st} value between Europe (Slovakia, Georgia, Southern Sweden 1, Southern Sweden 2, Slovenia, Northern Italy, Central Italy, and Spain) and North America (Alaska, Denali, Kenai, Admiralty 1, Admiralty 2, Baranof, Chichagof 1, and Chichagof 2) was lower than that between Hokkaido and the others (Table 2), supporting the results shown in Figures 5 and 7b. F_{st} values among the Hokkaido subpopulations (Table 3) were consistent with a closer relationship between Southern and Central Hokkaido, as indicated by the results of the first principal component of PCA (Figure 6).

In the neighbor-joining tree (Figure 4b) constructed by using identity-by-state distances between autosomal genomes, the Hokkaido and North American individuals comprise distinct clades embedded within a paraphyletic European group, with the individual from Russia most closely related to the Hokkaido clade which was also suggested in Figure 7a.

A plot of f_3 statistics (Figure 8) against geographical locality showed that the Russia, Kenai, and Denali individuals are more closely related to the Hokkaido population than are the other populations examined, which was also supported by the result of f_4 (Asiatic black bear, individuals from Denali, Kenai, and Russia; others from Europe or North America, individuals from Hokkaido), although the relationship between bears from Denali and Kenai, and other North American individuals was closer (Table 4).

In trees constructed by using TreeMix (Figure 9), the three groups appear as distinct clades. Both trees in Figure 9a, assuming no gene flow, and Figure 9b, assuming that one gene flow occurred, showed that the Russian individual lies outside the clade, including the European individuals. In addition, it indicates gene flow between the Asiatic black bear and the brown bears of Georgia.

I applied f_4 statistics to clarify the genetic relationship between the continental

population and the Hokkaido population. Values of f_4(Asiatic black bear, European populations; North American populations, individuals from Hokkaido) were calculated to investigate the genetic relationship between populations in Europe (Slovakia, Georgia, Sweden, Slovenia, Northern Italy, Central Italy, and Spain) and the Hokkaido population (Table 5), and values of f_4(Asiatic black bear, North American populations; the Russian individual, individuals from Hokkaido) were calculated to detect the genetic relationship between populations in North America (Alaska, Denali, Kenai, Admiralty, Baranof, and Chichagof) and those in Hokkaido (Table 6). While the values of f_4(Asiatic black bear, European populations; North American populations except Denali and Kenai, Hokkaido) indicated slightly close relatedness between Hokkaido individuals and European populations (f_4 = 0.0003500 to 0.001510, |Z score| > 3 except in two cases), the relatedness between European populations and individuals from Denali and Kenai (f_4 = –0.001644 to –0.000436, |Z score| > 3) was closer. Bears from Hokkaido and that from North America were not closely related to each other ($f4$ = –0.0019050 to –0.001230, |Z score| > 3).

Values for f_4(Asiatic black bear, X; Hokkaido 1, Hokkaido 2), where X indicates brown bears other than those from Hokkaido, were calculated to estimate allele-sharing bias within the Hokkaido populations. The analysis suggested that Southern Hokkaido 1 shares more alleles with European brown bears than with other Hokkaido individuals (Figure 10 and Table 7) although only f_4(Asiatic black bear, Spain; South Hokkaido 1, Eastern Hokkaido 1) and f_4(Asiatic black bear, Sweden; South Hokkaido 1, Eastern Hokkaido 1) were statistically significant (|Z score| > 3) and both Z scores were slightly above 3, indicating the statistical significance was marginal.

Demographic dynamics

Historical demography was reconstructed based on PSMC. This analysis indicated that the effective population size (N_e) of most European and North American brown bears increased about 120 thousand years ago (Figures 11a and 12). In contrast, none of the six Hokkaido individuals indicated an increase in population size at that time (Figure 11).

Discussion

This study aimed to reveal the local genetic differentiation of the Hokkaido brown bear population compared with the continental populations. The genetic diversity of the Hokkaido brown bears was not lower than the European endangered populations, but slightly lower than the other continental populations. Based on autosomal SNPs, the Hokkaido population is clearly distinguishable from other continental populations, and the nuclear genetic difference between different mtDNA lineages within Hokkaido was not observed. The expansion of the effective population size during the Eemian interglacial period confirmed for the European and North American individuals was not found for the Hokkaido individuals, so some ancestors of the Hokkaido population were inferred to have migrated into Hokkaido before the Eemian interglacial period.

Genetic diversity

Heterozygosity values indicated that the Hokkaido brown bears are higher in genetic diversity than the endangered brown bears in Europe, although the Hokkaido population has long been isolated from populations in continental Eurasia. This result is incongruent with previous studies based on major histocompatibility complex class-II *DQA* genes (Goda et al. 2009), DNA

fingerprinting (Tsuruga et al. 1994), and protein polymorphism (Tsuruga et al. 1996), in which the Hokkaido brown bears showed lower genetic diversity than other individuals. I conclude that the diversity of the whole genome has been maintained at a higher level than that of only coding regions as shown in the previous studies, as has also been reported for macaques (Osada et al. 2015). Previous studies have shown that the genetic diversity of the whole genome declines in cases of 1) long-term population decline and inbreeding (Xue et al. 2015; Benazzo et al. 2017), and 2) strong recent inbreeding (Prufer et al. 2014; Benazzo et al. 2017). Although the Hokkaido bears have experienced a population decline since the Last Glacial Period, 70,000–10,000 years ago (Figure 11b), my results indicated no events leading to a decline of genetic diversity in the whole genome.

Demography of brown bears

Matsuhashi et al. (1999) and Hirata et al. (2013) showed that three mtDNA lineages are distributed allopatrically in Southern, Central, and Eastern Hokkaido. My study also showed the same three lineages and the corresponding allopatric distributions. Most previous mtDNA analyses found that clade 3a included only two clades, the East European and Alaskan lineage (clade 3a1) and the central Hokkaido lineage (clade 3a2) (Hirata et al. 2013; Tumendemberel et al. 2019). However, an amplified product length polymorphism (APLP) analysis by Hirata et al. (2014) detected another haplotype from western Iran and the Caucasus (Eastern 2) in clade 3a that was distinct from clades 3a1 and 3a2. Consistent with this result, the haplotype from Georgia was included in clade 3a but not in clade 3a1.

The PCA and the genetic cluster analyses revealed apparent genetic differentiation among Hokkaido, European, and North American bears, with the Hokkaido individuals separate from both

the European and North American groups. The first principal component of PCA, the clustering of ADMIXTURE at $K = 2$, and F_{st} values all suggest that the nuclear genome of brown bears on Hokkaido differs from that in the continental populations. Analyses by Hirata et al. (2013) based on the whole mitogenome indicated that clade 3a2 in Central Hokkaido was the last of the three lineages (clades 4, Southern; 3b, Eastern; 3a2, Central) to migrate to Hokkaido, and that clade 3a1 (the sister group to clade 3a2) spread widely from Eastern Europe to Alaska via the Bering region after that. The fossil record is congruent with this result because no fossil record of clade 3a brown bears has been confirmed prior to 10 thousand years ago in North America (Leonard et al. 2000; Barnes et al. 2002), which could be later than the isolation of Hokkaido Island from the Eurasian Continent (Ohshima 1990).

In contrast, the neighbor-joining tree and f_3 statistics showed that the Hokkaido brown bears are most closely related to the individuals from Russia, Denali and Kenai, reflecting some genetic affinity between the Hokkaido population and individuals occurring relatively close by Hokkaido. Moreover, f_4 statistics suggested the Hokkaido bears are more closely related to European bears than North American bears except for Denali and Kenai. The results infer clade 3a migration route from the Eurasia continent onto Hokkaido, Denali and Kenai via the land bridges (Figure 13b). Matsuhashi et al. (1999) and Hirata et al. (2013) concluded based on mtDNA data that ancestral bears migrated to Hokkaido from continental Eurasia via Sakhalin Island. The sea depth between Hokkaido and Sakhalin is relatively shallow, so Hokkaido had been a part of the Eurasia continent rather than an islands before 12 thousand years ago (Ono 1990), which is consistent with the result in the present study. Mizumachi et al. (2021) analyzed mtDNA sequences from ancient and modern samples of brown bears on Sakhalin and found that only clade 3a1, which is distributed widely on the continent, occurs on Sakhalin. Although the

mtDNA haplogroups detected on Hokkaido are clearly different from those in continental Eurasia, admixture by male-biased dispersal between continental Eurasia and Hokkaido could have occurred prior to the opening of Soya Strait between Sakhalin and Hokkaido approximately 12 thousand years ago (Ohshima 1990). In addition, ancestors of the Denali and Kenai bears are estimated to have migrated to North America via Bering land bridge after migration onto Hokkaido because clade 3a1, which is not found in Hokkaido, distributes around Denali and Kenai (Leonard et al. 2000; Barnes et al. 2002). Closer relationship between Denali-Kenai and the European bears from Eurasia than that between Hokkaido and European bears is also reflected to the f_4 statistics.

The neighbor-joining tree based on autosomal genomic data showed brown bears divided into three groups (Hokkaido, Europe, and North America), all of which include mtDNA lineage 3a. This suggests that populations having mtDNA 3a haplotypes have dispersed across a wide range and contributed to current populations by hybridization among local populations. Although Matsuhashi et al. (2001) and Davison et al. (2011) found a clearly separated distribution of mtDNA lineages, the present results from the whole autosomal genome indicated that individuals from the same population may be closely related to each other even if their mtDNA haplogroups are different, which is consistent with the results of Hailer et al. (2012). This pattern could have resulted from wide male-biased dispersal (McLellan & Hovey 2001). Bidon et al. (2014) analyzing Y-chromosomal sequences indicated no allopatric distribution as shown in mtDNA analysis (Davison et al. 2011) and male-biased gene flow caused by sex-biased dispersal. It suggests that autosomal homogenization has occurred by male-biased gene flow within the groups after their dispersal.

More locally, values for f_4(Asiatic black bear, X; Hokkaido 1, Hokkaido 2) showed that

Southern Hokkaido 1 individual shared more alleles with European individuals than with other Hokkaido individuals. This suggests that the Southern Hokkaido population has been isolated by a stronger geographic barrier than the other Hokkaido populations; the sampling location (Kikonai) for individual Southern Hokkaido is located at the southernmost end of Hokkaido, where admixture with other Hokkaido populations may have been restricted. As a result, some genetic factors from the continent may have been maintained. More samples are needed, however, to elucidate the genetic features of the brown bears in Southern Hokkaido.

The results of PSMC detected no increase in N_e at around 120 thousand years ago for brown bear individuals from Hokkaido. The recovery in N_e observed for continental brown bears is generally correlated with increased temperatures in the Eemian interglacial period 130–114 thousand years ago (Miller et al. 2012; Cahill et al. 2013; Benazzo et al. 2017). The Hokkaido population appears to have undergone two demographic events. In the first event, ancestors of the Hokkaido population migrated to Hokkaido before the interglacial period and underwent a different demographic history from the continental population. Hirata et al. (2013) estimated that the Southern Hokkaido (clade 4) and Eastern Hokkaido (clade 3b) lineages derived from mtDNA continental lineages about 190 thousand years ago and 160 thousand years ago, respectively. Their population demography could have differed from that of continental populations after those times. The second demographic event was gene flow involving the autosomal genome into populations having different mtDNA haplogroups, as might be expected with male-biased dispersal; in this context, Hirata et al. (2017) demonstrated that male dispersal does occur between populations with different mtDNA haplogroups. The Central Hokkaido population (clade 3a2) likewise did not show the N_e recovery, although Hirata et al. (2013) estimated that it migrated to Hokkaido 50 thousand years ago. By dispersal, alleles of the Southern and Eastern

Hokkaido lineages have been shared with the Central Hokkaido population.

Demographic history scenario of brown bears in Hokkaido

This study aimed to clarify the demographic history of brown bears in Hokkaido from four points of view: genetic diversity, genetic structure and genealogy, demographic dynamics, and gene flow. From the results, I concluded the following scenario and showed it in Figure 13.

Brown bears migrated to Hokkaido before the Eemian interglacial period (Figure 13a) because the PSMC estimates indicated no historical increase in population size in Hokkaido. The divergence time of the Southern and Eastern Hokkaido mtDNA lineages (clades 4 and 3b) estimated by Hirata et al. (2013) supports this conclusion.

Hybridization between different lineages (Figure 13b, c) has occurred following migration because the Central Hokkaido lineage (clade 3a2), which is estimated to have migrated to Hokkaido after 50 thousand years ago (Hirata et al. 2013), also showed no N_e recovery in the interglacial period. The Y-chromosomal DNA analysis by Hirata et al. (2017) found no correlation between the genetic affinity of paternal brown bear haplotypes and the geographical distribution on Hokkaido. This suggests that populations having different mtDNA lineages underwent admixture due to male dispersal, contributing to the current structure of the Hokkaido population.

Isolation by distance (IBD) and geographic barriers have also affected the Hokkaido population, leading to hybridization bias between individuals. Southern Hokkaido 1 shared more alleles with the individuals from Europe than with other Hokkaido individuals, which reflects some maintenance of genetic factors from the continent. In Scandinavia, IBD has led to a strong correlation between genetic and geographic distances (Kopatz et al. 2014; Schregel et al. 2018),

and the Hokkaido population could likewise be affected. Separation of the Hokkaido population into three subpopulations as indicated by the first principal component in the PCA analysis, and higher F_{st} values between Eastern and Central-Southern Hokkaido individuals, indicate not only IBD but also some effect by a geographic barrier across the Eastern–Southern/Central boundary, although what is the geographic barrier is still unknown. This difference in F_{st} values was also observed by Hirata et al. (2017), although the cause remains unknown.

Chapter 3

Male-biased dispersal has contributed to the rapid expansion of the population of the brown bear *Ursus arctos* in Hokkaido Island following the near-expiration during the Last Glacial Maximum

Introduction

The process of the formation of the island's biodiversity has been an exciting topic for a long time, and there are still many questions about it (Patiño et al. 2017). Information on this topic contributes significantly to conserving the biodiversity in the recent extinction crisis of the island species (Frankham et al. 2010; Lomolino et al. 2016). Genetic differentiation resulting from geographical isolation, both between islands and within islands, has been found in numerous island species, even within the same species. For example, the endangered Pribilof Island shrew (*Sorex pribilofensis*) distributed on the islands near the North American continent was differentiated between populations of islands and the mainland (Wiens et al. 2022). Even within the insular populations, it is known that the genetic structure was formed in many taxa, such as the giant turtle (Bourgeois et al. 2020), horseshoe bat (Ikeda & Motokawa 2021), and Asiatic black bear (Ohnishi et al. 2009).

The diversity of island species depends on migration from the continent by two filters (Matthews & Triantis 2021). One is the dispersal filter, that is, whether the species can migrate from the continent to the island. The other is the environment filter, which refers to whether the species can adapt to the new environment after migration. Mammals have tended to be focused more on in terms of the dispersal filter. These species are considered a suitable model taxon for studying historical migrations because their movement has depended on the appearance of land bridges that appeared due to sea level changes. In fact, many phylogeographical studies of mammal populations have discussed the relationships between population demography and land bridges (Dobson 1994; Gaughran & vonHoldt 2022; Fu & Wen 2023). On the other hand, other various environmental factors can also trigger significant migrations. For instance, human migration into islands tends to result in species extinction (Rozzi et al. 2023), while climate

change promotes shifts in species habitat (Davis & Shaw 2001; Hewitt 2000). Thus, understanding the context of various biological, environmental, and geographical factors, and global climate changes is crucial for research on mammals' migration.

For the Hokkaido brown bears, Matsuhashi et al. (1999) and Hirata et al. (2013) identified three deeply diverged mtDNA lineages with varying divergence times ranging from hundreds of thousands of years ago to tens of thousands of years ago, each distributed across separate areas (Figure 14). The three lineages are speculated to have migrated to Hokkaido Island independently from the Eurasia continent through land bridges such as the Sohya land bridge, which appeared approximately 12,000 years ago (Ohshima 1990). In contrast, Hirata et al. (2017) found no clear genetic differentiation in Y-chromosomal DNA haplotypes in the Hokkaido bear population. Thus, an apparent mismatch in genetic structures between mtDNA and the Y-chromosomal DNA within the Hokkaido population may be attributed mainly to male-biased dispersal (Chapter 2), but the process that has been formed is still unknown. Therefore, further research using a genome-wide dataset is required to investigate the effect of male-biased dispersal on this question. In addition, the previous study (Matsuhashi et al. 1999) found that the Ishikari lowland is located on the border between areas where different mtDNA lineages are distributed. This result suggests the lowlands as geographic barriers, but any quantitative evaluation about which environmental factors affect the genetic structure formation of the Hokkaido brown bear populations has not been done yet.

In this study, I investigated the demographic history of the Hokkaido brown bear population. Firstly, using double digest restriction site associated DNA sequencing (ddRAD-seq) data, I analyzed the genetic structure and population demography of the Hokkaido bear population, focusing on autosomal and X-chromosomal SNP data. I compared the findings with previous mtDNA and Y-chromosomal DNA data (Matsuhashi et al. 1999; Hirata et al. 2017) and

integrated whole genome resequencing data from populations outside Hokkaido. Additionally, I examined the correlation between the genetic findings and environmental factors, such as elevation and climate changes, that may have influenced the brown bear dispersal over several centuries to ten millennia. Based on these results, I explore the population demography, considering the processes that lead to the separated distribution of three distinct mtDNA lineage clusters, alongside environmental factors, and assess the effect of sex-biased dispersal during this period.

Materials and methods

Sampling and sequencing for the Hokkaido bear population

Forty-nine brown bears from Hokkaido, collected by the Environmental and Geological Research Department, Hokkaido Research Organization, were used (Figure 14; Table 8). I selected samples from all subpopulations described as management units (Oshima Peninsula, Shakotan-Eniwa, Hidaka-Yubari, Doto-Sohya a, Doto-Sohya b, and Teshio-Mashike) based on the brown bear management plan of Hokkaido (Hokkaido 2017, 2022). The English names of these subpopulations are followed by Sato et al. (2005). The mtDNA and Y-chromosomal haplotypes followed previous studies (Matsuhashi et al. 1999; Hirata et al. 2017). Total genomic DNA was extracted from the tissue and muscle with a DNeasy Tissue & Blood Kit (QIAGEN) or QIAamp DNA Micro Kit (QIAGEN). The DNA concentration was measured using NanoDrop2000 (THERMO), and TE buffer (pH 8.0) was added to some DNA extraction to mess their DNA concentration up to 10 μg/ml.

After that, I applied ddRAD-seq to the samples. *Eco*RI and *Bgl*II were used as restriction enzymes to cut off DNA sequences following by Sakaguchi et al. (2015). The libraries were run

on an an Illumina HiSeq X sequencer using 150 bp paired-end mode at Macrogen (Kyoto, Japan).

Genotyping and SNP filtering

Pair-end sequencing data were filtered to exclude low-quality sequences using process_radtags (option: -c -q --index_index --retain_heade --disable_rad_check) in stacks ver. 2.5 (Catchen et al. 2013). Subsequently, the data were mapped to the reference sequence of the polar bear (GCF_017311325.1) using bowtie2 ver. 2.4.4 (Langmead & Salzberg 2012) and duplicate sequences were removed using samtools ver. 1.7 (Li et al. 2009). Genotypes were called by gstacks in stacks. The result was exported as a VCF file using population (option: --vcf --ordered-export) in stacks, which included information about which lineage each sample is belonged using -M option to confirm any significant bias in basic population genetic statistics, such as nucleotide diversity.

To obtain high-reliable genotyping data, I applied SNP filtration following some steps and made four datasets (Figure 15). First, SNP were selected, which the 30-mer starting from the site is unique in the genome, even allowing for two mismatches and the depth is more than three. Each of these mappability scores and depth is calculated using GenMap Genmap ver. 1.3.0 (Pockrandt et al. 2020) and vcftools ver. 0.1.17 (Danecek et al. 2011) filtered the depth > 3 using vcftools.

After separating genotyped sites data by the four chromosome class (unplaced scaffolds regarded as autosomes in this study, scaffolds from X chromosome, scaffolds from Y chromosome, and mitogenome) and selecting SNPs with a missing rate of ≤ 0.1 for all individuals and a missing rate of ≤ 0.2 for individuals, four datasets were created using PLINK

ver. 1.90 (Purcell et al. 2007). Of the four datasets, I selected SNPs located in non-coding regions for fastsimcoal2. All missing sites were excluded from landscape genetic analysis (Mantel test, Partial Matel test, and ResistanceGA). For genetic structure analyses (PCA, fineRADstructure, and ADMIXTURE), sites under linkage disequilibrium (LD) and observed minor alleles less than 2 in all individuals were excluded by using PLINK options "–indep-pairwise 50 5 0.5." and "--mac 2", respectively.

Whole genome data genotyping and SNP filtering

Whole genome re-sequencing data in previous studies (Miller et al. 2012; Cahill et al. 2013, 2015; Benazzo et al. 2017; Kumar et al. 2017; Barlow et al. 2018; Chapter 2) were used to calculate F_{st}, and Q statistics, and compare the populations between Hokkaido and others (Table 9). The raw sequence data were trimmed based on sequence quality, mapped to the reference genome, and called genotyping. This method was followed by Chapter 2 in this dissertation, except for the reference genome for mapping.

Genetic diversity and genetic structure

The number of heterozygous sites per individual was counted using the PLINK --het option.

To investigate the genetic structure, the principal components analysis, PCA, and fineRADstructure were done using PLINK with --pca option and fineRADstructure (Malinsky et al. 2018), respectively. Clustering analysis from $K = 1$ to $K = 10$ was also done using ADMIXTURE ver. 1.3 (Alexander et al. 2009). F_{st} was calculated by smartpca in eigenstrat (Patterson et al. 2006) to detect genetic differentiation between subpopulations.

Gene flow

I conducted three analyses to evaluate gene flow between the subpopulations and between the continental populations. First, visualization of gene flow between the Hokkaido subpopulations was done by EEMS (Petkova et al. 2016) with the number of modeled demes set to be 400 and Markov chain Monte Carlo (MCMC) chain comprising 100 million iterations each were run, discarding the first 10 million generations as burn-in, and sampling every 10,000th generation. The matrix of pairwise genetic differences was calculated using PLINK with --1-ibs option. Second, Q statistics evaluate migration bias between males and females, which evaluates the autosome-to-X genetic drift ratio (Chen et al. 2018; Keinan et al. 2009). If there is no bias in the effective population size and migration between males and females, the Q statistics value converges at 0.75. The formula was $Q = \ln(1 - 2{F_{\mathrm{st}}}^{A})/\ln(1 - 2{F_{\mathrm{st}}}^{X})$ following the previous studies (Chen et al. 2018; Keinan et al. 2009).

Demography

To infer the change in the effective population size, I applied fastsimcoal2 ver. 2.6 (Excoffier et al. 2021) and GONE (Santiago et al. 2020). For fastsimcoal2, I created the site frequency spectrum using easySFS (https://github.com/isaacovercast/easySFS). Monomorphic sites were not considered, so the current effective population size was fixed at N_e = 20,000, which means the number of individuals who can inbreed in Hokkaido is 10,000. Each of the five population demographic models (Figure 16) was simulated with the options (-n 100000 -M -m -q -L40 --removeZeroSFS) for 100 replications. The best model and parameters with the lowest

estimated log-likelihood value were chosen, then 100 bootstrap iterations were run with the same options. GONE was run with the options (cMMb = 1 and MAF = 0.05).

Correlation between genetic distance and elevation

Before calculation, I prepared the elevation data in Hokkaido from elevation and slope 1 km mesh data published by Ministry of Land, Infrastructure, Transport and Tourism of Japan (https://nlftp.mlit.go.jp/ksj/gml/datalist/KsjTmplt-G04-a.html).

For evaluation based on correlation with elevation, the Mantel test (Mantel 1967) and partial Mantel test (Smouse et al. 1986) were performed. I gathered the elevation on the line segment connecting two individuals for all pairs of sampling locations. I determined the following parameters based on four hypotheses: (a) Euclidean distance, (b) high elevation, (c) low elevation, and (d) high elevation difference is as resistance, respectively. I calculated five values for each hypothesis: (a) Euclidean distance between two individuals, (b) the mean elevation and the highest elevation in the elevation on the line segment connecting two individuals, (c) the difference between the lowest elevation in the elevation on the line segment connecting two individuals, and (d) the difference between the highest and lowest elevation in the elevation on the line segment connecting two individuals and its standard deviation (SD). This idea and method were followed by Ohnishi et al. (2019). In addition, I collected three datasets for genetic distance: mtDNA (Matsuhashi et al. 1999), Y-chromosomal DNA (Hirata et al. 2017), and autosomal DNA (this study). For mtDNA and Y-chromosomal DNA data, I calculated Bray–Curtis percentage dissimilarity as the genetic distance between individuals using the ecodist package ver. 2.0.9 in R ver. 4.2.1 (R core team 2022). Genetic distance for autosome was calculated by PLINK with --1-ibs option.

Mantel and partial Mantel tests for genetic distance and candidate elevation parameters were performed with 999 permutations using the vegan package ver. 2.6.4 in R with the options (method = spearman and permutations = 9999). In addition, ResistanceGA (Peterman 2018) was run with the default setting to evaluate how the elevation was resistant for the brown bears in Hokkaido.

Correlation between genetic distance and climate dynamics

To estimate the relative habitat suitability change along with past climate change, I constructed a habitat suitable model for the brown bear based on the current occurrence data and climate data (temperature and precipitation). The occurrence data described only as "HUMAN_OBSERVATION" from 1979 to 2013 north of the equator was downloaded from the Global Biodiversity Information Facility (GBIF, https://www.gbif.org, https://doi.org/10.15468/dl.mmst2x), then I filtered the data using the spThin package ver. 0.2.0 in R with the option (thin.par = 10). The current climate data published in Karger et al. (2017) was downloaded from the PaleoClim database (http://www.paleoclim.org/; Brown et al. 2018). I chose seven variables: bio7, 8, 9, 15, 17, 18, 19 in the current available BIOCLIM variables (Booth et al. 2014), which was not correlated with other available ($|r| < 0.7$) based on pairwise correlations by the ENMTools package ver. 1.0.7 in R (Warren et al. 2021).

I evaluated multiple relative habitat suitable models based on the maxent.jar JAVA program (Phillips et al. 2006) using the ENMeval package ver. 2.0.4 in R (Muscarella et al. 2014) with the options (method = 'randomkfold', algorithm = 'maxent.jar', fc = c("L","LQ","LQH"), and RMvalues = seq(0.5, 3, 0.5)) and chose the model which the AICc value was lowest. 10,000 background points were randomly selected as absence data. The model

was predicted using cloglog transformation to Present (Karger et al. 2017), mid-Holocene (8.326–4.2 ka) (Fordham et al. 2017), Last Glacial Maximum (ca. 21 ka) (Karger et al. 2023), and Last Interglacial (ca. 130 ka) (Otto-Bliesner et al. 2006) climate data. For mid-Holocene (8.326–4.2 ka) and Last Glacial Maximum (ca. 21 ka), three additional surfaces based on different climate models: the community climate system model, CCSM (Gent et al. 2011), the model for interdisciplinary research on climate model, MIROC-ESM (K-1 model developers 2004), and the Max-Planck-Inst. für Meteorologie climate model, MPI-ESM-P (Liepert & Lo 2013), downloaded from the WorldClim database ver. 1.4 (Hijmans et al. 2005), were used respectively.

Results

Genotyping

By genotyping ddRAD-seq data using stacks, I detected 1,915,799 SNPs for 49 individuals from the Hokkaido bear population. No significant bias in basic population genetic statistics, such as heterozygosity and nucleotide diversity, was found (Table 10). After the different SNP filtration to use the optimal SNPs dataset for each population genetic analysis, I used from 505 to 138,791 SNPs (Figure 15). The number of heterozygous sites per individual was 12,201–19,174 (Table 11), with no significant difference between subpopulations described as management units by Hokkaido Prefecture (2017, 2022).

Genetic structure and gene flow

PCA, fineRADstructure, and ADMIXTURE were applied to investigate genetic structures in the Hokkaido bear population. The genetic heterogeneity was shown in the first

principal component of PCA (n = 40, 33,559 SNPs; Figure 17a). The results utilized different colors to represent subpopulations (Oshima, Ishikari, Hidaka, Sohya, Doto, and Teshio), which corresponded to the designated management units (Oshima peninsula, Shakotan-Eniwa, Hidaka-Yubari, Doto-Sohya a, Doto-Sohya b, and Teshio-Mashike) as described by the Brown Bear Management Plan on Hokkaido (Hokkaido 2017, 2022). The South (Oshima and Ishikari) was well differentiated from the others (Hidaka, Sohya, and Doto) (Figure 17a). The fineRADstructure (Figure 17b) supported the grouping of the two subpopulations and indicated weak genetic differences between Sohya and Doto due to the absence of a defined separation (red arrows shown in Figures 17b, c, and d), which was also supported by the lowest F_{st} value between Sohya and Doto (Table 12). F_{st} values (0.084–0.093) between Ishikari and other subpopulations were relatively higher (Table 12).

The clustering analysis by ADMIXTURE (n = 40, 33,559 SNPs) estimated that a single population (K = 1) is the most likelihood in 10 patterns, indicating the division into subpopulations (K = 1 to K = 10) based on the standard error of the cross-validation error estimate (CV error). At the same time, the results of K = 2, 3, and 4 also showed the difference between the South and the others indicated by the results of PCA and fineRADstructure (Figure 18). For example, K = 2 showed the two subpopulations, the South and the others shown in Figure 17a.

The result estimated gene flow in the Hokkaido bear population using EEMS was shown in Figure 17c (n = 40, 138,791 SNPs). Compared with the elevation in Hokkaido (Figure 17d), the lower gene flow seemed to be more frequent in the lowlands, particularly in the Ishikari lowland, than in the highlands.

I calculated Q statistics, $\ln(1-2{F_{\mathrm{st}}}^{A})/\ln(1-2{F_{\mathrm{st}}}^{X})$followed by Chen et al. (2018) and Keinan et al. (2009), between the subpopulations in Hokkaido and between the populations (Hokkaido, North America, and Europe). All Q statistics between the subpopulations in Hokkaido (n = 39 obtained both autosomal and the X-chromosomal SNP data, autosome: 33,559 SNPs, X chromosome: 505 SNPs) were lower than 0.75, meaning that the genetic differentiation of X-chromosomal DNA is higher than the expected value under no sex-biased migration and number of spouses (Q values = 0.321–0.496; Table 13). Q statistics between Hokkaido and other populations (n = 18, autosome: 1,7178,876 SNPs, X chromosome: 398,711 SNPs) were lower than 0.75 (Q values = 0.308–0.403; Table 14), even considering the 95% confidence interval (CI), 0.157–0.560.

Demography

Using fastsimcoal2 (n = 41, 61,168 SNPs), I simulated five population demographic models: (a) One expansion, (b) one decline, (c) two expansions, (d) two declines, and (e) one bottleneck (Figure 16). A model in which one bottleneck has happened was most statistically supported (Table 15). Under the situation in which the generation time was 11 years (Benazzo et al. 2017; Cronin et al. 2009), the time starting the decline was 22,619 years ago (95% CI: 2,972–71,942), and the end was 1,155 years ago (95% CI: 1,227–35,616) (Figure 19). Another demography estimation software, GONE (n = 40, 138,791 SNPs; Figure 20), also indicated a recent rapid expansion of the effective population size from about one thousand years ago.

Correlation between genetic distance, landform, and climate dynamics

As a result of EEMS (shown above), I assumed that the lowland was resistant to disperse for the brown bears in Hokkaido. Two calculations, the Mantel and partial Mantel test, were done to investigate the assumption. The tests accessed the correlation between pairwise genetic distance and the elevation on the line segment connecting two individuals. Mantel and partial Mantel tests based on mtDNA revealed that, within pairs, the lower the elevation, the higher the genetic differentiation of the mtDNA, though the correlation was also influenced by isolation by distance (Tables 16 and 17). Using autosomal SNP data, both two tests supported only isolation by distance. In case of using the Y-chromosomal data, only the Mantel test indicated a weak correlation between the genetic differentiation and the high elevation between two individual pairs. Some previous studies suggested the limitation of Mantel and partial Mantel tests (Balkenhol et al. 2009; Meirmans 2012), so I run ResistanceGA to investigate whether the highland or lowland is resistant for bears' migration in Hokkaido. The results indicates that the lowland in Hokkaido acts as a barrier based on mtDNA and autosomal SNP data (Table 18 and Figure 21). On the other hand, when using the Y-chromosomal data, isolation by distance was strongly supported than barrier by the elevation.

I constructed a habitat suitable model to estimate the relative habitat suitability change along with past climate changes. By evaluating some relative habitat suitable models, a Maxent model with linear, quadratic, and hinge features, with RM values of 0.5, was chosen as the best model based on AICc (Table 19). The contributions and response curves of each environment variance were shown in Table 20 and Figure 22, respectively. The relative habitat suitability during (BIO7, 8, 9, 15, 17, 18, and 19) the last glacial maximum (LGM) about 21,000 years ago was estimated to be low in Hokkaido (Figure 23). This inference was also supported when the different climate model surfaces were used (Figures 24 and 25).

Discussion

This study aims to investigate the colonization history of the Hokkaido brown bear population, in relation to genetic structure mismatches between mtDNA and the Y-chromosomal, then evaluate the influence of the male-biased dispersal and environmental factors on the population demography. The results showed that the Hokkaido bear population was divided into the South (Oshima and Ishikari) and the others (Hidaka, Sohya, and Doto) subpopulations. Although admixture between the Hokkaido subpopulations ongoing, a weak difference in gene flow between the subpopulations was suggested and probably influenced by the lowlands, mainly for female brown bears. In the past, the Hokkaido bear population has experienced bottlenecks and a recent expansion, which could be caused by climate changes.

Population demography based on autosomal and X-chromosomal SNPs

The result (K = 1) of ADMIXTURE indicated that the population is not divided into multiple subpopulations, most likely based on CV error. It is because of the ongoing admixture between lineages in Hokkaido, as indicated by Chapter 2. Matsuhashi et al. (1999) reported the clearly separated distribution of the three mtDNA lineages, which was also supported by previous studies (Sato et al. 2011a; Shirane et al. 2018). On the other hand, the microsatellite analysis of Y-chromosomal did not support such a clear genetic structure (Hirata et al. 2017). The simulation by the previous studies (de Jong et al. 2023) estimated that the former population structure could not be detected in 100–1,000 generations, which are 1,100–11,000 years considering the brown bear generation time, about 11 years (Benazzo et al. 2017; Cronin et al. 2009). Thus, allele sharing between different mtDNA lineages (Hirata et al. 2013) has been caused rapidly and widely across

Hokkaido Island by male-biased dispersal.

While the admixture has already been done, the results of PCA, ADMIXTURE (K = 2, 3, and 4), and fineRADstructure detected weak genetic heterogeneity in Hokkaido. Significantly, the difference between the South (Oshima and Ishikari) and the others (Hidaka, Sohya, and Doto) (Figure 17a) was highest. Chapter 2 showed that the individuals from the South, especially from Oshima, were slightly different from others. The result could reflect that the ancestor from the South, mainly the clade 4 of mtDNA, has experienced migration from a different route, isolation, or both compared with the other lineages. Hirata et al. (2013) and Segawa et al. (2021) suggested that this subpopulation might have migrated from the continent to Honshu through Hokkaido and Soya land bridge (Ohshima 1990; Figure 23c). However, there is another possibility that the reverse route from Honshu to Hokkaido might have also occurred because the divergence time of clade 4, estimated about 194,000 years ago (Hirata et al. 2013), is older than the formation of the Korean Strait, during the last interglacial (Ohshima 1990). At present, it is hard to conclude the migration direction of clade 4, but further analysis, such as the ancient genome of fossils, might verify these hypotheses. Compared with the migration route hypotheses, the isolation of the South from the other regions is more likely to have happened due to the Ishikari lowland, at the boundary of the two subpopulations, and the contraction of suitable habitat in Hokkaido in the LGM (Figure 23c). The results of F_{st} indicated that Ishikari was the most genetically different from other subpopulations, despite Oshima, which is far from the Ishikari lowland, being considered the most isolated from other subpopulations (Figure 17d). This could be due to sampling bias because this study used only three samples as individuals from the Ishikari subpopulation. It is necessary to study further to solve the question and discuss the influence of the Ishikari lowland on the dispersal of the brown bear.

All Q statistics values of ddRAD-seq and whole-genome datasets were lower than the expected value, 0.75. The sex-biased process, which differs in effective population size between females and males, is known to cause the Q statistics values to deviate significantly from 0.75 (Keinan et al. 2009). Significantly, a sex bias in dispersal, lifespan, and breeding opportunity influences the Q statistics values (Webster & Wilson Sayres 2016). In the case of the brown bear, Q statistics would be lower than 0.75 by male-biased dispersal. The sex ratio and lifespan, in which the number of females is slightly larger than that of males, could also be reasons for affecting Q statistics values (Sato 2015; Shimozuru et al. 2022). If so, Q statistics could be higher in both situations because the female effective population size is more significant. In addition, following Chapter 1, there is no confirmed significant bias in the sex ratio in the population (Swenson et al. 1994) and difference in reproductive success between sexes (Shimozuru et al. 2019). Thus, this result can be explained due to the male-biased dispersal. The result that Q statistics between Hokkaido and the continents was lower than that between continental populations means the significant influence of the male-biased dispersal when the ancestor had migrated from the Eurasian Continent into Hokkaido Island. A mitochondrial lineage, clade 3a1, assumed to disperse about tens of thousands of years ago, is found widely in the North American and the Eurasian Continents, while it has yet to be found in Hokkaido. The result of Q statistics suggests that clade 3a1 migrated from the Eurasian Continent to Hokkaido, but only clade 3a2, as a sister subclade to clade 3a1, has been found on Hokkaido.

Fastsimcoal2 estimated that the Hokkaido population experienced a decline in the effective population size 22,616 years ago (95% CI: 2,972–71,942) and a rapid expansion recently, which was also supported by the analysis using GONE. Hirata et al. (2013) reported that each coalescent time of three mtDNA lineages in Hokkaido is about several tens of thousands of years ago (27,000–

42,000 years ago). In addition, the common ancestor of the Hokkaido brown bear was estimated to be about 53 thousand years ago based on Y-chromosomal analysis (Hirata et al. 2017). The decline of time estimation in this study is consistent with these times despite the wide confidence interval. The time is also closer to the LGM when many mammals moved on a large scale (Fu & Wen 2023). Therefore, the decline might have occurred due to climate change in the LGM, which is also supported by the lack of fossil records of brown bears on Hokkaido in the Late Pleistocene age (Takakuwa et al., 2007).

Correlation between genetic distance, landform, and climate dynamics

This study shows resistance to population colonization by searching for a correlation between landform and genetic distance based on maternal and paternal heritable markers in previous studies (Matsuhashi et al. 1999; Hirata et al. 2017) and nuclear variants. As a result, a negative correlation between low elevation and genetic distance for the mtDNA and autosomal SNP was observed, while that for the Y-chromosomal was not.

This study found that gene flow between the South subpopulations (Oshima and Ishikari) and the other subpopulations seems to be restricted by a wide lowland; the Ishikari lowland between them was the lowest within Hokkaido Island according to the results of F_{st} and EEMS. On the other hand, previous studies have suggested that highland and elevation variance were also barriers to dispersal for each American black bear in North America (Cushman et al. 2006; Short Bull et al. 2011) and the Asiatic black bear in Japan (Ohnishi et al. 2019). This study did not support both studies, although the partial Mantel test based on the Y-chromosomal DNA markers inferred a weak correlation between the highland and the genetic distance. There has been a brackish water lake on the Ishikari lowland in the mid-Holocene (Ishii & Hori 2016; Sagayama et al. 2010),

together with many oxbow lakes, and widespread peatlands (Ishii & Hori 2016). In addition, now along the lowlands in Hokkaido, cities and farm areas inferred as barriers for bears to move (Palm et al. 2023) are developed. For these reasons, the lowlands in Hokkaido may have posed challenges for brown bears to migrate for a long time.

While the lowland was inferred as a barrier to dispersal, the signature was not detected from the landscape genetic analysis using the Y-chromosomal DNA data. This is because male-biased dispersal significantly contributed to the colonization of the Hokkaido population. The genetic structure based on autosomal SNP in this study partially agrees with the genetic structure of mtDNA haplotypes, which shows genetic differentiation between the South subpopulation and others, whereas some genetic affinity is found within the Hokkaido population. Thus, the genetic structure based on autosomal SNP reflects both female philopatry and male-biased dispersal. That is, within Hokkaido, the autosomal and Y-chromosomal admixture between different areas of distribution of mtDNA lineages (Chapter 2) occurred due to the larger migration ability of male bears.

Relative habitat suitability for brown bears estimated by Maxent was low in the LGM. The trend, in which the habitat suitability was significantly changed in the LGM, was reported widely in the northern hemispheres (de Jong et al. 2023; Fu & Wen 2023; Luna-Aranguré et al. 2020). In Japan, the Japanese macaque (*Macaca fuscata*) also followed this (Ito et al. 2021). The northern and central areas of Hokkaido estimated not to be suitable for brown bears during the LGM, were covered with tundra (Dobson 1994). Igarashi (2016) estimated that Hokkaido was covered by coniferous forest and grassland extensively during the Last Glacial Maximum (LGM), based on a review of pollen data. These areas might not have been suitable for brown bears compared to the current predominant broad-leaved forest vegetation in Hokkaido (Igarashi 2016). Other

palynological studies (Okaura et al. 2007) indicate that oak nuts, a primary food resource for brown bears (Ohdachi & Aoi 1987; Sato et al. 2005), were scarce during the LGM. The lack of fossil records of brown bears on Hokkaido in the Late Pleistocene age (Takakuwa et al. 2007) supports the prediction that almost all areas were not suitable for the brown bear. From the result of fastsimcoal2 and the habitat suitability, the Hokkaido bear population would have experienced a decline during the LGM due to habitat reduction caused by climate changes.

Population demographic history of the brown bear in Hokkaido

Combining the previously reported multiple migrations theory with the results of this study, the following population demographic history can be inferred for the brown bear population in Hokkaido (Figure 26). Firstly, the ancestors of each mtDNA lineage had migrated into Hokkaido from the Eurasian Continent severally before the LGM. These lineages might have migrated from different routes and been distributed separately then, but at present, I cannot conclude clearly because further analyses that detect their genotypes, including ancient genome analysis, are needed. Next, during the Last Glacial Maximum (LGM), a population decline occurred due to a decrease in their suitable habitat, prompting the ancestors of each lineage to move south and establish subpopulations in different corners of Hokkaido. After that, a rapid expansion occurred through male-biased dispersal, forming a nuclear homogeneous population with the separated distribution of three mtDNA lineages, although there were some dispersal restrictions, such as geographical barriers like the Ishikari lowland.

This scenario supports the previous studies, suggesting *i)* dispersal barrier by lowland (Matsuhashi et al. 1999), *ii)* no findings of clade 3a1, which differentiated recently within Hokkaido (Itoh et al. 2012; Matsuhashi et al. 1999; Sato et al. 2011a; Shirane et al. 2018),

admixture between different lineages (Chapter 2; Hirata et al. 2017), and *iii)* slight genetic differentiation between the South and others in Hokkaido (Chapter 2). On the other hand, this scenario suggests no massive migration around the LGM, even though the Soya land bridge appeared at this time (Ohshima 1990).

Compared with the previous phylogeographic studies, this study suggests that not only sea levels but also other factors, such as climate change and landforms, are important in biogeography for large mammals. For mammals, the population demographic history profoundly depends on the formation of land bridges due to sea level changes (Salis et al. 2021; Wiens et al. 2022). Especially, the species distributed in present Japan could have experienced multiple land bridge formations caused by climate changes, resulting in their population demographic history (Dobson 1994; Mckay 2012; Millien-Parra & Jaeger 1999). However, other environmental factors may be equally important, even for the species that can easily move through land bridges, such as large mammals. I emphasize the importance of the verification of multiple factors, which would be clarified in future phylogeographic studies.

de Jong et al. (2023) proposed that the separated distribution of mitochondrial DNA lineages is a result of random fixation differences. Considering the results in this study, these random fixation disparities could have arisen by contraction associated with climate changes after multiple migrations from the Eurasia continent to Hokkaido. To fully validate this hypothesis, the transition of haplotype frequencies should ideally be revealed through the detection of ancient samples. Unfortunately, there is currently a lack of fossil records in Hokkaido (Takakuwa et al. 2007).

Although this study investigated the population demographic event that the previous studies missed, the correlation with natural selection could not be detected. The previous study

(Ohdachi et al. 1992) showed the latitude gradient on skull dimensions, which increases from south to north, in Hokkaido, so there might be differences in SNP relating to body size in Hokkaido. Further analysis of whole-genome resequencing for more samples is needed.

Conservation perspectives

It is essential to conserve and manage the brown bear population in Hokkaido. Although the population size has been stable recently (Japan Bear Network 2006; Hokkaido 2022), a massive decline in the number of individuals was caused by the spring cull, which was a hunting measure used to remove bears that could be a nuisance in the future around the 1990s (Takinami et al. 2021). In addition, some local subpopulations (Teshio-Mashike and Shakotan-Eniwa subpopulations) are assigned as threatened local populations (Ministry of the Environment 2020). Thus, a management plan of conservation and management is needed for the Hokkaido bear population.

Now, the population is managed based on the 2nd Brown Bear Management Plan on Hokkaido (Hokkaido 2022). Setting management units based on genetic data was not suggested in this management plan, although this consideration was in the 1st one. This study demonstrates that the subpopulations in Hokkaido correspond to the management units (Oshima, Ishikari, Hidaka, Sohya, and Doto) outlined in the 2nd Brown Bear Management Plan on Hokkaido (Hokkaido 2022), providing scientific support for the current management units. I would like to suggest that it is not just how to divide units, but how to maintain connectivity between units that is important. This perspective is also supported by the previous reviews on applying genetic data to wildlife management, considering connectivity as one of the conservation principles (Andrello et al. 2022; Nielsen et al. 2022). This study inferred that the lowland is a barrier to dispersed brown bears for a long time. Now the artifacts such as buildings, roads, and farms that brown bears tend to avoid,

as demonstrated by Palm et al (2023), are present in the area. Considering how to maintain connectivity through lowland areas while ensuring citizen safety will be crucial for the future management of brown bears on Hokkaido.

Chapter 4

Local genetic differences by sex-biased dispersal in brown bear *Ursus arctos* populations, revealed by whole genome sequencing

Introduction

The discrepancy between the phylogenic tree based on different genetic regions has been confirmed in many species. It has been observed not only between species (Kutschera et al. 2014) but also within species (Hailer et al. 2012; Chapter 2). Although investigating its formation process has long been fundamental in understanding its evolution, it remains a significant challenge due to considering various mechanisms. For example, incomplete lineage sorting (e.g., Feng et al. 2022), gene flow, which can result in mitochondrial capture or nuclear swamping (e.g., Rogers et al. 2019), and horizontal gene transfer (e.g., Kambayashi et al. 2022) are considered as causes. Given such a background, it is essential to employ not only improved technical methods but also comprehensive sampling across various habitats spanning different time periods. Comparing the results from such diverse samples, then, is crucial for unraveling the underlying processes.

The brown bear *Ursus arctos* is an example of a species exhibiting such a discrepancy between the phylogenic trees. At the inter-species level, mitochondrial DNA-based phylogenetic trees place the polar bear *Ursus maritimus* within a brown bear lineage, clade 2, distributed in the Admiralty, Baranof, and Chichagof (ABC) islands (Leonard et al. 2000). In contrast, phylogenetic trees estimated from the nuclear genome clearly show their differentiation (Hailer et al. 2012; Miller et al. 2012). Even at the intra-species level, multiple mitochondrial DNA (mtDNA) lineages with differing estimated divergence times are reported (Davison et al. 2011; Hirata et al. 2013; Lan et al. 2017), whereas the nuclear genome does not exhibit a clear differentiation between those lineages (Bidon et al. 2014; de Jong et al. 2023; Chapter 2). The discrepancy in the phylogenetic relationships has been attributed to a multitude of factors, including incomplete lineage sorting (Kutschera et al. 2014), male-biased dispersal (Bidon et al. 2014; Hirata et al. 2017), and hybridization with related species (Cahill et al. 2013, 2015, 2018; Lan et al. 2022; Liu et al. 2014;

Miller et al. 2012; Wang et al. 2022), which even includes hybridization with the extinct cave bear (Barlow et al. 2018). Such various factors and the complex relationship among them make it challenging to establish a clear and conclusive explanation.

Focusing on intra-species levels, de Jong et al. (2023) revealed admixture between populations leading to the erasure of the former genetic structure on the nuclear genome and suggested two inferences: *i*) the distribution of mtDNA haplotypes is due to incomplete lineage sorting and *ii*) autosomal genome reflects recent population demography by male-mediated gene flow. Although two inferences might have occurred partially in the population demography, both are not enough to fully explain the incongruences between the phylogenic trees of mtDNA and the nuclear genome for the brown bear. The hypothesis *i* was suggested based on the result of the multiple coalescent analysis of the Hokkaido and Scandinavian populations, which are only part of the brown bear populations. The brown bear distributes widely in the northern hemisphere and exhibits a broad genetic structure consisting of multiple mtDNA lineages (Davison et al. 2011; Hirata et al. 2013; Lan et al. 2017) with different divergence times distributed separately (Figure 27). The consistency between these appearance and divergence times is confirmed by many previous studies, including the studies using ancient sample data from different areas (da Silva Coelho et al. 2023; Edwards et al. 2011; Kosintsev et al. 2022; Molodtseva et al. 2022; Segawa et al., 2021). Thus, it is highly possible that such a broad genetic structure has not been formed only by incomplete lineage sorting, and some local populations observed the mtDNA lineage with ancient divergence times might have retained ancestral genetic characteristics on the nuclear genome. The hypothesis *ii* cannot explain the genetic distinctiveness of the brown bear subspecies in Himalaya, Mongolia, and Pakistan (de Jong et al. 2023; Tumendemberel et al. 2023), where an old divergent mitochondrial DNA haplotype was identified (Lan et al. 2017;

Tumendemberel et al. 2019). The genetic distinctiveness of the nuclear genome might reflect not only recent expansion mainly by male-biased dispersal but also local differences before the expansion. Hence, population genetic analysis is needed using samples from the population across the habitat, including ancient samples, to verify *i*) the correlation between the divergence time of the mtDNA lineages and the genetic distinctiveness on the nuclear genome and *ii*) the differences in the influence of recent expansion driven by male-biased dispersal between the populations.

In this study, I applied whole-genome resequencing to nine brown bears (Hirata et al. 2013, 2014) from the local Asian populations (Etorofu Island, Sakhalin, Far East, Kazakhstan, Tibet, Central Russia, and West Asia; Figure 27 and Table 21). These populations were found to exhibit distinct genetic characteristics from those on the Eurasian and North American continents based on mtDNA analyses (Hirata et al. 2013, 2014), so the difference in the nuclear genome might also persist. Combining them with the published modern genome data (Barlow et al. 2018; Benazzo et al. 2017; Cahill et al. 2013, 2015; Chapter 2; Kumar et al. 2017; Liu et al. 2014; Miller et al. 2012; Taylor et al. 2018; Wang et al. 2022) and ancient genome data (Barlow et al. 2018; Cahill et al. 2018; Lan et al. 2022; Segawa et al. 2021; Wang et al. 2022), population genomic analysis focused on the local differences in the phylogeny, demography, and gene flow. Based on the results obtained, this study verifies the correlation between mtDNA and nuclear genome and the impact of the recent dispersal to investigate the process such a significant discrepancy between the phylogenic tree at the intra-species level has occurred.

Materials and methods

Sampling and genome-sequencing

Nine skin or muscle samples collected by the Zoological Institute, Russian Academy of Sciences (Figure 27 and Table 21) were used from the local populations distributed in the Eurasian Continent and islands (Etorofu Island, Sakhalin, Far Eastern area, Kazakhstan, Tibet, Central Russia, and Western Asia) across the habitat of the brown bear (McLellan et al. 2017). From the samples, I extracted the total DNA using the DNeasy Blood & Tissue Kit (Qiagen, Hilden, Germany) and stored it at four or −20°C until used.

The 150 bp pair-end whole-genome resequencing on an Illumina Novaseq 6000 sequencer was applied to these samples by Macrogen Japan (Tokyo, Japan). The libraries were prepared using the TruSeq DNA Nano Sample Prep Kit (Illumina, San Diego, USA). The average of the total amount of sequence data per sample is 90 Gb.

Mapping and genotyping

I mapped raw sequence data to the reference sequence of the polar bear (GCF_017311325.1) and genotyped after a quality check. This method followed by the Materials and methods section in Chapter 2. Since I had to detect sex for individuals except for individuals included the group, ancient, Cave bear, and Ancient Polar shown in the “Group” column in Table 21 to analyze for sex-chromosomes, so I calculated the depth ratio on the scaffolds of the X chromosome (n = 5; NW_024423319.1–NW_024423323.1) and the Y chromosome (n = 19; NW_024423324.1– NW_024423342.1) by the following formula. If the depth ratio was > 1, we set the sex as female. After the detection, genotyping of SNVs on the scaffolds of the X chromosome for males was performed with the option --ploidy 1, and that of females with the option --ploidy 2 in GATK.

$$Depth\ ratio\ = \frac{depth\ for\ X-link\ scaffolds}{depth\ for\ Y-link\ scaffolds}$$

Due to the lower sequence quality of ancient samples, the method for genotyping was changed from that used for modern samples. Ancient samples (n = 11, samples from the group, ancient, Cave bear, and Ancient Polar shown in the "Group" column in Table 21) were genotyped by mpileup in samtools ver. 1.9 using -q 30 -Q 30 options and pileupCaller (https://github.com/stschiff/sequenceTools) with some options (--randomHaploid --skipTransitions) after mapping to the reference sequence. Such samples are sometimes not suitable for population genetic analysis because of the small amount of sequence data, so I calculated the ratio of the number of covered bases with depth >= 1 to the total bases of the reference sequence using a samtools ver. 1.15 command, samtools coverage, then used samples with a ratio of > 0.1.

For f_4 statistics and ancient DNA analysis, I used only scaffolds longer than 0.1 M bp and excluded the sex-linked scaffolds (n = 79) whose total length was approximately 99% of the total reference sequence length because most scaffolds were too short to be used for population genetic analysis and EIGENSOFT ver. 7.2.1 (Patterson et al. 2006) used in PCA do not accept the data contained more than 100 chromosomes.

Genetic diversity, genetic structure, phylogeny and demography

I calculated heterozygosity and run of homozygosity (ROH) per individual using PLINK ver. 1.9, using options --het for heterozygosity, and --homozyg-kb 500 and --homozyg-kb 2000 for ROH, respectively. The genetic structure of the brown bear (n = 54) worldwide was estimated by PCA and ADMIXTURE, followed by Chapter 2 of this dissertation. The relative scale of gene flow based on genetic distance and sampling location was calculated by EEMS (Petkova et al. 2016).

The number of modeled demes set to be 400 and Markov chain Monte Carlo (MCMC) chain comprising 20 million iterations each were run, discarding the first 10 million generations as burn-in, and sampling every 10,000th generation.

To obtain the whole mtDNA sequence, 37 whole-genome sequence data (with an asterisk on the "Getorganelle" column in Table 21) was assembled using getOrganelle with the option (-k 21,45,65,85,127). The 81 samples (Table 22) on the NCBI database were downloaded and added as sequence data. For sequence data, two rRNA genes, 22 tRNA genes, and 12 coding genes except for NADH dehydrogenase subunit 6 (ND6) sequences due to the heterogeneity of its nucleotide composition (Hirata et al. 2013) were extracted; gap sites were excluded. The final sequence length was 14,784 bp. The phylogenetic tree was constructed by the maximum-likelihood method using iqtree ver. 1.6.12 with the options (-m MFP -AICc -bb 1000 -alrt 1000) after alignment by the MUSCLE algorithm (Edgar 2004). The Asiatic black bear sample (Honshu; NCBI accession number: DRR250459) was used as an outgroup. Additionally, the divergence time for each mtDNA lineage was estimated using BEAST ver. 2.4.3 under the GTR substitution model. The relaxed clock lognormal and the coalescent constant population model were used. To calibrate divergence times, radiocarbon dates for ancient sequences, which is a mean age of 120 thousands of years ago for the ancient polar bear (GU573488; Lindqvist et al. 2010), 31.87 thousand years ago, 44 thousand years ago, and 409 thousand years ago for the cave bears (EU327344, NC011112, and KF437625; Bon et al. 2008, Krause et al. 2008, Dabney et al. 2013), were set. Trees were sampled every 10,000 generations from a total of 1,000,000,000 generations whose first 100,000,000 generations were described as burn-in. The maximum credibility tree was generated using TreeAnnotator in BEAST. Other options were followed by the "Divergence Time Estimation" tutorial by Taming the BEAST (Barido-Sottani et al. 2018).

The Y-chromosomal sequences were constructed from the vcf file using bcftools consensus ver. 1.9. Phylogenetic trees based on haplotype data were constructed following the same method as that of mtDNA. I used the American black bear sample (American_black_bear; Kumar et al. 2017) for the Y chromosomal tree as an outgroup.

To construct phylogenetic trees based on the autosomal and X-chromosomal SNPs, the identity-by-state of each pair was calculated using PLINK with the option (--distance square 1-ibs). This study interpreted the non-sex-linked scaffolds as autosomal scaffolds (n = 3,875). After the calculation of the genetic distance matrix, phylogenetic trees based on neighbor-joining methods (Saitou & Nei 1987) were constructed using the ape package on R (Paradis et al. 2004). I used the Asiatic black bear sample (Asiatic_black_bear) as an outgroup. PSMC (Li & Durbin 2011) was applied to all new samples and samples from the same or near group followed by Chapter 2.

Gene flow with inter- and intra-species

TreeMix (Pickrell & Pritchard 2012) was applied following by Chapter 2 to show the phylogenetic relationship and gene flow between groups or individuals. After running TreeMix, I evaluated how many migration times are more suitable using OptM (Fitak 2021).

Hybridization with the related species and gene flow between the brown bear populations were evaluated by f_4 statistics using Admixtools (Patterson et al. 2012). f_4(Outgroup, Polar bear; X, Kazakhstan(U13M)) and f_4(Outgroup, Cave bear; X, modern Polar bear), where X means the brown bear individuals, were calculated to detect hybridization with the polar bear and the cave bear, respectively. An alternative evaluation for hybridization with related species, f_4 ratio

(Patterson et al. 2012) was applied to infer the mixing proportions of an admixture event. I calculated the ratio of f_4 values, α for each related species shown below.

$$\alpha_{Polar\ bear} = \frac{\mathrm{f}_4(\text{Outgroup, Polar bear; X, Kazakhstan(U13M)})}{\mathrm{f}_4(\text{Outgroup, Polar bear; West Asia, Kazakhstan(U13M)})}$$

$$\alpha_{Cave\ bear} = \frac{\mathrm{f}_4(\text{Outgroup, Cave bear; X, modern Polar bear})}{\mathrm{f}_4(\text{Outgroup, Cave bear; North America, modern Polar bear})}$$

The percentage of the admixture proportion was then calculated following the below formula.

$$f_4 ratio\ (\%) = (1 - \alpha) \times 100$$

I created mtDNA consensus sequences of 63 bears from the vcf file using bcftools (Danecek et al. 2021) to detect modern brown bears whose mitochondrial DNA lineage is clade 3a1. Gene flow, driven by the recent expansion of mainly clade 3a1, was evaluated by the value of f_4(Outgroup, clade 3a1 in Europe; X, the modern brown bear excluding X) and of f_4(Outgroup, clade 3a1 in North America; X, the modern brown bear excluding X) using autosomal SNPs data. For evaluation of the recent expansion, the dataset only including modern samples was used because using as many sites as possible is suitable for evaluation. I used the American black bear (American_black_bear; Kumar et al. 2017) and the Asiatic black bear (Asiatic_black_bear; Kumar et al. 2017) as outgroup.

Species distribution model

The relative habitat suitability model of the polar bear was constructed using Maxent (Phillips et al. 2006) to compare with that of the brown bear. The workflow was the same as in Chapter 3, excluding the filtration methods of distribution points. Instead of the spThin package, gridSample in dismo package was used for the filtration, which is the extraction of one present point per 4,000 × 8,000 meshes covered with the northern hemisphere.

Results

I genotyped 42,906,277 SNPs for modern samples and 10,537,259 SNPs for ancient samples. I used two datasets, including only modern samples (dataset modern; n = 61, 42,906,277 SNPs) and both modern and ancient samples (dataset ancient and modern; n = 72, 10,537,259 SNPs). The coverage, which means the proportion of covered bases with depth >= 1 to the toral bases of the reference sequence (Table 21), was 10.14–91.59% (only modern samples: 81.26–91.59). The depth for modern samples was 6.85–55.11 (Table 21).

Genetic diversity, genetic structure, phylogeny, and demography

To assess the genetic diversity of the brown bear, I computed heterozygosity and ROH for each individual (Figure 28). Bears from Central Asia exhibited high heterozygosity and low ROH, while those of Etorofu Island (marked with an asterisk in Figure 28) displayed the opposite pattern.

The genetic structure was inferred by PCA, ADMIXTURE, and EEMS. PCA showed genetic affinity between individuals from geographically near locations (Figures 29a and 30). The first principal component reflected the genetic difference between the North American

individuals and others, whereas the second principal comportment divided the East Asian individuals from the European and West and Central Asian individuals, which was supported by the result of $K = 2$ and $K = 3$ in ADMIXTURE (Figure 31a, b). In addition, the third and fourth principal components showed the local distinction of the Kazakhstan and Tibetan individuals from others (Figure 29b), which was also shown in PCA based on the modern dataset (Figure 30) and $K = 4$ in ADMIXTURE (Figure 31c). The relative effective migration rate around the area was estimated low by EEMS (Figure 31d).

The phylogenetic trees based on mtDNA, X-chromosomal, autosomal, and Y-chromosomal DNA were constructed to investigate the identity and differentiation between the populations (Figure 32). Compared with the geographic discontinuities observed in mtDNA haplotypes (Davison et al. 2011), the trees based on the nuclear genome reflected affinity between nearby populations, as previously reported by de Jong et al. (2023) and Figure 4. Individuals from Kazakhstan and Western Asia, whose mtDNA haplotypes are minor, tended to exhibit distinctions from others, such as European, North American, and other Asian individuals. Individuals from Tibet were also observed this trend, but they were included within the same lineages as the European, North American, and other Asian individuals. The mtDNA lineages found in West Asia (clade 1_West Asia and clade 3_West Asia) were different from other lineages reported in the previous studies (Davison et al. 2011). Both of them diverged earlier than each related lineages (clade 1 and clade 3). These divergence time were, 253.2 thousand years ago (95%CI: 142.9–373.8 thousand years ago) and 138.6–145.8 (95%CI: 73.7–219.9 thousand years ago), respectively (Figure 33).

PSMC was applied to modern brown bear samples to estimate their population demography, shown per area (Figure 34). The effective population size of individuals from Tibet

was notably different from that of other Central Asian individuals (Figure 34a). Nearly identical trends were observed between the Hokkaido and Etorofu Island individuals (Figure 34b), as well as the West Asian and European individuals (Figure 34c). The size changes in the Far East, Sakhalin, and Hokkaido were similar until about one hundred thousand years ago, but thereafter, the effective population sizes in the Far East and Sakhalin were slightly larger than that in Hokkaido (Figure 34d).

Gene flow with inter- and intra-species

The population splits and mixtures were inferred using TreeMix (Figure 35). The phylogeny optimally estimated based on Δm (Figure 36), revealed a genetic affinity between nearby populations, consistent with the findings from the phylogenetic tree (Figure 33). The results (migration edge = 1, 2) indicate migration from the ABC island population to the polar bear. Additionally, the result (migration edge = 5) shows migration from the polar bear to the Hokkaido and Etorofu Island populations.

To compare the difference between populations in hybridization with related species, f_4(Outgroup, Polar bear; X, Kazakhstan(U13M)) and f_4(Outgroup, Cave bear; X, modern Polar bear), where X means the brown bear individuals, were calculated. The values of f_4(Outgroup, Polar bear; Hokkaido, Kazakhstan(U13M)) shown in Figure 37 and Table 23 were higher next to f_4(Outgroup, Polar bear; North America, Kazakhstan(U13M)) than f_4(Outgroup, Polar bear; East Asia excluded Etorofu Island, Kazakhstan(U13M)). The values of f_4(Outgroup, Polar bear; ancient brown bear, Kazakhstan(U13M)) were higher than those of f_4 values using modern samples from nearby areas as X. These trends were consistent regardless of the individuals used as the polar bear and were also supported when to use the only modern samples dataset (Table

24). The result of f_4(Outgroup, Cave bear; X, modern Polar bear) shows only f_4(American black bear, taxa *kudarensis*; Kazakhstan(U13M), modern Polar bear) and f_4(American black bear, taxa *kudarensis*; West Asia, modern Polar bear) were statistically significant (|Z score| > 3; Figure 38 and Table 25), although f_4(Asiatic black bear, taxa *kudarensis*; Kazakhstan(U13M), modern Polar bear) and f_4(Asiatic black bear, taxa *kudarensis*; West Asia, modern Polar bear) were not. The proportion of each gene flow was estimated by f_4 ratio (Figures 39, 40, Table 26, and 27). The proportion of gene flow from the polar bear or the cave bear to the brown bear was approximately 24.36% and 13.81%, respectively, considering only the values where X represents an individual with a statistically significant f_4 value.

In 49 brown bears, 3 (RF01, SJS01, and SLK1) and 7 (BB020, BB034, BB049, BB059, Den, GRZ, and WB039) individuals were identified as clade 3a1 in Europe and North America, respectively (Figure 27 and Table 21). The value of f_4(Outgroup, clade 3a1 in Europe; X, the modern brown bear excluding X) and f_4(Outgroup, clade 3a1 in North America; X, the modern brown bear excluding X) were calculated to infer the scale of gene flow driven by the recent expansion of mainly a mitochondrial DNA lineage, clade 3a1 (Figures 41 and 42). The Kazakhstan brown bear (only including U13M) has not been affected by the gene flow, compared with other populations (Tukey honestly significant difference test, $P < 0.05$). The West Asian brown bears were also confirmed the same trend only by the values of $f4$(Outgroup, clade 3a1 in North America; X, the modern brown bear excluding X). Both $f4$ statistics supported the influence from the recent gene flow to the Tibetan individuals. The Hokkaido and Etorofu Island populations have not been affected by the gene flow than the Far Eastern Asia population, only including U34 (Tukey honestly significant difference test, $P < 0.05$), whereas no statistically

significant differences between the Hokkaido and Etorofu Island populations and the Sakhalin population (only including AA1) were found.

Species distribution model

To compare the relative habitat suitability of the polar bear with that of the brown bear around Hokkaido (Figure 23), I constructed the species distribution model of the polar bear using Maxent shown in Tables 28 and 29, and Figure 43, projected the model to the surface showing ancient climate (Figure 44). In contrast to the result of the brown bear showing a significant shift in the relative habitat suitability after the LGM, the relative habitat suitability for the polar bear has kept low throughout the hundred thousand years.

Discussion

This study applied population genomic analysis to the brown bear, including nine new genome sequence data from individuals around the Eurasian Continent, to verify the correlation in genetic differences between the mtDNA lineages and the nuclear genome and the contribution of the scale of replacement driven by male-biased dispersal. Genetic differentiation between local populations, particularly around Kazakhstan, Tibet, and West Asia, where the ancient mtDNA lineages were confirmed, was observed. A geographic discontinuity in gene flow from the polar bear was found, with more alleles from the polar bear remaining in the Hokkaido and Etorofu Island populations compared to those of Far Eastern Asia. The results could be attributed to differences in the influence of the recent expansion, primarily driven by males, between the continental and island populations.

Genetic diversity of the brown bear

The genetic diversity of brown bears in Western and Central Asia was relatively higher than others. Although low migration around Western and Central Asia that EEMS showed has restricted gene flow from others and contributed to the significant distinctiveness of the populations from others, especially in Kazakhstan, Tibet, and Western Asia, as shown by genetic structure analysis, the population size around the area was inferred to have kept constantly, remaining the genetic diversity. In contrast, Tumendemberel et al. (2023) reported low heterozygosity of brown bears from Mongolia and Pakistan located near this area, and suggested the conservation necessity. Even with high genetic diversity, comprehensive monitoring research is necessary in Western and Central Asia.

In contrast to the high genetic diversity of West and Central Asian brown bears, that of the Etorofu Island individual was significantly lower than that of the Hokkaido individuals and as low as the Apennine brown bear, which has been recently endangered, although genetic affinity with the Hokkaido, suggested by mtDNA analysis (Hirata et al. 2013), was also found. These results suggest that the Etorofu Island population has experienced a bottleneck after isolation from the Hokkaido population. Some events, such as the founder effect and human activity (Kostenko et al. 2004), could be one of the causes of low genetic diversity. The number of brown bears on each island in the Kuril Archipelago is few, about 60–260 (Kostenko et al. 2004), so conservation plans and further genomic data are needed to monitor the population and evaluate the genetic diversity.

Demographic history of Western and Central Asia

PCA shows a clear difference of the Tibet and Kazakhstan populations from others, and this was also reflected in the phylogenetic tree. Previous studies (Hirata et al. 2013; Lan et al. 2017) reported minor mtDNA haplotypes, clade 5 for Tibet and clade 6 for Himaraya around the area. Ancestral genetic traits from those mtDNA lineages have still remained in this area due to geographical isolation from other populations, which is partially supported by ADMIXTURE in this study and the previous study (de Jong et al. 2023). Compared with the two populations, Tibetan individuals appear to be slightly more distinct from others than the Kazakhstan individual, as indicated by the results of PCA and PSMC that show a distinct population size change from others. By contrast, the result of f_4(Outgroup, clade 3a1 in Europe; X, the modern brown bear excluded X) showed the Tibetan population has been affected by the recent expansion more than the Kazakhstan individual. Thus, the slightly higher genetic differentiation in Tibet individuals may be attributed to a more ancient population demographic history predating the recent expansion. Further analyses are warranted considering the limitations of the current sampling.

PCA, ADMIXTURE, PSMC, and TreeMix indicated that the Western Asian population was relatively similar to the European populations. On the other hand, the phylogeny based on the Y-chromosomal DNA sequence revealed that the Western Asian individuals were diverged earliest among the brown bear lineages examined in this study (Figure 32d): this finding is consistent with de Jong et al. (2023). Additionally, the values of f_4(Outgroup, clade 3a1 in North America; X, the modern brown bear excluding X) did not support the gene flow from the recent expansion. Minor mtDNA haplogroups, which were more closely related to the European lineages and not detected in other areas, were reported in the previous studies (Ashrafzadeh et al. 2016; Hirata et al. 2014; Mizumachi et al. 2020). Consequently, it is inferred that the Western

Asian population diverged from the European population before the recent expansion and has remained isolated from others.

The brown bears in Central Russia (Krasnojarsk and ProvBalakhtinsky District, Russia) were identified as an admixture between other populations (Europe, North America, and Hokkaido populations). Both major mtDNA lineages, clade 3a1, and clade 3b, with clade 3b diverging earlier than clade 3a1, were found around the area (Hirata et al. 2014). In the nearby region, northern Mongolia, Tumendemberel et al. (2023) reported a mtDNA lineage that diverged earlier than clade 3, despite low bootstrap values. Combining these results, the populations around Central Russia have formed by admixture between ancestral and recent expansion populations.

f_4 and f_4 ratios detected hybridization between a cave bear *kudarensis*, and the brown bear in Western Asia and Kazakhstan. The cave bear *kudarensis* are widely distributed on the Eurasian Continent several hundred thousand years ago (Knapp et al. 2009), suggesting that hybridization could have occurred during that period. Barlow et al. (2021) proposed gene flow between the cave bear, excluding the cave bear *kudarensis* and the common ancestor of the European and Western Asian populations. The results of this study may reflect additional gene flow from the cave bear. On the other hand, f_4(Asiatic black bear, Cave bear; X, modern Polar bear) values were not statistically significant. Gene flow between the American black bear, the brown bear, and the polar bear was estimated by *D* statistics (Kumar et al. 2017). This gene flow could be a cause of the statistical significance of f_4(American black bear, Cave bear; X, modern Polar bear) because the value of f_4(W, X; Y, Z) statistics also become negative significantly in case of gene flow between W and Z. Although whether f_4 values when other bears were set as an

outgroup were statistically significant or not is a matter of, alleles from hybridization with the cave bear might have persisted, especially in these populations.

Demographic history of Etorofu Island and Hokkaido

PSMC analysis revealed a difference in population size between the islands (Hokkaido and Etorofu Island) and the mainland (Sakhalin and the Far East) from approximately 100,000 years ago, indicating a potential influence of the recent expansion scale. f_4 statistics estimated that the Far East individual shares more alleles from the recent divergent lineage, the 3a1 lineage, than other East Asia and Hokkaido individuals, while no statistical difference was observed between the Sakhalin and Hokkaido populations. The findings suggest that the ancestor of the Far Eastern individual was most affected by the recent dispersal, whereas the ancestor of the Sakhalin individual originated from admixture between recent dispersal individuals and those from Hokkaido.

TreeMix (migration edges = 5) and f_4 statistics confirmed more hybridization between the polar bear and the brown bear in Hokkaido and Etorofu Island than in other Eastern Asian areas, partially aligning with findings by de Jong et al. (2023) shows gene flow between the Hokkaido population and the polar bear. Previous studies (Cahill et al. 2013, 2015) identified that the North American population, particularly individuals around the ABC islands, harbors the most alleles from the polar bear among brown bear populations. These imply geographically discontinuous gene flow from the polar bear. Two scenarios regarding this discontinuity are considered: *i*) gene flow by recent expansion, replacing major alleles in the population on the Eurasian Continent, as suggested by de Jong et al. (2023), and *ii*) gene flow from the polar bear only to the Hokkaido and Etorofu Island populations. The results of PSMC and f_4(Outgroup,

clade 3a1 in Europe; X, the modern brown bear excluding X) in this study suggest that scenario *i*) is more likely because these results reflected that the Hokkaido and Etorofu Island populations have been affected by the recent expansion very little. In addition, the relative habitat suitability of the polar bear around Hokkaido, estimated by Maxent, has been low. Additionally, ancient brown bears tended to share more alleles from the polar bear than modern brown bears distributed near their collected places, also supported by Cahill et al. (2018). Thus, it is more likely that the ancestor of the brown bear possessed more alleles from the polar bear than modern brown bears, and the recent expansion replaced these alleles with the alleles observed today.

The multi-layered genetic structure could explain the process of formation of the discrepancy between the phylogenic trees.

de Jong et al. (2023) inferred the incomplete lineage sorting of mtDNA based on the multiple coalescent analysis, which shows individuals classified with different mtDNA lineages from the same populations coalesce more frequently than individuals classified in the same mtDNA lineage from different populations. This suggestion was also supported by the part of the result about the discrepancy between phylogenetic trees based on mtDNA and nuclear genome in this study (Figure 32). However, this study also emphasized local genetic differentiation, especially in Kazakhstan, Tibet, and West Asia, reflected in the contemporary genetic structure, population demography, and gene flow from related species. These populations do not include a clade 3a1 that diverged recently but mtDNA lineages that diverged before clade 3a1. Thus, the local genetic differentiation could be from the genetic characteristics of the ancestral populations and relate to the difference of mtDNA lineages with the deep divergence time. In this context, incomplete lineage sorting alone could not fully explain the observed difference in phylogenetic trees between

mtDNA and nuclear genome.

de Jong et al. (2023) proposed that gene flow driven by recent dispersal can rapidly erase genomic evidence of former population structure from simulations. Combining the result and the geographic discontinuity in the gene flow from the polar bear, they discussed that the isolated populations from the continent (e.g., Hokkaido and ABC islands) preserve polar bear genetic material. This trend was also applied to the individuals from the Etorofu island near Hokkaido. The results of f_4(Outgroup, clade 3a1; X, the modern brown bear excluding X) suggested that this pattern has been formed by the scale of the recent male-biased dispersal. In addition, the f_4 statistics also showed that the individual from Kazakhstan has fewer alleles from the recent divergent lineage than others and more alleles from the cave bear. It means that some populations even on the Eurasia continent, could have retained the ancestral genetic traits. Thus, the impact of the recent expansion driven by male-biased is heterogeneous and different by the populations.

Based on these findings, the multi-layered genetic structure of the brown bear genome (Figure 45), which is both the retention of ancestral genetic traits (Figure 45a) and the replacement of these traits with new ones due to the recent expansion by male-biased dispersal (Figure 45b) is, reflected in the contemporary genetic structure (Figure 45c), is plausible to explain the incongruences between the phylogenic trees of mtDNA and the nuclear genome for the brown bear. This genetic structure's idea is same as that of the human. The genetic structure of humans is composed of multi-genetic traits from multiple migrations at different times (e.g., Tassi et al. 2015). For example, the current Japanese population consists of two main genetic layers from Jomon hunter-gatherers and rice-farming Yayoi migrants and more genetic layers from different migrations by genome-wide genetic data (Osada & Kawai 2021). While the genetic structure of other species, like *Rattus rattus* (Puckett et al. 2020), is inferred to

incorporate such multi-layers reflecting population demography at different times, the presence of multi-layers in the genetic structure of species other than humans remains largely unknown due to the lack of worldwide genome-wide data. This study successfully addressed this challenge by concentrating on the brown bear, a species that reported abundant genome data from various sampling locations worldwide at different times and well-documented local genetic variations.

The reason causing the difference in the influence of the recent expansion driven by male-biased dispersal could have arisen primarily due to climate changes. For example, climate change lets sea-level fluctuations leading to the land bridges, and the glacial ice covering the land. These environmental changes facilitated migration to new environments while occasionally imposing restrictions. As demonstrated in the demographic history outlined in Chapter 3, it makes the effective population size contraction. The diverse environmental factors in each area underscore the significance of directing attention to local demographic history.

While this study revealed the variation in brown bear populations, it is necessary to note that not all brown bear populations were involved for the study. For example, individuals from the northern part of Russia, Kunashiri Island, and around the border between East Russia and China were not included due to a lack of samples. Such sampling biases, referred to as Wallacean shortfall, have the potential to overlook genetic diversity and pose challenges in assessing future extinction risks (Lomolino et al. 2016). Additionally, this study and other studies (Cahill et al. 2018; Segawa et al. 2024) showed the genetic differentiation between precent and ancient populations, providing valuable insights into the evolution of the brown bear. Integrating genomic data from individuals across various distribution areas and time periods would offer a more comprehensive understanding of the evolutionary processes and contribute to the conservation of these genetic diversity.

Chapter 5. General discussion

This dissertation concentrated on the population demography of the brown bear (Figure 1) in each chapter to assess the long-term effect of sex-biased dispersal on population demography. Chapter 2 specifically focuses on the Hokkaido population, utilizing whole-genome resequencing and population genetic analysis to investigate its genetic characteristics. The very slight differences based on different mtDNA lineages suggest admixture and genetic homogenization driven by male-biased dispersal. Chapter 3 evaluated the long-term effect of male-biased dispersal and environmental factors on the colonization of the Hokkaido population, employing ddRAD-seq. Male-biased dispersal was found to have played a role in the rapid population formation after a contraction due to low habitat suitability caused by climate changes. Chapter 4 focuses on verifying local genetic variation in brown bear populations in and around the Eurasian Continent (Hokkaido, Etorofu Island, Sakhalin, Far East area, Kazakhstan, Tibet, Central Russia, and the Caucasus) through whole-genome resequencing. Both the influence of recent expansion caused by male-biased dispersal and the ancestral genetic diversity reflected in the brown bear nuclear genome shaped the local genetic variation of brown bear populations. Based on the data, this dissertation shows the population demographic history of the brown bear (Figure 46) and the significant influence of male-biased dispersal in it.

Comparison with the previous studies

Such a clear mismatch pattern of the genetic structure between maternal inheritance (e.g., mtDNA) and paternal inheritance (e.g. Y-chromosomal DNA) is reported rarely in other studies focusing on different species, despite sex-biased dispersal being a phenomenon observed in

various species, from plants (Ghazoul 2005) to vertebrates (Trochet et al. 2016). In the case of the brown bear, the replaced alleles driven by male-biased dispersal are widespread, leading to significant admixture with the ancestral population, genetic homogenization, and inconsistencies in the phylogeny between mtDNA and the nuclear genome. On the contrary, previous studies focusing on fishers (Tucker et al. 2017), gibbons (Matsudaira et al. 2018), chimpanzees (Mitchell et al. 2018), humans (Seielstad et al. 1998), and dolphins (Andrews et al. 2013) did not reveal such a clear and significant mismatch on a wide scale. This difference is attributed to limitations in sampling across wide areas, variations in the number of variants and loci used in different inheritable regions, and other factors such as the social systems influencing the result. The reason for observing the clear mismatch of the genetic structure would solve these problems by focusing on the brown bear, which is discussed below in detail.

Long-term effect of the sex-biased dispersal

In this dissertation, I identified the significant contribution of male-biased dispersal in *i)* migration into new habitats, *ii)* rapid colonization, and *iii)* formation pattern of intra- and inter-species hybridization, resulting in the mismatch of genetic structure patterns between mtDNA and the Y-chromosomal DNA.

Using and comparing with different inheritance DNA regions made it possible to accurately detect the long-term effect of male-biased dispersal in gene flow over multiple generations. Utilizing tens of thousands of SNP data with bisexual inheritance. This dissertation was able to detect subtle differentiation in male-biased dispersal within and between bear populations, which was not evident when relying solely on haplotype data, such as only mitochondrial DNA and the Y-chromosomal DNA, although this dissertation also partially agrees with the previous studies,

such as local genetic diversity in the part on the Eurasian Continent (see Chapter 4).

Focusing on the brown bear allows for a practical evaluation of male-biased dispersal. In the case of other animals, the influence of other factors, such as the social systems, must be considered. The research for the plants is also challenging because most of them do not disperse widely by themselves. Compared with the case of other species, the brown bear could be evaluated only with male-biased dispersal because it moves randomly by itself regardless of the society of the brown bear. By addressing multiple challenges in evaluating sex-biased dispersal, this dissertation significantly contributes to understanding the process of population formation influenced by environmental factors and the long-term effect of sex-biased dispersal.

The influence of the global climate change dynamics

In the population demographic history of the brown bear, not only the sex-biased dispersal but also the environmental factors, especially climate changes, have a significant influence because those are pivotal factors in determining whether the individuals can move. For instance, Chapter 3 shows the reduction of the relatively suitable habitat for brown bears during the LGM, when the contraction of the effective population size also occurred. In fact, climate changes have led to species extinction, shifts in habitat, or adaptations to new environments (Davis & Shaw 2001; de Lafontaine et al. 2018; Hewitt 2000).

Previous phylogeographic studies focusing on the Japanese archipelago tended to discuss the demographic history with land bridge connecting the mainland (Dobson 1994; Dobson & Kawamura 1998; Mckay 2012; Millien-Parra & Jaeger 1999), but other environmental factors are also important, as shown in Chapter 3. Especially, climate change is crucial. Iwase et al. (2012) suggested that the extinction of megafauna on the Japanese archipelago in the late Pleistocene were

changes in the ecosystem driven by climatic changes based on fossil recodes. In the case of the brown bear, the dramatic feeding habit shift from carnivorousness to herbivorousness at this time was inferred based on stable isotope ratio analysis (Rey-Iglesia et al. 2019; Segawa et al. 2021), so climate changes could have affected the brown bear population considerably. Thus, verification and discussion combined with multiple environmental factors such as landform dynamics and climate changes are important to clarify the process of the brown bear's evolution.

Future issue

While climate change is a crucial factor in the population demographic history of the brown bear, potentially driving shifts in feeding habits, this dissertation was not able to investigate the genetic basis relating to adaptation to climate changes. In Chapter 4, it was revealed that the Honshu brown bear reported by Segawa et al. (2021), which went extinct approximately 17,000 years ago (Takakuwa et al. 2007), had more alleles by the gene flow from the polar bear than the current individuals. The significant rapid increase in temperature on a global scale occurred from the LGM to the Holocene when the Honshu brown bears went extinct (Osman et al. 2022), so the difference in allele frequency may be one of the reasons for the extinction of the brown bear in Honshu, as it struggled to adapt to climate changes.

The genome analysis proves to be an effective and versatile method for understanding population demographic history. For example, comparing allele frequencies between past and current populations using ancient genomic analysis allows the detection of dramatic changes in allele frequencies associated with local adaptation (e.g., Kirch et al. 2021). These further analyses might explore evidence of selection and elucidate the relationship between climate changes and local adaptation.

Reference

Alexander DH, Novembre J, Lange K. 2009. Fast model-based estimation of ancestry in unrelated individuals. *Genome Research*. 19: 1655–1664.

Andrello M, D'aloia C, Dalongeville A, Escalante MA, Guerrero J, Perrier C, Torres-Florez JP, Xuereb A, Manel S. 2022. Evolving spatial conservation prioritization with intraspecific genetic data. *Trends in Ecology & Evolution*. 37: 553–564.

Andrews KR, Perrin WF, Oremus M, Karczmarski L, Bowen BW, Puritz JB, Toonen RJ. 2013. The evolving male: Spinner dolphin (*Stenella longirostris*) ecotypes are divergent at Y chromosome but not mtDNA or autosomal markers. *Molecular Ecology*. 22: 2408–2423.

Ashrafzadeh MR, Kaboli M, Naghavi MR. 2016. Mitochondrial DNA analysis of Iranian brown bears (*Ursus arctos*) reveals new phylogeographic lineage. *Mammalian Biology*. 81: 1–9.

Babraham Bioinformatics. 2011. FastQC: a quality control tool for high throughput sequence data. Available from: https://www.bioinformatics.babraham.ac.uk/projects/fastqc/. last accessed 3 November, 2023.

Balkenhol N, Waits LP, Dezzani RJ. 2009. Statistical approaches in landscape genetics: An evaluation of methods for linking landscape and genetic data. *Ecography*. 32: 818–830.

Barido-Sottani J, et al. 2018. Taming the BEAST—A community teaching material resource for BEAST 2. *Systematic biology*. 67: 170–174.

Barlow A, et al. 2018. Partial genomic survival of cave bears in living brown bears. *Nature Ecology & Evolution*. 2: 1563–1570.

Barlow A, et al. 2021. Middle Pleistocene genome calibrates a revised evolutionary history of extinct cave bears. *Current Biology*. 31: 1771–1779.

Barnes I, Matheus P, Shapiro B, Jensen D, Cooper A. 2002. Dynamics of Pleistocene population

extinctions in Beringian brown bears. *Science*. 295: 2267–2270.

Benazzo A, et al. 2017. Survival and divergence in a small group: the extraordinary genomic history of the endangered Apennine brown bear stragglers. *Proceedings of the National Academy of Sciences*. 114: 9589–9597.

Bidon T, Janke A, Fain SR, Eiken HG, Hagen SB, Saarma U, Hallström BM, Lecomte N, Hailer F. 2014. Brown and polar bear Y chromosomes reveal extensive male-biased gene flow within brother lineages. *Molecular Biology and Evolution*. 31: 1353–1363.

Bolger AM, Lohse M, Usadel B. 2014. Trimmomatic: a flexible trimmer for Illumina sequence data. *Bioinformatics*. 30: 2114–2120.

Bon C, Berthonaud V, Maksud F, Labadie K, Poulain J, Artiguenave F, Wincker P, Aury JM, and Elalouf JM. 2012. Coprolites as a source of information on the genome and diet of the cave hyena. *Proceedings of the Royal Society B: Biological Sciences*. 279: 2825–2830.

Booth TH, Nix HA, Busby JR, Hutchinson MF. 2014. bioclim: The first species distribution modelling package, its early applications and relevance to most current MaxEnt studies. *Diversity and Distributions*. 20: 1–9.

Bossart JL, Pashley Prowell D. 1998. Genetic estimates of population structure and gene flow: Limitations, lessons and new directions. *Trends in Ecology and Evolution*. 13: 202–206.

Bourgeois YXC, Bertrand JAM, Delahaie B, Holota H, Thébaud C, Milá B. 2020. Differential divergence in autosomes and sex chromosomes is associated with intra-island diversification at a very small spatial scale in a songbird lineage. *Molecular Ecology*. 29: 1137–1153.

Brown JL, Hill DJ, Dolan AM, Carnaval AC, Haywood AM. 2018. PaleoClim, high spatial resolution paleoclimate surfaces for global land areas. *Scientific Data*. 5: Article 1.

Cahill JA, et al. 2013. Genomic evidence for island population conversion resolves conflicting

theories of polar bear evolution. *PLoS Genetics*. 9: e1003345.

Cahill JA, Stirling I, Kistler L, Salamzade R, Ersmark E, Fulton TL, Stiller M, Green RE, Shapiro B. 2015. Genomic evidence of geographically widespread effect of gene flow from polar bears into brown bears. *Molecular Ecology*. 24: 1205–1217.

Cahill JA, et al. 2018. Genomic evidence of widespread admixture from polar bears into brown bears during the last ice age. *Molecular Biology and Evolution*. 35: 1120–1129.

Catchen J, Hohenlohe PA, Bassham S, Amores A, Cresko WA. 2013. Stacks: An analysis tool set for population genomics. *Molecular Ecology*. 22: 3124–3140.

Chen ZH, Zhang M, Lv FH, Ren X, Li WR, Liu MJ, Nam K, Bruford MW, Li MH. 2018. Contrasting patterns of genomic diversity reveal accelerated genetic drift but reduced directional selection on X-chromosome in wild and domestic sheep species. *Genome Biology and Evolution*. 10: 1282–1297.

Coia V, et al. 2013. Demographic histories, isolation and social factors as determinants of the genetic structure of Alpine linguistic groups. *PLoS ONE*. 8: e81704.

Colangelo P, Loy A, Huber D, Gomerčić T, Taglianti AV, Ciucci P. 2012. Cranial distinctiveness in the Apennine brown bear: genetic drift effect or ecophenotypic adaptation? *Biological Journal of the Linnean Society*. 107: 15–26.

Cronin MA, Amstrup SC, Talbot SL, Sage GK, Amstrup KS. 2009. Genetic variation, relatedness, and effective population size of polar bears (*Ursus maritimus*) in the southern Beaufort sea, Alaska. *Journal of Heredity*. 100: 681–690.

Cushman SA, McKelvey KS, Hayden J, Schwartz MK. 2006. Gene flow in complex landscapes: Testing multiple hypotheses with causal modeling. *The American Naturalist*. 168: 486–499.

Dabney J, et al. 2013 Complete mitochondrial genome sequence of a Middle Pleistocene cave bear reconstructed from ultrashort DNA fragments. *Proceedings of the National Academy of Sciences*. 110: 15758–15763.

Danecek P, et al. 2011. The variant call format and VCFtools. *Bioinformatics*. 27: 2156–2158.

Danecek P, et al. 2021. Twelve years of SAMtools and BCFtools. *Gigascience*. 10: giab008.

Davis MB, Shaw RG. 2001. Range Shifts and Adaptive Responses to Quaternary Climate Change. *Science*. 292: 673–679.

Davison J, et al. 2011. Late-Quaternary biogeographic scenarios for the brown bear (*Ursus arctos*), a wild mammal model species. *Quaternary Science Reviews*. 30: 418–430.

da Silva Coelho FA, et al. 2023. Ancient bears provide insights into Pleistocene ice age refugia in Southeast Alaska. *Molecular Ecology*. 32: 3641–3656.

de Jong MJ, et al. 2023. Range-wide whole-genome resequencing of the brown bear reveals drivers of intraspecies divergence. *Communications Biology*. 6: Article 1.

de Lafontaine G, Napier JD, Petit RJ, Hu FS. 2018. Invoking adaptation to decipher the genetic legacy of past climate change. *Ecology*. 99: 1530–1546.

de Oliveira ME, Saranholi BH, Dirzo R, Galetti Jr PM. 2022. A review of philopatry and dispersal in felids living in an anthropised world. *Mammal Review*. 52: 208–220.

Dobson M. 1994. Patterns of distribution in Japanese land mammals. *Mammal Review*. 24: 91–111.

Dobson M, Kawamura Y. 1998. Origin of the Japanese land mammal fauna: allocation of extant species to historically-based categories. *The Quaternary Research (Daiyonki-Kenkyu)*. 37: 385–395.

Edgar RC. 2004. MUSCLE: Multiple sequence alignment with high accuracy and high

throughput. *Nucleic Acids Research*. 32: 1792–1797.

Edwards CJ, et al. 2011. Ancient hybridization and an Irish origin for the modern polar bear matriline. *Current biology*, 21: 1251–1258.

Endo Y, Osada N, Mano T, Masuda R. 2021. Demographic history of the brown bear (*Ursus arctos*) on Hokkaido Island, Japan, based on whole-genomic sequence analysis. *Genome Biology and Evolution*. 13: evab195.

Excoffier L, Marchi N, Marques DA, Matthey-Doret R, Gouy A, Sousa VC. 2021. fastsimcoal2: Demographic inference under complex evolutionary scenarios. *Bioinformatics*. 37: 4882–4885.

Feng S, et al. 2022. Incomplete lineage sorting and phenotypic evolution in marsupials. *Cell*. 185: 1646–1660.e18.

Fitak RR. 2021. OptM: estimating the optimal number of migration edges on population trees using TreeMix. *Biology Methods and Protocols*. 6: bpab017.

Fordham DA, Saltré F, Haythorne S, Wigley TML, Otto-Bliesner BL, Chan KC, Brook BW. 2017. PaleoView: A tool for generating continuous climate projections spanning the last 21 000 years at regional and global scales. *Ecography*. 40: 1348–1358.

Frankham R, Ballou J, Briscoe D. 2010. Introduction to Conservation Genetics: Second Edition. New York, USA: Cambridge University Press.

Fu J, Wen L. 2023. Impacts of Quaternary glaciation, geological history and geography on animal species history in continental East Asia: A phylogeographic review. *Molecular Ecology*. 32: 4497–4514.

Gaughran SJ, vonHoldt B. 2022. Pleistocene parades of carnivores into North America. *Molecular Ecology*. 31: 6387–6389.

Gent PR, et al. 2011. The community climate system model version 4. *Journal of Climate*. 24: 4973–4991.

Ghazoul J. 2005. Pollen and seed dispersal among dispersed plants. *Biological Reviews*. 80: 413–443.

Goda N, Mano T, Masuda R. 2009. Genetic diversity of the MHC class-II DQA gene in brown bears (*Ursus arctos*) on Hokkaido, northern Japan. *Zoological science*. 26: 530–535.

Green RE, et al. 2010. A draft sequence of the Neandertal genome. *Science*. 328: 710-722.

Greenwood PJ. 1980. Mating systems, philopatry and dispersal in birds and mammals. *Animal Behaviour*. 28: 1140–1162.

Hailer F, Kutschera VE, Hallström BM, Klassert D, Fain SR, Leonard JA, Ulfur A, Janke A. 2012. Nuclear genomic sequences reveal that polar bears are an old and distinct bear lineage. *Science*. 336: 344–347.

Hewitt G. 2000. The genetic legacy of the Quaternary ice ages. *Nature*. 405: Article 6789.

Hijmans RJ, Cameron SE, Parra JL, Jones PG, Jarvis A. 2005. Very high resolution interpolated climate surfaces for global land areas. *International Journal of Climatology*. 25: 1965–1978.

Hirata D, Mano T, Abramov AV, Baryshnikov GF, Kosintsev PA, Vorobiev AA, Raichev GV, Tsunoda H, Kaneko Y, Murata K, et al. 2013. Molecular phylogeography of the brown bear (*Ursus arctos*) in northeastern Asia based on analyses of complete mitochondrial DNA sequences. *Molecular biology and Evolution*. 30: 1644–1652.

Hirata D, Abramov AV, Baryshnikov GF, Masuda R. 2014. Mitochondrial DNA haplogrouping of the brown bear, *Ursus arctos* (Carnivora: Ursidae) in Asia, based on a newly developed APLP analysis. *Biological Journal of the Linnean Society*. 111: 627–635.

Hirata D, Mano T, Abramov AV, Baryshnikov GF, Kosintsev PA, Murata K, Masuda R. 2017.

Paternal phylogeographic structure of the brown bear (*Ursus arctos*) in northeastern Asia and the effect of male-mediated gene flow to insular populations. *Zoological Letters*. 3: 1–13.

Hokkaido. 2017. The 1st Brown Bear Management Plan on Hokkaido. Hokkaido, Japan: Hokkaido. (in Japanese)

Hokkaido. 2022. The 2nd Brown Bear Management Plan on Hokkaido. Hokkaido, Japan: Hokkaido. (in Japanese)

Holekamp KE, Sawdy MA. 2019. The evolution of matrilineal social systems in fissiped carnivores. *Philosophical Transactions of the Royal Society B: Biological Sciences*. 374: 20180065.

Hudson RR, Slatkin M, Maddison WP. 1992. Estimation of levels of gene flow from DNA sequence data. *Genetics*. 132: 583–589.

Igarashi Y. 2016. Vegetation and climate during the LGM and the last deglaciation on Hokkaido and Sakhalin Islands in the northwest Pacific. *Quaternary International*. 425: 28–37.

Ikeda Y, Motokawa M. 2021. Phylogeography of the Japanese greater horseshoe bat *Rhinolophus nippon* (Mammalia: Chiroptera) in Northeast Asia: New insight into the monophyly of the Japanese populations. *Ecology and Evolution*. 11: 18181–18195.

Ishii Y, Hori K. 2016. Formation and infilling of oxbow lakes in the Ishikari lowland, northern Japan. *Quaternary International*. 397: 136–146.

Ito T, et al. 2021. Phylogeographic history of Japanese macaques. *Journal of Biogeography*. 48: 1420–1431.

Itoh T, Sato Y, Kobayashi K, Mano T, Iwata R. 2012. Effective dispersal of brown bears (*Ursus arctos*) in eastern Hokkaido, inferred from analyses of mitochondrial DNA and

microsatellites. *Mammal Study*. 37: 29–41.

Iwase A, Hashizume J, Izuho M, Takahashi K, Sato H. 2012. Timing of megafaunal extinction in the late Late Pleistocene on the Japanese Archipelago. *Quaternary International*. 255: 114–124.

Japan Bear Network. 2006. Understanding Asian Bears to Secure Their Future. Ibaraki, Japan: Japan Bear Network.

K-1 model developers. 2004. K-1CoupledGCM(MIROC) Description. Center for Climate System Research (Univ. of Tokyo), National Institute for Environmental Studies, and Frontier Research Center for Global Change. http://www.ccsr.u-tokyo.ac.jp/kyosei/hasumi/MIROC/tech-repo.pdf last accessed 3 November, 2023.

Kambayashi, C, et al. 2022. Geography-dependent horizontal gene transfer from vertebrate predators to their prey. *Molecular Biology and Evolution*. 39: msac052.

Karger DN, Conrad O, Böhner J, Kawohl T, Kreft H, Soria-Auza RW, Zimmermann NE, Linder HP, Kessler M. 2017. Climatologies at high resolution for the earth's land surface areas. *Scientific Data*. 4: Article 1.

Karger DN, Nobis MP, Normand S, Graham CH, Zimmermann NE. 2023. CHELSA-TraCE21k – high-resolution (1 km) downscaled transient temperature and precipitation data since the Last Glacial Maximum. *Climate of the Past*. 19: 439–456.

Keinan A, Mullikin JC, Patterson N, Reich D. 2007. Measurement of the human allele frequency spectrum demonstrates greater genetic drift in East Asians than in Europeans. *Nature genetics*. 39:1251–1255.

Keinan A, Mullikin JC, Patterson N, Reich D. 2009. Accelerated genetic drift on chromosome X during the human dispersal out of Africa. *Nature Genetics*. 41: 66–70.

Kirch M, Romundset A, Gilbert MTP, Jones FC, Foote AD. 2021. Ancient and modern stickleback genomes reveal the demographic constraints on adaptation. *Current Biology*. 31: 2027–2036.

Knapp M, et al. 2009. First DNA sequences from Asian cave bear fossils reveal deep divergences and complex phylogeographic patterns. *Molecular Ecology*. 18: 1225–1238.

Kopatz A, Eiken HG, Aspi J, Kojola I, Tobiassen C, Tirronen KF, Danilov PI, Hagen SB. 2014. Admixture and gene flow from Russia in the recovering Northern European brown bear (*Ursus arctos*). *PLoS One*. 9: e97558.

Kosintsev PA, Bocherens H, Kirillova IV, Levchenko VA, Zazovskaya EP, Trofimova SS, Lan T, Lindqvist C. 2022. Palaeoecological and genetic analyses of Late Pleistocene bears in Asiatic Russia. *Boreas*. 51: 465–480.

Kostenko VA, Nesterenko VA, Trukhin AM. 2004. Mammals of the Kuril Archipelago. Vladivostok, Russia: Dalnauka. (in Russia)

Krause J et al. 2008 Mitochondrial genomes reveal an explosive radiation of extinct and extant bears near the Miocene–Pliocene boundary. *BMC Evolutionary Biology*. 8: 220.

Kuijper B, Johnstone RA. 2017. How sex-biased dispersal affects sexual conflict over care. *The American Naturalist*. 189: 501–514.

Kumar S, Stecher G, Li M, Knyaz C, Tamura K. 2018. MEGA X: molecular evolutionary genetics analysis across computing platforms. *Molecular Biology and Evolution*. 35: 1547–1549.

Kumar V, Lammers F, Bidon T, Pfenninger M, Kolter L, Nilsson MA, Janke A. 2017. The evolutionary history of bears is characterized by gene flow across species. *Scientific Reports*. 7: 1–10.

Kutschera VE, Bidon T, Hailer F, Rodi JL, Fain SR, Janke A. 2014. Bears in a forest of gene trees: Phylogenetic inference is complicated by incomplete lineage sorting and gene flow. *Molecular Biology and Evolution*. 31: 2004–2017.

Lan T, Gill S, Bellemain E, Bischof R, Nawaz MA, Lindqvist C. 2017. Evolutionary history of enigmatic bears in the Tibetan plateau–Himalaya region and the identity of the yeti. *Proceedings of the Royal Society B: Biological Sciences*. 284.

Lan T, et al. 2022. Insights into bear evolution from a Pleistocene polar bear genome. *Proceedings of the National Academy of Sciences*. 119.

Langmead B, Salzberg SL. 2012. Fast gapped-read alignment with Bowtie 2. *Nature Methods*. 9: Article 4.

Lawson Handley LJ, Perrin N. 2007. Advances in our understanding of mammalian sex-biased dispersal. *Molecular Ecology*. 16: 1559–1578.

Lemaître JF, et al. 2020. Sex differences in adult lifespan and aging rates of mortality across wild mammals. *Proceedings of the National Academy of Sciences*. 117: 8546–8553.

Leonard JA, Wayne RK, Cooper A. 2000. Population genetics of Ice Age brown bears. *Proceedings of the National Academy of Sciences*. 97: 1651–1654.

Li H, Durbin R. 2009. Fast and accurate short read alignment with Burrows-Wheeler transform. *Bioinformatics*. 25: 1754–1760.

Li H, Handsaker B, Wysoker A, Fennell T, Ruan J, Homer N, Marth G, Abecasis G, Durbin R. 2009. The sequence alignment/map format and SAMtools. *Bioinformatics*. 25: 2078–2079.

Li H, Durbin R. 2011. Inference of human population history from individual whole-genome sequences. *Nature*. 475: 493–496.

Li XY, Kokko H. 2019. Sex-biased dispersal: A review of the theory. *Biological Reviews*. 94:

721–736.

Liepert BG, Lo F. 2013. CMIP5 update of 'Inter-model variability and biases of the global water cycle in CMIP3 coupled climate models.' *Environmental Research Letters*. 8: 029401.

Lindqvist C et al. 2010 Complete mitochondrial genome of a Pleistocene jawbone unveils the origin of polar bear. *Proceedings of the National Academy of Sciences*. 107: 5053–5057.

Liu S, et al. 2014. Population genomics reveal recent speciation and rapid evolutionary adaptation in polar bears. *Cell*. 157: 785–794.

Lomolino MV, Riddle BR, Whittaker RJ. Biogeography. 5th ed. 2016. Sunderland: Sinauer Associates, Inc.

Luna-Aranguré C, Soberón J, Vázquez-Domínguez E. 2020. A tale of four bears: Environmental signal on the phylogeographical patterns within the extant *Ursus* species. *Journal of Biogeography*. 47: 472–486.

Malinsky M, Trucchi E, Lawson DJ, Falush D. 2018. RADpainter and fineRADstructure: population inference from RADseq data. *Molecular Biology and Evolution*. 35: 1284–1290.

Mantel N. 1967. The detection of disease clustering and a generalized regression approach. *Cancer Research*. 27: 209–220.

Mathieson I, et al. 2015. Genome-wide patterns of selection in 230 ancient Eurasians. *Nature*. 528: 499-503.

Matsudaira K, Ishida T, Malaivijitnond S, Reichard UH. 2018. Short dispersal distance of males in a wild white-handed gibbon (*Hylobates lar*) population. *American Journal of Physical Anthropology*. 167: 61–71.

Matsuhashi T, Masuda R, Mano T, Yoshida MC. 1999. Microevolution of the mitochondrial DNA control region in the Japanese brown bear (*Ursus arctos*) population. *Molecular*

Biology and Evolution. 16: 676–684.

Matsuhashi T, Masuda R, Mano T, Murata K, Aiurzaniin A. 2001. Phylogenetic relationships among worldwide populations of the brown bear *Ursus arctos*. *Zoological Science*. 18: 1137–1143.

Matthews TJ, Triantis K. 2021. Island biogeography. *Current Biology*. 31: R1201–R1207.

Mckay BD. 2012. A new timeframe for the diversification of Japan's mammals. *Journal of Biogeography*. 39: 1134–1143.

McKenna A, et al. 2010. The Genome Analysis Toolkit: a MapReduce framework for analyzing next-generation DNA sequencing data. *Genome Research*. 20: 1297–1303.

McLellan BN, Hovey FW. 2001. Natal dispersal of grizzly bears. *Canadian Journal of Zoology*. 79: 838–844.

McLellan BN, Proctor MF, Huber D, Michel S. 2017. *Ursus arctos* (amended version of 2017 assessment). The IUCN Red List of Threatened Species 2017. Version 2016.2.

McPherson FJ, Chenoweth PJ. 2012. Mammalian sexual dimorphism. *Animal Reproduction Science*. 131: 109–122.

Meirmans G. 2012. The trouble with isolation by distance. *Molecular Ecology*. 21: 2839–2846.

Miller W, et al. 2012. Polar and brown bear genomes reveal ancient admixture and demographic footprints of past climate change. *Proceedings of the National Academy of Sciences*. 109: 2382–2390.

Millien-Parra V, Jaeger JJ. 1999. Island biogeography of the Japanese terrestrial mammal assemblages: An example of a relict fauna. *Journal of Biogeography*. 26: 959–972.

Ministry of the Environment. 2020. Red List 2020 of Ministry of the Environment, Government of Japan. https://www.env.go.jp/press/107905.html. last accessed 3 November, 2023. (in

Japanese)

Mitchell MW, Locatelli S, Abwe EE, Ghobrial L, Gonder MK. 2018. Male-driven differences in chimpanzee (*Pan troglodytes*) population genetic structure across three habitats in Cameroon and Nigeria. *International Journal of Primatology*. 39: 581–601.

Mizumachi K, Spassov N, Kostov D, Raichev EG, Peeva S, Hirata D, Nishita Y, Kaneko Y, Masuda R. 2020. Mitochondrial haplogrouping of the ancient brown bears (*Ursus arctos*) in Bulgaria, revealed by the APLP method. *Mammal Research*. 65: 413–421.

Mizumachi K, Gorbunov SV, Vasilevski AA, Amano T, Ono H, Kosintsev PA, Hirata D, Nishita Y, Masuda R. 2021. Phylogenetic relationships of ancient brown bears (*Ursus arctos*) on Sakhalin Island, revealed by APLP and PCR-direct sequencing analyses of mitochondrial DNA. *Mammal Research*. 66: 95–102.

Molodtseva AS, et al. 2022. Phylogeography of ancient and modern brown bears from eastern Eurasia. *Biological Journal of the Linnean Society*. 135: 722–733.

Muscarella R, Galante PJ, Soley-Guardia M, Boria RA, Kass JM, Uriarte M, Anderson RP. 2014. ENMeval: An R package for conducting spatially independent evaluations and estimating optimal model complexity for Maxent ecological niche models. *Methods in Ecology and Evolution*. 5: 1198–1205.

Musharoff S, Shringarpure S, Bustamante CD, Ramachandran S. 2019. The inference of sex-biased human demography from whole-genome data. *PLoS Genetics*. 15: e1008293.

Nielsen ES, Hanson JO, Carvalho SB, Beger M, Henriques R, Kershaw F, Von der Heyden S. 2022. Molecular ecology meets systematic conservation planning. *Trends in Ecology & Evolution*. 38: 143–155.

Novembre J, et al. 2008. Genes mirror geography within Europe. *Nature*. 456: 98-101.

Ohdachi S, Aoi T. 1987. Food habits of brown bears in Hokkaido, Japan. *Bears: Their Biology and Management*. 7: 215.

Ohdachi S, Aoi T, Manot T, Tsubotat T. 1992. Growth, sexual dimorphism, and geographical variation of skull dimensions of the brown bear *Ursus arctos* in Hokkaido. *Journal of the Mammalogical Society of Japan*. 17: 27–47.

Ohnishi N, Uno R, Ishibashi Y, Tamate HB, Oi T. 2009. The influence of climatic oscillations during the Quaternary Era on the genetic structure of Asian black bears in Japan. *Heredity*. 102: 579–589.

Ohnishi N, Osawa T, Yamamoto T, Uno R. 2019. Landscape heterogeneity in landform and land use provides functional resistance to gene flow in continuous Asian black bear populations. *Ecology and Evolution*. 9: 4958–4968.

Ohshima K. 1990. The history of straits around the Japanese islands in the late-quaternary. *The Quaternary Research (Daiyonki-Kenkyu)*. 29: 193–208 (in Japanese with an English abstract)

Okaura T, Quang ND, Ubukata M, Harada K. 2007. Phylogeographic structure and late Quaternary population history of the Japanese oak *Quercus mongolica* var. *crispula* and related species revealed by chloroplast DNA variation. *Genes & Genetic Systems*. 82: 465–477.

Ono Y. 1990. The northern landbridge of Japan. *The Quaternary Research (Daiyonki-Kenkyu)*. 29: 183–192. (in Japanese with an English abstract)

Osada N, Hettiarachchi N, Babarinde AI, Saitou N, Blancher A. 2015. Whole-genome sequencing of six Mauritian cynomolgus macaques (*Macaca fascicularis*) reveals a genome-wide pattern of polymorphisms under extreme population bottleneck. *Genome Biology and*

Evolution. 7: 821–830.

Osada N, Kawai Y. 2021. Exploring models of human migration to the Japanese archipelago using genome-wide genetic data. *Anthropological Science*. 129: 45–58.

Osman MB, Tierney JE, Zhu J, Tardif R, Hakim GJ, King J, Poulsen CJ. 2021. Globally resolved surface temperatures since the Last Glacial Maximum. *Nature*. 599: 239-244.

Otto-Bliesner BL, Marshall SJ, Overpeck JT, Miller GH, Hu A, CAPE LAST INTERGLACIAL PROJECT MEMBERS. 2006. Simulating arctic climate warmth and icefield retreat in the last interglaciation. *Science*. 311: 1751–1753.

Packer C. 1979. Inter-troop transfer and inbreeding avoidance in *Papio anubis*. *Animal behaviour*. 27: 1–36.

Palm EC, et al. 2023. Corridor-based approach with spatial cross-validation reveals scale-dependent effects of geographic distance, human footprint and canopy cover on grizzly bear genetic connectivity. *Molecular Ecology*. 3: 5211–5227.

Paradis E, Claude J, Strimmer K. 2004. APE: Analyses of Phylogenetics and Evolution in R language. *Bioinformatics*. 20: 289–290.

Patiño J, et al. 2017. A roadmap for island biology: 50 fundamental questions after 50 years of The Theory of Island Biogeography. *Journal of Biogeography*. 44: 963–983.

Patterson N, Price AL, Reich D. 2006. Population structure and eigenanalysis. *PLoS Genetics*. 2: e190.

Patterson N, Moorjani P, Luo Y, Mallick S, Rohland N, Zhan Y, Genschoreck T, Webster T, Reich D. 2012. Ancient admixture in human history. *Genetics*. 192: 1065–1093.

Peterman WE. 2018. ResistanceGA: An R package for the optimization of resistance surfaces using genetic algorithms. *Methods in Ecology and Evolution*. 9: 1638–1647.

Petkova D, Novembre J, Stephens M. 2016. Visualizing spatial population structure with estimated effective migration surfaces. *Nature Genetics*. 48: Article 1.

Phillips SJ, Anderson RP, Schapire RE. 2006. Maximum entropy modeling of species geographic distributions. *Ecological Modelling*. 190: 231–259.

Pickrell J, Pritchard J. 2012. Inference of population splits and mixtures from genome-wide allele frequency data. *PLoS Genetics*. 8: e1002967.

Pockrandt C, Alzamel M, Iliopoulos CS, Reinert K. 2020. GenMap: ultra-fast computation of genome mappability. *Bioinformatics*. 36: 3687–3692.

Pongracz JD, Paetkau D, Branigan M, Richardson E. 2017. Recent hybridization between a polar bear and grizzly bears in the Canadian Arctic. *Arctic*. 70: 151–160.

Prufer K, et al. 2014. The complete genome sequence of a Neanderthal from the Altai Mountains. *Nature*. 505: 43–49.

Puckett EE, Orton D, Munshi‐South J. 2020. Commensal rats and humans: integrating rodent phylogeography and zooarchaeology to highlight connections between human societies. *Bioessays*. 42: 1900160.

Purcell S, et al. 2007. PLINK: a tool set for whole-genome association and population-based linkage analyses. *The American journal of human genetics*. 81: 559–575.

R Core Team 2022. R: A language and environment for statistical computing. R Foundation for Statistical Computing, Vienna, Austria. https://www.r-project.org/. last accessed 2 October, 2023.

Ragsdale AP, Weaver TD, Atkinson EG, Hoal EG, Möller M, Henn BM, Gravel S. 2023. A weakly structured stem for human origins in Africa. *Nature*. 1-9.

Randi E, Gentile L, Boscagli G, Huber D, Roth HU. 1994. Mitochondrial DNA sequence divergence among some west European brown bear (*Ursus arctos L.*) populations. Lessons for conservation. *Heredity*. 73: 480–489.

Reich D, et al. 2010. Genetic history of an archaic hominin group from Denisova Cave in Siberia. *Nature*. 468: 1053-1060.

Rey-Iglesia A, García-Vázquez A, Treadaway EC, van der Plicht J, Baryshnikov GF, Szpak P, Bocherens H, Boeskorov GG, Lorenzen ED. 2019. Evolutionary history and palaeoecology of brown bear in North-East Siberia re-examined using ancient DNA and stable isotopes from skeletal remains. *Scientific Reports*. 9.

Rogers J, et al. 2019. The comparative genomics and complex population history of *Papio* baboons. *Science Advances*. 5.

Rozzi R, et al. 2023. Dwarfism and gigantism drive human-mediated extinctions on islands. *Science*. 379: 1054–1059.

Sagayama T, Tonosaki T, Kondo T, Okamura S, Sato K. 2010. Stratigraphy and paleoenvironment of Upper Pleistocene to Holocene sediments in the Ishikari Plain, Hokkaido, Japan. *The Journal of the Geological Society of Japan*. 116: 13–26.

Saitou N, Nei M. 1987. The neighbor-joining method: A new method for reconstructing phylogenetic trees. *Molecular Biology and Evolution*. 4: 406–425.

Sakaguchi S, et al. 2015. High-throughput linkage mapping of Australian white cypress pine (*Callitris glaucophylla*) and map transferability to related species. *Tree Genetics & Genome*s. 11: 1–12.

Salis AT, et al. 2021. Lions and brown bears colonized North America in multiple synchronous waves of dispersal across the Bering Land Bridge. *Molecular Ecology*. 31: 6407–6421.

Santiago E, Novo I, Pardiñas AF, Saura M, Wang J, Caballero A. 2020. Recent demographic history inferred by high-resolution analysis of linkage disequilibrium. *Molecular Biology and Evolution*. 37: 3642–3653.

Sato Y, Mano T, Takatsuki S. 2005. Stomach contents of brown bears *Ursus arctos* in Hokkaido, Japan. *Wildlife Biology*. 11: 133–144.

Sato Y, Itoh T, Mori Y, Satoh Y, Mano T. 2011. Dispersal of male bears into peripheral habitats inferred from mtDNA haplotypes. *Ursus*. 22: 120–132.

Sato Y, Nakamura H, Ishifune Y, Ohtaishi N. 2011. The white-colored brown bears of the Southern Kurils. *Ursus*. 22: 84–90.

Sato Y. 2015. *Ursus arctos* Linnaeus, 1758. Ohdachi SD, Ishibashi Y, Iwasa MA, Saitoh T, Sellers SB. Eds., The wild mammals of Japan Second Edition. pp. 240–242. Kyoto, Japan: Shoukadoh Book Sellers.

Schliep KP. 2011. Phangorn: phylogenetic analysis in R. *Bioinformatics*. 27: 592–593.

Schregel J, Remm J, Eiken HG, Swenson JE, Saarma U, Hagen SB. 2018. Multi-level patterns in population genetics: variogram series detects a hidden isolation-by-distance-dominated structure of Scandinavian brown bears *Ursus arctos*. *Methods in Ecology and Evolution*. 9: 1324–1334.

Segawa T, et al. 2021. Ancient DNA reveals multiple origins and migration waves of extinct Japanese brown bear lineages. *Royal Society Open Science*. 8: 210518.

Segawa T, Rey-Iglesia A, Lorenzen ED, Westbury MV. 2024. The origins and diversification of Holarctic brown bear populations inferred from genomes of past and present populations. *Proceedings of the Royal Society B*. 291: 20232411.

Seielstad MT, Minch E, Cavalli-Sforza LL. 1998. Genetic evidence for a higher female migration

rate in humans. *Nature Genetics*. 20: Article 3.

Shimozuru M, et al. 2019. Incidence of multiple paternity and inbreeding in high-density brown bear populations on the shiretoko Peninsula, Hokkaido, Japan. *Journal of Heredity*. 110: 321–331.

Shimozuru M, et al. 2022. Estimation of breeding population size using DNA-based pedigree reconstruction in brown bears. *Ecology and Evolution*. 12: e9246.

Shirane Y, et al. 2018. Sex-biased natal dispersal in Hokkaido brown bears revealed through mitochondrial DNA analysis. *European Journal of Wildlife Research*. 64: 1–12.

Shirane Y, et al. 2019. Sex-biased dispersal and inbreeding avoidance in Hokkaido brown bears. *Journal of Mammalogy*. 100: 1317–1326.

Short Bull RA, et al. 2011. Why replication is important in landscape genetics: American black bear in the Rocky Mountains. *Molecular Ecology*. 20: 1092–1107.

Smouse PE, Long JC, Sokal RR. 1986. Multiple regression and correlation extensions of the Mantel test of matrix correspondence. *Systematic Biology*. 35: 627–632.

Swenson JE, Sandegren F, Bjärvall A, Söderberg A, Wabakken P, Franzén R. 1994. Size, trend, distribution and conservation of the brown bear *Ursus arctos* population in Sweden. *Biological Conservation*. 70: 9–17.

Takakuwa Y, Anezaki T, Toshiyuki K. 2007. Fossil of the brown bear from Fuji-do cave, Ueno Village, Gunma Prefecture, Japan. *Bulletin of the Gunma Museum of Natural History*. 11: 63–72. (in Japanese with English abstract)

Takinami H, Ishiyama N, Takafumi H, Kubo T, Tomita K, Tsujino M, Nakamura F. 2021. Young citizen sensors for managing large carnivores: Lessons from 40 years of monitoring a brown bear population. *Conservation Science and Practice*. 3: e484.

Talbot SL, Shields GF. 1996. Phylogeography of brown bears (*Ursus arctos*) of Alaska and paraphyly within the Ursidae. *Molecular phylogenetics and evolution*. 5: 477–494.

Tassi F, Ghirotto S, Mezzavilla M, Vilaça ST, De Santi L, Barbujani G. 2015. Early modern human dispersal from Africa: genomic evidence for multiple waves of migration. *Investigative genetics*. 6: 1–16.

Taylor GA, et al. 2018. The genome of the North American brown bear or grizzly: *Ursus arctos* ssp. *horribilis*. *Genes*. 9: 598.

Trochet A, Courtois EA, Stevens VM, Baguette M, Chaine A, Schmeller DS, Clobert J. 2016. Evolution of sex-biased dispersal. *Quarterly Review of Biology*. 91: 297–320.

Tsuruga H, Mano T, Yamanaka M, Kanagawa H. 1994. Estimate of genetic variations in Hokkaido brown bears (*Ursus arctos yesoensis*) by DNA fingerprinting. *The Japanese Journal of Veterinary Research*. 42: 127–136.

Tsuruga H, Mano T, Yamano S, Kanagawa H. 1996. Lack of protein polymorphism in Hokkaido brown bears (*Ursus arctos yesoensis*). *Honyurui-Kagaku(Mammaliam Science)*. 36: 59–62. (in Japanese)

Tucker JM, Allendorf FW, Truex RL, Schwartz MK. 2017. Sex-biased dispersal and spatial heterogeneity affect landscape resistance to gene flow in fisher. *Ecosphere*. 8: e01839.

Tumendemberel O, et al. 2019. Phylogeography, genetic diversity, and connectivity of brown bear populations in Central Asia. *PLoS One*. 14: e0220746.

Tumendemberel O, Hendricks SA, Hohenlohe PA, Sullivan J, Zedrosser A, Sæbø M, Proctor MF, Koprowski JL, Waits LP. 2023. Range-wide evolutionary relationships and historical demography of brown bears (*Ursus arctos*) revealed by whole-genome sequencing of isolated central Asian populations. *Molecular Ecology*. 32: 5156–5169.

Waits L, Taberlet P, Swenson JE, Sandegren F, Franzén R. 2000. Nuclear DNA microsatellite analysis of genetic diversity and gene flow in the Scandinavian brown bear (*Ursus arctos*). *Molecular Ecology*. 9: 4.

Warren DL, et al. 2021. ENMTools 1.0: An R package for comparative ecological biogeography. *Ecography*. 44: 504–511.

Wang MS, et al. 2022. A polar bear paleogenome reveals extensive ancient gene flow from polar bears into brown bears. *Nature Ecology and Evolution*. 1–9.

Webster TH, Wilson Sayres MA. 2016. Genomic signatures of sex-biased demography: Progress and prospects. *Current Opinion in Genetics and Development*. 41: 62–71.

Wiens BJ, Combe FJ, Dickerson B, Divine LM, Padula VM, Sage GK, Talbot SL, Hope AG 2022. Genetic drift drives rapid speciation of an Arctic insular endemic shrew (*Sorex pribilofensis*). *Molecular Ecology*. 31: 5231–5248.

Xue Y, et al. 2015. Mountain gorilla genomes reveal the impact of long-term population decline and inbreeding. *Science*. 348: 242–245.

Zedrosser A, Støen OG, Sæbø S, Swenson JE. 2007. Should I stay or should I go? Natal dispersal in the brown bear. *Animal Behaviour*. 74: 369–376.

Figures and Tables

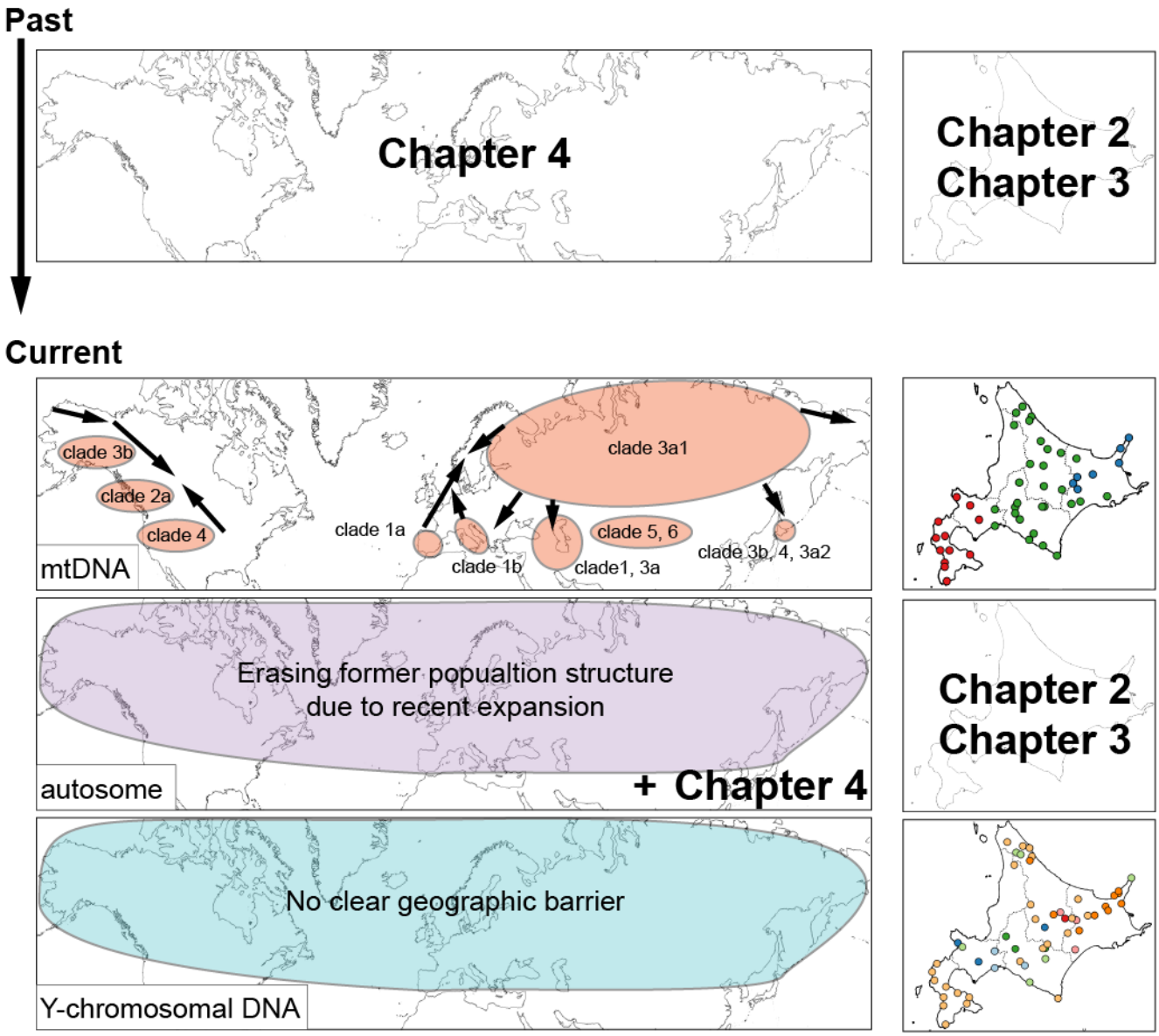

Figure 1. The population demographic history of the brown bear verified in the previous studies and discussed in this article. The worldwide maps showing the genetic structure based on mtDNA, autosome, and Y-chromosomal DNA were drawn based on the previous studies (Davison et al. 2011, Bidon et al. 2014, de Jong et al. 2023). The maps of the genetic structure in Hokkaido were followed by Matsuhashi et al. (1999) and Hirata et al. (2017). The chapter names shown in this figure mean which periods each chapter focused on.

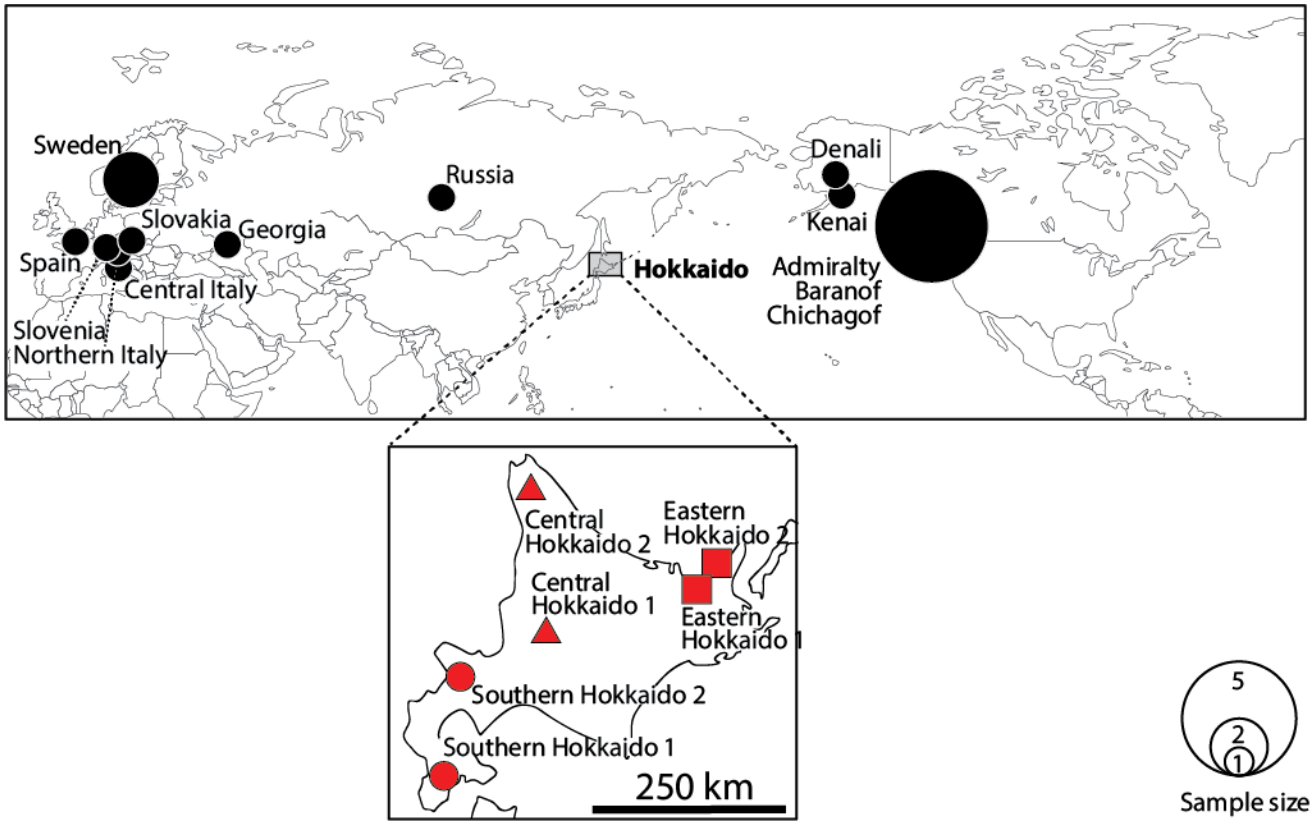

Figure 2. Sampling locations for brown bears used for the study in Chapter 2. The size of the circles on the above world map shows the number of samples from various regions. The Hokkaido map shows sample numbers from previous studies (Matsuhashi et al. 1999; Hirata et al. 2017). The shapes for Hokkaido individuals indicate the mtDNA lineage: circle, Southern Hokkaido (clade 4); triangle, Central Hokkaido (clade 3a2); and square, Eastern Hokkaido (clade 3b).

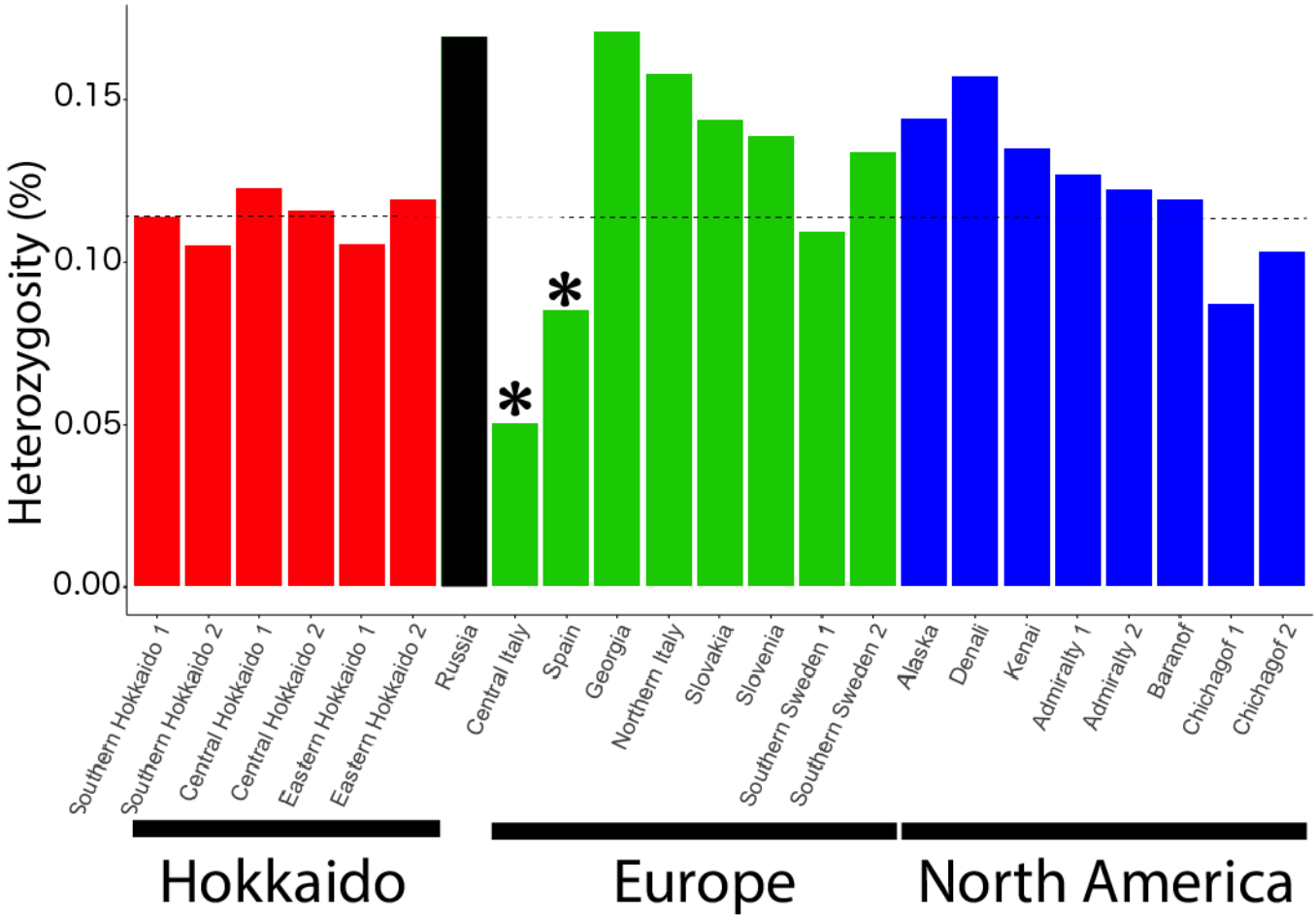

Figure 3. Heterozygosity for all brown bears examined. The names of the individuals are shown below. Asterisks indicate individuals from the endangered population in Europe. The dashed line means the average of the Hokkaido population.

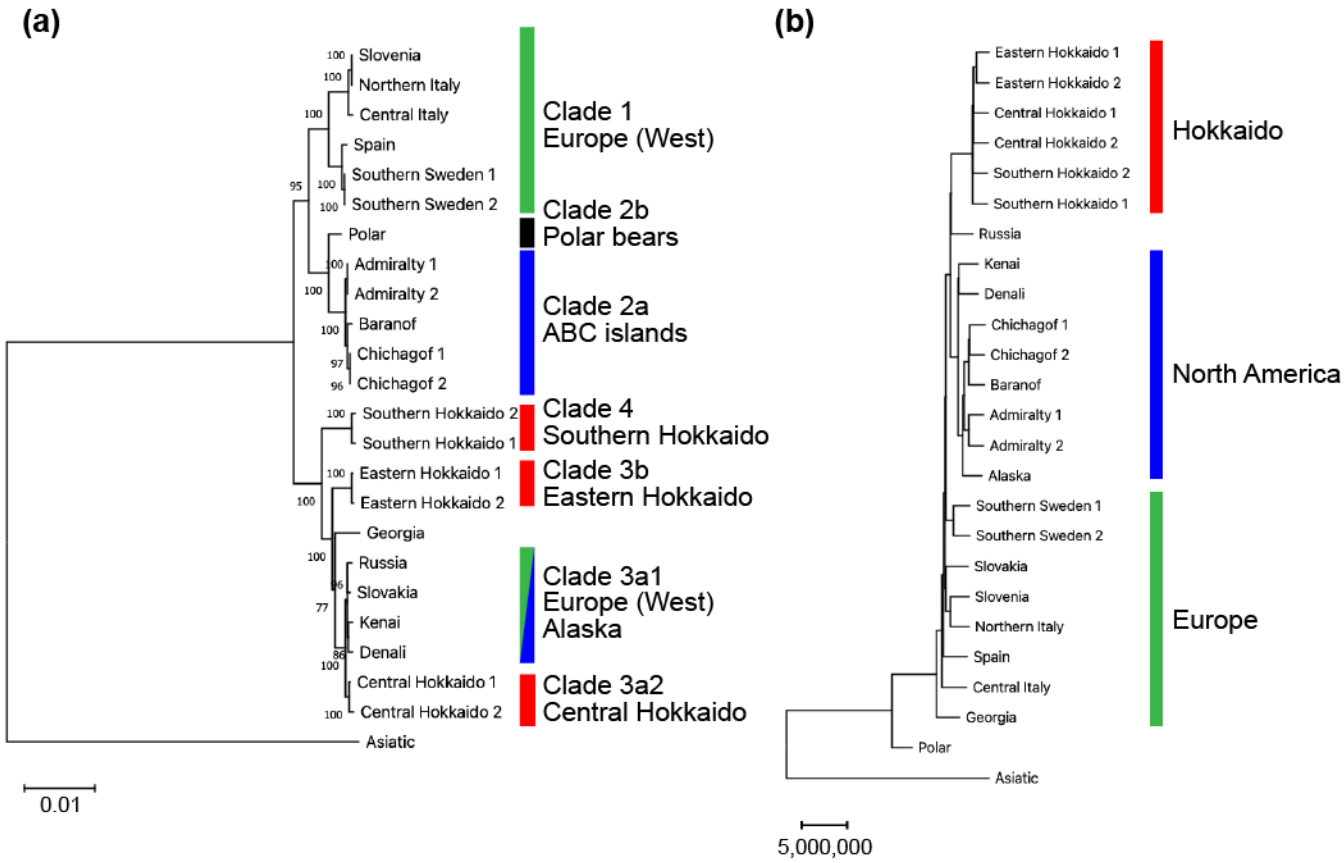

Figure 4. Phylogenetic tree based on the mitogenome (a) and autosomal genomic data (b). Numbers on internal branches are bootstrap values in percent. Clade designations to the right refer to Hirata et al. (2013). The Alaskan brown bear was removed from the result because I could not successfully assemble the mitochondrial DNA sequence using its sequence data (SRR7758718). The autosomal phylogenetic tree was constructed by the Neighbor-joining method. The colors in this figure mean which populations were included mainly in each lineage; red means Hokkaido, green means Europe, and blue means North America.

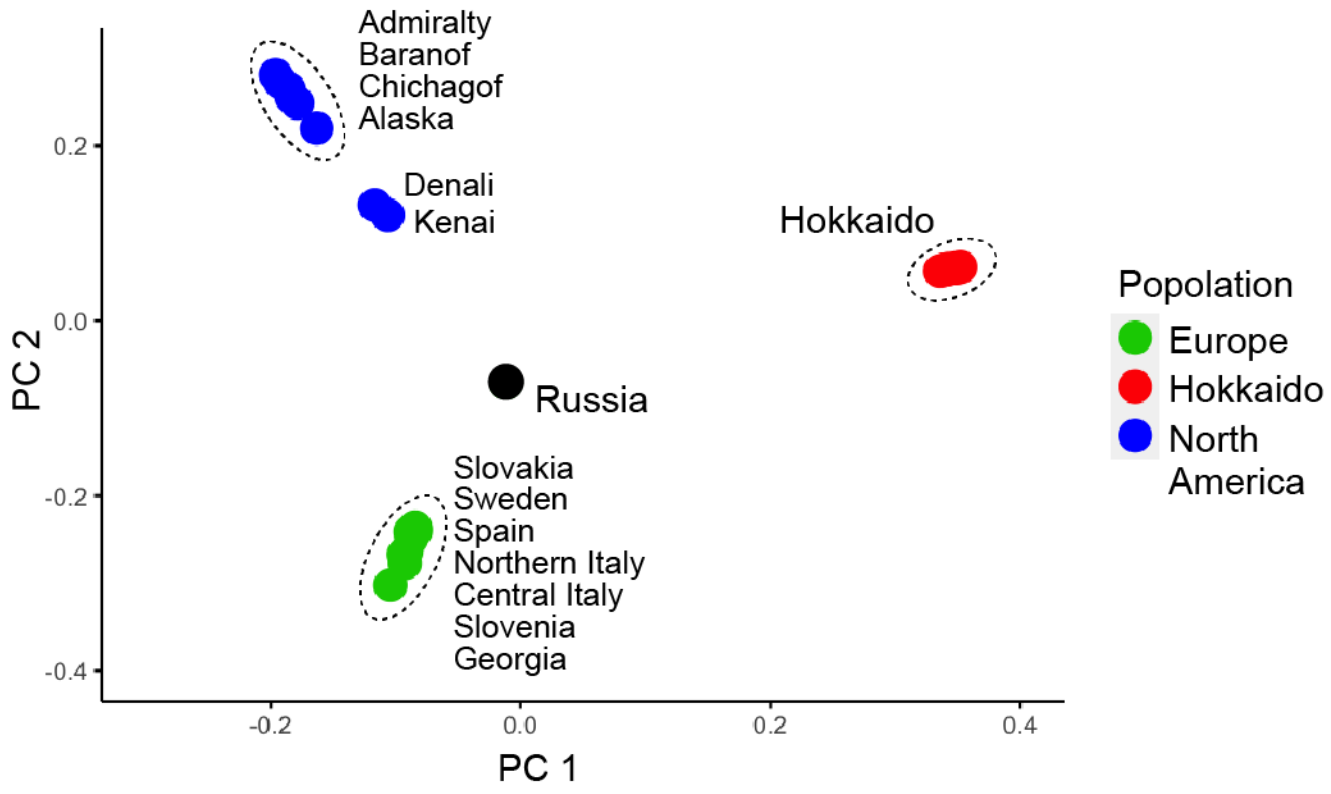

Figure 5. Principal component analysis (PCA) for all brown bears. The horizontal axis shows the first principal component, and the vertical axis the second principal component.

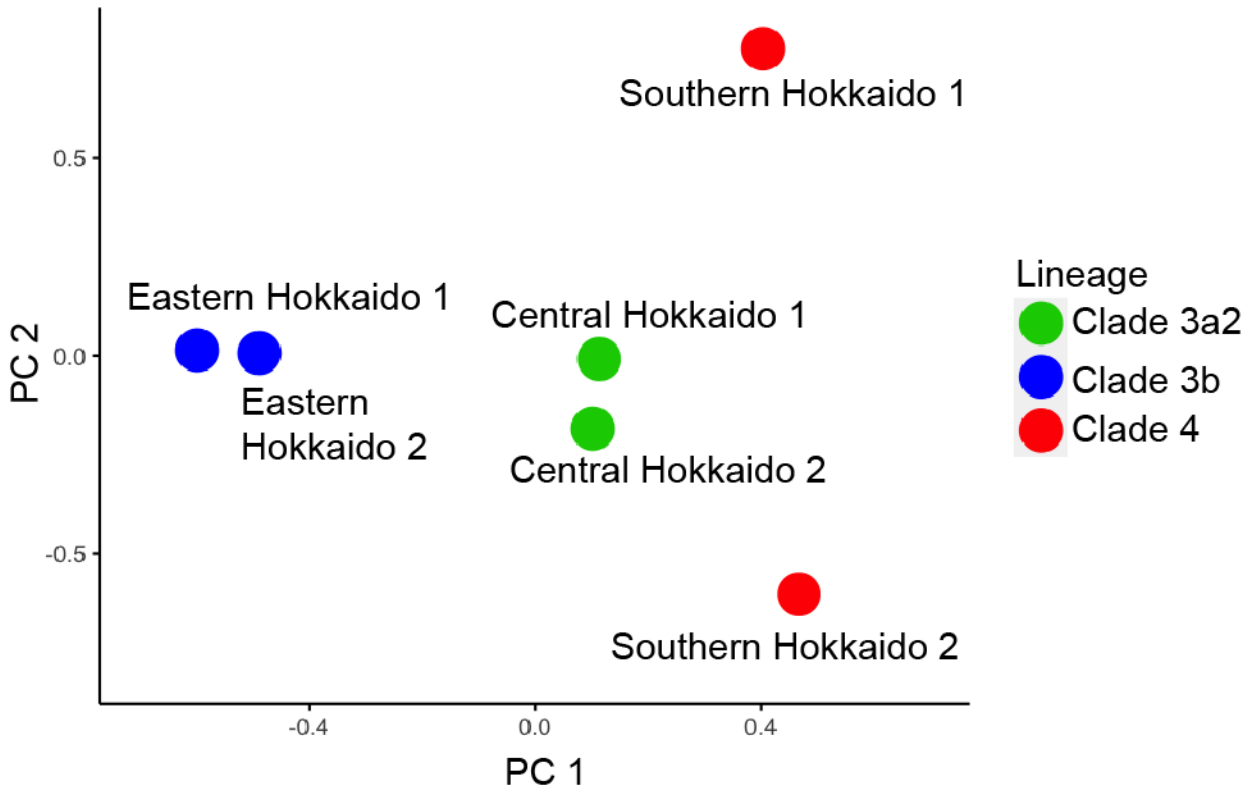

Figure 6. PCA for only the Hokkaido population, with the sample names labeled. The horizontal axis shows the first principal component, and the vertical axis the second principal component.

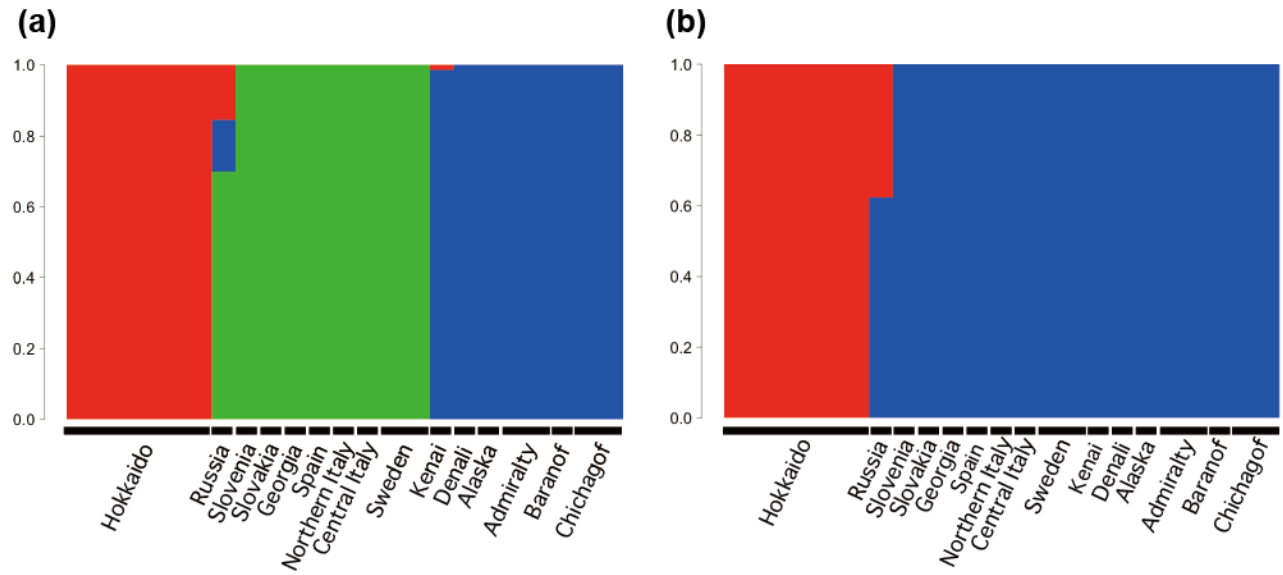

Figure 7. ADMIXTURE analyses at *K*=3 (a) and *K*=2 (b). Population or individual names are labeled at the bottom.

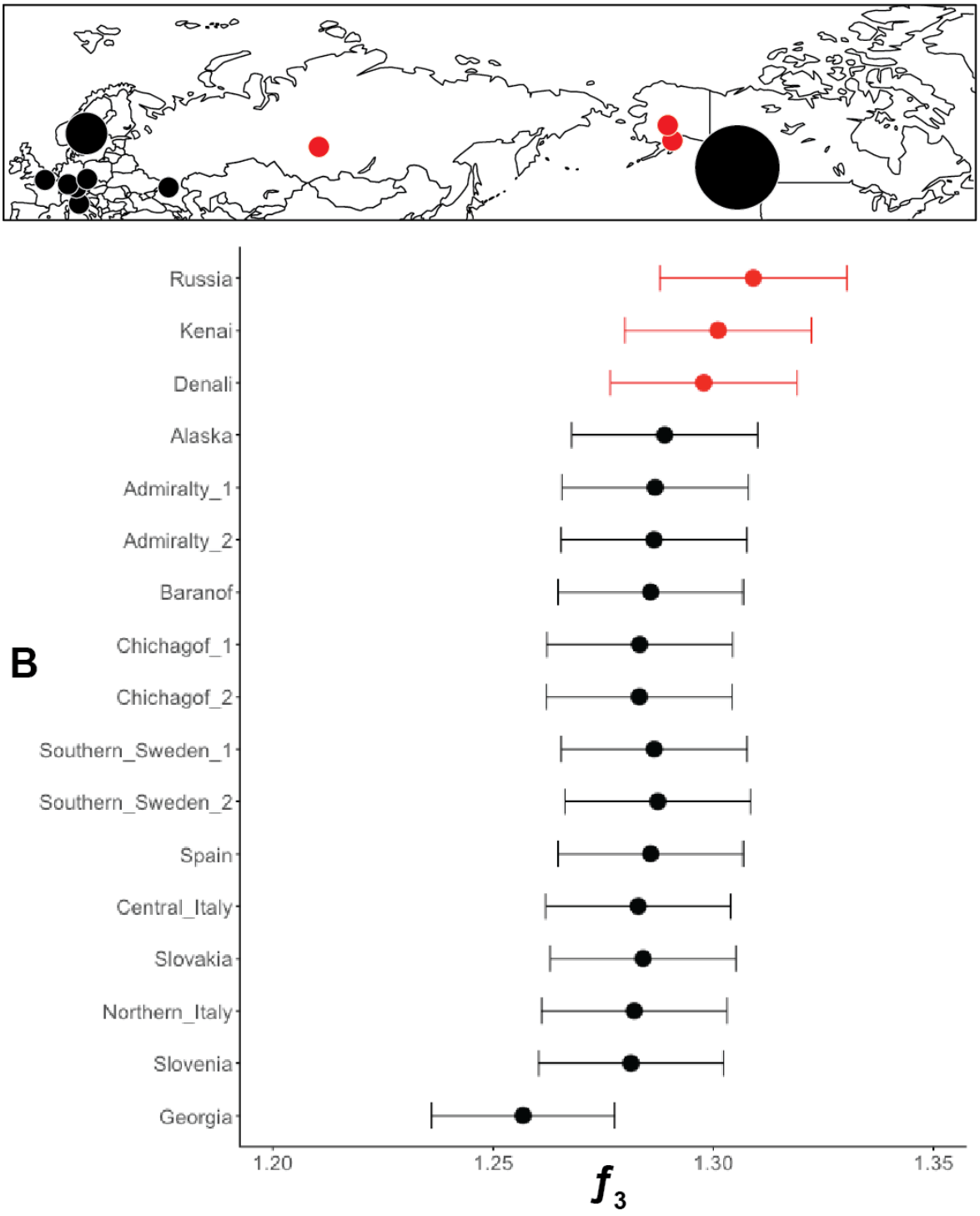

Figure 8. Correlation between *f*3(Hokkaido, B, Asiatic black bear) and geographical locality, with "B" indicating the brown bear individuals listed on the vertical axis. Higher values indicate a closer relationship between Hokkaido and B. Circle shading corresponds between the upper map and lower graph.

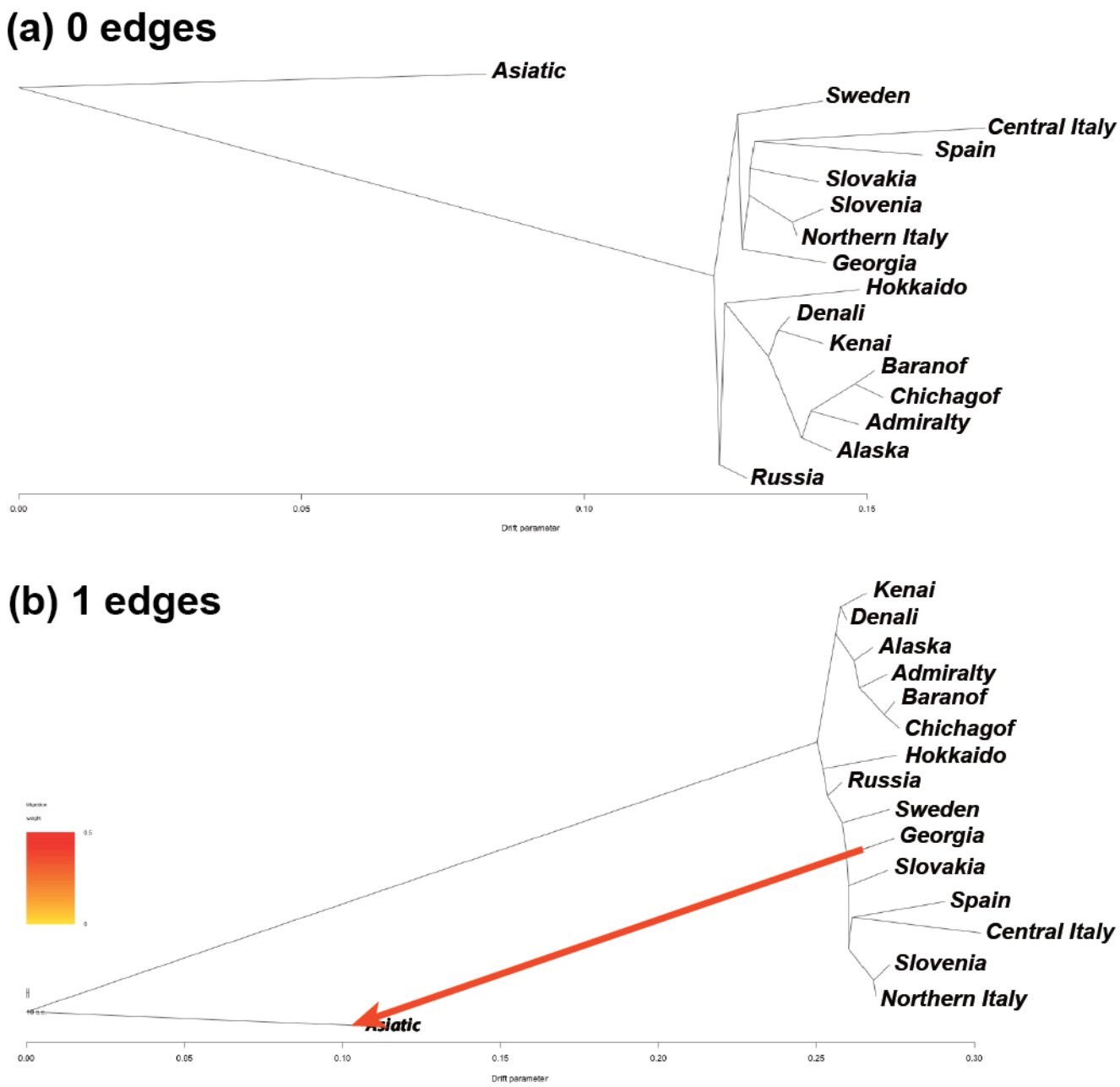

Figure 9. TreeMix analysis. 0 edges, assuming no genetic drift (a). 1 edge, assuming that genetic drift occurred (b). The arrow in (b) indicates gene flow, with the colored scale at the left indicating migration weight (ratio of gene flow).

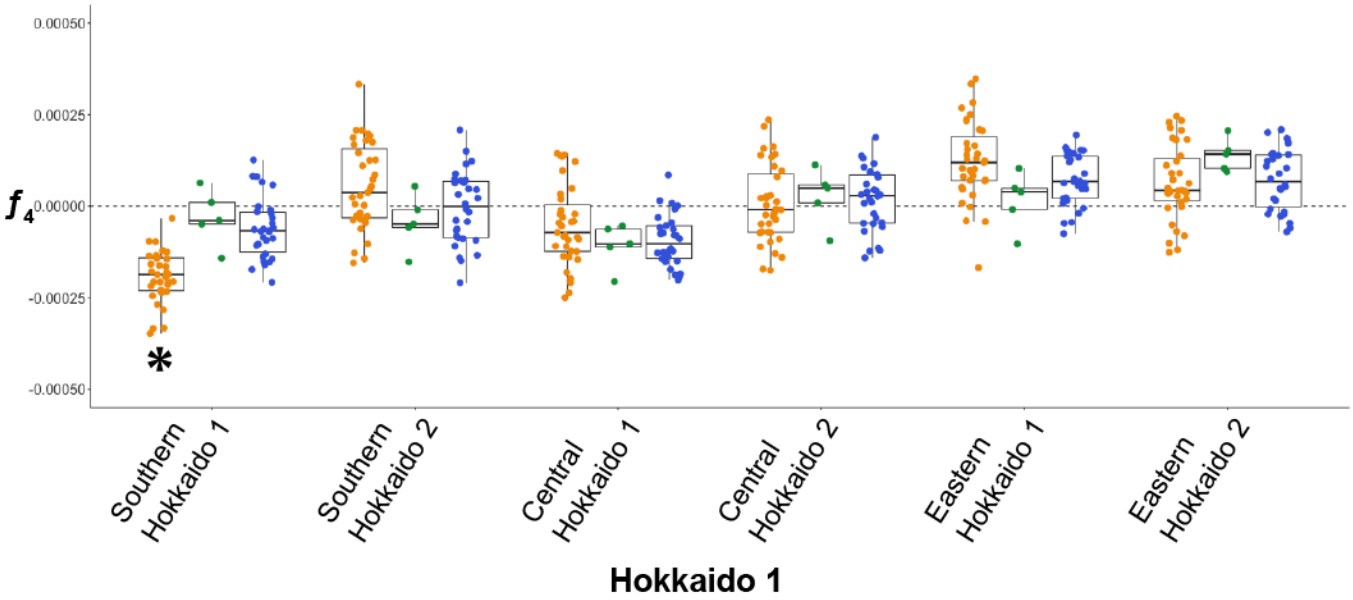

Figure 10. Range of values for f_4(Asiatic black bear, X; Hokkaido 1, Hokkaido 2). For each boxplot, the boxes range from the 25th to 75th percentiles and the lines extend to 1.5 times the distance from the 25th to 75th percentile. The lines inside the boxes indicate the median value. The dots indicate $f4$ values, with different shading indicating the population from which X derives: orange, European population (Slovakia, Georgia, Sweden, Slovenia, Northern Italy, Central Italy, and Spain); blue, North American population (Alaska, Denali, Kenai, Admiralty, Baranof, and Chichagof); green, Russian population. Hokkaido 1 and Hokkaido 2 indicate individuals from Hokkaido. Lower values mean that more alleles are shared between Hokkaido 1 and X. Asterisks indicate mean the range of values of $f4$(Asiatic black bear, the European population; Southern Hokkaido 1, Hokkaido 2).

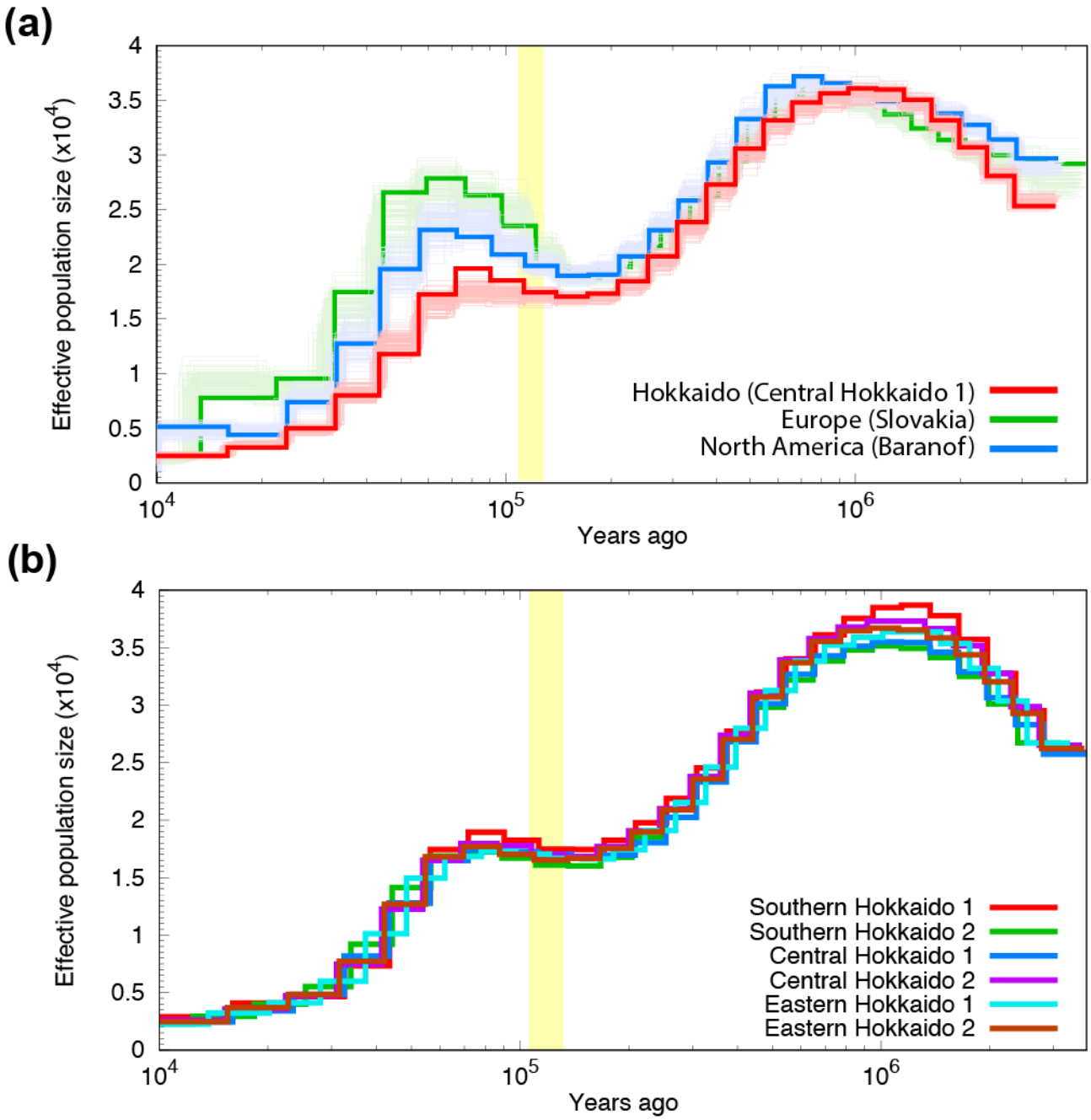

Figure 11. Pairwise sequentially Markovian coalescent (PSMC) estimates of brown bear effective population size (N_e) through time. Comparison of results including individual Central Hokkaido 1 and two individuals from Europe and North America (Slovakia and Baranof) (a). Results for all Hokkaido individuals (b). The vertical gray shading indicates the Eemian interglacial period (130–114 Kya).

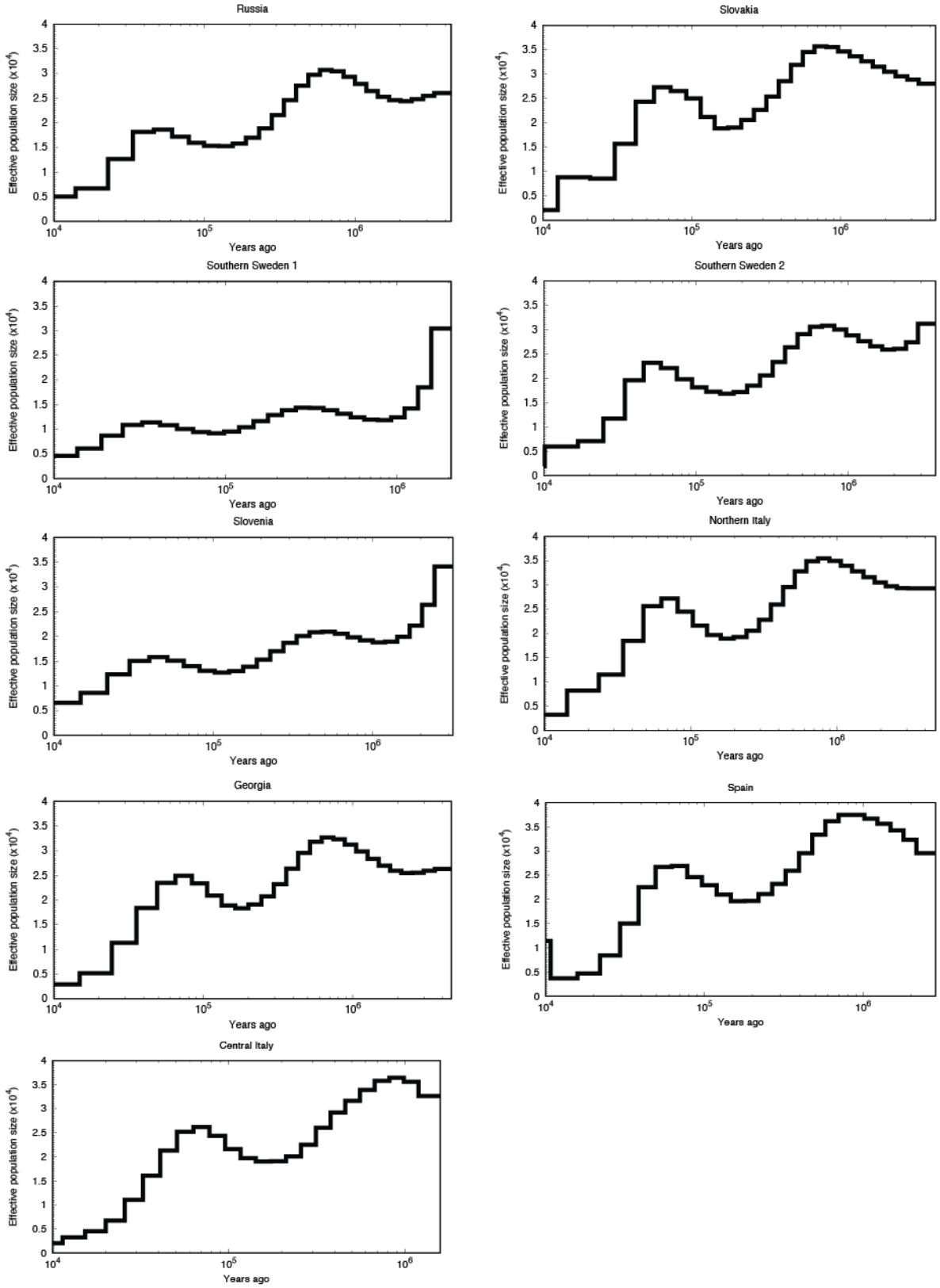

Figure 12. PSMC analysis. All individuals are from areas other than Hokkaido.

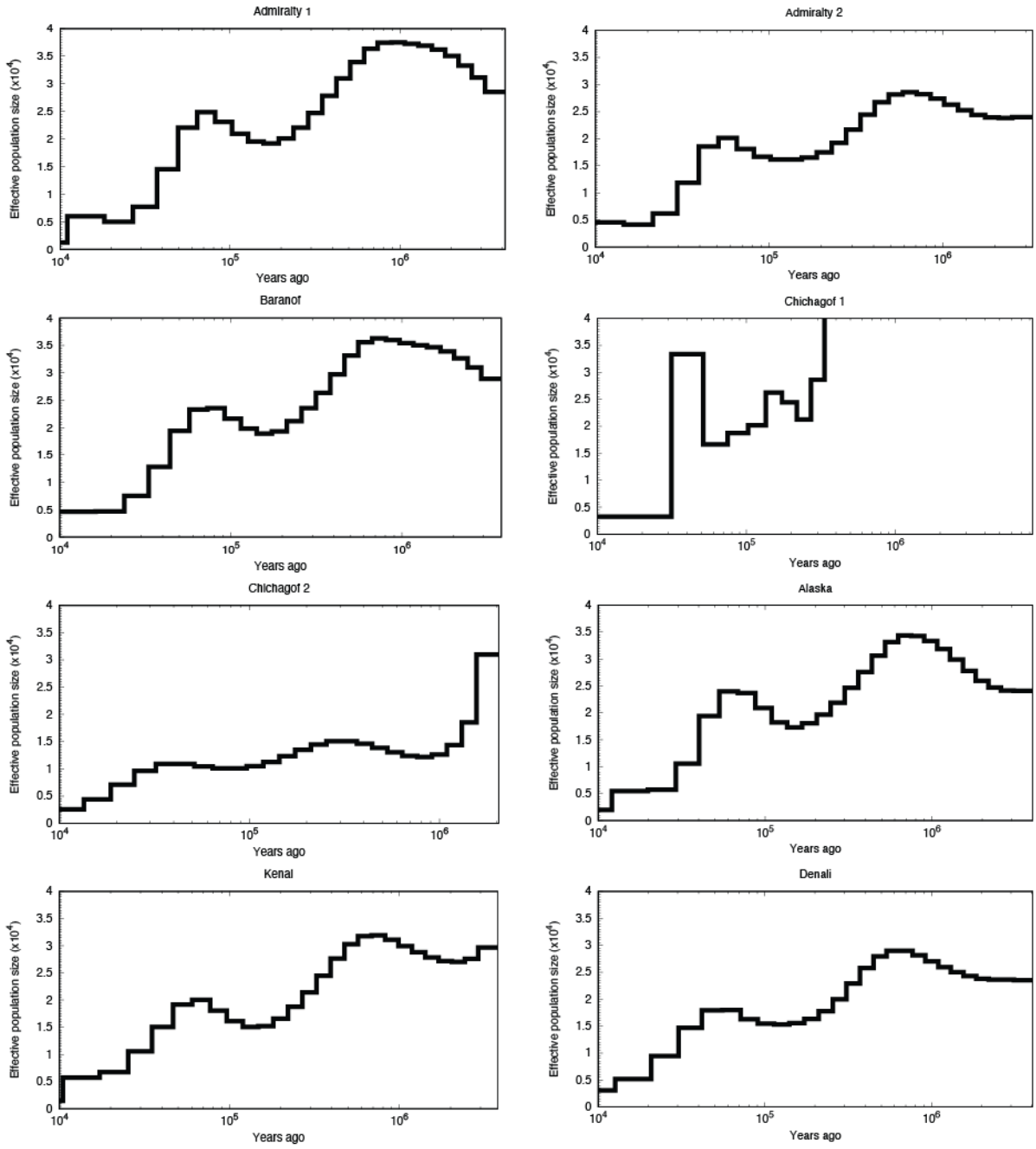

Figure 12. (Continued)

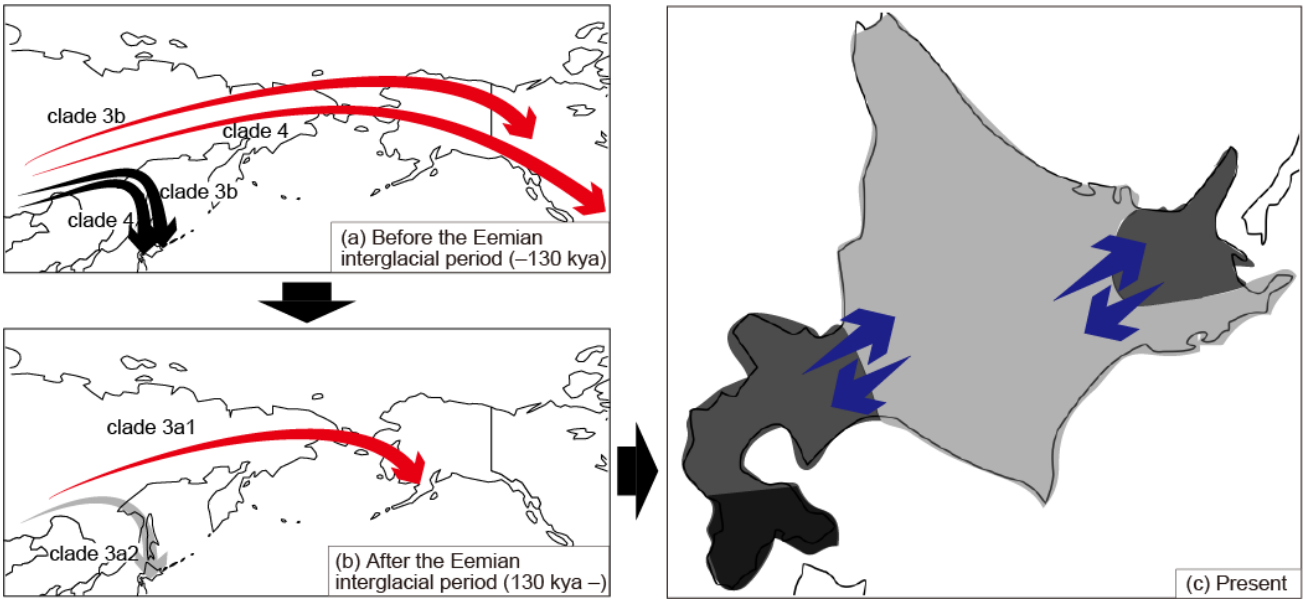

Figure 13. Demographic history of brown bears in Hokkaido. Before the Eemian interglacial period (-130 Kya) (a). After the Eemian interglacial period (130 Kya –) (b). Present (c). Red arrows mean the dispersal of the continental lineages. Blue arrows mean migration between subpopulations.

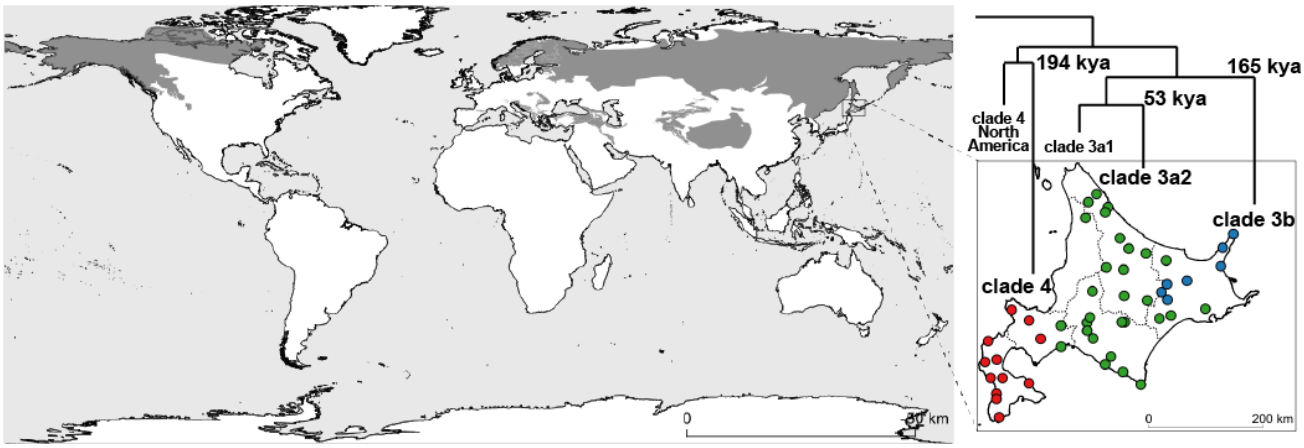

Figure 14. Habitat of brown bears and sampling location of specimens used for the study in Chapter 3. The grep polygons on the left side of the world map show the distribution of brown bears (McLellan et al. 2017). The dot on the right map colored by mt DNA lineages (red, clade 4; green, clade 3a2; blue, clade 3b) shows the sampling location of 49 individuals in this study. The dashed lines mean the management unit described by the Brown Bear Management Plan on Hokkaido (Hokkaido, 2017, 2022).

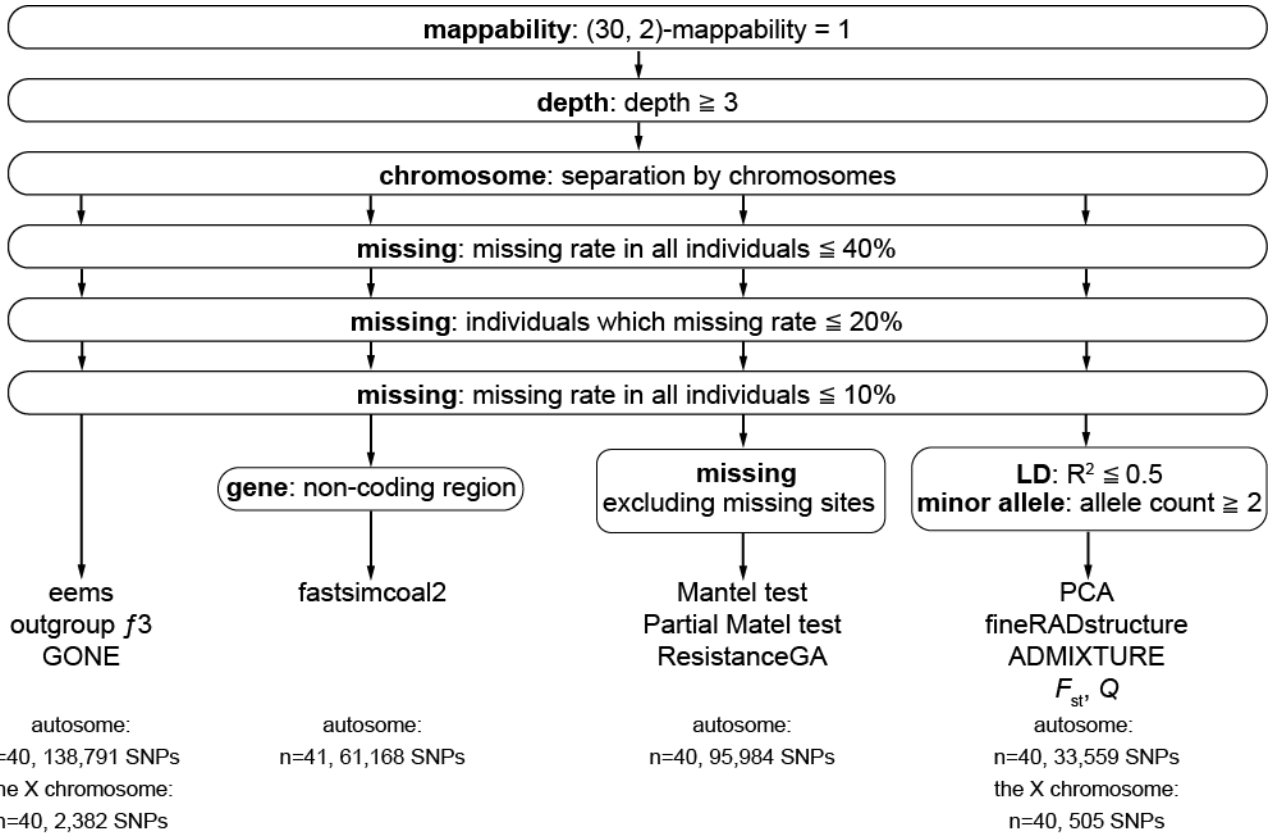

Figure 15. Workflow on SNP filtration.

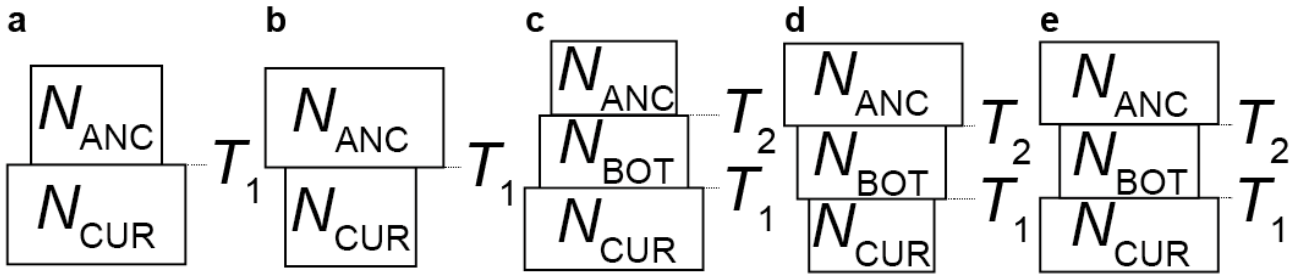

Figure 16. Five Population demographic models simulated by fastsimcoal2.

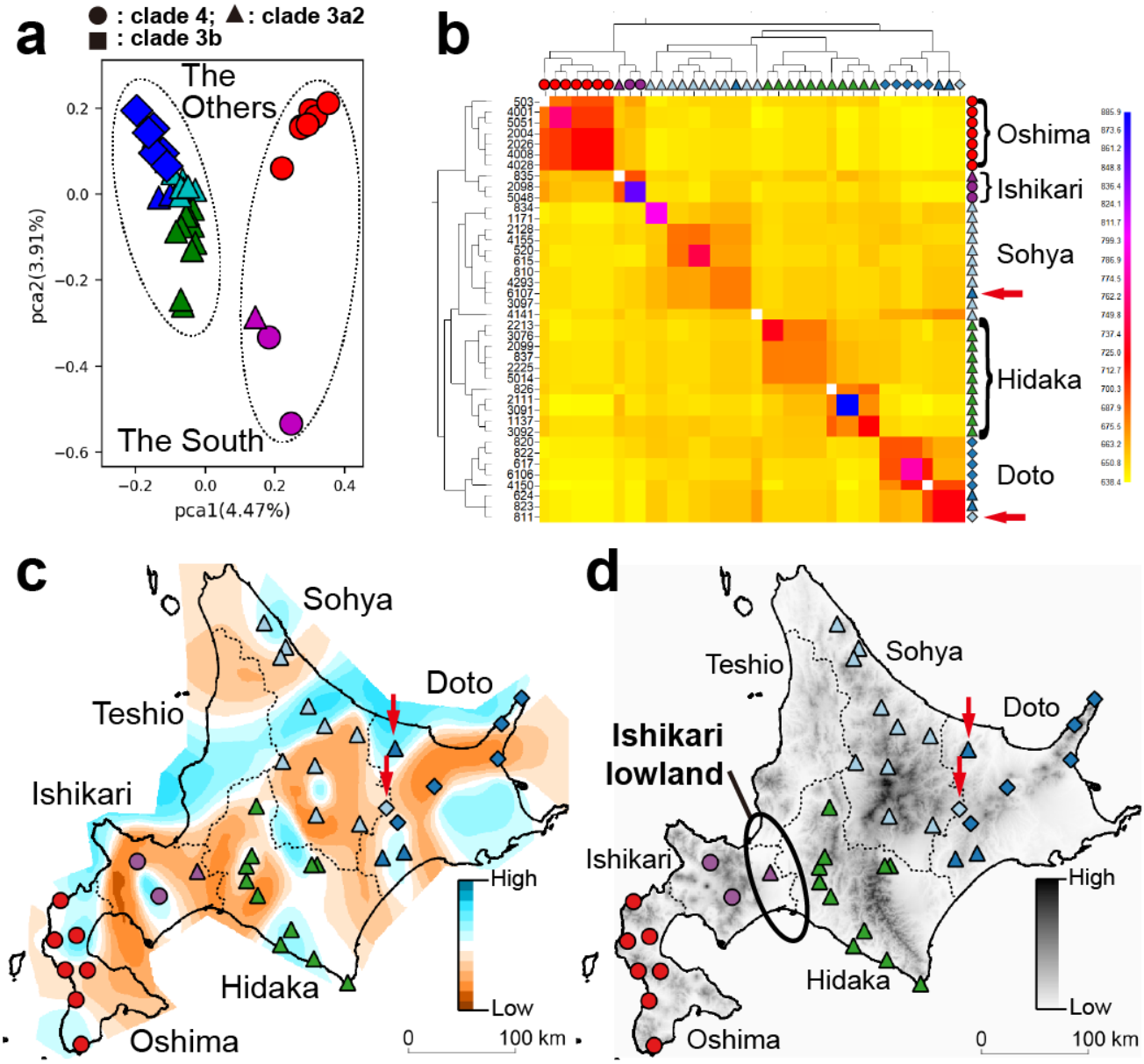

Figure 17. Genetic structure of the brown bear subpopulations in Hokkaido. The dot colors mean the subpopulation. Red corresponds to Oshima, purple to Ishikari, green to Hidaka, light blue to Sohya, and blue to Doto. The individual from Teshio was excluded from this analysis because they did not pass the SNP filtration. The dot shape means the mtDNA haplotypes (Matsuhashi et al., 1999) (circle: clade 4, triangle: clade 3a2, square: clade 3b). The arrow shown in Figures 2b, 2c, and 2d means the individuals categorized into different subpopulations from the sampling location by fineRADstructure. The result of PCA (a), fineRADstructure (b), and EEMS (c) were shown, respectively. The elevation in Hokkaido is shown in (d).

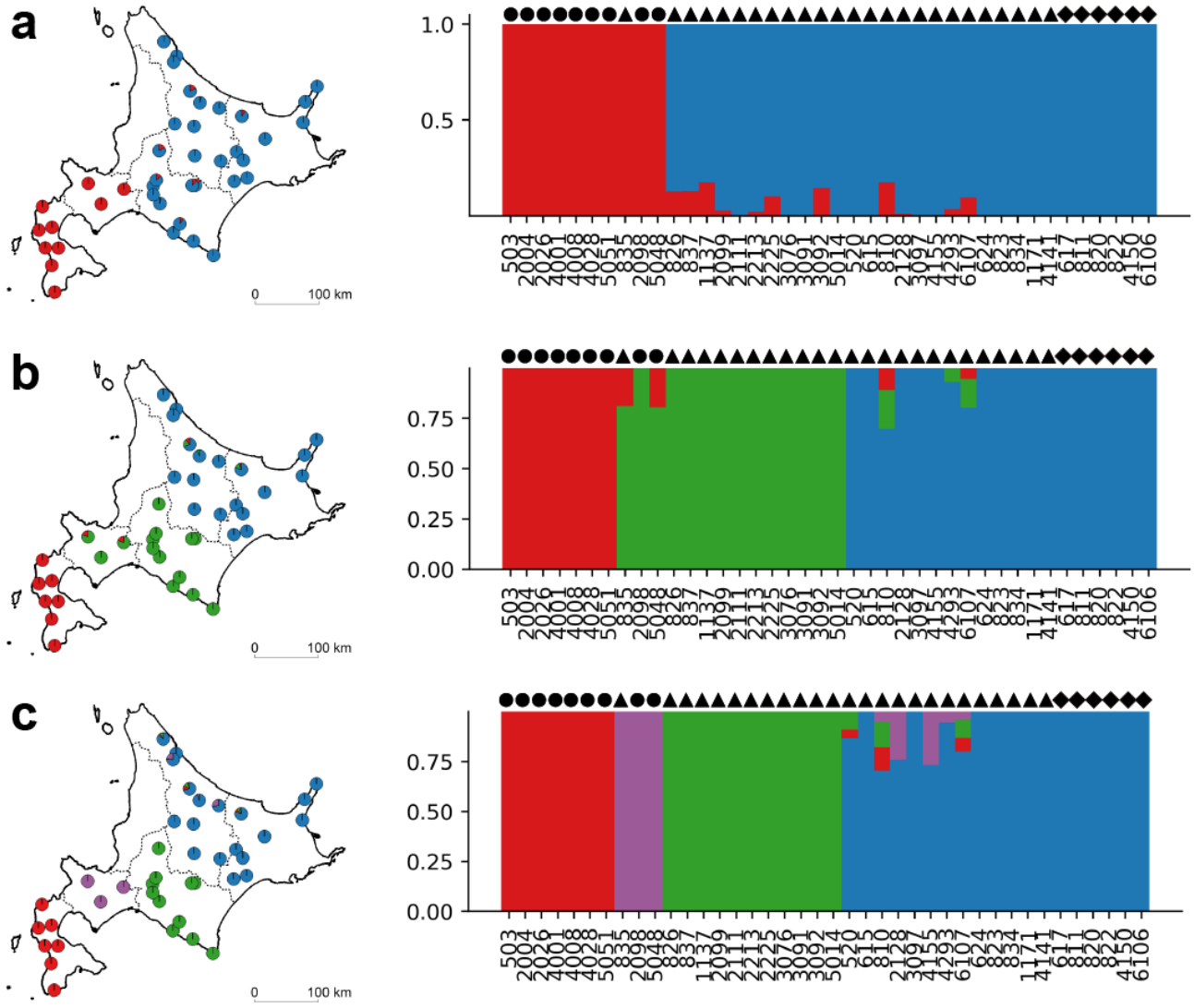

Figure 18. ADMIXTURE (right) and the distribution (left). The shapes shown above the result of ADMIXTURE indicate the types of mtDNA lineages for each individual (Matsuhashi et al., 1999) (circle: clade 4, triangle: clade 3a2, square: clade 3b). (a) *K*=2, (b)*K*=3, and (c) *K*=4.

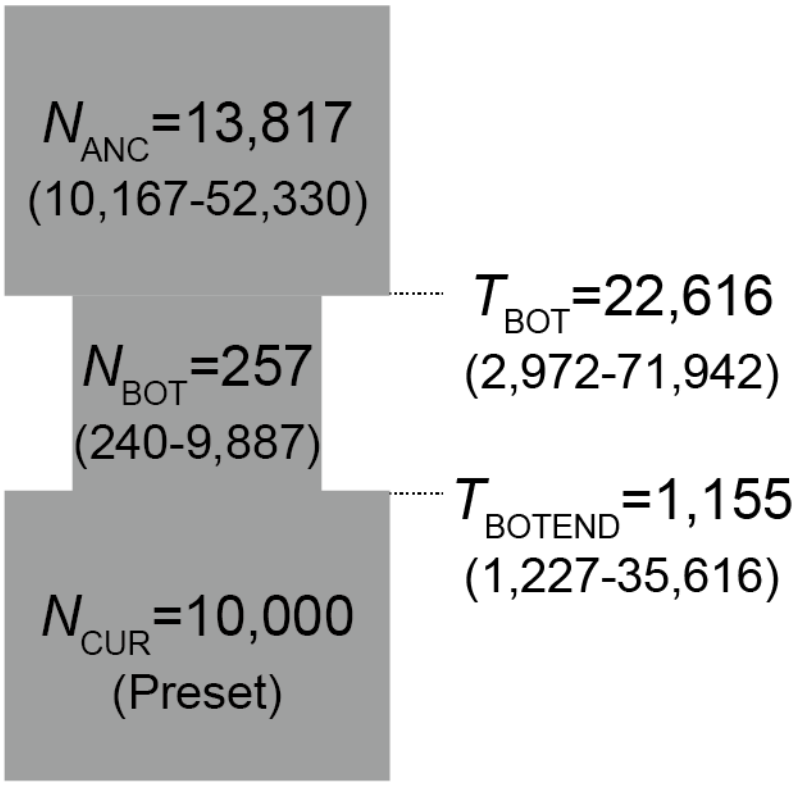

Figure 19. The best demographic model supported by fastsimcoal2. *T* means years corrected under the generation time being set as 11 years. *N* means the number of individuals included in the effective population.

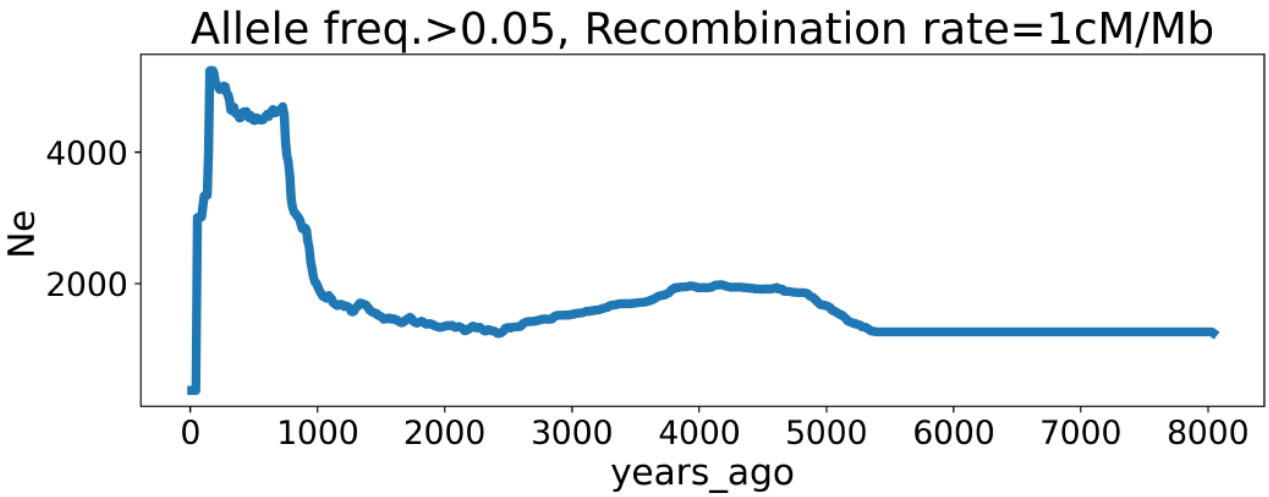

Figure 20. Recent effective population size change estimated by GONE.

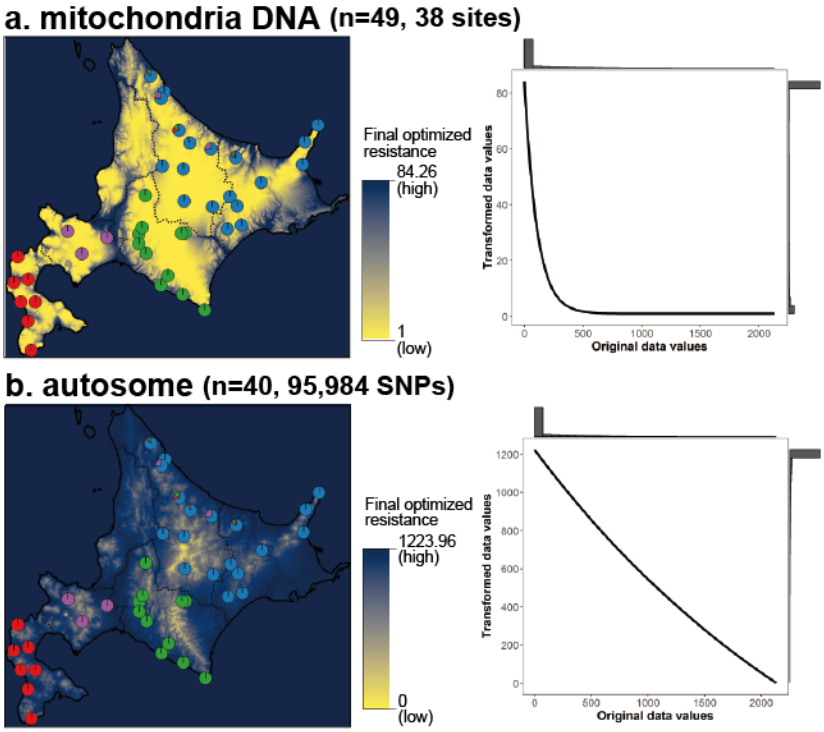

Figure 21. Final optimized resistance for the mitochondria DNA (a) and autosome (b). In the pictures on the left side, the higher the resistance is, the darker the color, which means the resistance is. Pie charts in the maps show the result of ADMIXTURE (shown in Figure Supplemental Figure 3c). Pictures on the right side show the correlation between original elevation values and transformed values.

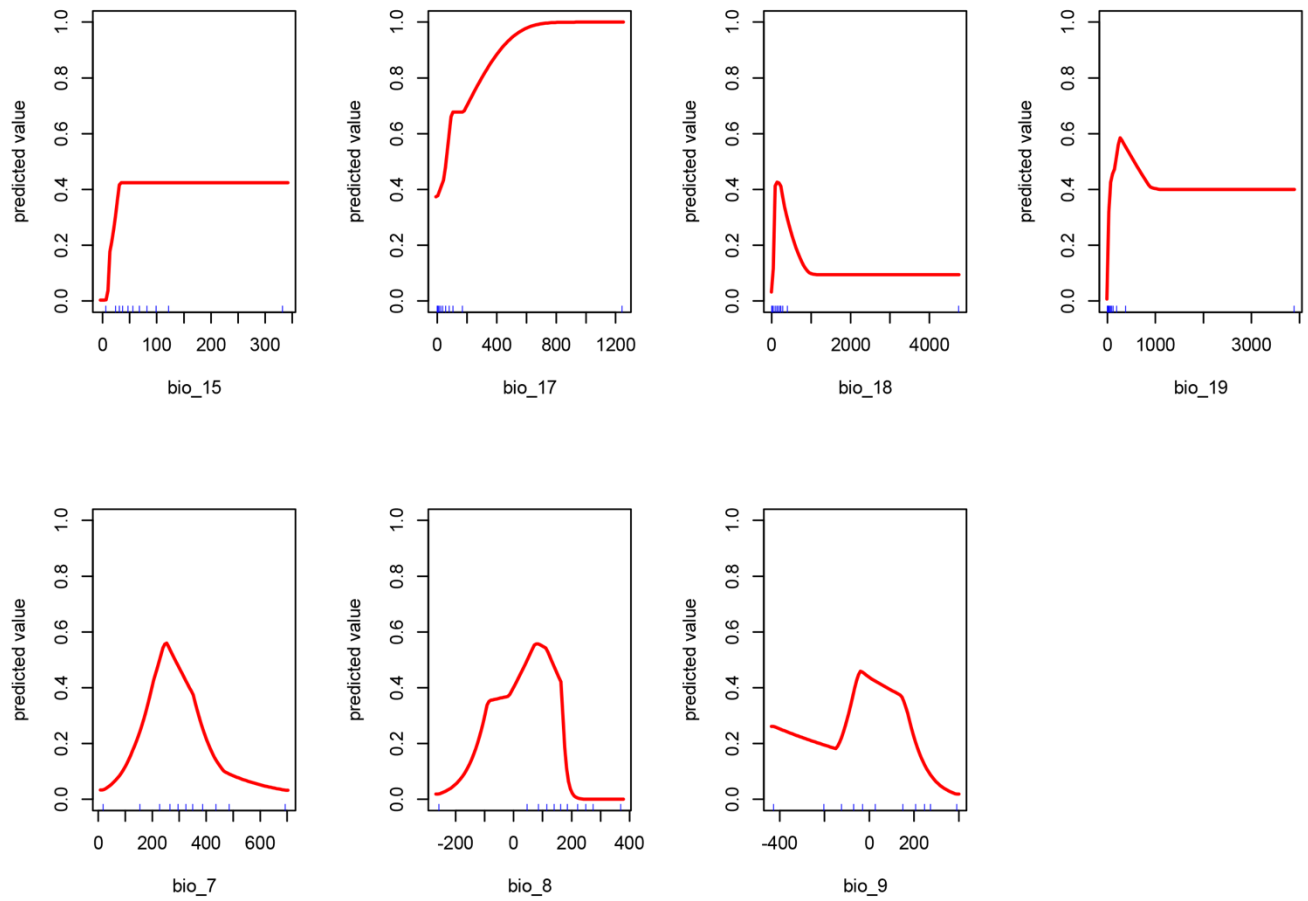

Figure 22. Response curves of each environmental variance in the best model. The curves show the predicted value (Y-axis) changes in each environmental variance (X-axis).

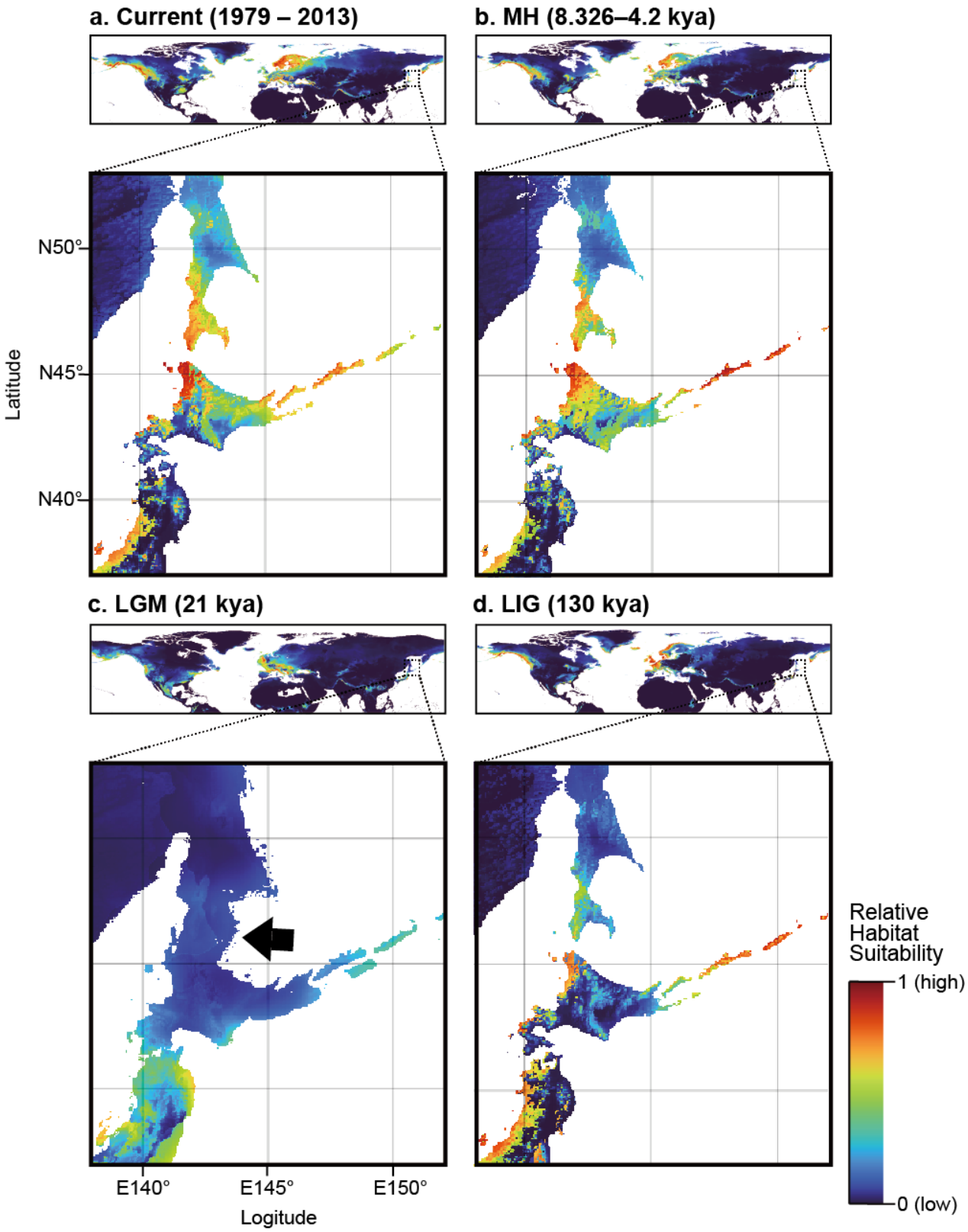

Figure 23. Inferred change of relative habitat suitability using Maxent. Each picture shows the result of the Current (a), the Middle Holocene (b), the Last Glacial Period (c), and the Last Inter Glacial (d). The black arrow in Figure 4c means the Soya land bridge.

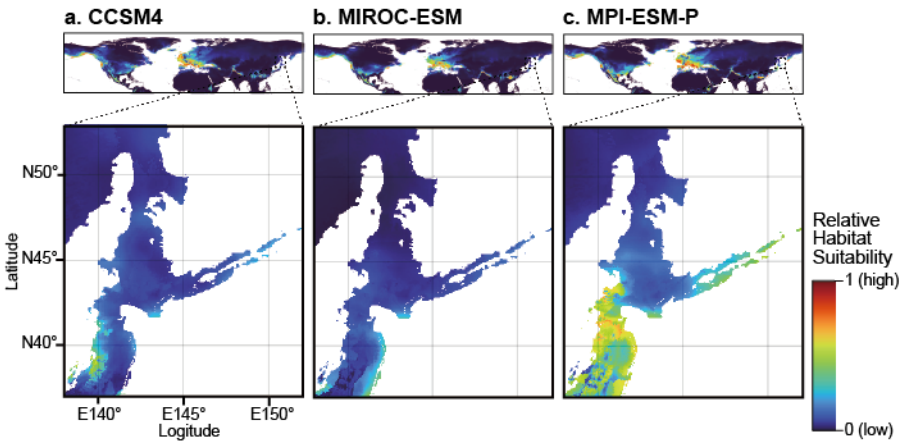

Figure 24. Relative habitat suitability using Maxent in the Last Glacial Period. Each picture shows the result using CCSM4 (a), MIROC-ESM (b), and MPI-ESM-P (c).

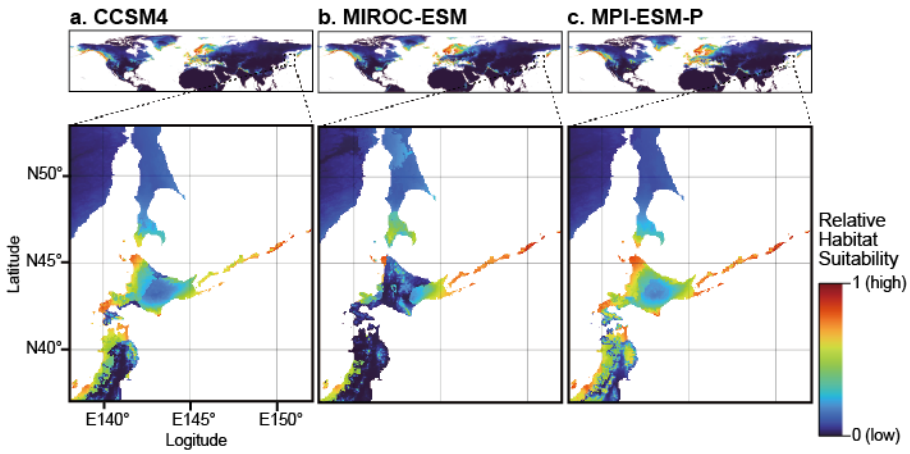

Figure 25. Relative habitat suitability using Maxent in the Middle Holocene. Each picture shows the result using CCSM4 (a), MIROC-ESM (b), and MPI-ESM-P (c).

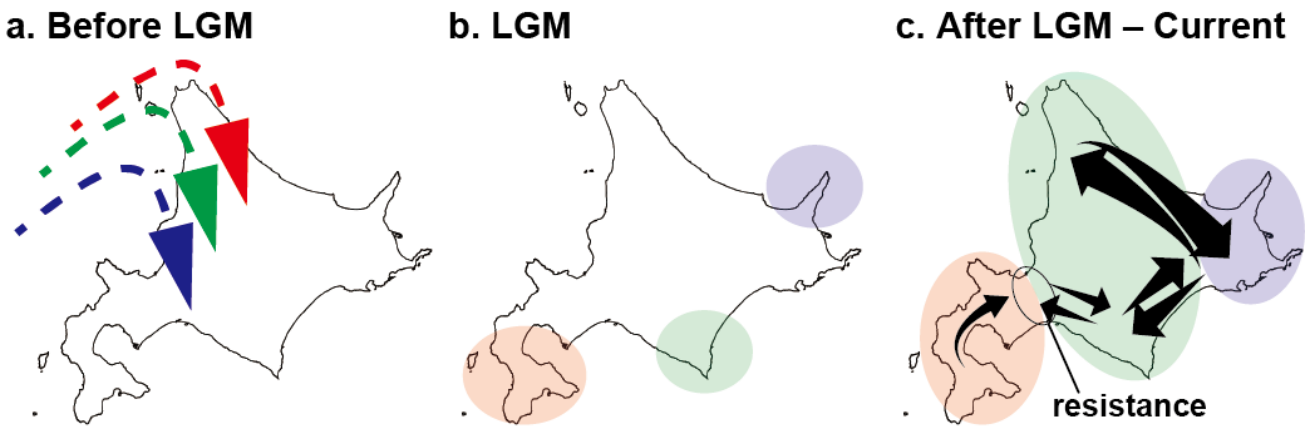

Figure 26. Demographic history scenario of the Hokkaido brown bear population. Each picture means before LGM (a), LGM (b), and after LGM–Current (c).

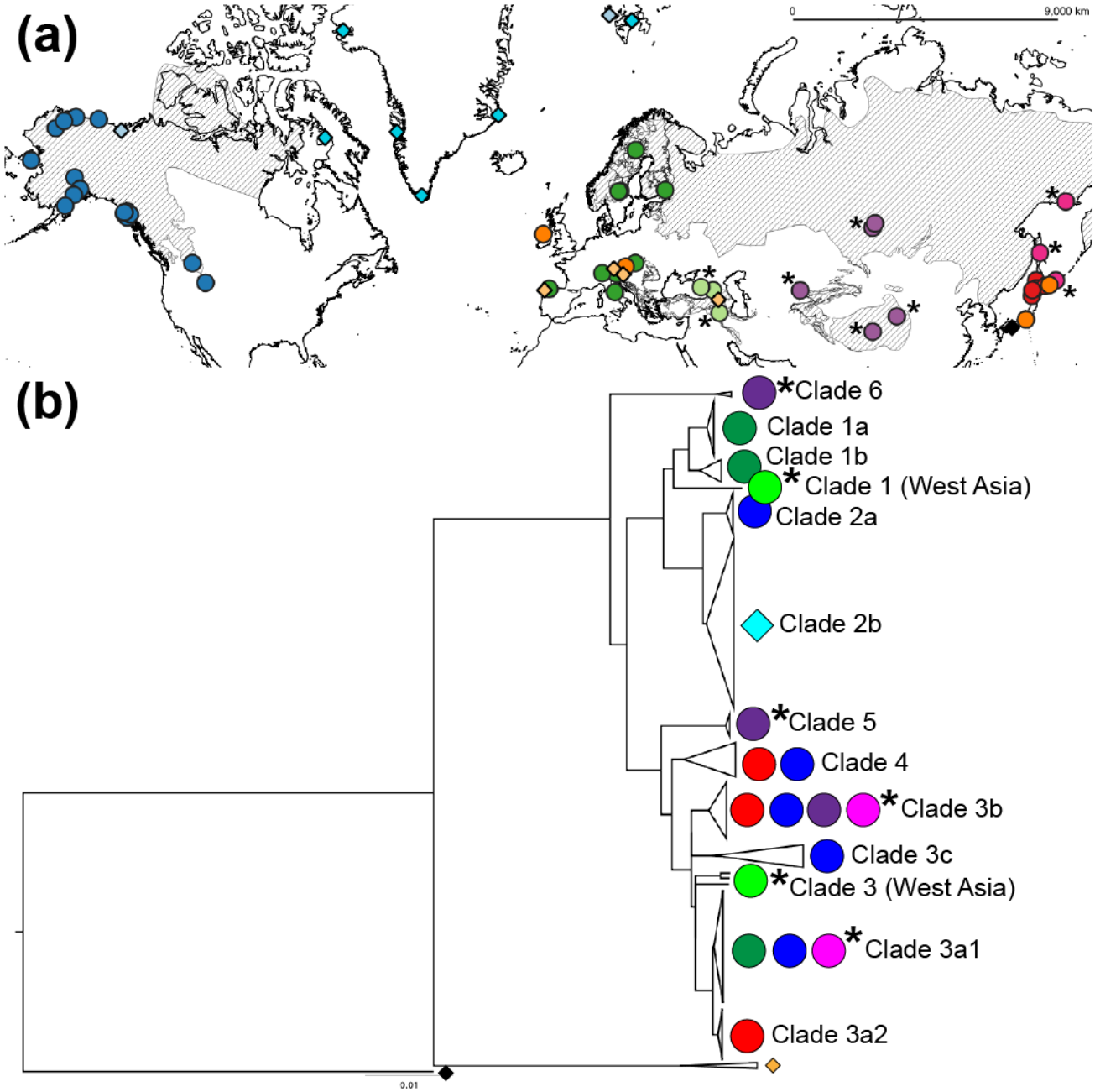

Figure 27. Sampling locations for bears used in this article excluded outgroup (a) and phylogenetic tree of the brown bear's mtDNA lineages (b). The shaded area reflects the current habitat of the brown bear (McLellan et al. 2017). The colors of dots mean groups (Table 23); each dot is included (ancient brown bear, dark orange; ancient polar bear, light blue; cave bear, light orange; brown bear from West Asia, light green; brown bear from Central Asia, purple; brown bear from East Asia, pink; Europe, green; Hokkaido, red; North America, blue). These shapes mean species (square, the polar bear or cave bear; circle, the brown bear). The asterisks shown near the dots mean new sequence data reported in this article. These sampling locations were inferred by the collected region (Hirata et al. 2014) and habitat of the brown bear (McLellan et al. 2017). 2 samples (GT_1 and Asiatic_black_bear) were not shown in this map because these individuals are from zoos.

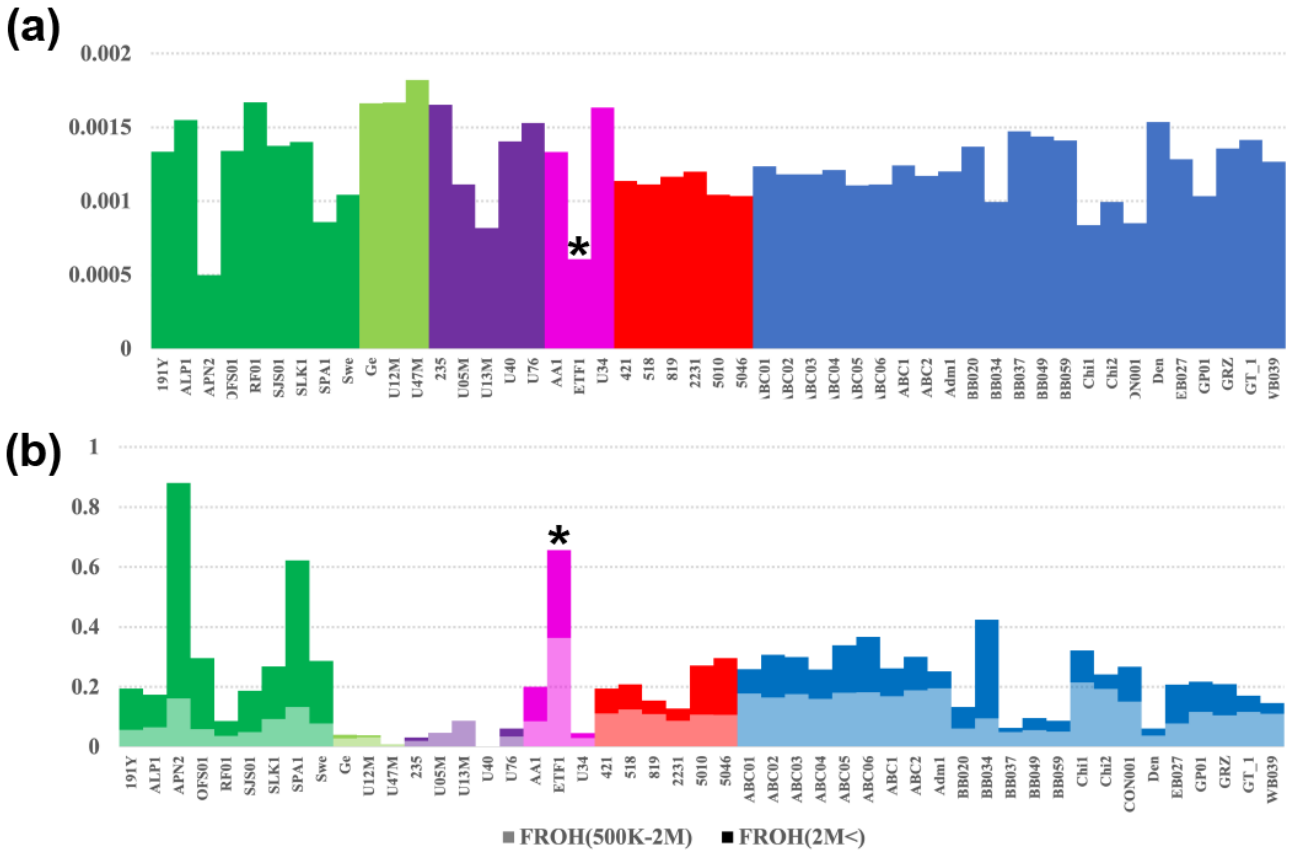

Figure 28. Genetic diversity per sample based on the heterozygosity (a) and frequency of the run of homozygosity (b). The result for an individual from Etorofu Island is denoted with an asterisk placed at the top of the bar.

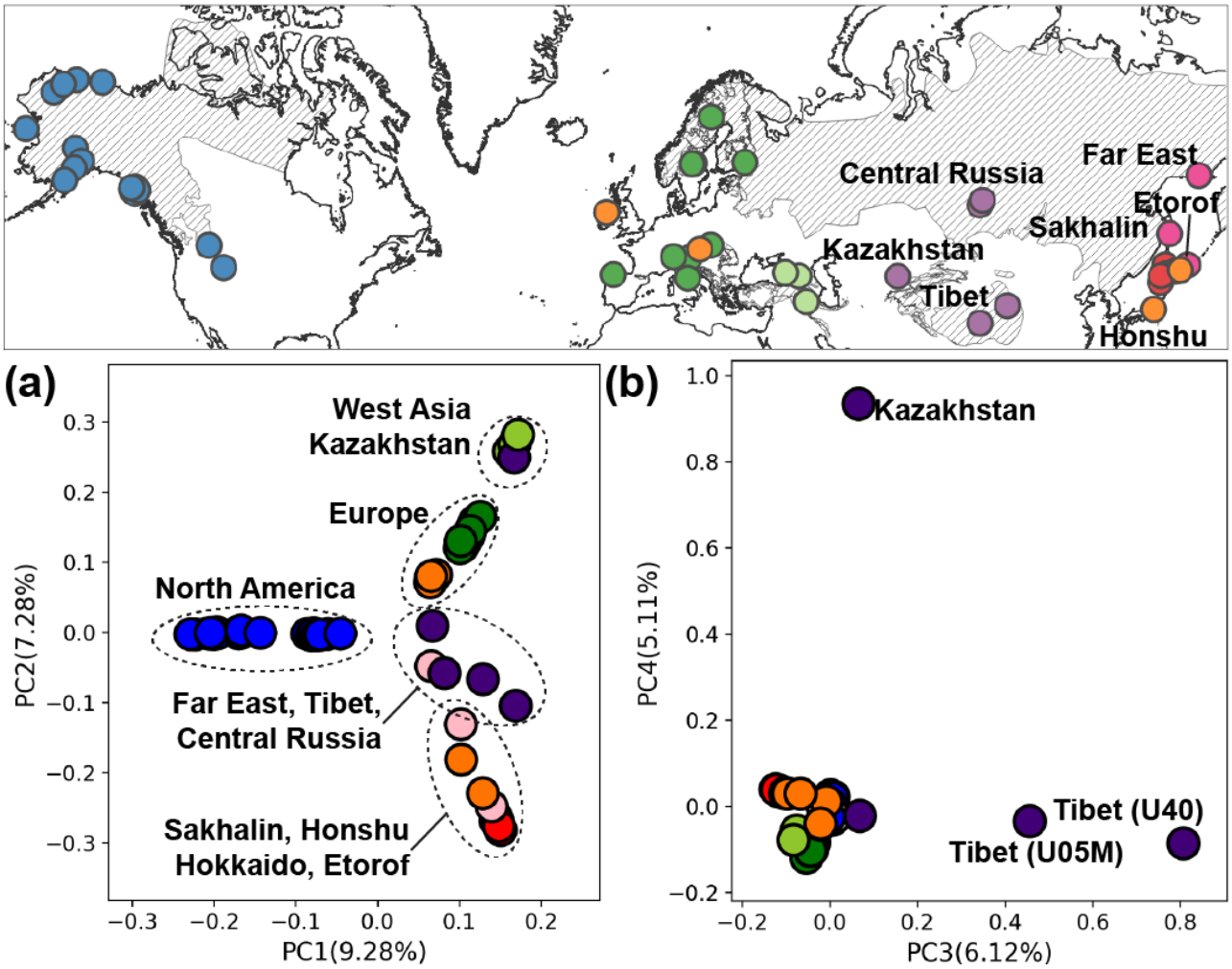

Figure 29. PCA of both modern and ancient samples. The results of the first and second principal components are presented in (a), and the third and fourth principal components results are depicted in (b). The colors of dots on the PCA mean groups and correspond with the color shown in the worldwide map.

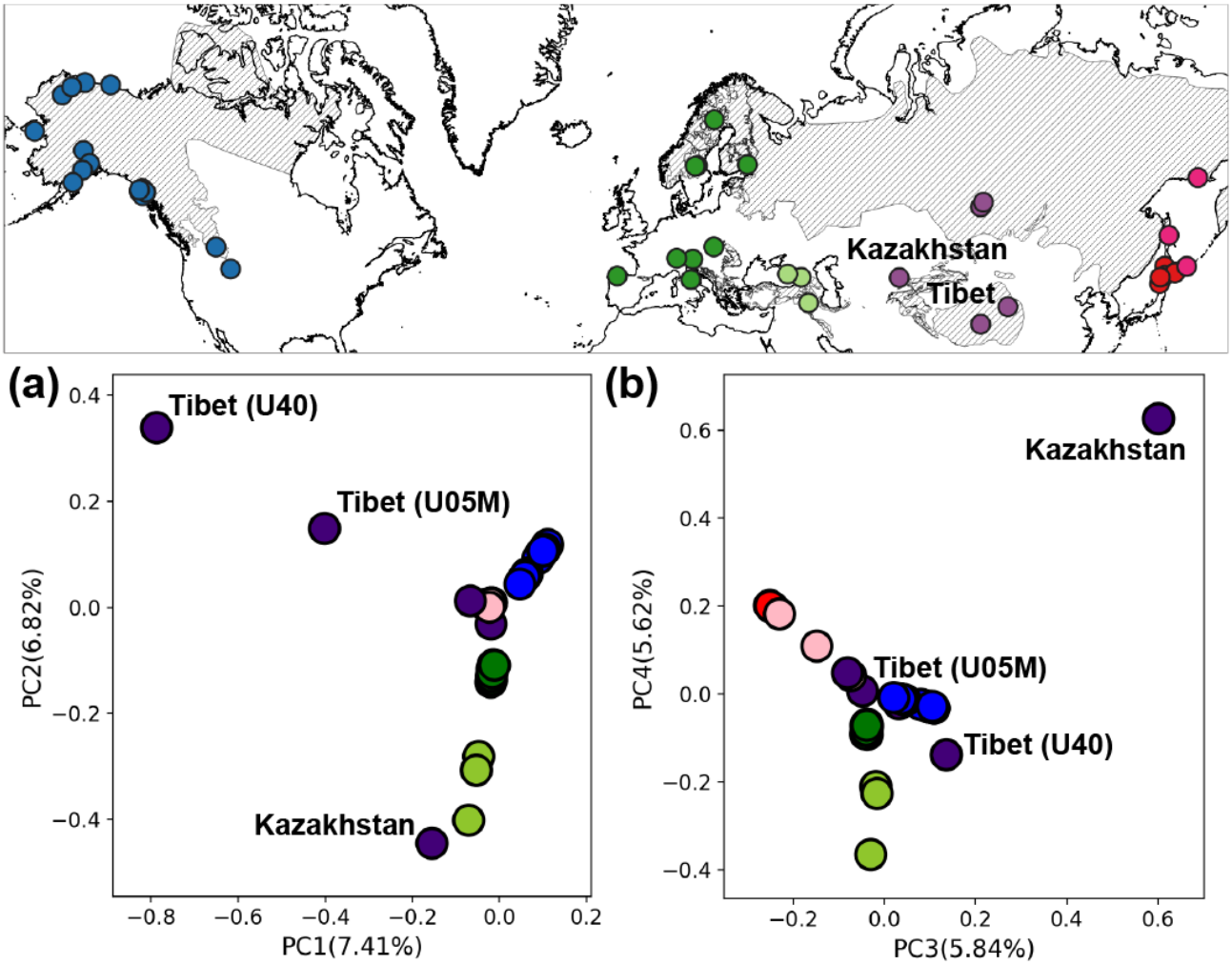

Figure 30. PCA of only modern samples. The results of PCA 1 and PCA 2 are presented in (a), and PCA 3 and PCA 4 results are depicted in (b). The colors of dots on the PCA mean groups and correspond with the color shown in the worldwide map.

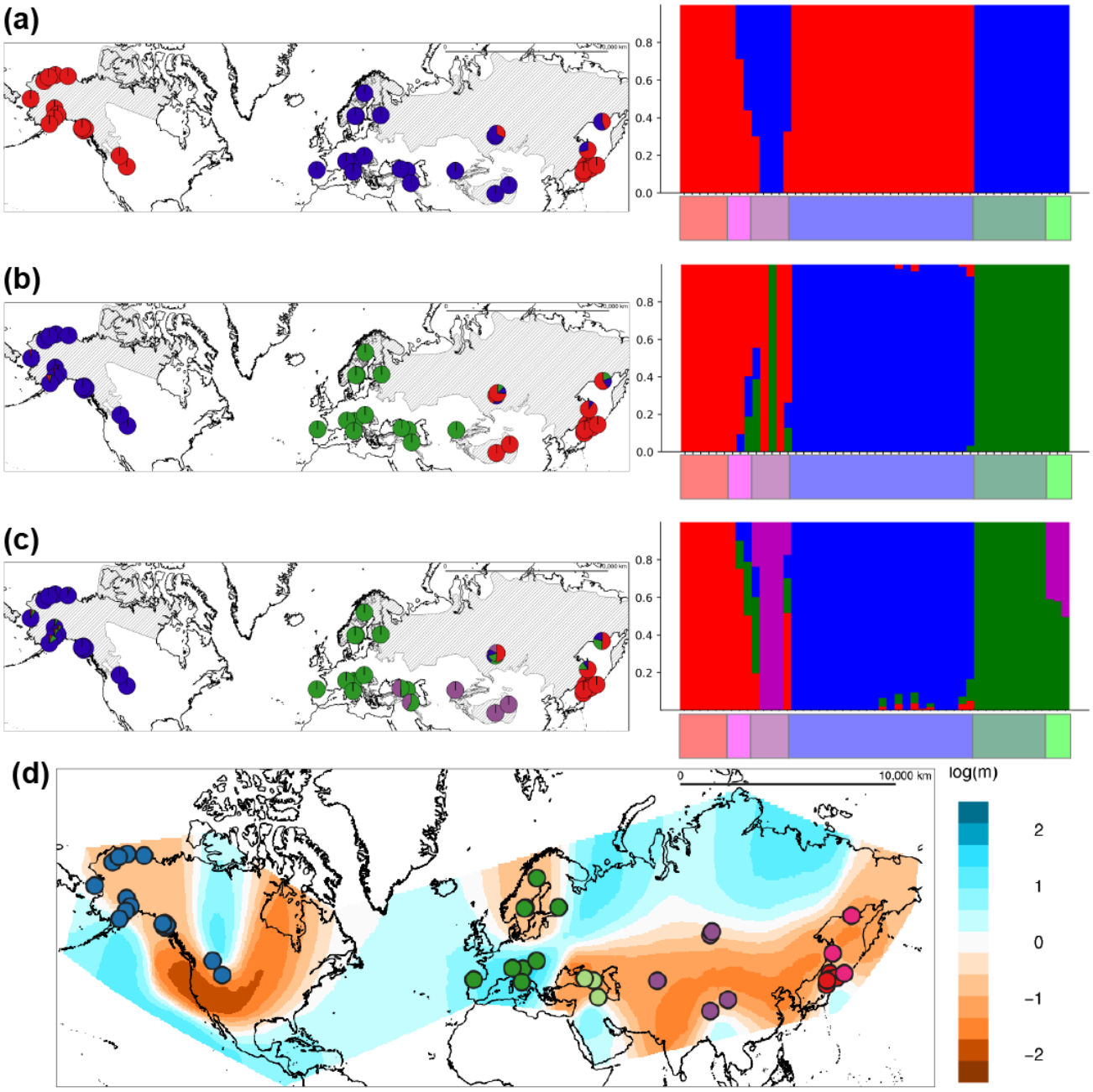

Figure 31. Genetic structure. This figure shows the result of each analysis: ADMIXTURE (*K*=2) (a), ADMIXTURE (*K*=3) (b), ADMIXTURE (*K*=4) (c), and EEMS (d), corresponding with the sampling locations. The bar colors below the result of ADMIXTURE correspond with the dot colors in Figure 31d. One sample (GT_1) was excluded in EEMS because I could not find the information about its capturing place in detail.

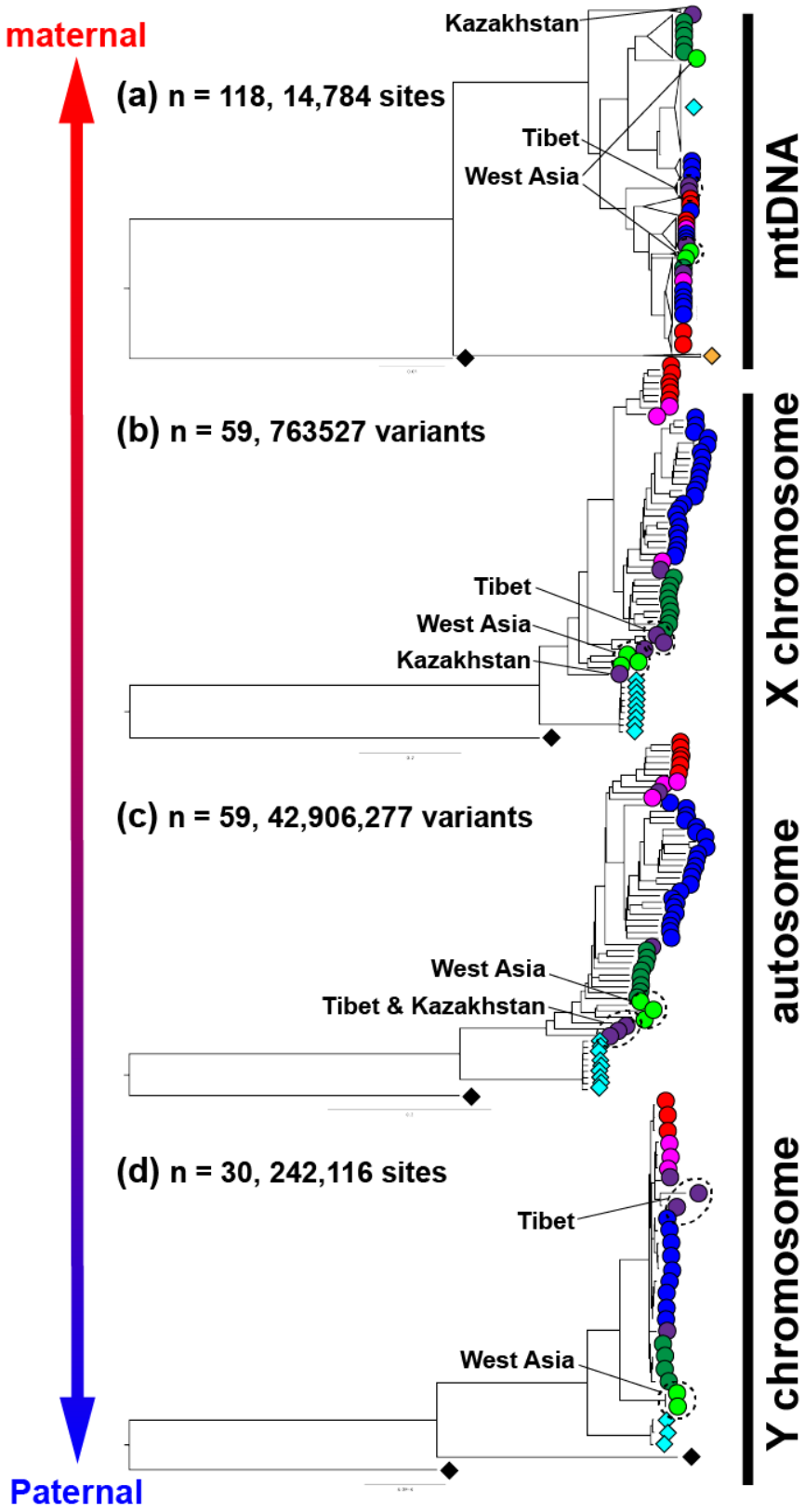

Figure 32. Phylogenetic trees for four different heritable regions. Each tree was constructed based on mitochondrial DNA (a), X chromosome (b), autosome (c), and Y chromosome (d). The number of individuals and total sites or variants are shown in each tree. The dot shape and color correspond to the dots shown in Figure 27.

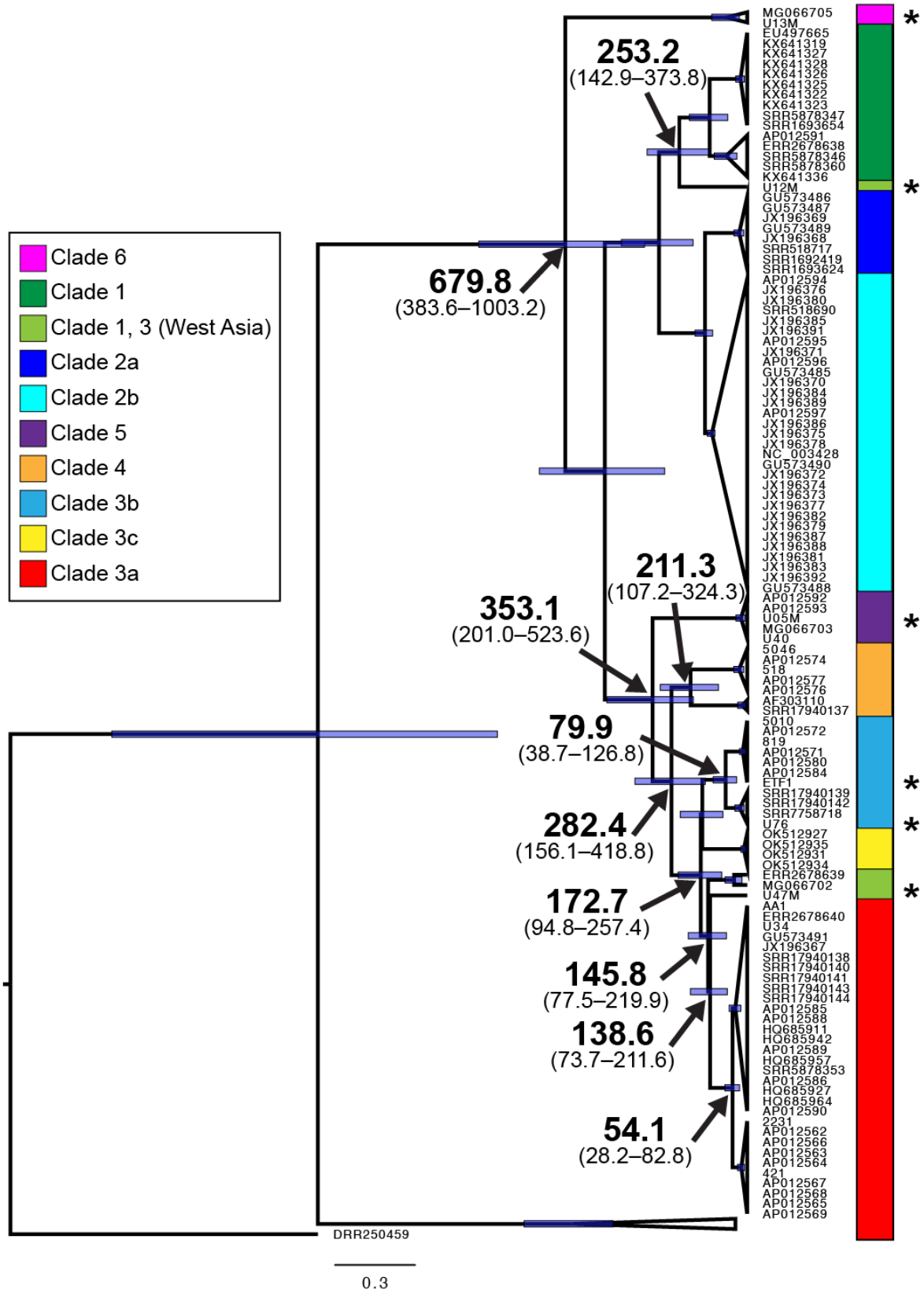

Figure 33. Phylogenetic tree based on the mitochondrial DNA sequence and these divergence times (thousand years ago). The number of individuals and total sites is the same as Figure 32a.

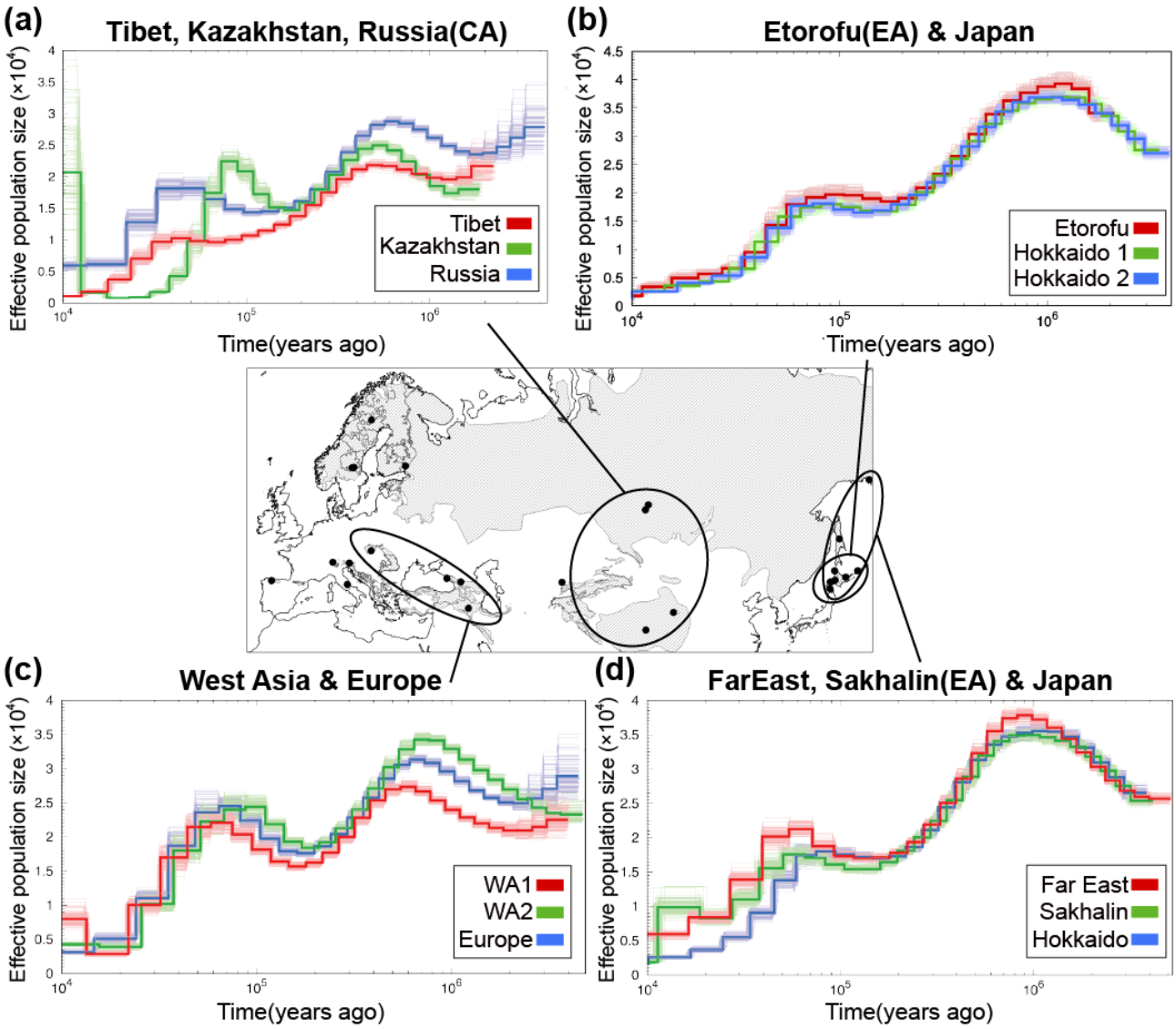

Figure 34. PSMC. Each figure shows the result of the Central Asia (a), the Hokkaido and Etorofu Island (b), the West Asia and Europe (c), and the Hokkaido and East Asia (d).

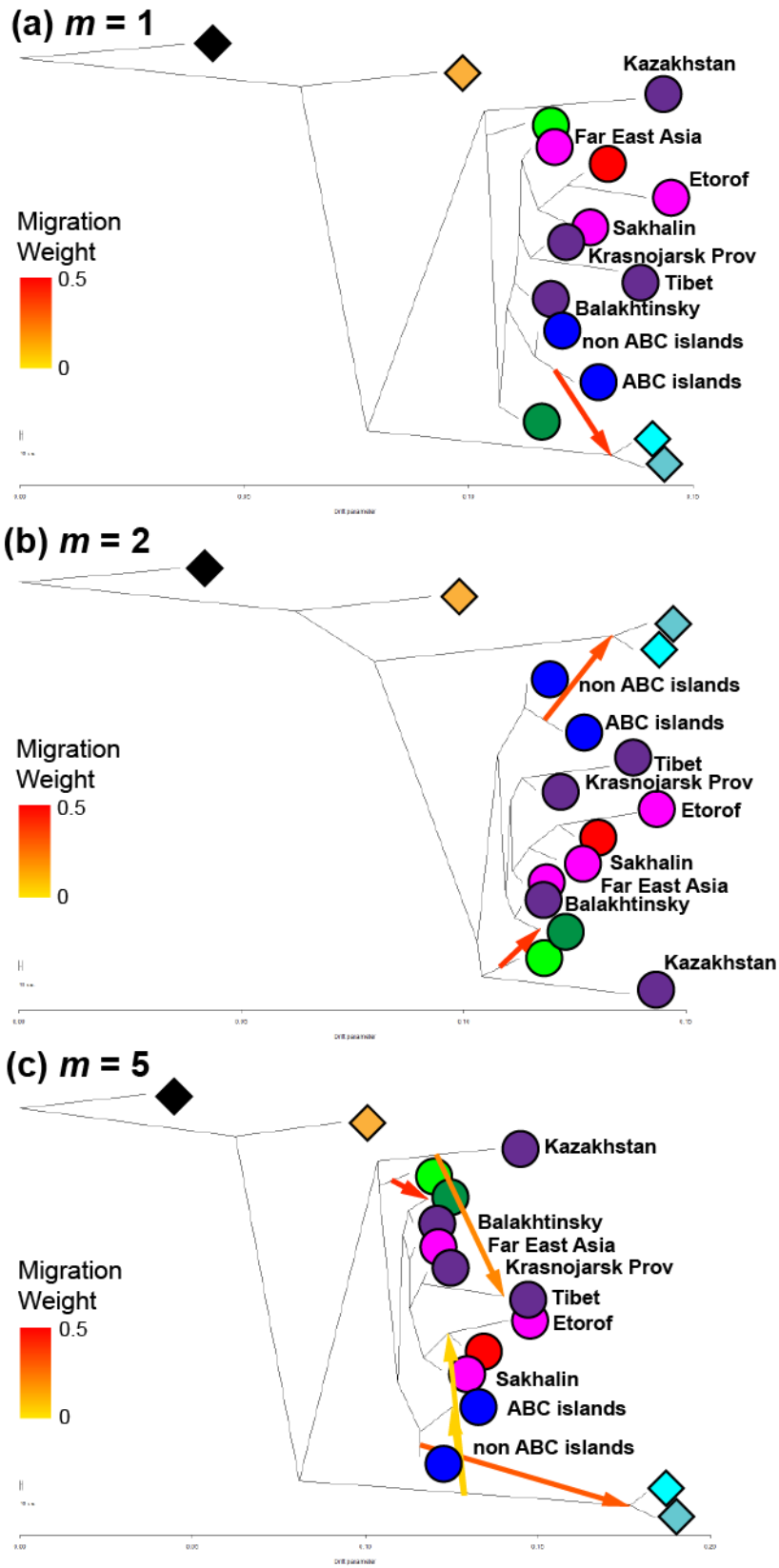

Figure 35. TreeMix. The figure shows the results of different the number of migrations: *m* = 1 (a), *m* = 2 (b), *m* = 5 (c). The geographical names shown next to the circles mean each sample applied in the analysis without including each Group described in Table 23.

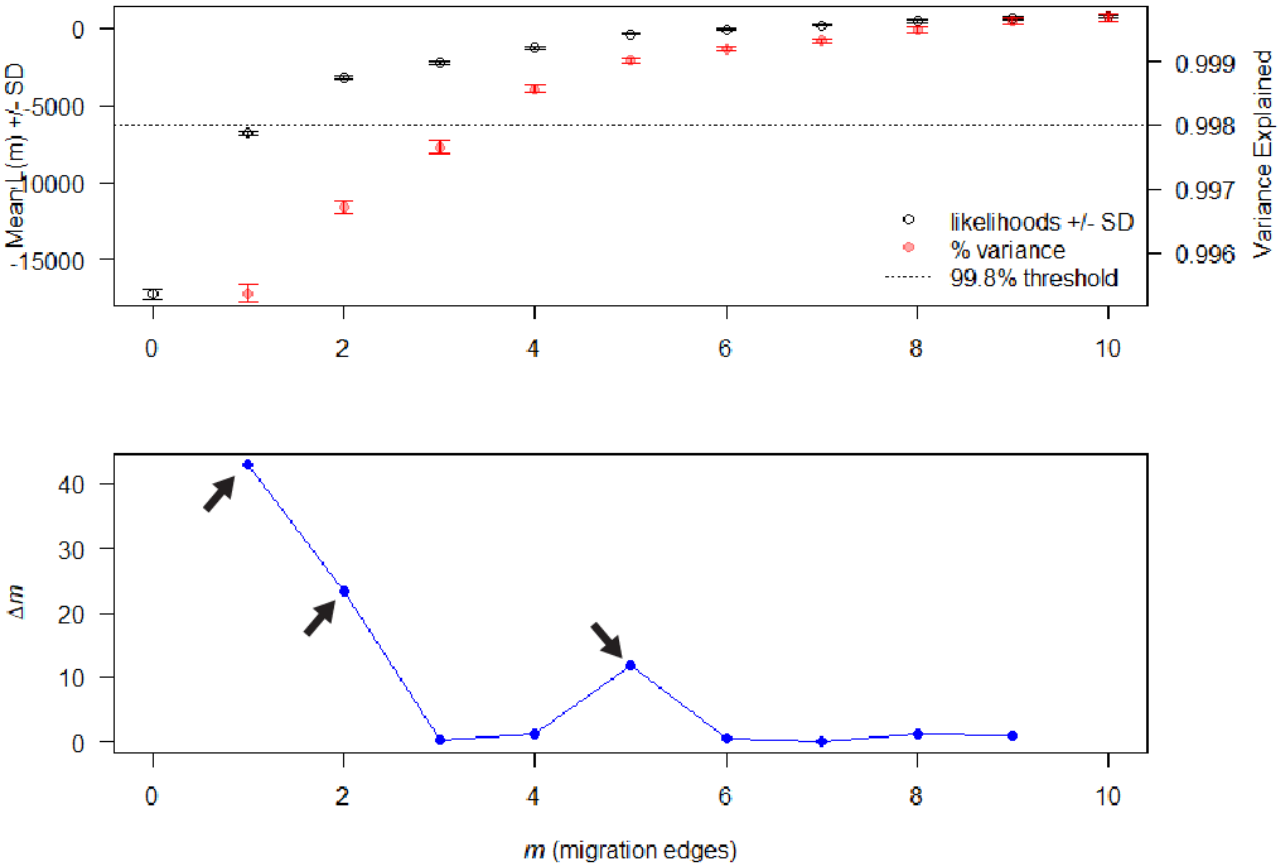

Figure 36. The optimal number of migration edges using OptM. The figure on the top shows the mean and standard deviation (SD) for the composite likelihood L(m) per migration edges. The figure on the bottom shows Δ*m*, whose higher value means a more optimal migration edge. The arrows shown on the bottom figure mean their results were shown in Figure 34.

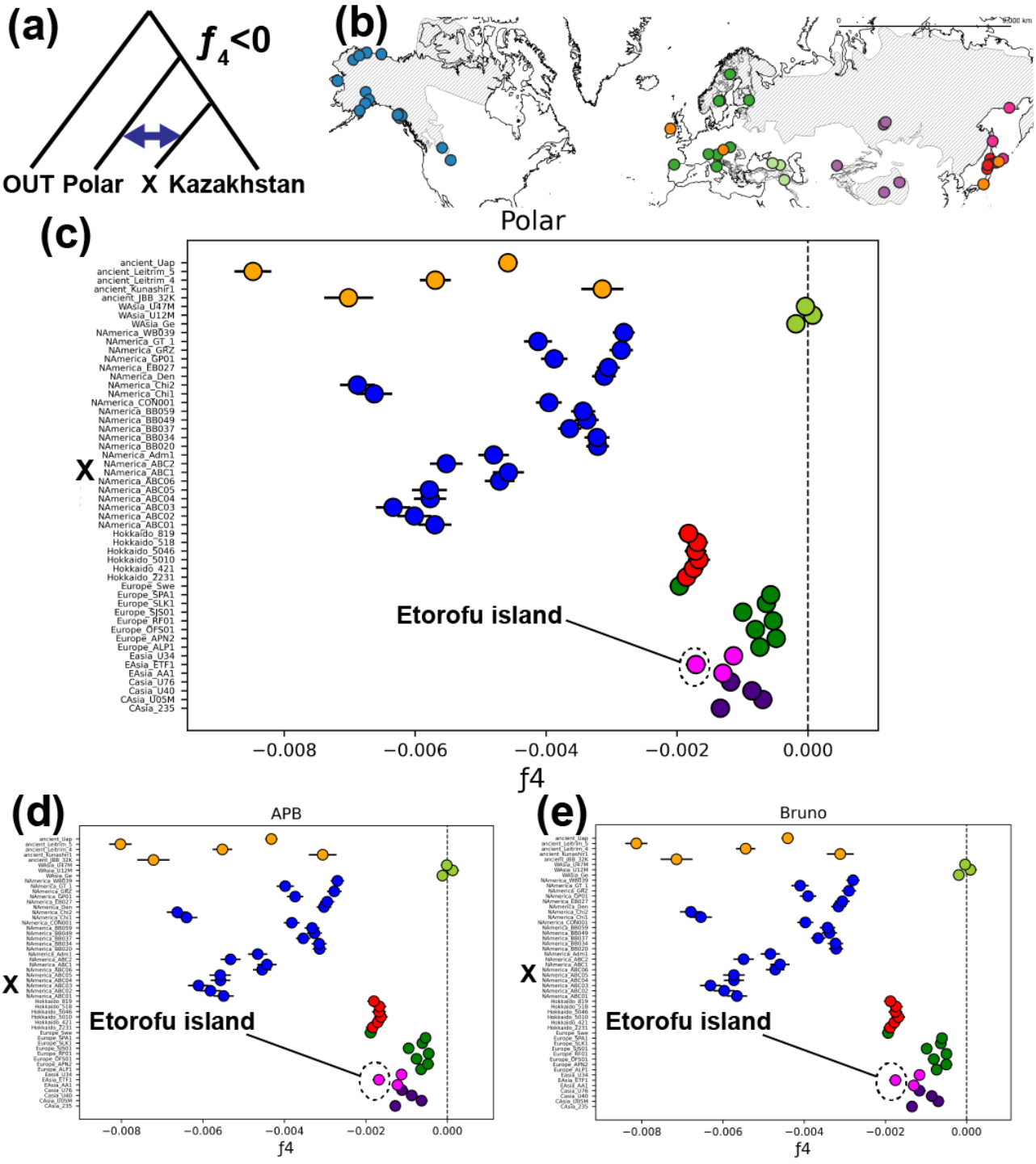

Figure 37. f_4(Asiatic black bear, Polar bear; X, Kazakhstan(U13M)) values. If f_4 value was lower than 0, gene flow between Polar bear and X, which means the brown bear individual, is supported (a). The dot colors are correlated with the dot colors on the worldwide map (b). Each figure shows the result of f_4(Asiatic black bear, modern Polar bear; X, Kazakhstan(U13M)) (c), f_4(Asiatic black bear, APB, an ancient Polar bear; X, Kazakhstan(U13M)) (d), and f_4(Asiatic black bear, Bruno, an ancient Polar bear; X, Kazakhstan(U13M)) (e). The absolute values of Z scores were 3 <, excluding the values when X was the individual from West Asia.

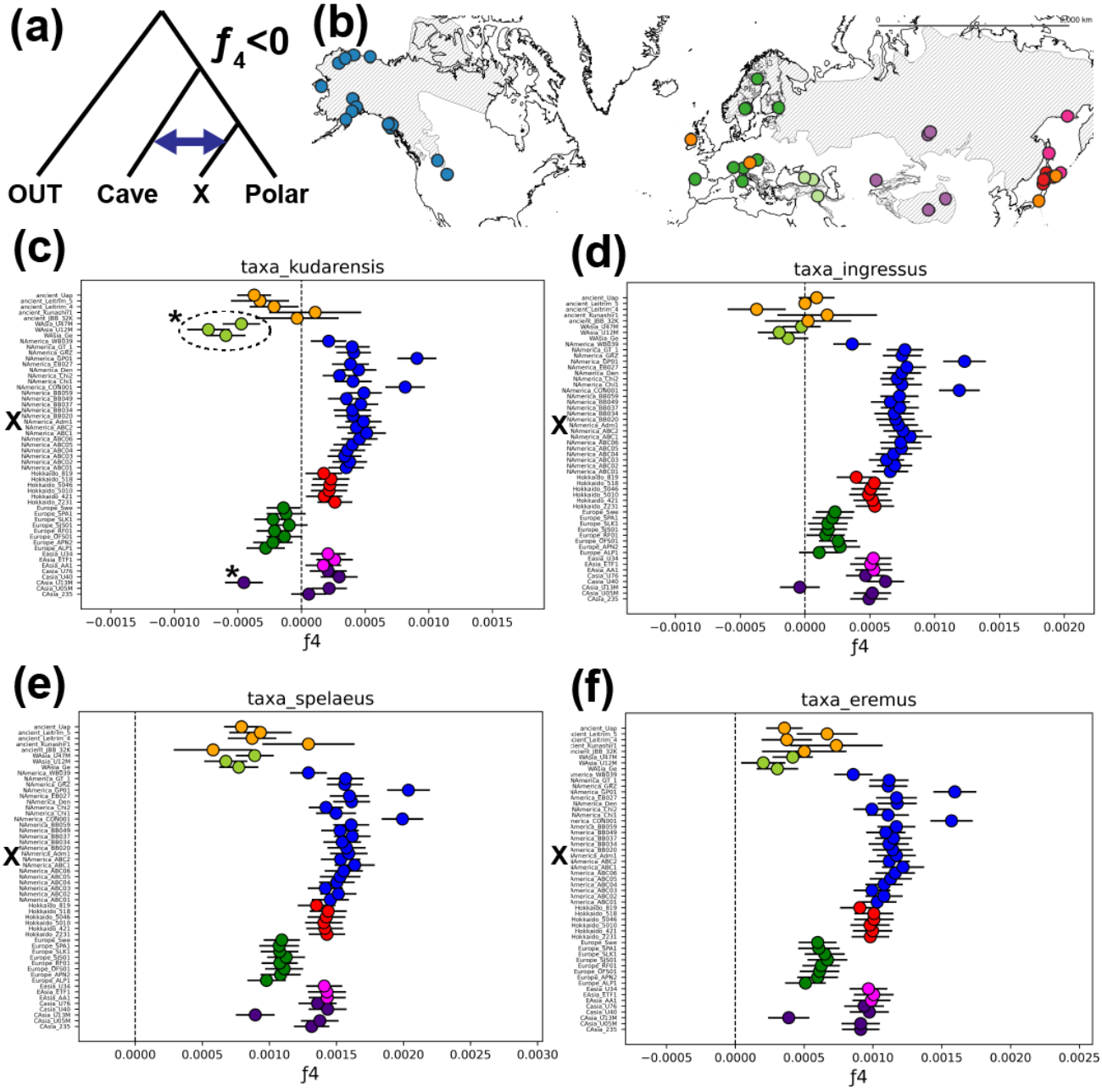

Figure 38. f_4(American black bear, Cave bear; X, modern Polar bear) values. If f_4 value was lower than 0, gene flow between Cave bear and X, which means the brown bear individual, is supported (a). The dot colors are correlated with the dot colors on the worldwide map (b). Each figure shows the result of f_4(American black bear, HV74(taxa *kudarensis*); X, Polar bear) (c), f_4(American black bear, GS136(taxa *ingressus*); X, Polar bear) (d), and f_4(American black bear, E_VD_1838(taxa *spelaeus*); X, Polar bear) (e), and f_4(American black bear, WK01(taxa *eremus*); X, Polar bear) (f). Only values shown with an asterisk were confirmed statistically significant (|Z score| > 3).

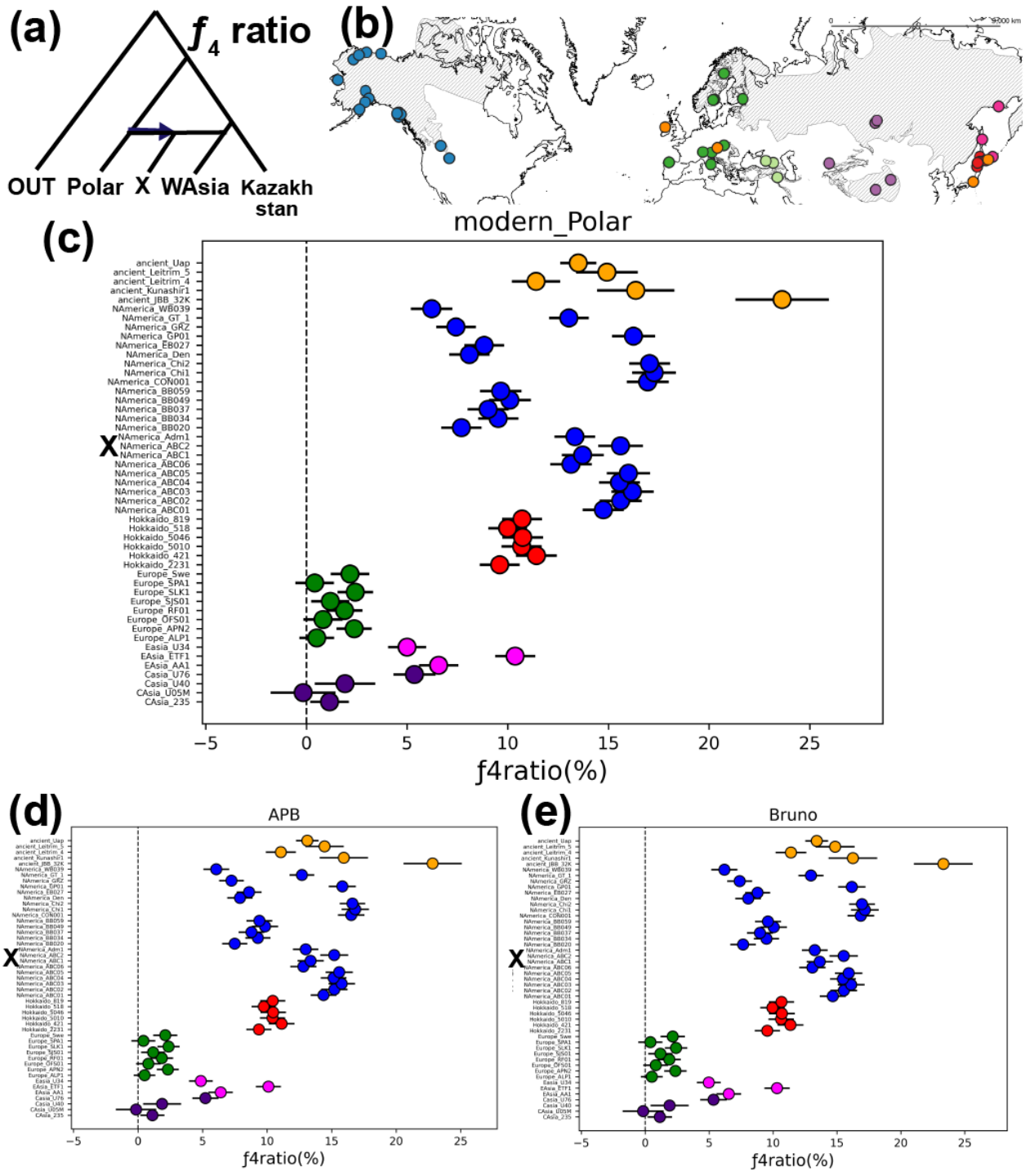

Figure 39. The percentage of the admixture proportion from the polar bear based on f_4 ratio. f_4 ratio (%) means the proportion of gene flow from the polar bear to X, which represent a brown bear individual (a). The dot colors correlate with those on the world map (b). Each figure shows the result when the polar bear is the modern polar bear (c), APB is an ancient polar bear (d), and Bruno is an ancient polar bear (e).

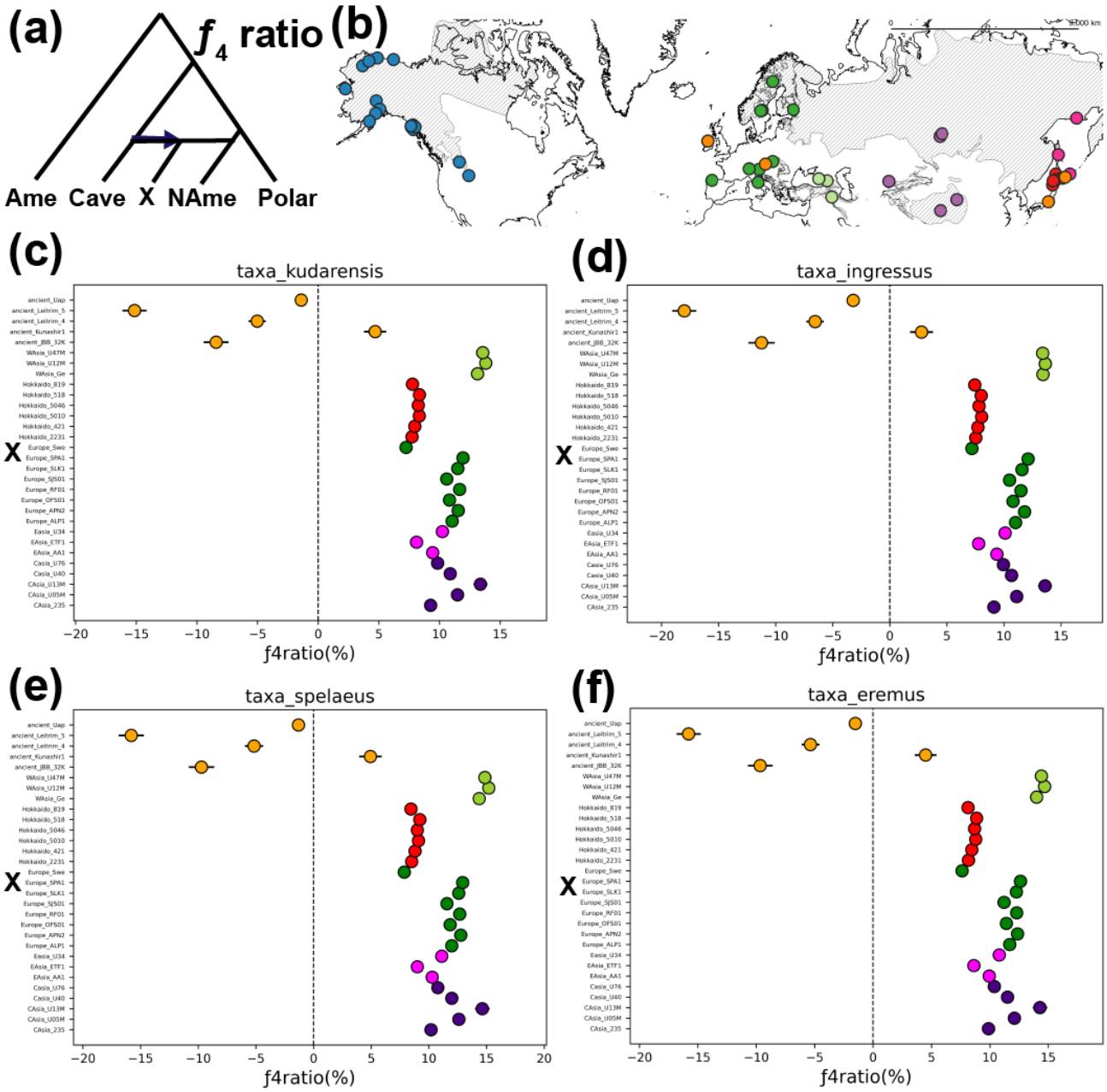

Figure 40. The percentage of the admixture proportion from the cave bear based on f_4 ratio. f_4 ratio (%) means the proportion of gene flow from the cave bear to X, which represent a brown bear individual (a). The dot colors correlate with those on the world map (b). Each figure shows the result when the cave bear is HV74(taxa *kudarensis*) (c), GS136(taxa *ingressus*) (d), E_VD_1838(taxa *spelaeus*) (e), and WK01(taxa *eremus*).

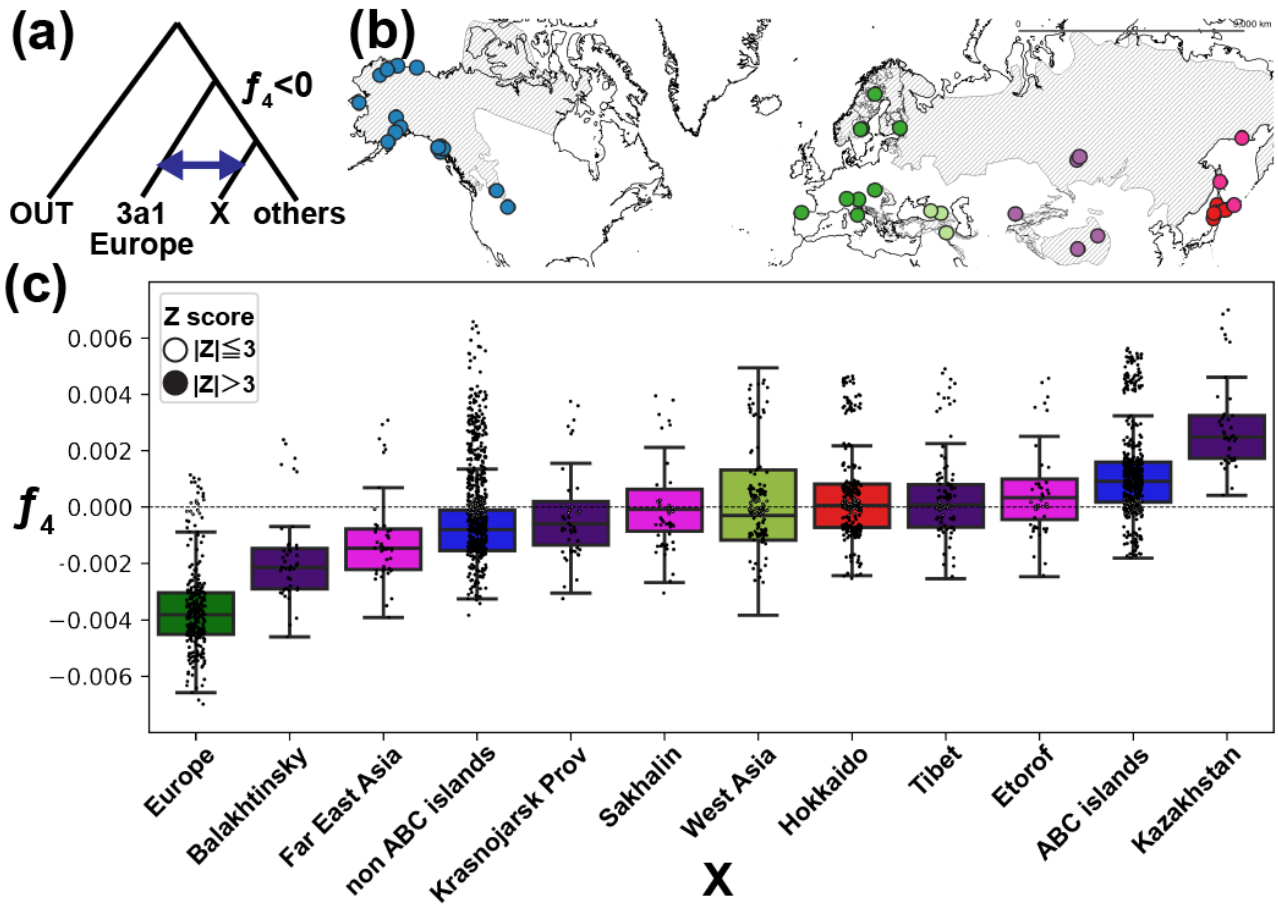

Figure 41. f_4(Outgroup, clade 3a1 in Europe; X, the modern brown bear excluding X) values. Where f_4 value is lower than 0, the gene flow between clade 3a1 in Europe and X, which means the brown bear individual, is supported.

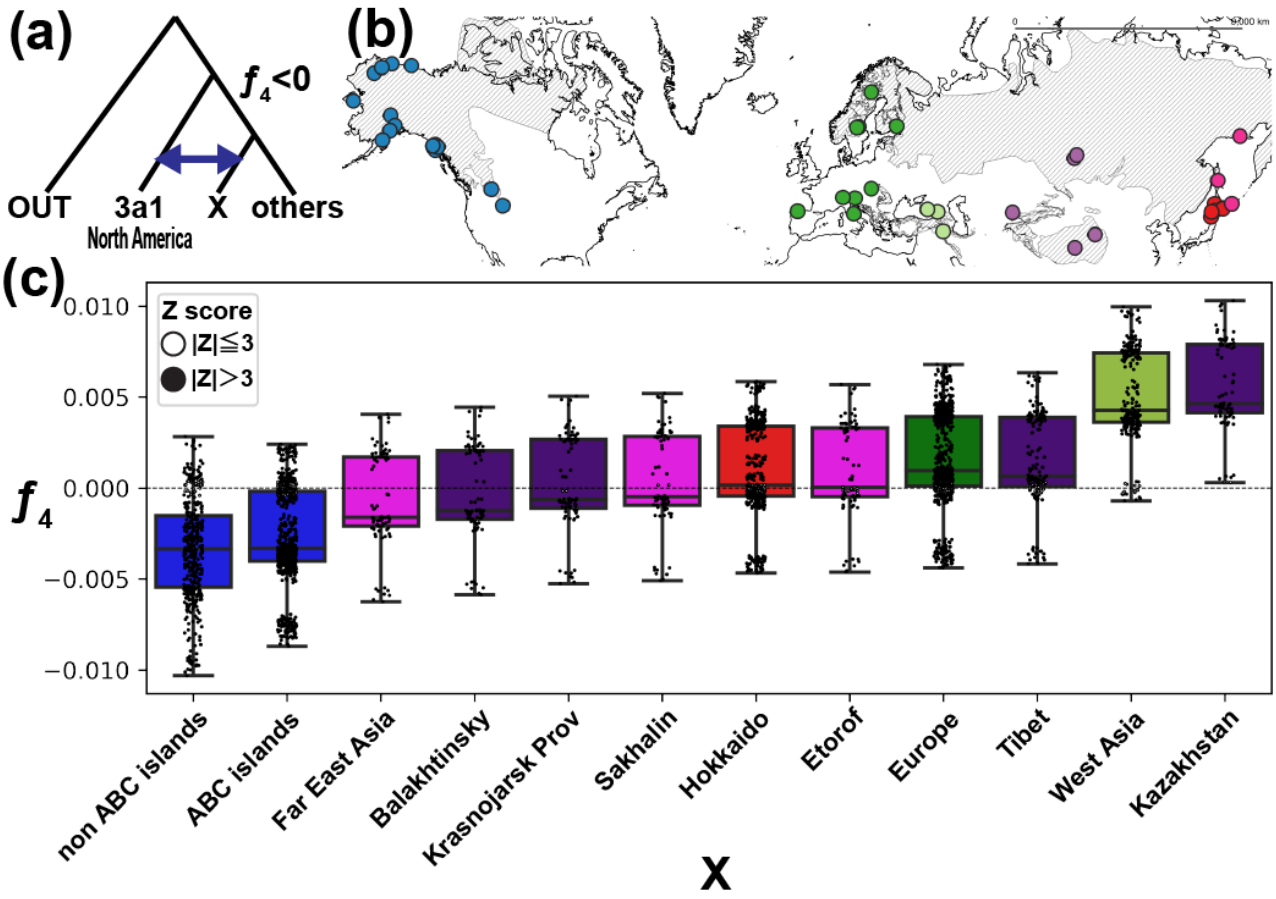

Figure 42. f_4(Outgroup, clade 3a1 in North America; X, the modern brown bear excluding X) values. Where f_4 value is lower than 0, the gene flow between clade 3a1 in North America and X, which means the brown bear individual, is supported.

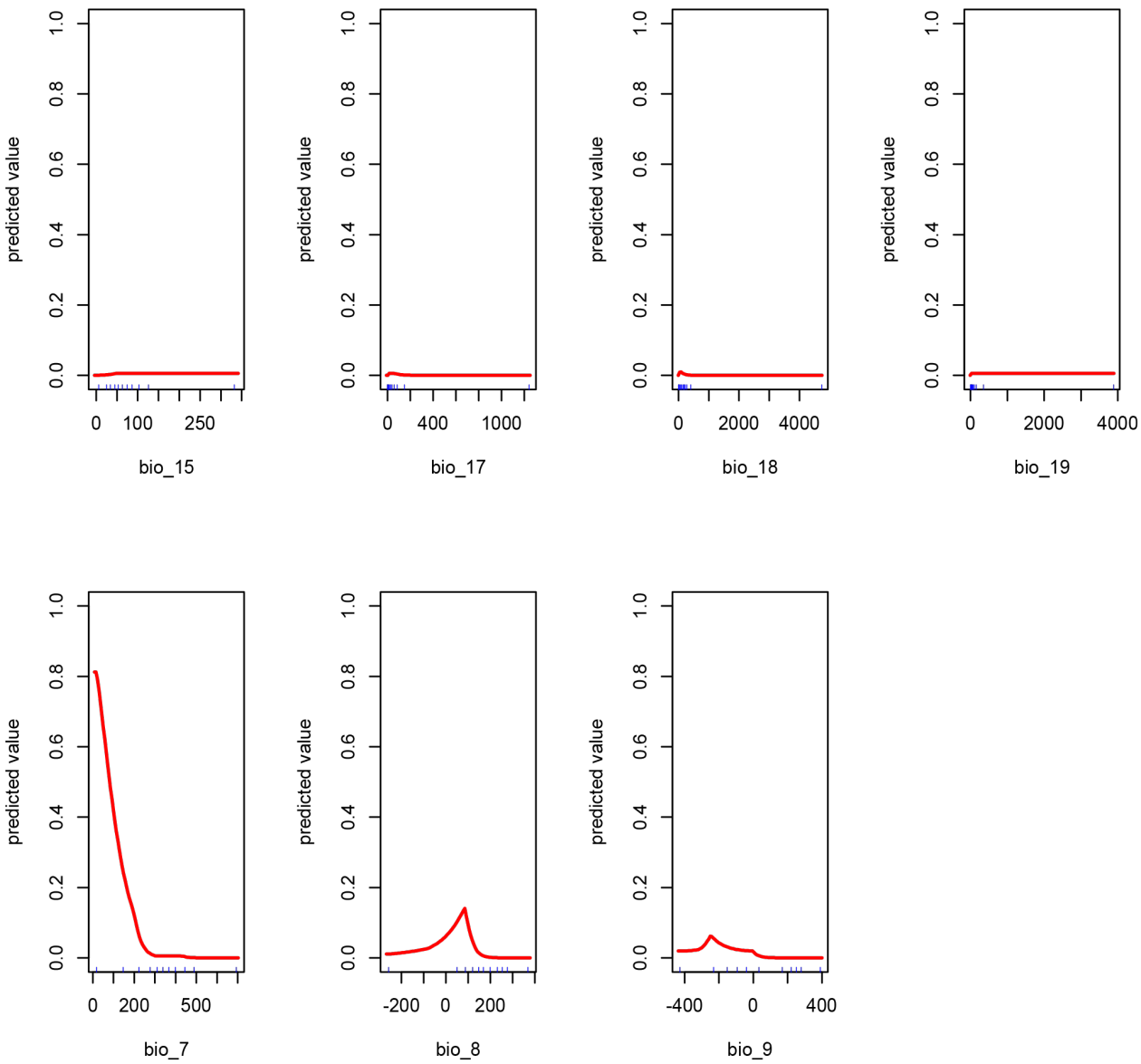

Figure 43. Response curves of each environmental variance in the best model. The curves show the predicted value (Y-axis) changes in each environmental variance (X-axis).

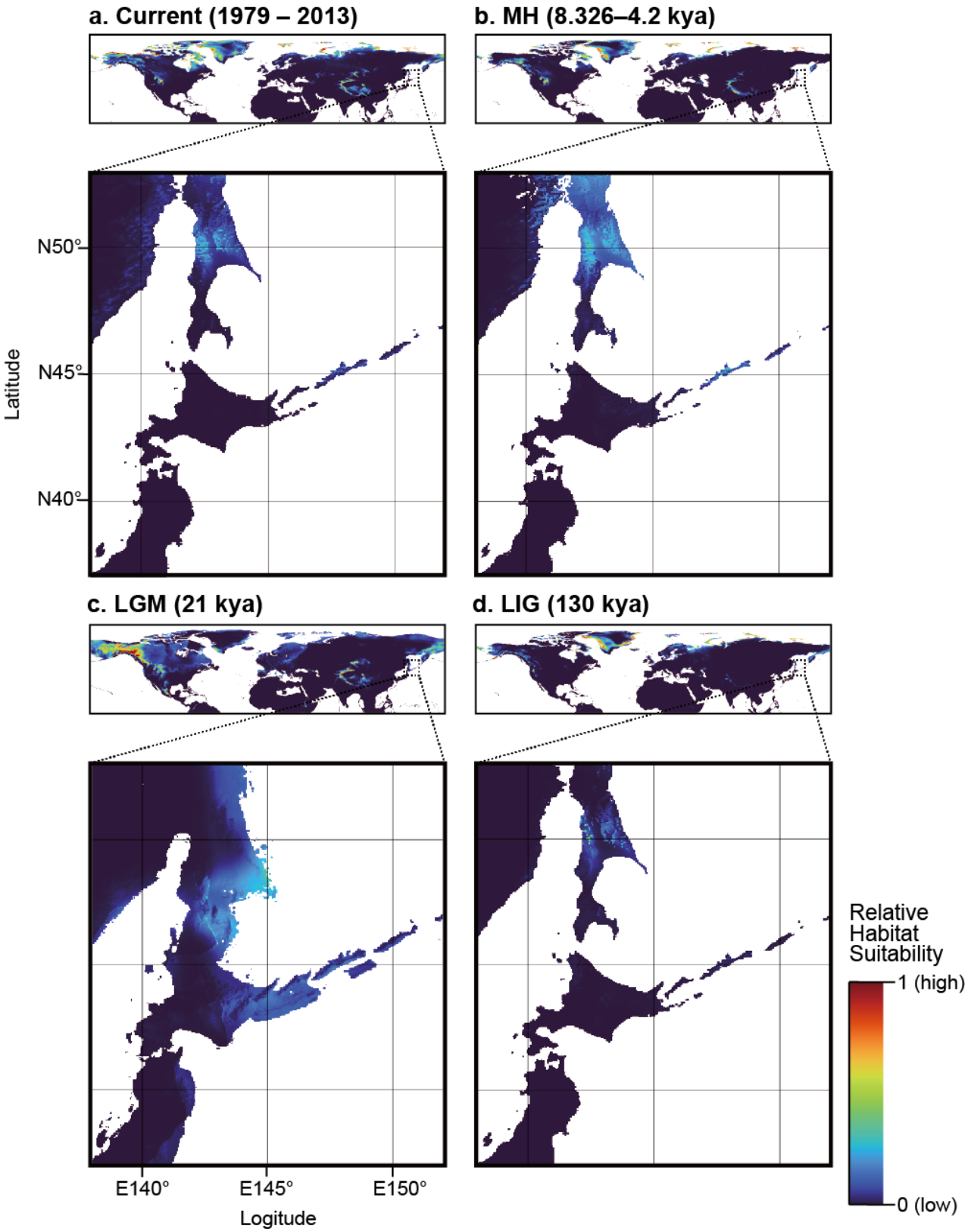

Figure 44. Inferred change of relative habitat suitability of the polar bear. Each picture shows the result of the Current (a), the Middle Holocene (b), the Last Glacial Period (c), and the Last Inter Glacial (d).

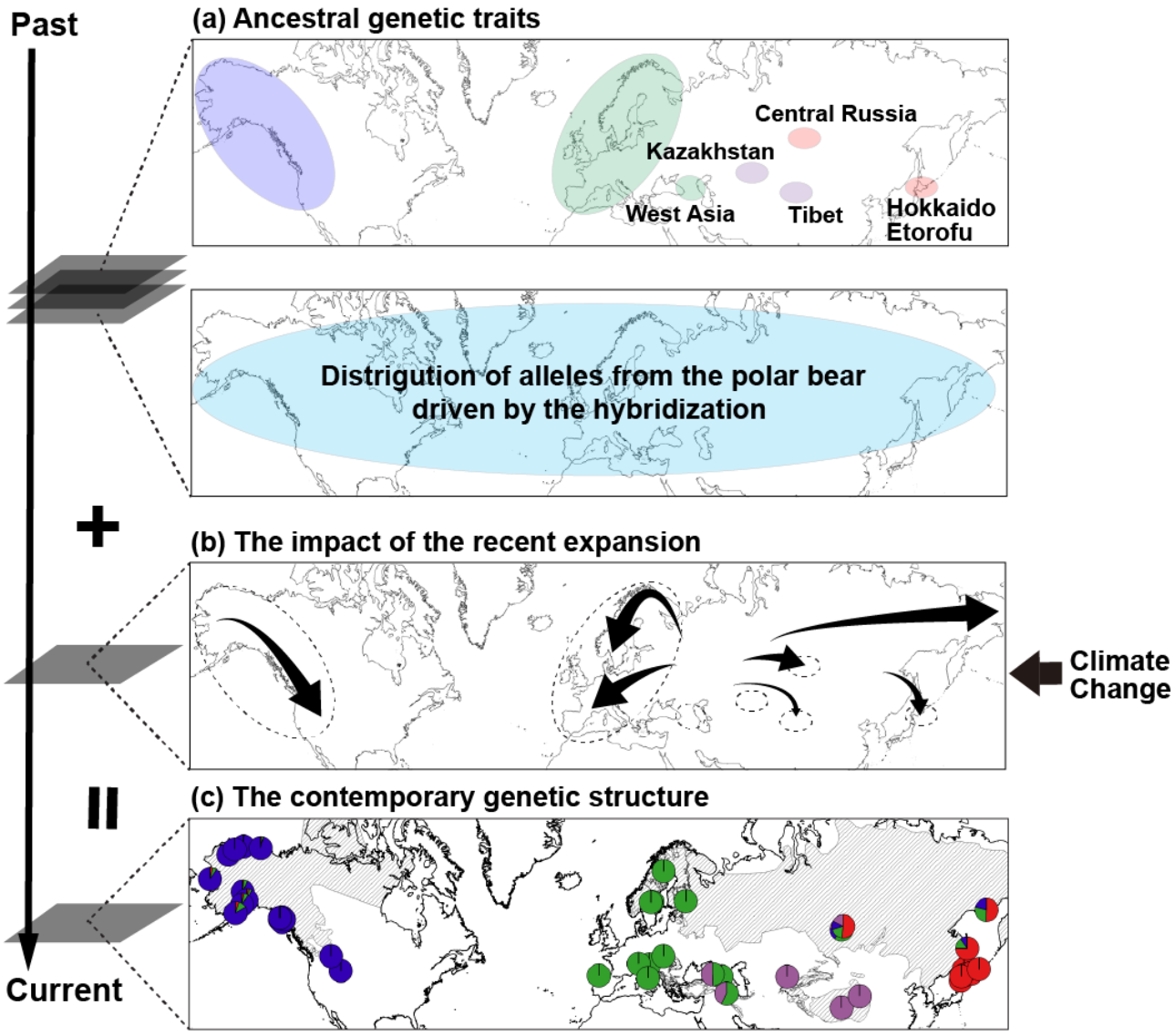

Figure 45. Multi layers in the genetic structure of the brown bear populations inferred by the results of this study. (a) Ancestral genetic traits before the recent expansion and (b) the scale of the recent expansion. The upper and lower figures in Figure 31c represent the ancestral genetic structure and allele frequency driven by hybridization with the polar bear, respectively. The bolder the arrows shown in (b), the greater the impact of the recent expansion estimated by f_4 statistics.

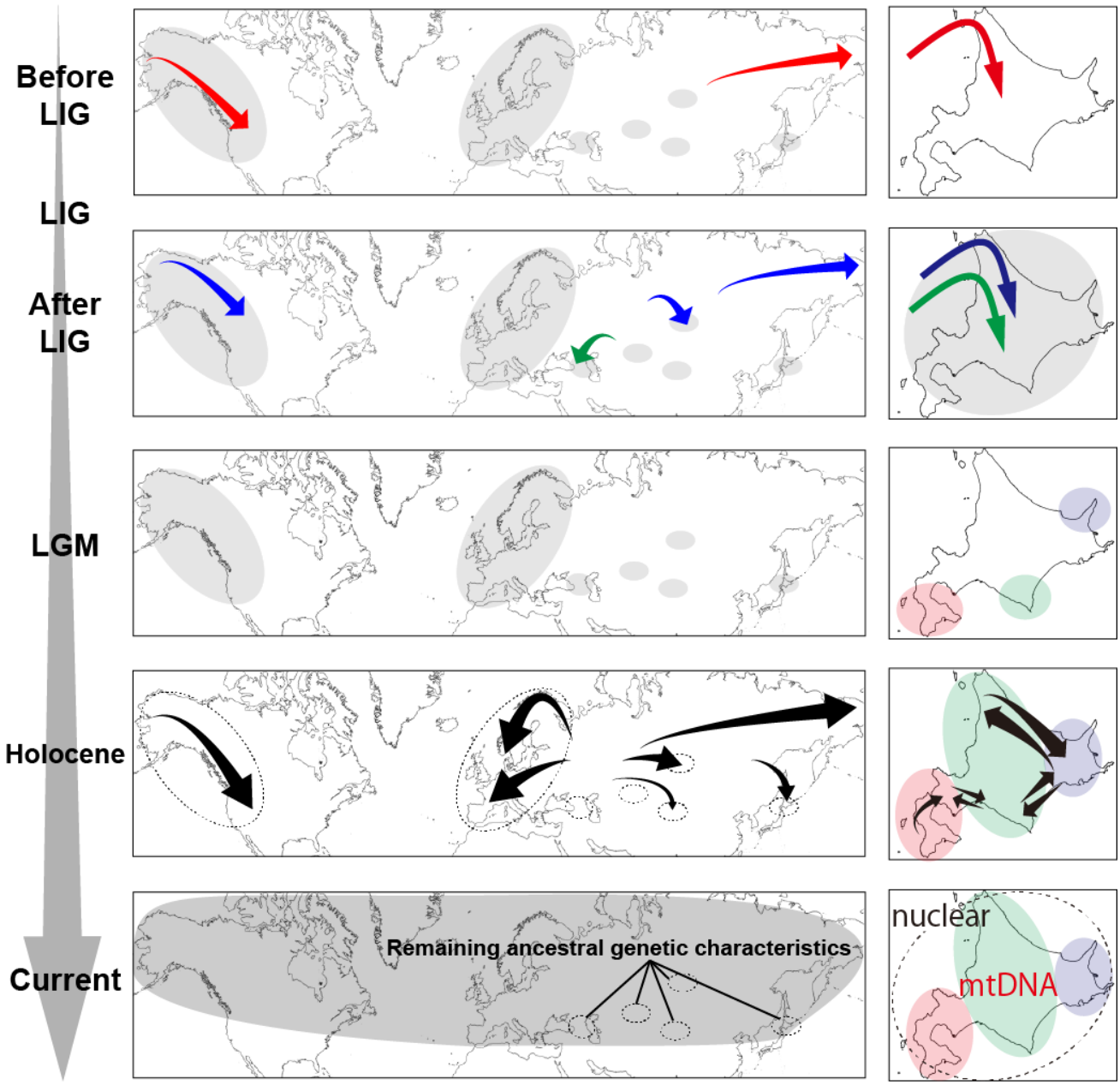

Figure. 46. Conclusion of this dissertation. The scenario about the population demographic history of the brown bear, based on the results in this thesis, is shown in chronological order from top to bottom. The red, green blue arrows and circles mean the clade 4, 3b, and clade 3a except for 3a1, respectively. Grey circles represent populations that share the same alleles more than other populations.

Table 1. List of bear samples examined in this study.

Species	Sample name	Population	Sampling location	Sex	Reads aligned to the polar bear genome	Proportion of the genome covered (%)	Number of SNPs	Mean depth per individual	Instrument model	NCBI accession number	Reference	Remarks
Brown bear	Southern Hokkaido 1 (518)	Hokkaido	Kikonai, Hokkaido, Japan	F	688,637,360	96.6%	4,271,702	38.79	Illumina Hiseq X	DRR276774	-	
Brown bear	Southern Hokkaido 2 (5046)	Hokkaido	Kyowa, Hokkaido, Japan	M	895,857,288	98.3%	4,216,493	54.87	Illumina Hiseq X	DRR276775	-	
Brown bear	Central Hokkaido 1 (2231)	Hokkaido	Bibai, Hokkaido, Japan	F	900,845,720	98.3%	4,329,119	53.74	Illumina Hiseq X	DRR276776	-	
Brown bear	Central Hokkaido 2 (421)	Hokkaido	Toyotomi, Hokkaido, Japan	M	842,793,684	97.6%	4,285,305	50.02	Illumina Hiseq X	DRR276777	-	
Brown bear	Eastern Hokkaido 1 (5010)	Hokkaido	Kiyosato, Hokkaido, Japan	F	879,591,070	98.1%	4,218,591	52.47	Illumina Hiseq X	DRR276778	-	
Brown bear	Eastern Hokkaido 2 (5046)	Hokkaido	Syari, Hokkaido, Japan	M	861,014,212	97.9%	4,305,849	52.15	Illumina Hiseq X	DRR276779	-	
Brown bear	Russia	Russia	Balakhtinsky District, Russia	Unknown	365,300,696	98.2%	4,631,827	18.21	NextSeq 5000	ERR2678640	Barlow et al. (2018)	
Brown bear	Slovakia	Slovakia	Slovakia	M	424,613,162	98.7%	4,550,141	19.03	Illumina Hiseq 2000	SRR5878353	Benazzo et al. (2017)	
Brown bear	Georgia	Georgia	Great Caucasus, Georgia	Unknown	426,436,048	98.1%	4,748,290	20.87	NextSeq 5000	ERR2678639	Barlow et al. (2018)	
Brown bear	Southern Sweden 1	Sweden	Dalarna, Sweden	F	177,684,578	98.5%	4,153,172	9.62	Illumina Hiseq 2000	SRR1693654	Cahill et al. (2015)	
Brown bear	Southern Sweden 2	Sweden	Östanvik, Furudal, Sweden	F	380,222,608	99.2%	4,437,314	15.00	Illumina Genome Analyzer 2	SRR935626	Liu et al. (2014)	
Brown bear	Slovenia	Slovenia	Hrusica, Slovenia	Unknown	162,367,312	98.4%	4,395,974	9.51	NextSeq 5000	ERR2678638	Barlow et al. (2018)	
Brown bear	Northern Italy	Northern Italy	Alps, northern Italy	F	421,229,138	98.4%	4,648,341	18.54	Illumina Hiseq 2000	SRR5878346	Benazzo et al. (2017)	
Brown bear	Central Italy	Central Italy	Apennine, central Italy	M	416,965,160	98.4%	3,934,064	18.65	Illumina Hiseq 2000	SRR5878360	Benazzo et al. (2017)	
Brown bear	Spain	Spain	Spain	M	470,415,352	97.4%	4,170,113	21.38	Illumina Hiseq 2000	SRR5878347	Benazzo et al. (2017)	
Brown bear	Alaska	Alaska	Toronto Zoo (from unknown locality in Alaska, USA)	M	858,533,614	98.5%	4,479,501	25.36	Illumina Hiseq X	SRR7758718	Taylor et al. (2018)	No mitochondrial DNA data included
Brown bear	Denali	Denali	Denali, Alaska, USA	F	361,222,718	98.7%	4,454,847	20.28	Illumina Hiseq 2000	SRR830337	Cahill et al. (2013)	
Brown bear	Kenai	Kenai	Kenai, AK, USA	F	1,074,684,010	99.2%	4,318,747	17.03	Illumina Hiseq 2000	SRR518713	Miller et al. (2012)	
Brown bear	Admiralty 1	Admiralty	Admiralty Island, AK, USA	F	948,621,596	99.4%	4,188,549	36.42	Illumina Hiseq 2000	SRR518711	Miller et al. (2012)	
Brown bear	Admiralty 2	Admiralty	Admiralty Island, AK, USA	F	1,074,684,010	99.2%	4,124,981	20.91	Illumina Hiseq 2000	SRR830213	Cahill et al. (2013)	
Brown bear	Baranof	Baranof	Baranof Island, AK, USA	M	1,121,237,882	99.1%	4,065,687	32.42	Illumina Hiseq 2000	SRR518717	Miller et al. (2012)	
Brown bear	Chichagof 1	Chichagof	Chichagof island, AK, USA	F	148,325,262	98.7%	3,726,121	8.61	Illumina Hiseq 2000	SRR1692419	Cahill et al. (2015)	
Brown bear	Chichagof 2	Chichagof	Chichagof island, AK, USA	F	164,831,768	98.5%	3,838,312	9.15	Illumina Hiseq 2000	SRR1693624	Cahill et al. (2015)	
Asiatic black bear	Asiatic	-	Zoo Madrid, Spain	F	338,940,868	98.0%	-	-	Illumina Hiseq 2000	ERR946787	Kumar et al. (2017)	
Polar bear	Polar	-	Dalian Hutan Marine Animal Protection and Research Institute, China	M	-	-	-	-	Illumina Genome Analyzer 2	GCF_000687225.1	Liu et al. (2014)	Reference genome

Numbered sample designations from previous studies (Matsuhashi et al. 1999; Hirata et al. 2017) are in parentheses.

Table 2. Autosomal F_{st} values among groups of bears representing the Hokkaido, European, and North American populations.

	Hokkaido	Europe
Hokkaido	-	-
Europe	0.228 (0.0012)	-
North America	0.262 (0.0014)	0.156 (0.0008)

Europe includes eight individuals (Slovakia, Georgia, Southern Sweden 1, Southern Sweden 2, Slovenia, Northern Italy, Central Italy, and Spain). North America includes eight individuals (Alaska, Denali, Kenai, Admiralty 1, Admiralty 2, Baranof, Chichagof 1, and Chichagof 2). Hokkaido includes six indivduals, two each from Central, Eastern, and Southern Hokkaido. Standard deviation (SD) values are in parentheses.

Table 3. Autosomal F_{st} values for three subpopulations in

	Southern Hokkaido	Central Hokkaido
Southern Hokkaido	-	-
Central Hokkaido	0.035 (0.0032)	-
Eastern Hokkaido	0.082 (0.0042)	0.061 (0.0039)

Southern Hokkaido includes two individuals (Southern Hokkaido 1 and Southern Hokkaido 2). Central Honshu includes 2 individuals (Central Hokkaido 1 and Central Hokkaido 2). Eastern Hokkaido includes 2 individuals (Eastern Hokkaido 1 and Eastern Hokkaido 2). Standard deviation (SD) values are in parentheses.

Table 4. Values for the *f* 4 (Asiatic black bear, Denali, Kenai, and Russia; other Europe or North America, Hokkaido) statistic.

Asiatic black bear	Denali, Kenai, and Russia	other Europe or North America	Hokkaido	*f*4	Standard Error	Z score
Asiatic	Denali	Alaska	Hokkaido	-0.007981	0.000242318	-32.936
Asiatic	Denali	Admiralty 1	Hokkaido	-0.007572	0.000232741	-32.534
Asiatic	Denali	Admiralty 2	Hokkaido	-0.007351	0.000244422	-30.075
Asiatic	Denali	Baranof	Hokkaido	-0.006455	0.000242032	-26.67
Asiatic	Denali	Chichagof 2	Hokkaido	-0.006184	0.000231394	-26.725
Asiatic	Denali	Chichagof 1	Hokkaido	-0.006087	0.000234557	-25.951
Asiatic	**Denali**	**Southern Sweden 1**	**Hokkaido**	**0.000406**	**0.000152861**	**2.656**
Asiatic	**Denali**	**Southern Sweden 2**	**Hokkaido**	**0.000416**	**0.000156039**	**2.666**
Asiatic	**Denali**	**Spain**	**Hokkaido**	**0.000846**	**0.000161543**	**5.237**
Asiatic	**Denali**	**Spain**	**Hokkaido**	**0.000846**	**0.000161543**	**5.237**
Asiatic	**Denali**	**Slovakia**	**Hokkaido**	**0.001188**	**0.000148593**	**7.995**
Asiatic	**Denali**	**Central Italy**	**Hokkaido**	**0.001556**	**0.000175542**	**8.864**
Asiatic	**Denali**	**Northern Italy**	**Hokkaido**	**0.001563**	**0.000146307**	**10.683**
Asiatic	**Denali**	**Slovenia**	**Hokkaido**	**0.001647**	**0.000154026**	**10.693**
Asiatic	**Denali**	**Georgia**	**Hokkaido**	**0.006165**	**0.000152625**	**40.393**
Asiatic	Kenai	Alaska	Hokkaido	-0.007325	0.000251295	-29.149
Asiatic	Kenai	Admiralty 1	Hokkaido	-0.006442	0.000228951	-28.137
Asiatic	Kenai	Admiralty 2	Hokkaido	-0.006389	0.00023936	-26.692
Asiatic	Kenai	Baranof	Hokkaido	-0.005593	0.000239703	-23.333
Asiatic	Kenai	Chichagof 2	Hokkaido	-0.005325	0.000241332	-22.065
Asiatic	Kenai	Chichagof 1	Hokkaido	-0.005141	0.000227247	-22.623
Asiatic	**Kenai**	**Southern Sweden 2**	**Hokkaido**	**0.0006**	**0.000168209**	**3.567**
Asiatic	**Kenai**	**Southern Sweden 1**	**Hokkaido**	**0.000639**	**0.000166363**	**3.841**
Asiatic	**Kenai**	**Spain**	**Hokkaido**	**0.001022**	**0.000172025**	**5.941**
Asiatic	**Kenai**	**Slovakia**	**Hokkaido**	**0.001209**	**0.000165662**	**7.298**
Asiatic	**Kenai**	**Central Italy**	**Hokkaido**	**0.001596**	**0.000179649**	**8.884**
Asiatic	**Kenai**	**Northern Italy**	**Hokkaido**	**0.001715**	**0.000155838**	**11.005**
Asiatic	**Kenai**	**Slovenia**	**Hokkaido**	**0.001824**	**0.000155155**	**11.756**
Asiatic	**Kenai**	**Georgia**	**Hokkaido**	**0.006423**	**0.000160937**	**39.91**
Asiatic	**Russia**	**Southern Sweden 2**	**Hokkaido**	**0.000095**	**0.000158598**	**0.599**
Asiatic	**Russia**	**Southern Sweden 1**	**Hokkaido**	**0.00024**	**0.000161834**	**1.483**
Asiatic	**Russia**	**Spain**	**Hokkaido**	**0.000516**	**0.000165226**	**3.123**
Asiatic	**Russia**	**Slovakia**	**Hokkaido**	**0.00059**	**0.000166479**	**3.544**
Asiatic	**Russia**	**Central Italy**	**Hokkaido**	**0.00111**	**0.000187373**	**5.924**
Asiatic	**Russia**	**Northern Italy**	**Hokkaido**	**0.001112**	**0.000169409**	**6.564**
Asiatic	**Russia**	**Slovenia**	**Hokkaido**	**0.001216**	**0.000168328**	**7.224**
Asiatic	**Russia**	**Alaska**	**Hokkaido**	**0.00198**	**0.00016601**	**11.927**
Asiatic	**Russia**	**Admiralty 1**	**Hokkaido**	**0.002325**	**0.00016356**	**14.215**
Asiatic	**Russia**	**Baranof**	**Hokkaido**	**0.00233**	**0.000179645**	**12.97**
Asiatic	**Russia**	**Admiralty 2**	**Hokkaido**	**0.002426**	**0.000167924**	**14.447**
Asiatic	**Russia**	**Chichagof 2**	**Hokkaido**	**0.002684**	**0.000172151**	**15.591**
Asiatic	**Russia**	**Chichagof 1**	**Hokkaido**	**0.002856**	**0.000167822**	**17.018**
Asiatic	**Russia**	**Georgia**	**Hokkaido**	**0.006068**	**0.000168917**	**35.923**

The values highlighted in grey indicate |Z score| > 3 considered significant. The rows in bold font indicate *f*4 > 0

Table 5. Values for the f 4 (Asiatic black bear, Europe; North America, Hokkaido) statistic.

Asiatic black bear	Europe	North America	Hokkaido	$f4$	Standard Error	Z score
Asiatic	Central Italy	Admiralty	Hokkaido	0.001112	0.00015150	7.340
Asiatic	Georgia	Admiralty	Hokkaido	0.000794	0.00011985	6.625
Asiatic	Northern Italy	Admiralty	Hokkaido	0.000858	0.00013816	6.210
Asiatic	Slovakia	Admiralty	Hokkaido	0.000935	0.00014743	6.342
Asiatic	Slovenia	Admiralty	Hokkaido	0.000714	0.00014363	4.971
Asiatic	Spain	Admiralty	Hokkaido	0.000825	0.00014995	5.502
Asiatic	Sweden	Admiralty	Hokkaido	0.000724	0.00013923	5.200
Asiatic	Central Italy	Alaska	Hokkaido	0.000590	0.00015633	3.774
Asiatic	Georgia	Alaska	Hokkaido	0.000547	0.00012730	4.297
Asiatic	Northern Italy	Alaska	Hokkaido	0.000471	0.00015111	3.117
Asiatic	Slovakia	Alaska	Hokkaido	0.000487	0.00015564	3.129
Asiatic	Slovenia	Alaska	Hokkaido	0.000470	0.00015137	3.105
Asiatic	Spain	Alaska	Hokkaido	0.000459	0.00016499	2.782
Asiatic	**Sweden**	**Alaska**	**Hokkaido**	**0.000350**	0.00015178	**2.306**
Asiatic	Central Italy	Baranof	Hokkaido	0.001175	0.00016538	7.105
Asiatic	Georgia	Baranof	Hokkaido	0.000907	0.00013809	6.568
Asiatic	Northern Italy	Baranof	Hokkaido	0.001112	0.00015995	6.952
Asiatic	Slovakia	Baranof	Hokkaido	0.000961	0.00016580	5.796
Asiatic	Slovenia	Baranof	Hokkaido	0.000849	0.00015775	5.382
Asiatic	Spain	Baranof	Hokkaido	0.000863	0.00017281	4.994
Asiatic	Sweden	Baranof	Hokkaido	0.000904	0.00015738	5.744
Asiatic	**Central Italy**	**Chichagof**	**Hokkaido**	**0.001510**	0.00014875	**10.151**
Asiatic	Georgia	Chichagof	Hokkaido	0.001132	0.00013220	8.563
Asiatic	Northern Italy	Chichagof	Hokkaido	0.001417	0.00014046	10.088
Asiatic	Slovakia	Chichagof	Hokkaido	0.001331	0.00014307	9.303
Asiatic	Slovenia	Chichagof	Hokkaido	0.001166	0.00014351	8.125
Asiatic	Spain	Chichagof	Hokkaido	0.001322	0.00015665	8.439
Asiatic	Sweden	Chichagof	Hokkaido	0.001171	0.00014471	8.092
Asiatic	Central Italy	Denali	Hokkaido	-0.000839	0.00015839	-5.297
Asiatic	**Georgia**	**Denali**	**Hokkaido**	**-0.000436**	0.00011495	**-3.793**
Asiatic	Northern Italy	Denali	Hokkaido	-0.000979	0.00013710	-7.141
Asiatic	Slovakia	Denali	Hokkaido	-0.001031	0.00013955	-7.388
Asiatic	Slovenia	Denali	Hokkaido	-0.001015	0.00014146	-7.175
Asiatic	Spain	Denali	Hokkaido	-0.001096	0.00015469	-7.085
Asiatic	Sweden	Denali	Hokkaido	-0.001334	0.00014139	-9.435
Asiatic	Central Italy	Kenai	Hokkaido	-0.001317	0.00015778	-8.347
Asiatic	Georgia	Kenai	Hokkaido	-0.000697	0.00012994	-5.364
Asiatic	Northern Italy	Kenai	Hokkaido	-0.001346	0.00014495	-9.286
Asiatic	Slovakia	Kenai	Hokkaido	-0.001529	0.00015139	-10.100
Asiatic	Slovenia	Kenai	Hokkaido	-0.001356	0.00014552	-9.318
Asiatic	Spain	Kenai	Hokkaido	-0.001440	0.00015690	-9.178
Asiatic	**Sweden**	**Kenai**	**Hokkaido**	**-0.001644**	0.00014547	**-11.301**

The rows highlighted in grey indicate |Z score| < 3, which is not considered significant. The rows in bold font indicate the maximum and minimum values for $f4$(Asiatic black bear, Europe; North America excluding Denali and Kenai, Hokkaido) and $f4$(Asiatic black bear, Europe; Denali and Kenai, Hokkaido).

Table 6. Values for the $f4$(Asiatic black bear, North America; Russia, Hokkaido) statistic.

Asiatic black bear	North America	Russia	Hokkaido	$f4$	Standard Error	Z score
Asiatic	**Admiralty**	**Russia**	**Hokkaido**	**-0.001230**	0.00014057	**-8.750**
Asiatic	Alaska	Russia	Hokkaido	-0.001257	0.00014234	-8.831
Asiatic	Baranof	Russia	Hokkaido	-0.001420	0.00015197	-9.344
Asiatic	Chichagof	Russia	Hokkaido	-0.001384	0.00013864	-9.983
Asiatic	**Denali**	**Russia**	**Hokkaido**	**-0.001905**	0.00014481	**-13.155**
Asiatic	Kenai	Russia	Hokkaido	-0.001881	0.00015601	-12.057

Rows in bold correspond to the maximum and minimum values for $f4$(Asiatic black bear, North America; Russia, Hokkaido).

Table 7. Values for the *f*4(Asiatic black bear, X; Hokkaido 1, Hokkaido 2) statistic.

Asiatic black bear	X	Hokkaido1	Hokkaido2	*f*4	Standard Error	Z score
Asiatic	Admiralty	Central Hokkaido 1	Central Hokkaido 2	-0.000137	0.00009282	-1.476
Asiatic	Admiralty	Central Hokkaido 1	Eastern Hokkaido 1	-0.000194	0.00010636	-1.824
Asiatic	Admiralty	Central Hokkaido 1	Eastern Hokkaido 2	-0.000185	0.00011084	-1.669
Asiatic	Admiralty	Central Hokkaido 1	Southern Hokkaido 1	-0.000126	0.00010056	-1.253
Asiatic	Admiralty	Central Hokkaido 1	Southern Hokkaido 2	-0.000045	0.00009890	-0.455
Asiatic	Alaska	Central Hokkaido 1	Central Hokkaido 2	-0.000079	0.00011351	-0.696
Asiatic	Alaska	Central Hokkaido 1	Eastern Hokkaido 1	-0.000126	0.00010881	-1.158
Asiatic	Alaska	Central Hokkaido 1	Eastern Hokkaido 2	-0.000201	0.00011693	-1.719
Asiatic	Alaska	Central Hokkaido 1	Southern Hokkaido 1	-0.000058	0.00011717	-0.495
Asiatic	Alaska	Central Hokkaido 1	Southern Hokkaido 2	0.000008	0.00011594	0.069
Asiatic	Baranof	Central Hokkaido 1	Central Hokkaido 2	-0.000188	0.00010968	-1.714
Asiatic	Baranof	Central Hokkaido 1	Eastern Hokkaido 1	-0.000144	0.00011111	-1.296
Asiatic	Baranof	Central Hokkaido 1	Eastern Hokkaido 2	-0.000128	0.00011819	-1.083
Asiatic	Baranof	Central Hokkaido 1	Southern Hokkaido 1	-0.000081	0.00011005	-0.736
Asiatic	Baranof	Central Hokkaido 1	Southern Hokkaido 2	-0.000150	0.00010965	-1.368
Asiatic	Central Italy	Central Hokkaido 1	Central Hokkaido 2	-0.000022	0.00011640	-0.189
Asiatic	Central Italy	Central Hokkaido 1	Eastern Hokkaido 1	-0.000030	0.00011811	-0.254
Asiatic	Central Italy	Central Hokkaido 1	Eastern Hokkaido 2	-0.000072	0.00011707	-0.615
Asiatic	Central Italy	Central Hokkaido 1	Southern Hokkaido 1	0.000136	0.00011429	1.190
Asiatic	Central Italy	Central Hokkaido 1	Southern Hokkaido 2	-0.000198	0.00012230	-1.619
Asiatic	Chichagof	Central Hokkaido 1	Central Hokkaido 2	-0.000116	0.00009355	-1.240
Asiatic	Chichagof	Central Hokkaido 1	Eastern Hokkaido 1	-0.000137	0.00010163	-1.348
Asiatic	Chichagof	Central Hokkaido 1	Eastern Hokkaido 2	-0.000089	0.00010710	-0.831
Asiatic	Chichagof	Central Hokkaido 1	Southern Hokkaido 1	0.000015	0.00010135	0.148
Asiatic	Chichagof	Central Hokkaido 1	Southern Hokkaido 2	-0.000073	0.00010657	-0.685
Asiatic	Denali	Central Hokkaido 1	Central Hokkaido 2	-0.000031	0.00010915	-0.284
Asiatic	Denali	Central Hokkaido 1	Eastern Hokkaido 1	-0.000152	0.00011218	-1.355
Asiatic	Denali	Central Hokkaido 1	Eastern Hokkaido 2	-0.000173	0.00011556	-1.497
Asiatic	Denali	Central Hokkaido 1	Southern Hokkaido 1	0.000001	0.00020000	0.005
Asiatic	Denali	Central Hokkaido 1	Southern Hokkaido 2	-0.000063	0.00011270	-0.559
Asiatic	Georgia	Central Hokkaido 1	Central Hokkaido 2	-0.000012	0.00008451	-0.142
Asiatic	Georgia	Central Hokkaido 1	Eastern Hokkaido 1	-0.000083	0.00008655	-0.959
Asiatic	Georgia	Central Hokkaido 1	Eastern Hokkaido 2	-0.000123	0.00008761	-1.404
Asiatic	Georgia	Central Hokkaido 1	Southern Hokkaido 1	0.000122	0.00008316	1.467
Asiatic	Georgia	Central Hokkaido 1	Southern Hokkaido 2	-0.000085	0.00009004	-0.944
Asiatic	Kenai	Central Hokkaido 1	Central Hokkaido 2	-0.000008	0.00011940	-0.067
Asiatic	Kenai	Central Hokkaido 1	Eastern Hokkaido 1	-0.000075	0.00010917	-0.687
Asiatic	Kenai	Central Hokkaido 1	Eastern Hokkaido 2	-0.000053	0.00011726	-0.452
Asiatic	Kenai	Central Hokkaido 1	Southern Hokkaido 1	0.000085	0.00011486	0.740
Asiatic	Kenai	Central Hokkaido 1	Southern Hokkaido 2	-0.000123	0.00012035	-1.022
Asiatic	Northern Italy	Central Hokkaido 1	Central Hokkaido 2	-0.000109	0.00009706	-1.123
Asiatic	Northern Italy	Central Hokkaido 1	Eastern Hokkaido 1	-0.000250	0.00010052	-2.487
Asiatic	Northern Italy	Central Hokkaido 1	Eastern Hokkaido 2	-0.000181	0.00010523	-1.720
Asiatic	Northern Italy	Central Hokkaido 1	Southern Hokkaido 1	0.000033	0.00010443	0.316
Asiatic	Northern Italy	Central Hokkaido 1	Southern Hokkaido 2	-0.000146	0.00010815	-1.350
Asiatic	Russia	Central Hokkaido 1	Central Hokkaido 2	-0.000112	0.00011606	-0.965
Asiatic	Russia	Central Hokkaido 1	Eastern Hokkaido 1	-0.000103	0.00012047	-0.855
Asiatic	Russia	Central Hokkaido 1	Eastern Hokkaido 2	-0.000206	0.00013180	-1.563
Asiatic	Russia	Central Hokkaido 1	Southern Hokkaido 1	-0.000063	0.00012257	-0.514
Asiatic	Russia	Central Hokkaido 1	Southern Hokkaido 2	-0.000054	0.00011714	-0.461
Asiatic	Slovakia	Central Hokkaido 1	Central Hokkaido 2	0.000048	0.00010787	0.445

Asiatic	Slovakia	Central Hokkaido 1	Eastern Hokkaido 1	-0.000124	0.00010830	-1.145
Asiatic	Slovakia	Central Hokkaido 1	Eastern Hokkaido 2	-0.000043	0.00011026	-0.390
Asiatic	Slovakia	Central Hokkaido 1	Southern Hokkaido 1	0.000144	0.00011009	1.308
Asiatic	Slovakia	Central Hokkaido 1	Southern Hokkaido 2	0.000019	0.00011047	0.172
Asiatic	Slovenia	Central Hokkaido 1	Central Hokkaido 2	-0.000022	0.00010329	-0.213
Asiatic	Slovenia	Central Hokkaido 1	Eastern Hokkaido 1	-0.000092	0.00010502	-0.876
Asiatic	Slovenia	Central Hokkaido 1	Eastern Hokkaido 2	-0.000041	0.00010963	-0.374
Asiatic	Slovenia	Central Hokkaido 1	Southern Hokkaido 1	0.000140	0.00011236	1.246
Asiatic	Slovenia	Central Hokkaido 1	Southern Hokkaido 2	-0.000046	0.00010979	-0.419
Asiatic	Spain	Central Hokkaido 1	Central Hokkaido 2	-0.000080	0.00010652	-0.751
Asiatic	Spain	Central Hokkaido 1	Eastern Hokkaido 1	-0.000209	0.00011200	-1.866
Asiatic	Spain	Central Hokkaido 1	Eastern Hokkaido 2	-0.000090	0.00011236	-0.801
Asiatic	Spain	Central Hokkaido 1	Southern Hokkaido 1	0.000138	0.00011138	1.239
Asiatic	Spain	Central Hokkaido 1	Southern Hokkaido 2	-0.000054	0.00011563	-0.467
Asiatic	Sweden	Central Hokkaido 1	Central Hokkaido 2	-0.000139	0.00010491	-1.325
Asiatic	Sweden	Central Hokkaido 1	Eastern Hokkaido 1	-0.000237	0.00010395	-2.280
Asiatic	Sweden	Central Hokkaido 1	Eastern Hokkaido 2	-0.000137	0.00010498	-1.305
Asiatic	Sweden	Central Hokkaido 1	Southern Hokkaido 1	0.000097	0.00010695	0.907
Asiatic	Sweden	Central Hokkaido 1	Southern Hokkaido 2	-0.000110	0.00010417	-1.056
Asiatic	Admiralty	Central Hokkaido 2	Central Hokkaido 1	0.000137	0.00009282	1.476
Asiatic	Admiralty	Central Hokkaido 2	Eastern Hokkaido 1	-0.000056	0.00010409	-0.538
Asiatic	Admiralty	Central Hokkaido 2	Eastern Hokkaido 2	-0.000048	0.00010412	-0.461
Asiatic	Admiralty	Central Hokkaido 2	Southern Hokkaido 1	0.000011	0.00009821	0.112
Asiatic	Admiralty	Central Hokkaido 2	Southern Hokkaido 2	0.000093	0.00009617	0.967
Asiatic	Alaska	Central Hokkaido 2	Central Hokkaido 1	0.000079	0.00011351	0.696
Asiatic	Alaska	Central Hokkaido 2	Eastern Hokkaido 1	-0.000047	0.00011033	-0.426
Asiatic	Alaska	Central Hokkaido 2	Eastern Hokkaido 2	-0.000123	0.00010724	-1.147
Asiatic	Alaska	Central Hokkaido 2	Southern Hokkaido 1	0.000021	0.00011932	0.176
Asiatic	Alaska	Central Hokkaido 2	Southern Hokkaido 2	0.000087	0.00011585	0.751
Asiatic	Baranof	Central Hokkaido 2	Central Hokkaido 1	0.000188	0.00010968	1.714
Asiatic	Baranof	Central Hokkaido 2	Eastern Hokkaido 1	0.000044	0.00011224	0.392
Asiatic	Baranof	Central Hokkaido 2	Eastern Hokkaido 2	0.000060	0.00011111	0.540
Asiatic	Baranof	Central Hokkaido 2	Southern Hokkaido 1	0.000107	0.00012063	0.887
Asiatic	Baranof	Central Hokkaido 2	Southern Hokkaido 2	0.000039	0.00010569	0.369
Asiatic	Central Italy	Central Hokkaido 2	Central Hokkaido 1	0.000022	0.00011640	0.189
Asiatic	Central Italy	Central Hokkaido 2	Eastern Hokkaido 1	-0.000008	0.00012308	-0.065
Asiatic	Central Italy	Central Hokkaido 2	Eastern Hokkaido 2	-0.000049	0.00011061	-0.443
Asiatic	Central Italy	Central Hokkaido 2	Southern Hokkaido 1	0.000158	0.00012650	1.249
Asiatic	Central Italy	Central Hokkaido 2	Southern Hokkaido 2	-0.000175	0.00011864	-1.475
Asiatic	Chichagof	Central Hokkaido 2	Central Hokkaido 1	0.000116	0.00009355	1.240
Asiatic	Chichagof	Central Hokkaido 2	Eastern Hokkaido 1	-0.000021	0.00010244	-0.205
Asiatic	Chichagof	Central Hokkaido 2	Eastern Hokkaido 2	0.000027	0.00010547	0.256
Asiatic	Chichagof	Central Hokkaido 2	Southern Hokkaido 1	0.000131	0.00010100	1.297
Asiatic	Chichagof	Central Hokkaido 2	Southern Hokkaido 2	0.000042	0.00009524	0.441
Asiatic	Denali	Central Hokkaido 2	Central Hokkaido 1	0.000031	0.00010915	0.284
Asiatic	Denali	Central Hokkaido 2	Eastern Hokkaido 1	-0.000121	0.00010891	-1.111
Asiatic	Denali	Central Hokkaido 2	Eastern Hokkaido 2	-0.000141	0.00010829	-1.302
Asiatic	Denali	Central Hokkaido 2	Southern Hokkaido 1	0.000032	0.00010959	0.292
Asiatic	Denali	Central Hokkaido 2	Southern Hokkaido 2	-0.000032	0.00010191	-0.314
Asiatic	Georgia	Central Hokkaido 2	Central Hokkaido 1	0.000012	0.00008451	0.142
Asiatic	Georgia	Central Hokkaido 2	Eastern Hokkaido 1	-0.000071	0.00009149	-0.776
Asiatic	Georgia	Central Hokkaido 2	Eastern Hokkaido 2	-0.000111	0.00009737	-1.140
Asiatic	Georgia	Central Hokkaido 2	Southern Hokkaido 1	0.000134	0.00009280	1.444

Asiatic	Georgia	Central Hokkaido 2	Southern Hokkaido 2	-0.000073	0.00009023	-0.809
Asiatic	Kenai	Central Hokkaido 2	Central Hokkaido 1	0.000008	0.00011940	0.067
Asiatic	Kenai	Central Hokkaido 2	Eastern Hokkaido 1	-0.000068	0.00011486	-0.592
Asiatic	Kenai	Central Hokkaido 2	Eastern Hokkaido 2	-0.000045	0.00011421	-0.394
Asiatic	Kenai	Central Hokkaido 2	Southern Hokkaido 1	0.000093	0.00012109	0.768
Asiatic	Kenai	Central Hokkaido 2	Southern Hokkaido 2	-0.000115	0.00012273	-0.937
Asiatic	Northern Italy	Central Hokkaido 2	Central Hokkaido 1	0.000109	0.00009706	1.123
Asiatic	Northern Italy	Central Hokkaido 2	Eastern Hokkaido 1	-0.000140	0.00009729	-1.439
Asiatic	Northern Italy	Central Hokkaido 2	Eastern Hokkaido 2	-0.000072	0.00010714	-0.672
Asiatic	Northern Italy	Central Hokkaido 2	Southern Hokkaido 1	0.000142	0.00011008	1.290
Asiatic	Northern Italy	Central Hokkaido 2	Southern Hokkaido 2	-0.000037	0.00010914	-0.339
Asiatic	Russia	Central Hokkaido 2	Central Hokkaido 1	0.000112	0.00011606	0.965
Asiatic	Russia	Central Hokkaido 2	Eastern Hokkaido 1	0.000009	0.00010588	0.085
Asiatic	Russia	Central Hokkaido 2	Eastern Hokkaido 2	-0.000094	0.00011520	-0.816
Asiatic	Russia	Central Hokkaido 2	Southern Hokkaido 1	0.000049	0.00011722	0.418
Asiatic	Russia	Central Hokkaido 2	Southern Hokkaido 2	0.000058	0.00011240	0.516
Asiatic	Slovakia	Central Hokkaido 2	Central Hokkaido 1	-0.000048	0.00010787	-0.445
Asiatic	Slovakia	Central Hokkaido 2	Eastern Hokkaido 1	-0.000172	0.00010997	-1.564
Asiatic	Slovakia	Central Hokkaido 2	Eastern Hokkaido 2	-0.000090	0.00010369	-0.868
Asiatic	Slovakia	Central Hokkaido 2	Southern Hokkaido 1	0.000096	0.00010714	0.896
Asiatic	Slovakia	Central Hokkaido 2	Southern Hokkaido 2	-0.000028	0.00010646	-0.263
Asiatic	Slovenia	Central Hokkaido 2	Central Hokkaido 1	0.000022	0.00010329	0.213
Asiatic	Slovenia	Central Hokkaido 2	Eastern Hokkaido 1	-0.000070	0.00009887	-0.708
Asiatic	Slovenia	Central Hokkaido 2	Eastern Hokkaido 2	-0.000019	0.00010160	-0.187
Asiatic	Slovenia	Central Hokkaido 2	Southern Hokkaido 1	0.000162	0.00011305	1.433
Asiatic	Slovenia	Central Hokkaido 2	Southern Hokkaido 2	-0.000024	0.00010256	-0.234
Asiatic	Spain	Central Hokkaido 2	Central Hokkaido 1	0.000080	0.00010652	0.751
Asiatic	Spain	Central Hokkaido 2	Eastern Hokkaido 1	-0.000130	0.00011149	-1.166
Asiatic	Spain	Central Hokkaido 2	Eastern Hokkaido 2	-0.000010	0.00010870	-0.092
Asiatic	Spain	Central Hokkaido 2	Southern Hokkaido 1	0.000218	0.00011208	1.945
Asiatic	Spain	Central Hokkaido 2	Southern Hokkaido 2	0.000026	0.00011017	0.236
Asiatic	Sweden	Central Hokkaido 2	Central Hokkaido 1	0.000139	0.00010491	1.325
Asiatic	Sweden	Central Hokkaido 2	Eastern Hokkaido 1	-0.000098	0.00009849	-0.995
Asiatic	Sweden	Central Hokkaido 2	Eastern Hokkaido 2	0.000002	0.00008333	0.024
Asiatic	Sweden	Central Hokkaido 2	Southern Hokkaido 1	0.000236	0.00010645	2.217
Asiatic	Sweden	Central Hokkaido 2	Southern Hokkaido 2	0.000029	0.00010211	0.284
Asiatic	Admiralty	Eastern Hokkaido 1	Central Hokkaido 1	0.000194	0.00010636	1.824
Asiatic	Admiralty	Eastern Hokkaido 1	Central Hokkaido 2	0.000056	0.00010409	0.538
Asiatic	Admiralty	Eastern Hokkaido 1	Eastern Hokkaido 2	0.000008	0.00009195	0.087
Asiatic	Admiralty	Eastern Hokkaido 1	Southern Hokkaido 1	0.000067	0.00010229	0.655
Asiatic	Admiralty	Eastern Hokkaido 1	Southern Hokkaido 2	0.000149	0.00011119	1.340
Asiatic	Alaska	Eastern Hokkaido 1	Central Hokkaido 1	0.000126	0.00010881	1.158
Asiatic	Alaska	Eastern Hokkaido 1	Central Hokkaido 2	0.000047	0.00011033	0.426
Asiatic	Alaska	Eastern Hokkaido 1	Eastern Hokkaido 2	-0.000075	0.00009894	-0.758
Asiatic	Alaska	Eastern Hokkaido 1	Southern Hokkaido 1	0.000068	0.00011166	0.609
Asiatic	Alaska	Eastern Hokkaido 1	Southern Hokkaido 2	0.000134	0.00011111	1.206
Asiatic	Baranof	Eastern Hokkaido 1	Central Hokkaido 1	0.000144	0.00011111	1.296
Asiatic	Baranof	Eastern Hokkaido 1	Central Hokkaido 2	-0.000044	0.00011224	-0.392
Asiatic	Baranof	Eastern Hokkaido 1	Eastern Hokkaido 2	0.000016	0.00010526	0.152
Asiatic	Baranof	Eastern Hokkaido 1	Southern Hokkaido 1	0.000063	0.00011475	0.549
Asiatic	Baranof	Eastern Hokkaido 1	Southern Hokkaido 2	-0.000006	0.00012766	-0.047
Asiatic	Central Italy	Eastern Hokkaido 1	Central Hokkaido 1	0.000030	0.00011811	0.254
Asiatic	Central Italy	Eastern Hokkaido 1	Central Hokkaido 2	0.000008	0.00012308	0.065

Asiatic	Central Italy	Eastern Hokkaido 1	Eastern Hokkaido 2	-0.000042	0.00011170	-0.376
Asiatic	Central Italy	Eastern Hokkaido 1	Southern Hokkaido 1	0.000165	0.00012259	1.346
ma0822	Central Italy	Eastern Hokkaido 1	Southern Hokkaido 2	-0.000168	0.00012834	-1.309
Asiatic	Chichagof	Eastern Hokkaido 1	Central Hokkaido 1	0.000137	0.00010163	1.348
Asiatic	Chichagof	Eastern Hokkaido 1	Central Hokkaido 2	0.000021	0.00010244	0.205
Asiatic	Chichagof	Eastern Hokkaido 1	Eastern Hokkaido 2	0.000047	0.00009572	0.491
Asiatic	Chichagof	Eastern Hokkaido 1	Southern Hokkaido 1	0.000151	0.00010464	1.443
Asiatic	Chichagof	Eastern Hokkaido 1	Southern Hokkaido 2	0.000063	0.00011270	0.559
Asiatic	Denali	Eastern Hokkaido 1	Central Hokkaido 1	0.000152	0.00011218	1.355
Asiatic	Denali	Eastern Hokkaido 1	Central Hokkaido 2	0.000121	0.00010891	1.111
Asiatic	Denali	Eastern Hokkaido 1	Eastern Hokkaido 2	-0.000020	0.00009615	-0.208
Asiatic	Denali	Eastern Hokkaido 1	Southern Hokkaido 1	0.000153	0.00010797	1.417
Asiatic	Denali	Eastern Hokkaido 1	Southern Hokkaido 2	0.000089	0.00010867	0.819
Asiatic	Georgia	Eastern Hokkaido 1	Central Hokkaido 1	0.000083	0.00008655	0.959
Asiatic	Georgia	Eastern Hokkaido 1	Central Hokkaido 2	0.000071	0.00009149	0.776
Asiatic	Georgia	Eastern Hokkaido 1	Eastern Hokkaido 2	-0.000040	0.00007782	-0.514
Asiatic	Georgia	Eastern Hokkaido 1	Southern Hokkaido 1	0.000206	0.00008766	2.350
Asiatic	Georgia	Eastern Hokkaido 1	Southern Hokkaido 2	-0.000002	0.00010526	-0.019
Asiatic	Kenai	Eastern Hokkaido 1	Central Hokkaido 1	0.000075	0.00010917	0.687
Asiatic	Kenai	Eastern Hokkaido 1	Central Hokkaido 2	0.000068	0.00011486	0.592
Asiatic	Kenai	Eastern Hokkaido 1	Eastern Hokkaido 2	0.000023	0.00010599	0.217
Asiatic	Kenai	Eastern Hokkaido 1	Southern Hokkaido 1	0.000160	0.00011756	1.361
Asiatic	Kenai	Eastern Hokkaido 1	Southern Hokkaido 2	-0.000047	0.00011899	-0.395
Asiatic	Northern Italy	Eastern Hokkaido 1	Central Hokkaido 1	0.000250	0.00010052	2.487
Asiatic	Northern Italy	Eastern Hokkaido 1	Central Hokkaido 2	0.000140	0.00009729	1.439
Asiatic	Northern Italy	Eastern Hokkaido 1	Eastern Hokkaido 2	0.000069	0.00009163	0.753
Asiatic	Northern Italy	Eastern Hokkaido 1	Southern Hokkaido 1	0.000283	0.00010826	2.614
Asiatic	Northern Italy	Eastern Hokkaido 1	Southern Hokkaido 2	0.000103	0.00011123	0.926
Asiatic	Russia	Eastern Hokkaido 1	Central Hokkaido 1	0.000103	0.00012047	0.855
Asiatic	Russia	Eastern Hokkaido 1	Central Hokkaido 2	-0.000009	0.00010588	-0.085
Asiatic	Russia	Eastern Hokkaido 1	Eastern Hokkaido 2	-0.000103	0.00010088	-1.021
Asiatic	Russia	Eastern Hokkaido 1	Southern Hokkaido 1	0.000039	0.00011890	0.328
Asiatic	Russia	Eastern Hokkaido 1	Southern Hokkaido 2	0.000049	0.00011639	0.421
Asiatic	Slovakia	Eastern Hokkaido 1	Central Hokkaido 1	0.000124	0.00010830	1.145
Asiatic	Slovakia	Eastern Hokkaido 1	Central Hokkaido 2	0.000172	0.00010997	1.564
Asiatic	Slovakia	Eastern Hokkaido 1	Eastern Hokkaido 2	0.000081	0.00009866	0.821
Asiatic	Slovakia	Eastern Hokkaido 1	Southern Hokkaido 1	0.000268	0.00010690	2.507
Asiatic	Slovakia	Eastern Hokkaido 1	Southern Hokkaido 2	0.000143	0.00011413	1.253
Asiatic	Slovenia	Eastern Hokkaido 1	Central Hokkaido 1	0.000092	0.00010502	0.876
Asiatic	Slovenia	Eastern Hokkaido 1	Central Hokkaido 2	0.000070	0.00009887	0.708
Asiatic	Slovenia	Eastern Hokkaido 1	Eastern Hokkaido 2	0.000051	0.00009156	0.557
Asiatic	Slovenia	Eastern Hokkaido 1	Southern Hokkaido 1	0.000233	0.00010572	2.204
Asiatic	Slovenia	Eastern Hokkaido 1	Southern Hokkaido 2	0.000046	0.00010698	0.430
Asiatic	Spain	Eastern Hokkaido 1	Central Hokkaido 1	0.000209	0.00011200	1.866
Asiatic	Spain	Eastern Hokkaido 1	Central Hokkaido 2	0.000130	0.00011149	1.166
Asiatic	Spain	Eastern Hokkaido 1	Eastern Hokkaido 2	0.000119	0.00010025	1.187
Asiatic	Spain	Eastern Hokkaido 1	Southern Hokkaido 1	0.000348	0.00011440	3.042
Asiatic	Spain	Eastern Hokkaido 1	Southern Hokkaido 2	0.000155	0.00012128	1.278
Asiatic	Sweden	Eastern Hokkaido 1	Central Hokkaido 1	0.000237	0.00010395	2.280
Asiatic	Sweden	Eastern Hokkaido 1	Central Hokkaido 2	0.000098	0.00009849	0.995
Asiatic	Sweden	Eastern Hokkaido 1	Eastern Hokkaido 2	0.000101	0.00009173	1.101
Asiatic	Sweden	Eastern Hokkaido 1	Southern Hokkaido 1	0.000334	0.00010460	3.193
Asiatic	Sweden	Eastern Hokkaido 1	Southern Hokkaido 2	0.000128	0.00010518	1.217

Asiatic	Admiralty	Eastern Hokkaido 2	Central Hokkaido 1	0.000185	0.00011084	1.669
Asiatic	Admiralty	Eastern Hokkaido 2	Central Hokkaido 2	0.000048	0.00010412	0.461
Asiatic	Admiralty	Eastern Hokkaido 2	Eastern Hokkaido 1	-0.000008	0.00009195	-0.087
Asiatic	Admiralty	Eastern Hokkaido 2	Southern Hokkaido 1	0.000059	0.00010190	0.579
Asiatic	Admiralty	Eastern Hokkaido 2	Southern Hokkaido 2	0.000141	0.00010813	1.304
Asiatic	Alaska	Eastern Hokkaido 2	Central Hokkaido 1	0.000201	0.00011693	1.719
Asiatic	Alaska	Eastern Hokkaido 2	Central Hokkaido 2	0.000123	0.00010724	1.147
Asiatic	Alaska	Eastern Hokkaido 2	Eastern Hokkaido 1	0.000075	0.00009894	0.758
Asiatic	Alaska	Eastern Hokkaido 2	Southern Hokkaido 1	0.000144	0.00011410	1.262
Asiatic	Alaska	Eastern Hokkaido 2	Southern Hokkaido 2	0.000209	0.00011023	1.896
Asiatic	Baranof	Eastern Hokkaido 2	Central Hokkaido 1	0.000128	0.00011819	1.083
Asiatic	Baranof	Eastern Hokkaido 2	Central Hokkaido 2	-0.000060	0.00011111	-0.540
Asiatic	Baranof	Eastern Hokkaido 2	Eastern Hokkaido 1	-0.000016	0.00010526	-0.152
Asiatic	Baranof	Eastern Hokkaido 2	Southern Hokkaido 1	0.000047	0.00011353	0.414
Asiatic	Baranof	Eastern Hokkaido 2	Southern Hokkaido 2	-0.000022	0.00011111	-0.198
Asiatic	Central Italy	Eastern Hokkaido 2	Central Hokkaido 1	0.000072	0.00011707	0.615
Asiatic	Central Italy	Eastern Hokkaido 2	Central Hokkaido 2	0.000049	0.00011061	0.443
Asiatic	Central Italy	Eastern Hokkaido 2	Eastern Hokkaido 1	0.000042	0.00011170	0.376
Asiatic	Central Italy	Eastern Hokkaido 2	Southern Hokkaido 1	0.000207	0.00012715	1.628
Asiatic	Central Italy	Eastern Hokkaido 2	Southern Hokkaido 2	-0.000126	0.00012689	-0.993
Asiatic	Chichagof	Eastern Hokkaido 2	Central Hokkaido 1	0.000089	0.00010710	0.831
Asiatic	Chichagof	Eastern Hokkaido 2	Central Hokkaido 2	-0.000027	0.00010547	-0.256
Asiatic	Chichagof	Eastern Hokkaido 2	Eastern Hokkaido 1	-0.000047	0.00009572	-0.491
Asiatic	Chichagof	Eastern Hokkaido 2	Southern Hokkaido 1	0.000104	0.00010216	1.018
Asiatic	Chichagof	Eastern Hokkaido 2	Southern Hokkaido 2	0.000016	0.00010959	0.146
Asiatic	Denali	Eastern Hokkaido 2	Central Hokkaido 1	0.000173	0.00011556	1.497
Asiatic	Denali	Eastern Hokkaido 2	Central Hokkaido 2	0.000141	0.00010829	1.302
Asiatic	Denali	Eastern Hokkaido 2	Eastern Hokkaido 1	0.000020	0.00009615	0.208
Asiatic	Denali	Eastern Hokkaido 2	Southern Hokkaido 1	0.000173	0.00010860	1.593
Asiatic	Denali	Eastern Hokkaido 2	Southern Hokkaido 2	0.000109	0.00010481	1.040
Asiatic	Georgia	Eastern Hokkaido 2	Central Hokkaido 1	0.000123	0.00008761	1.404
Asiatic	Georgia	Eastern Hokkaido 2	Central Hokkaido 2	0.000111	0.00009737	1.140
Asiatic	Georgia	Eastern Hokkaido 2	Eastern Hokkaido 1	0.000040	0.00007782	0.514
Asiatic	Georgia	Eastern Hokkaido 2	Southern Hokkaido 1	0.000245	0.00009252	2.648
Asiatic	Georgia	Eastern Hokkaido 2	Southern Hokkaido 2	0.000038	0.00009360	0.406
Asiatic	Kenai	Eastern Hokkaido 2	Central Hokkaido 1	0.000053	0.00011726	0.452
Asiatic	Kenai	Eastern Hokkaido 2	Central Hokkaido 2	0.000045	0.00011421	0.394
Asiatic	Kenai	Eastern Hokkaido 2	Eastern Hokkaido 1	-0.000023	0.00010599	-0.217
Asiatic	Kenai	Eastern Hokkaido 2	Southern Hokkaido 1	0.000138	0.00012052	1.145
Asiatic	Kenai	Eastern Hokkaido 2	Southern Hokkaido 2	-0.000070	0.00011844	-0.591
Asiatic	Northern Italy	Eastern Hokkaido 2	Central Hokkaido 1	0.000181	0.00010523	1.720
Asiatic	Northern Italy	Eastern Hokkaido 2	Central Hokkaido 2	0.000072	0.00010714	0.672
Asiatic	Northern Italy	Eastern Hokkaido 2	Eastern Hokkaido 1	-0.000069	0.00009163	-0.753
Asiatic	Northern Italy	Eastern Hokkaido 2	Southern Hokkaido 1	0.000214	0.00011637	1.839
Asiatic	Northern Italy	Eastern Hokkaido 2	Southern Hokkaido 2	0.000035	0.00011551	0.303
Asiatic	Russia	Eastern Hokkaido 2	Central Hokkaido 1	0.000206	0.00013180	1.563
Asiatic	Russia	Eastern Hokkaido 2	Central Hokkaido 2	0.000094	0.00011520	0.816
Asiatic	Russia	Eastern Hokkaido 2	Eastern Hokkaido 1	0.000103	0.00010088	1.021
Asiatic	Russia	Eastern Hokkaido 2	Southern Hokkaido 1	0.000142	0.00011639	1.220
Asiatic	Russia	Eastern Hokkaido 2	Southern Hokkaido 2	0.000152	0.00011394	1.334
Asiatic	Slovakia	Eastern Hokkaido 2	Central Hokkaido 1	0.000043	0.00011026	0.390
Asiatic	Slovakia	Eastern Hokkaido 2	Central Hokkaido 2	0.000090	0.00010369	0.868
Asiatic	Slovakia	Eastern Hokkaido 2	Eastern Hokkaido 1	-0.000081	0.00009866	-0.821

Asiatic	Slovakia	Eastern Hokkaido 2	Southern Hokkaido 1	0.000186	0.00010845	1.715
Asiatic	Slovakia	Eastern Hokkaido 2	Southern Hokkaido 2	0.000062	0.00011091	0.559
Asiatic	Slovenia	Eastern Hokkaido 2	Central Hokkaido 1	0.000041	0.00010963	0.374
Asiatic	Slovenia	Eastern Hokkaido 2	Central Hokkaido 2	0.000019	0.00010160	0.187
Asiatic	Slovenia	Eastern Hokkaido 2	Eastern Hokkaido 1	-0.000051	0.00009156	-0.557
Asiatic	Slovenia	Eastern Hokkaido 2	Southern Hokkaido 1	0.000182	0.00011037	1.649
Asiatic	Slovenia	Eastern Hokkaido 2	Southern Hokkaido 2	-0.000005	0.00010638	-0.047
Asiatic	Spain	Eastern Hokkaido 2	Central Hokkaido 1	0.000090	0.00011236	0.801
Asiatic	Spain	Eastern Hokkaido 2	Central Hokkaido 2	0.000010	0.00010870	0.092
Asiatic	Spain	Eastern Hokkaido 2	Eastern Hokkaido 1	-0.000119	0.00010025	-1.187
Asiatic	Spain	Eastern Hokkaido 2	Southern Hokkaido 1	0.000229	0.00011589	1.976
Asiatic	Spain	Eastern Hokkaido 2	Southern Hokkaido 2	0.000036	0.00012329	0.292
Asiatic	Sweden	Eastern Hokkaido 2	Central Hokkaido 1	0.000137	0.00010498	1.305
Asiatic	Sweden	Eastern Hokkaido 2	Central Hokkaido 2	-0.000002	0.00008333	-0.024
Asiatic	Sweden	Eastern Hokkaido 2	Eastern Hokkaido 1	-0.000101	0.00009173	-1.101
Asiatic	Sweden	Eastern Hokkaido 2	Southern Hokkaido 1	0.000234	0.00011207	2.088
Asiatic	Sweden	Eastern Hokkaido 2	Southern Hokkaido 2	0.000027	0.00010547	0.256
Asiatic	Admiralty	Southern Hokkaido	Central Hokkaido 1	0.000126	0.00010056	1.253
Asiatic	Admiralty	Southern Hokkaido	Central Hokkaido 2	-0.000011	0.00009821	-0.112
Asiatic	Admiralty	Southern Hokkaido	Eastern Hokkaido 1	-0.000067	0.00010229	-0.655
Asiatic	Admiralty	Southern Hokkaido	Eastern Hokkaido 2	-0.000059	0.00010190	-0.579
Asiatic	Admiralty	Southern Hokkaido	Southern Hokkaido 2	0.000082	0.00009832	0.834
Asiatic	Alaska	Southern Hokkaido	Central Hokkaido 1	0.000058	0.00011717	0.495
Asiatic	Alaska	Southern Hokkaido	Central Hokkaido 2	-0.000021	0.00011932	-0.176
Asiatic	Alaska	Southern Hokkaido	Eastern Hokkaido 1	-0.000068	0.00011166	-0.609
Asiatic	Alaska	Southern Hokkaido	Eastern Hokkaido 2	-0.000144	0.00011410	-1.262
Asiatic	Alaska	Southern Hokkaido	Southern Hokkaido 2	0.000066	0.00011498	0.574
Asiatic	Baranof	Southern Hokkaido	Central Hokkaido 1	0.000081	0.00011005	0.736
Asiatic	Baranof	Southern Hokkaido	Central Hokkaido 2	-0.000107	0.00012063	-0.887
Asiatic	Baranof	Southern Hokkaido	Eastern Hokkaido 1	-0.000063	0.00011475	-0.549
Asiatic	Baranof	Southern Hokkaido	Eastern Hokkaido 2	-0.000047	0.00011353	-0.414
Asiatic	Baranof	Southern Hokkaido	Southern Hokkaido 2	-0.000069	0.00011349	-0.608
Asiatic	Central Italy	Southern Hokkaido	Central Hokkaido 1	-0.000136	0.00011429	-1.190
Asiatic	Central Italy	Southern Hokkaido	Central Hokkaido 2	-0.000158	0.00012650	-1.249
Asiatic	Central Italy	Southern Hokkaido	Eastern Hokkaido 1	-0.000165	0.00012259	-1.346
Asiatic	Central Italy	Southern Hokkaido	Eastern Hokkaido 2	-0.000207	0.00012715	-1.628
Asiatic	Central Italy	Southern Hokkaido	Southern Hokkaido 2	-0.000333	0.00012435	-2.678
Asiatic	Chichagof	Southern Hokkaido	Central Hokkaido 1	-0.000015	0.00010135	-0.148
Asiatic	Chichagof	Southern Hokkaido	Central Hokkaido 2	-0.000131	0.00010100	-1.297
Asiatic	Chichagof	Southern Hokkaido	Eastern Hokkaido 1	-0.000151	0.00010464	-1.443
Asiatic	Chichagof	Southern Hokkaido	Eastern Hokkaido 2	-0.000104	0.00010216	-1.018
Asiatic	Chichagof	Southern Hokkaido	Southern Hokkaido 2	-0.000088	0.00010390	-0.847
Asiatic	Denali	Southern Hokkaido	Central Hokkaido 1	-0.000001	0.00020000	-0.005
Asiatic	Denali	Southern Hokkaido	Central Hokkaido 2	-0.000032	0.00010959	-0.292
Asiatic	Denali	Southern Hokkaido	Eastern Hokkaido 1	-0.000153	0.00010797	-1.417
Asiatic	Denali	Southern Hokkaido	Eastern Hokkaido 2	-0.000173	0.00010860	-1.593
Asiatic	Denali	Southern Hokkaido	Southern Hokkaido 2	-0.000064	0.00010323	-0.620
Asiatic	Georgia	Southern Hokkaido	Central Hokkaido 1	-0.000122	0.00008316	-1.467
Asiatic	Georgia	Southern Hokkaido	Central Hokkaido 2	-0.000134	0.00009280	-1.444
Asiatic	Georgia	Southern Hokkaido	Eastern Hokkaido 1	-0.000206	0.00008766	-2.350
Asiatic	Georgia	Southern Hokkaido	Eastern Hokkaido 2	-0.000245	0.00009252	-2.648
Asiatic	Georgia	Southern Hokkaido	Southern Hokkaido 2	-0.000207	0.00009155	-2.261
Asiatic	Kenai	Southern Hokkaido	Central Hokkaido 1	-0.000085	0.00011486	-0.740

Asiatic	Kenai	Southern Hokkaido	Central Hokkaido 2	-0.000093	0.00012109	-0.768
Asiatic	Kenai	Southern Hokkaido	Eastern Hokkaido 1	-0.000160	0.00011756	-1.361
Asiatic	Kenai	Southern Hokkaido	Eastern Hokkaido 2	-0.000138	0.00012052	-1.145
Asiatic	Kenai	Southern Hokkaido	Southern Hokkaido 2	-0.000208	0.00012352	-1.684
Asiatic	Northern Italy	Southern Hokkaido	Central Hokkaido 1	-0.000033	0.00010443	-0.316
Asiatic	Northern Italy	Southern Hokkaido	Central Hokkaido 2	-0.000142	0.00011008	-1.290
Asiatic	Northern Italy	Southern Hokkaido	Eastern Hokkaido 1	-0.000283	0.00010826	-2.614
Asiatic	Northern Italy	Southern Hokkaido	Eastern Hokkaido 2	-0.000214	0.00011637	-1.839
Asiatic	Northern Italy	Southern Hokkaido	Southern Hokkaido 2	-0.000179	0.00010462	-1.711
Asiatic	Russia	Southern Hokkaido	Central Hokkaido 1	0.000063	0.00012257	0.514
Asiatic	Russia	Southern Hokkaido	Central Hokkaido 2	-0.000049	0.00011722	-0.418
Asiatic	Russia	Southern Hokkaido	Eastern Hokkaido 1	-0.000039	0.00011890	-0.328
Asiatic	Russia	Southern Hokkaido	Eastern Hokkaido 2	-0.000142	0.00011639	-1.220
Asiatic	Russia	Southern Hokkaido	Southern Hokkaido 2	0.000010	0.00011494	0.087
Asiatic	Slovakia	Southern Hokkaido	Central Hokkaido 1	-0.000144	0.00011009	-1.308
Asiatic	Slovakia	Southern Hokkaido	Central Hokkaido 2	-0.000096	0.00010714	-0.896
Asiatic	Slovakia	Southern Hokkaido	Eastern Hokkaido 1	-0.000268	0.00010690	-2.507
Asiatic	Slovakia	Southern Hokkaido	Eastern Hokkaido 2	-0.000186	0.00010845	-1.715
Asiatic	Slovakia	Southern Hokkaido	Southern Hokkaido 2	-0.000125	0.00010794	-1.158
Asiatic	Slovenia	Southern Hokkaido	Central Hokkaido 1	-0.000140	0.00011236	-1.246
Asiatic	Slovenia	Southern Hokkaido	Central Hokkaido 2	-0.000162	0.00011305	-1.433
Asiatic	Slovenia	Southern Hokkaido	Eastern Hokkaido 1	-0.000233	0.00010572	-2.204
Asiatic	Slovenia	Southern Hokkaido	Eastern Hokkaido 2	-0.000182	0.00011037	-1.649
Asiatic	Slovenia	Southern Hokkaido	Southern Hokkaido 2	-0.000187	0.00010661	-1.754
Asiatic	Spain	Southern Hokkaido	Central Hokkaido 1	-0.000138	0.00011138	-1.239
Asiatic	Spain	Southern Hokkaido	Central Hokkaido 2	-0.000218	0.00011208	-1.945
Asiatic	Spain	Southern Hokkaido	Eastern Hokkaido 1	-0.000348	0.00011440	-3.042
Asiatic	Spain	Southern Hokkaido	Eastern Hokkaido 2	-0.000229	0.00011589	-1.976
Asiatic	Spain	Southern Hokkaido	Southern Hokkaido 2	-0.000192	0.00011566	-1.660
Asiatic	Sweden	Southern Hokkaido	Central Hokkaido 1	-0.000097	0.00010695	-0.907
Asiatic	Sweden	Southern Hokkaido	Central Hokkaido 2	-0.000236	0.00010645	-2.217
Asiatic	Sweden	Southern Hokkaido	Eastern Hokkaido 1	-0.000334	0.00010460	-3.193
Asiatic	Sweden	Southern Hokkaido	Eastern Hokkaido 2	-0.000234	0.00011207	-2.088
Asiatic	Sweden	Southern Hokkaido	Southern Hokkaido 2	-0.000207	0.00009942	-2.082
Asiatic	Admiralty	Southern Hokkaido	Central Hokkaido 1	0.000045	0.00009890	0.455
Asiatic	Admiralty	Southern Hokkaido	Central Hokkaido 2	-0.000093	0.00009617	-0.967
Asiatic	Admiralty	Southern Hokkaido	Eastern Hokkaido 1	-0.000149	0.00011119	-1.340
Asiatic	Admiralty	Southern Hokkaido	Eastern Hokkaido 2	-0.000141	0.00010813	-1.304
Asiatic	Admiralty	Southern Hokkaido	Southern Hokkaido 1	-0.000082	0.00009832	-0.834
Asiatic	Alaska	Southern Hokkaido	Central Hokkaido 1	-0.000008	0.00011594	-0.069
Asiatic	Alaska	Southern Hokkaido	Central Hokkaido 2	-0.000087	0.00011585	-0.751
Asiatic	Alaska	Southern Hokkaido	Eastern Hokkaido 1	-0.000134	0.00011111	-1.206
Asiatic	Alaska	Southern Hokkaido	Eastern Hokkaido 2	-0.000209	0.00011023	-1.896
Asiatic	Alaska	Southern Hokkaido	Southern Hokkaido 1	-0.000066	0.00011498	-0.574
Asiatic	Baranof	Southern Hokkaido	Central Hokkaido 1	0.000150	0.00010965	1.368
Asiatic	Baranof	Southern Hokkaido	Central Hokkaido 2	-0.000039	0.00010569	-0.369
Asiatic	Baranof	Southern Hokkaido	Eastern Hokkaido 1	0.000006	0.00012766	0.047
Asiatic	Baranof	Southern Hokkaido	Eastern Hokkaido 2	0.000022	0.00011111	0.198
Asiatic	Baranof	Southern Hokkaido	Southern Hokkaido 1	0.000069	0.00011349	0.608
Asiatic	Central Italy	Southern Hokkaido	Central Hokkaido 1	0.000198	0.00012230	1.619
Asiatic	Central Italy	Southern Hokkaido	Central Hokkaido 2	0.000175	0.00011864	1.475
Asiatic	Central Italy	Southern Hokkaido	Eastern Hokkaido 1	0.000168	0.00012834	1.309
Asiatic	Central Italy	Southern Hokkaido	Eastern Hokkaido 2	0.000126	0.00012689	0.993

Asiatic	Central Italy	Southern Hokkaido	Southern Hokkaido 1	0.000333	0.00012435	2.678
Asiatic	Chichagof	Southern Hokkaido	Central Hokkaido 1	0.000073	0.00010657	0.685
Asiatic	Chichagof	Southern Hokkaido	Central Hokkaido 2	-0.000042	0.00009524	-0.441
Asiatic	Chichagof	Southern Hokkaido	Eastern Hokkaido 1	-0.000063	0.00011270	-0.559
Asiatic	Chichagof	Southern Hokkaido	Eastern Hokkaido 2	-0.000016	0.00010959	-0.146
Asiatic	Chichagof	Southern Hokkaido	Southern Hokkaido 1	0.000088	0.00010390	0.847
Asiatic	Denali	Southern Hokkaido	Central Hokkaido 1	0.000063	0.00011270	0.559
Asiatic	Denali	Southern Hokkaido	Central Hokkaido 2	0.000032	0.00010191	0.314
Asiatic	Denali	Southern Hokkaido	Eastern Hokkaido 1	-0.000089	0.00010867	-0.819
Asiatic	Denali	Southern Hokkaido	Eastern Hokkaido 2	-0.000109	0.00010481	-1.040
Asiatic	Denali	Southern Hokkaido	Southern Hokkaido 1	0.000064	0.00010323	0.620
Asiatic	Georgia	Southern Hokkaido	Central Hokkaido 1	0.000085	0.00009004	0.944
Asiatic	Georgia	Southern Hokkaido	Central Hokkaido 2	0.000073	0.00009023	0.809
Asiatic	Georgia	Southern Hokkaido	Eastern Hokkaido 1	0.000002	0.00010526	0.019
Asiatic	Georgia	Southern Hokkaido	Eastern Hokkaido 2	-0.000038	0.00009360	-0.406
Asiatic	Georgia	Southern Hokkaido	Southern Hokkaido 1	0.000207	0.00009155	2.261
Asiatic	Kenai	Southern Hokkaido	Central Hokkaido 1	0.000123	0.00012035	1.022
Asiatic	Kenai	Southern Hokkaido	Central Hokkaido 2	0.000115	0.00012273	0.937
Asiatic	Kenai	Southern Hokkaido	Eastern Hokkaido 1	0.000047	0.00011899	0.395
Asiatic	Kenai	Southern Hokkaido	Eastern Hokkaido 2	0.000070	0.00011844	0.591
Asiatic	Kenai	Southern Hokkaido	Southern Hokkaido 1	0.000208	0.00012352	1.684
Asiatic	Northern Italy	Southern Hokkaido	Central Hokkaido 1	0.000146	0.00010815	1.350
Asiatic	Northern Italy	Southern Hokkaido	Central Hokkaido 2	0.000037	0.00010914	0.339
Asiatic	Northern Italy	Southern Hokkaido	Eastern Hokkaido 1	-0.000103	0.00011123	-0.926
Asiatic	Northern Italy	Southern Hokkaido	Eastern Hokkaido 2	-0.000035	0.00011551	-0.303
Asiatic	Northern Italy	Southern Hokkaido	Southern Hokkaido 1	0.000179	0.00010462	1.711
Asiatic	Russia	Southern Hokkaido	Central Hokkaido 1	0.000054	0.00011714	0.461
Asiatic	Russia	Southern Hokkaido	Central Hokkaido 2	-0.000058	0.00011240	-0.516
Asiatic	Russia	Southern Hokkaido	Eastern Hokkaido 1	-0.000049	0.00011639	-0.421
Asiatic	Russia	Southern Hokkaido	Eastern Hokkaido 2	-0.000152	0.00011394	-1.334
Asiatic	Russia	Southern Hokkaido	Southern Hokkaido 1	-0.000010	0.00011494	-0.087
Asiatic	Slovakia	Southern Hokkaido	Central Hokkaido 1	-0.000019	0.00011047	-0.172
Asiatic	Slovakia	Southern Hokkaido	Central Hokkaido 2	0.000028	0.00010646	0.263
Asiatic	Slovakia	Southern Hokkaido	Eastern Hokkaido 1	-0.000143	0.00011413	-1.253
Asiatic	Slovakia	Southern Hokkaido	Eastern Hokkaido 2	-0.000062	0.00011091	-0.559
Asiatic	Slovakia	Southern Hokkaido	Southern Hokkaido 1	0.000125	0.00010794	1.158
Asiatic	Slovenia	Southern Hokkaido	Central Hokkaido 1	0.000046	0.00010979	0.419
Asiatic	Slovenia	Southern Hokkaido	Central Hokkaido 2	0.000024	0.00010256	0.234
Asiatic	Slovenia	Southern Hokkaido	Eastern Hokkaido 1	-0.000046	0.00010698	-0.430
Asiatic	Slovenia	Southern Hokkaido	Eastern Hokkaido 2	0.000005	0.00010638	0.047
Asiatic	Slovenia	Southern Hokkaido	Southern Hokkaido 1	0.000187	0.00010661	1.754
Asiatic	Spain	Southern Hokkaido	Central Hokkaido 1	0.000054	0.00011563	0.467
Asiatic	Spain	Southern Hokkaido	Central Hokkaido 2	-0.000026	0.00011017	-0.236
Asiatic	Spain	Southern Hokkaido	Eastern Hokkaido 1	-0.000155	0.00012128	-1.278
Asiatic	Spain	Southern Hokkaido	Eastern Hokkaido 2	-0.000036	0.00012329	-0.292
Asiatic	Spain	Southern Hokkaido	Southern Hokkaido 1	0.000192	0.00011566	1.660
Asiatic	Sweden	Southern Hokkaido	Central Hokkaido 1	0.000110	0.00010417	1.056
Asiatic	Sweden	Southern Hokkaido	Central Hokkaido 2	-0.000029	0.00010211	-0.284
Asiatic	Sweden	Southern Hokkaido	Eastern Hokkaido 1	-0.000128	0.00010518	-1.217
Asiatic	Sweden	Southern Hokkaido	Eastern Hokkaido 2	-0.000027	0.00010547	-0.256
Asiatic	Sweden	Southern Hokkaido	Southern Hokkaido 1	0.000207	0.00009942	2.082

The values highlighted in grey indicate |Z score| > 3 considered significant.

Table 8. Sampling data used in this study.

mtDNA lineage	subpopulation	Sample name	analysis_autosome	analysis_demography	analysis_X chromosome	analysis_mtDNA	analysis_Y chromosome	longitude	latitude	sex	haplotype(mtDNA)	haplotype(chr Y)
clade 3a2	Sohya	421					*	141.902	45.106	M	-	BR01_05
clade 3a2	Sohya	427				*	*	142.152	44.898	M	HB-07	BR01_06
clade 3a2	Sohya	520	*	*	*	*	*	142.34	45.023	M	HB-08	BR01_05
clade 3a2	Sohya	615	*	*	*	*	*	142.59	44.815	M	HB-02	BR01_05
clade 3a2	Doto	624	*	*	*	*		143.902	43.065	F	HB-02	-
clade 3a2	Sohya	810	*	*	*	*		142.84	44.315	F	HB-02	-
clade 3a2	Doto	823	*	*	*	*		143.652	43.023	F	HB-02	-
clade 3a2	Hidaka	826	*	*	*	*	*	142.902	42.982	M	HB-04	BR01_07
clade 3a2	Sohya	834	*	*	*	*	*	142.902	43.398	M	HB-01	BR01_09
clade 3a2	Ishikari	835	*	*	*	*	*	141.528	42.94	M	HB-05	BR01_08
clade 3a2	Hidaka	837	*	*	*	*	*	142.84	42.982	M	HB-04	BR01_05
clade 3a2	Sohya	901				*		142.152	44.898	F	HB-09	-
clade 3a2	Ishikari	910				*	*	141.528	42.607	M	HB-05	BR01_08
clade 3a2	Hidaka	916					*	142.965	43.065	M	-	BR01_05
clade 3a2	Hidaka	917					*	141.84	43.232	M	-	BR01_07
clade 3a2	Doto	931					*	143.777	43.523	M	-	BR01_03
clade 3a2	Hidaka	1137	*	*	*	*		142.215	43.482	F	HB-02	-
clade 3a2	Hidaka	1151					*	142.34	42.648	M	-	BR01_08
clade 3a2	Sohya	1171	*	*	*	*		142.902	43.815	F	HB-03	-
clade 3a2	Sohya	1176					*	142.652	43.565	M	-	BR01_05
clade 3a2	Doto	2078		*	*	*		144.652	43.148	F	HB-02	-
clade 3a2	Hidaka	2099	*	*	*	*	*	142.215	42.732	M	HB-04	BR01_05
clade 3a2	Hidaka	2111	*	*	*	*	*	142.09	42.982	M	HB-02	BR01_07
clade 3a2	Sohya	2128	*	*	*	*	*	142.527	44.731	M	HB-02	BR01_04
clade 3a2	Hidaka	2213	*	*	*	*	*	142.465	42.315	M	HB-04	BR01_06
clade 3a2	Hidaka	2225	*	*	*	*		142.59	42.44	F	HB-04	-
clade 3a2	Hidaka	3076	*	*	*	*		142.84	42.19	F	HB-04	-
clade 3a2	Hidaka	3091	*	*	*	*		142.09	42.857	F	HB-02	-
clade 3a2	Hidaka	3092	*	*	*	*		142.152	43.065	F	HB-02	-
clade 3a2	Sohya	3097	*	*	*	*	*	142.527	43.857	M	HB-02	BR01_05
clade 3a2	Hidaka	3126					*	142.902	42.773	M	-	BR01_06
clade 3a2	Sohya	4135					*	143.527	43.273	M	-	BR01_05
clade 3a2	Sohya	4141	*	*	*	*		143.402	43.315	F	HB-02	-
clade 3a2	Sohya	4149					*	143.652	43.565	M	-	BR01_05
clade 3a2	Sohya	4155	*	*	*	*		143.402	44.065	F	HB-02	-
clade 3a2	Teshio	4251				*	*	142.09	44.648	M	HB-02	BR01_05
clade 3a2	Sohya	4293	*	*	*	*		143.027	44.148	F	HB-06	-
clade 3a2	Hidaka	5014	*	*	*	*	*	143.215	41.982	M	HB-04	BR01_05
clade 3a2	Sohya	5074					*	142.277	44.856	M	-	BR01_06
clade 3a2	Sohya	6001					*	142.527	44.981	M	-	BR01_05
clade 3a2	Sohya	6065					*	143.152	43.648	M	-	BR01_04
clade 3a2	Sohya	6077					*	143.465	43.565	M	-	BR01_02
clade 3a2	Doto	6081					*	144.59	43.773	M	-	BR01_04
clade 3a2	Doto	6107	*	*	*	*	*	143.84	43.94	M	HB-02	BR01_05
clade 3b	Doto	617	*	*	*	*	*	145.027	43.815	M	HB-11	BR01_04
clade 3b	Doto	747					*	144.965	44.023	M	-	BR01_04
clade 3b	Sohya	811	*	*	*	*		143.715	43.44	F	HB-13	-
clade 3b	Doto	819					*	144.84	43.982	M	-	BR01_04
clade 3b	Doto	820	*	*	*	*		145.09	44.107	F	HB-10	-
clade 3b	Doto	822	*	*	*	*	*	145.34	44.315	M	HB-12	BR01_06
clade 3b	Doto	927					*	144.965	44.065	M	-	BR01_04
clade 3b	Doto	4148					*	143.715	42.94	M	-	BR01_03
clade 3b	Doto	4150	*	*	*	*	*	143.84	43.315	M	HB-13	BR01_04
clade 3b	Doto	4162				*		143.84	43.565	F	HB-13	-
clade 3b	Doto	4296					*	144.09	43.607	M	-	BR01_05
clade 3b	Sohya	6071					*	143.34	43.69	M	-	BR01_03
clade 3b	Doto	6106	*	*		*	*	144.277	43.607	M	HB-13	BR01_04
clade 3b	Doto	6115					*	144.652	43.69	M	-	BR01_04
clade 4	Oshima	503	*	*	*	*	*	139.965	42.69	M	HB-16	BR01_05
clade 4	Oshima	515				*	*	140.84	42.023	M	HB-17	BR01_05
clade 4	Oshima	526					*	140.528	42.107	M	-	BR01_05
clade 4	Oshima	815					*	140.778	41.898	M	-	BR01_05
clade 4	Ishikari	1119				*		140.465	43.19	F	HB-15	-
clade 4	Oshima	2004	*	*	*	*		140.278	42.107	F	HB-17	-
clade 4	Oshima	2026	*	*	*	*		140.028	42.107	M	HB-17	-
clade 4	Oshima	2027					*	140.153	42.023	M	-	BR01_05
clade 4	Oshima	2030					*	139.84	42.523	M	-	BR01_05
clade 4	Ishikari	2098	*	*	*	*	*	141.09	42.732	M	HB-14	BR01_09
clade 4	Ishikari	2109					*	140.528	43.107	M	-	BR01_09
clade 4	Oshima	4001	*	*	*	*	*	140.153	41.857	M	HB-17	BR01_05
clade 4	Oshima	4008	*	*	*	*	*	139.903	42.357	M	HB-16	BR01_05
clade 4	Oshima	4025				*		140.153	41.773	M	HB-17	-
clade 4	Oshima	4028	*	*	*	*		140.153	42.398	F	HB-16	-
clade 4	Oshima	4048					*	140.215	42.232	M	-	BR01_05
clade 4	Ishikari	5046					*	140.653	43.023	M	-	BR01_06
clade 4	Ishikari	5048	*	*	*	*		140.84	43.023	F	HB-14	-
clade 4	Oshima	5051	*	*	*	*	*	140.215	41.482	M	HB-17	BR01_05

Asterisks mean that each sample was included in each dataset.

Table 9. WGS data in this study.

species	Area	Population	Sample name (in this study)	sex	place	SRA accession	remarks	reference
Ursus arctos	Europe	West Europe	191Y	NA	Hrusica, Slovenia	ERR2678638		Barlow et al. (2018)
Ursus arctos	Europe	West Europe	ALP1	F	Alps, North Italy	SRR5878346		Benazzo et al. (2017)
Ursus arctos	Europe	West Europe	APN2	M	Apennine, Central Italy	SRR5878360		Benazzo et al. (2017)
Ursus arctos	Europe	East Europe	SLK1	M	Slovakia	SRR5878353		Benazzo et al. (2017)
Ursus arctos	Europe	West Europe	SPA1	M	Spain	SRR5878347		Benazzo et al. (2017)
Ursus arctos	Europe	West Europe	Swe	F	Dalarna, Sweden	SRR1693654		Cahill et al. (2015)
Ursus arctos	Hokkaido	Hokkaido	518	F	Kikonai, Hokkaido, Japan	DRR276774		Endo et al. (2021)
Ursus arctos	Hokkaido	Hokkaido	5046	M	Kyowa, Hokkaido, Japan	DRR276775		Endo et al. (2021)
Ursus arctos	Hokkaido	Hokkaido	421	M	Toyotomi, Hokkaido, Japan	DRR276777		Endo et al. (2021)
Ursus arctos	Hokkaido	Hokkaido	2231	F	Bibai, Hokkaido, Japan	DRR276776		Endo et al. (2021)
Ursus arctos	Hokkaido	Hokkaido	5010	F	Kiyosato, Hokkaido, Japan	DRR276778		Endo et al. (2021)
Ursus arctos	Hokkaido	Hokkaido	819	M	Syari, Hokkaido, Japan	DRR276779		Endo et al. (2021)
Ursus arctos	NorthAmerica	ABC	ABC2	M	Baranof Island, AK, USA	SRR518717		Miller et al. (2012)
Ursus arctos	NorthAmerica	ABC	Adm1	F	Admiralty Island, AK, ABC	SRR830213		Cahill et al. (2013)
Ursus arctos	NorthAmerica	ABC	Chi1	F	Chichagof island, AK, USA	SRR1692419		Cahill et al. (2015)
Ursus arctos	NorthAmerica	ABC	Chi2	F	Chichagof island, AK, USA	SRR1693624		Cahill et al. (2015)
Ursus arctos	NorthAmerica	Alaska	Den	F	Denali, Alaska, USA	SRR830337		Cahill et al. (2013)
Ursus arctos	NorthAmerica	Alaska	GT_1	M	Toronto zoo (from somewhere of Alaska), USA	SRR7758718		Taylor et al. (2018)

Table 10. The result of genotyping by stacks.

Population	Private	Sites	Variant sites	Polymorphic sites	% polymorphic loci	Numbver of individuals			P*			Observed heterozygosity			Observed homozygosity			Expected heterozigosity			Expected homozygosity			π			F_{IS}		
						Mean	Var	StdErr	Mean	Var	StdErr	Mean	Var	StdErr	Mean	Var	StdErr	Mean	Var	StdErr	Mean	Var	StdErr	Mean	Var	StdErr	Mean	Var	StdErr
# Variant positions																													
# Pop ID	Private					Num_Indv	Var	StdErr	P	Var	StdErr	Obs_Het	Var	StdErr	Obs_Hom	Var	StdErr	Exp_Het	Var	StdErr	Exp_Hom	Var	StdErr	Pi	Var	StdErr	Fis	Var	StdErr
clade 3a2	767452					8.70822	66.55163	0.00589	0.80568	0.0315	0.00013	0.08563	0.04341	0.00015	0.91437	0.04341	0.00015	0.25011	0.03735	0.00014	0.74989	0.03735	0.00014	0.29504	0.06144	0.00018	0.48993	0.26164	0.00589
clade 3b	116472					2.72202	3.78683	0.00165	0.9083	0.02879	0.00014	0.07691	0.04842	0.00019	0.92309	0.04842	0.00019	0.10902	0.0356	0.00016	0.89098	0.0356	0.00016	0.14402	0.06927	0.00022	0.11832	0.11558	0.00165
clade 4	176195					3.7495	10.24401	0.00265	0.89409	0.03018	0.00014	0.07739	0.04497	0.00018	0.92261	0.04497	0.00018	0.12903	0.03805	0.00016	0.87097	0.03805	0.00016	0.16311	0.06837	0.00022	0.16353	0.14846	0.00265
# All positions (variant and fixed)																													
# Pop ID	Private	Sites	Variant_Sites	Polymorphic_Sites	%Polymorphic_Loci	Num_Indv	Var	StdErr	P	Var	StdErr	Obs_Het	Var	StdErr	Obs_Hom	Var	StdErr	Exp_Het	Var	StdErr	Exp_Hom	Var	StdErr	Pi	Var	StdErr	Fis	Var	StdErr
clade 3a2	767452	382251004	1921106	1469006	0.3843	7.12506	61.31577	0.0004	0.99902	0.00035	0	0.00043	0.00025	0	0.99957	0.00025	0	0.00126	0.0005	0	0.99874	0.0005	0	0.00148	0.00074	0	0.00246	0.00252	0.0004
clade 3b	116472	249898321	1396355	378879	0.15161	2.64062	3.6585	0.00012	0.99949	0.00021	0	0.00043	0.0003	0	0.99957	0.0003	0	0.00061	0.00026	0	0.99939	0.00026	0	0.0008	0.0005	0	0.00066	0.00072	0.00012
clade 4	176195	306851250	1463228	504516	0.16442	3.72782	9.86104	0.00018	0.99949	0.0002	0	0.00037	0.00024	0	0.99963	0.00024	0	0.00062	0.00026	0	0.99938	0.00026	0	0.00078	0.00045	0	0.00078	0.00083	0.00018

Table 11. The number of heterozygous sites of the Hokkaido population per individual.

mtDNA lineage	Region	Sample name	Number of homozygous sites	Number of sites	Number of heterozygous sites
clade 3a2	Sohya	520	89,587	106,312	16,725
clade 3a2	Sohya	615	90,046	106,520	16,474
clade 3a2	Doto	624	87,821	105,208	17,387
clade 3a2	Sohya	810	90,896	106,418	15,522
clade 3a2	Doto	823	91,086	106,530	15,444
clade 3a2	Hidaka	826	90,130	106,549	16,419
clade 3a2	Doto	834	89,846	105,026	15,180
clade 3a2	Ishikari	835	89,693	103,258	13,565
clade 3a2	Hidaka	837	92,021	106,460	14,439
clade 3a2	Hidaka	1137	89,649	106,417	16,768
clade 3a2	Doto	1171	90,312	106,066	15,754
clade 3a2	Hidaka	2099	88,753	106,108	17,355
clade 3a2	Hidaka	2111	94,012	106,527	12,515
clade 3a2	Sohya	2128	87,484	105,380	17,896
clade 3a2	Hidaka	2213	89,737	105,720	15,983
clade 3a2	Hidaka	2225	89,397	106,011	16,614
clade 3a2	Hidaka	3076	87,469	104,347	16,878
clade 3a2	Hidaka	3091	89,526	106,094	16,568
clade 3a2	Hidaka	3092	88,339	105,007	16,668
clade 3a2	Sohya	3097	94,539	106,740	12,201
clade 3a2	Doto	4141	86,531	101,848	15,317
clade 3a2	Sohya	4155	86,323	105,497	19,174
clade 3a2	Sohya	4293	89,313	106,374	17,061
clade 3a2	Hidaka	5014	84,346	103,006	18,660
clade 3a2	Sohya	6107	89,506	106,412	16,906
clade 3b	Doto	617	90,454	106,132	15,678
clade 3b	Doto	811	90,485	106,619	16,134
clade 3b	Doto	820	88,200	104,530	16,330
clade 3b	Doto	822	90,287	106,568	16,281
clade 3b	Doto	4150	90,344	106,416	16,072
clade 3b	Doto	6106	89,052	103,053	14,001
clade 4	Oshima	503	89,685	106,046	16,361
clade 4	Oshima	2004	88,506	103,866	15,360
clade 4	Oshima	2026	90,476	106,545	16,069
clade 4	Ishikari	2098	91,214	104,201	12,987
clade 4	Oshima	4001	90,107	104,682	14,575
clade 4	Oshima	4008	90,366	106,396	16,030
clade 4	Oshima	4028	90,569	106,452	15,883
clade 4	Ishikari	5048	91,809	106,709	14,900
clade 4	Oshima	5051	90,545	106,309	15,764

Table 12. F_{st} between subpopulations based on autosomal data.

	Oshima	Ishikari	Hidaka	Sohya
Ishikari	0.090			
Hidaka	0.054	0.087		
Sohya	0.051	0.084	0.026	
Doto	0.061	0.093	0.035	0.018

All SE values were lower than 0.01

Table 13. Q statistics between the subpopulations in Hokkaido.

	Oshima	Ishikari	Hidaka	Sohya
Ishikari	0.376 (0.273–0.558)			
Hidaka	0.386 (0.316–0.472)	0.496 (0.361–0.749)		
Sohya	0.461 (0.369–0.586)	0.477 (0.351–0.671)	0.441(0.342–0.589)	
Doto	0.351 (0.284–0.439)	0.330 (0.266–0.440)	0.336(0.266–0.440)	0.321(0.234–0.470)

The values in the parentheses means 95% CI calculated based on F_{st} and that of SE.

Table 14. Q statistics between the three populations.

	Hokkaido	Europe
Europe	0.308(0.157–0.476)	
North America	0.403(0.237–0.560)	0.67(0.565–0.800)

The values in the parentheses means 95% CI calculated based on F_{st} and that of SE.

Table 15. The result of the parameters in all models on fastsimcoal2.

	a. One expansion model	b. One decline model	c. Two expansions model	d. Two declines model	e. One bottleneck model
NANC	525	14,903	389	28,354	13,817
NANC 95CI+	524	10,104	199	10,626	10,167
NANC 95CI-	579	10,379	1,292	26,571	52,330
NBOT	-	-	545	16,976	257
NBOT 95CI+	-	-	549	10,424	240
NBOT 95CI-	-	-	2,707	24,354	9,887
T1	1,144	2,470,457	116,512	34,318,207	22,616
T1 95CI+	1,155	1,235	1,685	1,232	2,972
T1 95CI-	1,303	19,563	128,205	996,440	71,942
T2	-	-	1,188	4,438,368	1,155
T2 95CI+	-	-	1,194	1,144	1,227
T2 95CI-	-	-	3,333	1,754	35,616

NCUR=10000, N/2, T*11

Table 16. Mantel r values on Mantel test.

Hypothesis	Barrier	Autosome (n=40, 95,984 SNPs)	Mitochondrial DNA (n=49, 38 sites)	Y-chromosomal DNA (n=54, 3 locus)
Distance	Distance	0.1944*	0.6495**	0.08563
High elev.	Mean	-0.00858	-0.1827	0.1036*
	Max	0.08725*	0.1244**	0.1186**
Low elev.	Min	0.1623	0.6258**	-0.0009369
Variant elv.	Max-Min	0.1073**	0.1957**	0.1138**
	SD	0.09859*	0.1622**	0.0885*

*:$P < 0.05$, **; $P < 0.01$

Table 17. Mantel r value on partial Mantel test.

Hypothesis	Barrier	Autosome (n=40, 95,984 SNPs)		Mitochondrial DNA (n=49, 38 sites)		Y-chromosomal DNA (n=54, 3 locus)	
		*G*B/D*	*G*D/B*	*G*B/D*	*G*D/B*	*G*B/D*	*G*D/B*
high elev.	Mean	0.00245	0.1942*	-0.2541	0.6637**	0.09979*	0.08099
	Max	0.02209	0.1757*	-0.1884	0.6585**	0.09258*	0.04246
low elev.	Min	0.05415	0.1211*	0.4162**	0.4628**	-0.06345	0.10640**
variant elv.	Max-Min	0.02734	0.1653*	-0.1561	0.6430**	0.08351	0.03647
	SD	0.04008	0.1729*	-0.0932	0.6414**	0.06251	0.05836

*:$P < 0.05$, **; $P < 0.01$

Table 18. The result of resistanceGA.

Surface	obj.func_LL	k	AIC	AICc	ΔAICc	ωi	R2m	R2c	LL	Equation
autosome										
elev	4021.72955	4	-8035.4591	-8034.3162	0	0.60414111	0.25732415	0.89510809	4021.72955	Inverse Monomolecular
Distance	4018.89752	2	-8033.795	-8033.4707	0.8455	0.39585889	0.20436188	0.87804776	4018.89752	
Null	3772.30368	1	-7542.6074	-7542.5021	491.8141	9.662E-108	0	0.72017896	3772.30368	
mtDNA										
elev	1391.35269	4	-2774.7054	-2773.7963	0	1	0.69497836	0.95896767	1391.35269	Inverse Monomolecular
Distance	1163.26027	2	-2322.5205	-2322.2597	451.536618	8.914E-99	0.52348297	0.69325959	1163.26027	
Null	732.83711	1	-1463.6742	-1463.5891	1310.20717	3.105E-285	0	0.3102302	732.83711	
chrY										
Distance	7640.15639	2	-15276.313	-15276.077	0	0.90808719	0.06463797	0.41187112	7640.15639	
elev	7640.15639	4	-15272.313	-15271.496	4.581	0.09191281	0.06463797	0.41187112	7640.15639	Distance
Null	7591.42984	1	-15180.86	-15180.783	95.294	1.842E-21	0	0.31956679	7591.42984	

Table 19. All results to evaluate the relative habitat suitable models.

rm	fc	tune.args	auc.train	auc.diff.avg	auc.diff.sd	auc.val.avg	auc.val.sd	AICc	delta.AICc	w.AIC	ncoef
0.5	LQH	rm.0.5_fc.LQH	0.9617574	0.00334575	0.00266748	0.9602009	0.00332275	40259.84	0	1	103
1	LQH	rm.1_fc.LQH	0.9598793	0.00314924	0.00277304	0.958662	0.0033415	40330.14	70.30285	5.4191E-16	75
1.5	LQH	rm.1.5_fc.LQH	0.9587625	0.002994	0.00270117	0.9576856	0.0032733	40401.98	142.1427	1.3618E-31	66
2	LQH	rm.2_fc.LQH	0.9578547	0.00289075	0.00284359	0.956822	0.00324877	40456.66	196.81928	1.8249E-43	54
2.5	LQH	rm.2.5_fc.LQH	0.9571295	0.00277631	0.00279353	0.9561991	0.00319997	40514.94	255.10125	4.0315E-56	50
3	LQH	rm.3_fc.LQH	0.9566933	0.0027177	0.00285443	0.9557039	0.0032136	40556.88	297.04226	3.1484E-65	47
0.5	LQ	rm.0.5_fc.LQ	0.938079	0.00553135	0.00348196	0.9377329	0.00555117	41259.96	1000.12065	6.707E-218	10
1	LQ	rm.1_fc.LQ	0.9349832	0.00539948	0.00345423	0.9346579	0.00552461	41418.75	1158.91522	2.212E-252	9
1.5	LQ	rm.1.5_fc.LQ	0.9335195	0.00539126	0.00359845	0.9331622	0.00564126	41518.84	1259.00354	4.082E-274	7
2	LQ	rm.2_fc.LQ	0.9313931	0.0053258	0.00364016	0.9314928	0.00547915	41647.34	1387.50211	5.102E-302	9
2.5	LQ	rm.2.5_fc.LQ	0.9293915	0.00517059	0.00367341	0.9292428	0.00547765	41767.61	1507.76791	0	8
3	LQ	rm.3_fc.LQ	0.9286674	0.00518213	0.00374663	0.9282997	0.00565183	41817.45	1557.61499	0	7
0.5	L	rm.0.5_fc.L	0.8694984	0.00362313	0.00136266	0.8690011	0.00345218	43918.88	3659.03887	0	7
1.5	L	rm.1.5_fc.L	0.8686489	0.0036758	0.00145815	0.8681661	0.00357487	43926.23	3666.3877	0	6
2	L	rm.2_fc.L	0.8683045	0.00368173	0.00143588	0.867911	0.00359651	43926.35	3666.51551	0	6
1	L	rm.1_fc.L	0.8689176	0.00361821	0.00150001	0.868454	0.00353446	43927.19	3667.35322	0	6
2.5	L	rm.2.5_fc.L	0.8679473	0.00371475	0.00138637	0.8675824	0.00363878	43927.82	3667.98528	0	6
3	L	rm.3_fc.L	0.8675717	0.00377501	0.00136378	0.8672126	0.00369805	43930.21	3670.37238	0	6

The rows highlighted in grey indicate the model chosen as the best model based on AICc

Table 20. Contributions of each environment variance in the best model.

variance	contribution(%)
bio_17	45.5721
bio_8	32.9288
bio_7	13.4466
bio_9	3.4719
bio_18	2.2736
bio_15	1.8269
bio_19	0.4801

Table 21. Sample list used as genome data in this study.

Sample name	species	Group	Getorganelle	mtDNAlineage	NCBI accession number	NCBI accession number (mtDNA)	sex	sex_test_result	coverage (%)	depth	Sampling_location	genotyping	using_multiple_fastq_files(Y/N)	reference
American_black_bear	*Ursus americanus*	Out group	-	-	SRS347023	-	M	M	89.90	20.69	Anchorage, AK, USA	modern	N	Kumar et al. (2017)
JBB_32K	*Ursus arctos*	ancient	-	-	DRS195621	-	NA	NA	10.54	-	Japan:Gunma, Ueno Village	ancient	Y	Segawa et al. (2021)
Kunashir1	*Ursus arctos*	ancient	-	-	SRS3444839	-	NA	NA	10.14	-	Kuril Islands	ancient	Y	Cahill et al. (2018)
Leitrim_4	*Ursus arctos*	ancient	-	-	SRS3444835	-	NA	NA	20.46	-	Poll na mBŽar Cave, Co. Leitrim, Ireland	ancient	Y	Cahill et al. (2018)
Leitrim_5	*Ursus arctos*	ancient	-	-	SRS3444834	-	NA	NA	15.47	-	Poll na mBŽar Cave, Co. Leitrim, Ireland	ancient	Y	Cahill et al. (2018)
Uap	*Ursus arctos*	ancient	-	-	ERS2582837	-	NA	NA	72.05	-	Winden Cave, Austria	ancient	Y	Barlow et al. (2018)
235	*Ursus arctos*	C_Asia	*	3a1	ERS2582840	-	NA	M	88.16	17.25	Balakhtinsky District, Russia	modern	N	Barlow et al. (2018)
U05M	*Ursus arctos*	C_Asia	*	5			NA	M	88.37	23.04	Tibetan plateau, Qinghai, Serg-tchu (upper Huang Ho)	modern	Y	Hirata et al. (2014)
U13M	*Ursus arctos*	C_Asia	*	6			NA	F	88.25	25.94	Kazakhstan, Karatau Mts.	modern	Y	Hirata et al. (2014)
U40	*Ursus arctos*	C_Asia	*	5			NA	M	85.06	10.65	Tibetan plateau, mountains to west from Kukunor Lake	modern	N	Hirata et al. (2014)
U76	*Ursus arctos*	C_Asia	*	3b			NA	M	89.71	38.47	Russia, Krasnojarsk Prov	modern	N	Hirata et al. (2014)
Ge	*Ursus arctos*	Caucasus	*	3a_WestAsia	ERS2582839	-	NA	M	89.02	19.96	Great Caucasus, Georgia	modern	N	Barlow et al. (2018)
U12M	*Ursus arctos*	Caucasus	*	1_WestAsia			NA	M	89.24	31.68	Western Iran, Oshnoviyeh, SW from Urmia Lake	modern	Y	Hirata et al. (2014)
U47M	*Ursus arctos*	Caucasus	*	3a_WestAsia			NA	F	88.31	23.87	Western Caucasus, Sochi	modern	Y	Hirata et al. (2014)
AA1	*Ursus arctos*	E_Asia	*	3a1			M	M	90.30	43.33	Sakhalin	modern	N	Hirata et al. (2013)
ETF1	*Ursus arctos*	E_Asia	*	3b			M	M	89.70	34.54	Etorofu	modern	N	Hirata et al. (2013)
U34	*Ursus arctos*	E_Asia	*	3a1			NA	M	90.49	41.71	North-East Siberia, Kolymskyi Mts.	modern	N	Hirata et al. (2014)
191Y	*Ursus arctos*	Europe	*	1b	ERS2582838	-	NA	M	84.49	8.53	Hrusica, Slovenia	modern	N	Barlow et al. (2018)
ALP1	*Ursus arctos*	Europe	*	1b	SRS2393233	-	F	F	87.15	16.28	Alps, North Italy	modern	N	Benazzo et al. (2017)
APN2	*Ursus arctos*	Europe	*	1b	SRS2393224	-	M	M	88.04	16.20	Apennine, Central Italy	modern	N	Benazzo et al. (2017)
OFS01	*Ursus arctos*	Europe	-	1a	SRS459921	-	F	F	88.25	25.83	Östanvik, Furudal, Sweden	modern	Y	Liu et al. (2014)
RF01	*Ursus arctos*	Europe	-	3a1	SRS459923	-	F	F	88.04	22.67	Ruokolahti, Finland	modern	Y	Liu et al. (2014)
SJS01	*Ursus arctos*	Europe	-	3a1	SRS459922	-	F	F	86.81	13.17	Slakka, Jokkmokk	modern	Y	Liu et al. (2014)
SLK1	*Ursus arctos*	Europe	*	3a1	SRS2393230	-	M	M	88.30	16.75	Slovakia	modern	N	Benazzo et al. (2017)
SPA1	*Ursus arctos*	Europe	*	1a	SRS2393232	-	M	M	88.33	18.35	Spain	modern	N	Benazzo et al. (2017)
Swe	*Ursus arctos*	Europe	*	1a	SRS779830	-	F	F	81.59	7.59	Dalarna, Sweden	modern	N	Cahill et al. (2015)
421	*Ursus arctos*	Hokkaido	*	3a2	DRS203666	-	M	M	90.33	40.87	Toyotomi, Hokkaido, Japan	modern	N	Endo et al. (2021)
518	*Ursus arctos*	Hokkaido	*	4	DRS203663	-	F	F	88.62	34.51	Kikonai, Hokkaido, Japan	modern	N	Endo et al. (2021)
819	*Ursus arctos*	Hokkaido	*	3b	DRS203668	-	M	M	90.30	41.50	Syari, Hokkaido, Japan	modern	N	Endo et al. (2021)
2231	*Ursus arctos*	Hokkaido	*	3a2	DRS203665	-	F	F	89.31	42.62	Bibai, Hokkaido, Japan	modern	N	Endo et al. (2021)
5010	*Ursus arctos*	Hokkaido	*	3b	DRS203667	-	F	F	89.10	41.85	Kiyosato, Hokkaido, Japan	modern	N	Endo et al. (2021)
5046	*Ursus arctos*	Hokkaido	*	4	DRS203664	-	M	M	90.46	43.67	Kyowa, Hokkaido, Japan	modern	N	Endo et al. (2021)
ABC01	*Ursus arctos*	NorthAmerica	-	2a	SRS459924	-	NA	M	89.21	21.70	Ford Arm, Alexander Archipelago, Baranof Island	modern	Y	Liu et al. (2014)
ABC02	*Ursus arctos*	NorthAmerica	-	2a	SRS459925	-	NA	F	87.55	19.42	Baranof Lake / Salmon Lake, Alexander Archipelago, Baranof Island	modern	Y	Liu et al. (2014)
ABC03	*Ursus arctos*	NorthAmerica	-	2a	SRS459926	-	NA	M	89.15	20.69	N Shore of Tenakee Inlet, Alexander Archipelago, Chichagof Island	modern	Y	Liu et al. (2014)
ABC04	*Ursus arctos*	NorthAmerica	-	2a	SRS459927	-	NA	M	89.04	20.47	Saltery Bay, Tenakee Inlet, Alexander Archipelago, Chichagof Island	modern	Y	Liu et al. (2014)
ABC05	*Ursus arctos*	NorthAmerica	-	2a	SRS459928	-	NA	F	88.30	24.22	Between Whitestone Harbor and Freshwater Bay, Alexander Archipelago, Chichagof Island	modern	Y	Liu et al. (2014)
ABC06	*Ursus arctos*	NorthAmerica	-	2a	SRS459929	-	NA	F	87.86	20.39	South arm of Hood Bay, Alexander Archipelago, Admiralty Island	modern	Y	Liu et al. (2014)
ABC1	*Ursus arctos*	NorthAmerica	-	2a	SRS347020	-	F	F	89.77	47.24	Admiralty Island, AK, USA	modern	Y	Miller et al. (2012)
ABC2	*Ursus arctos*	NorthAmerica	*	2a	SRS347021	-	M	M	89.53	27.00	Baranof Island, AK, USA	modern	N	Miller et al. (2012)
Adm1	*Ursus arctos*	NorthAmerica	-	2a	SRS412588	-	F	F	85.92	17.22	Admiralty Island, AK, ABC	modern	N	Cahill et al. (2013)
BB020	*Ursus arctos*	NorthAmerica	*	3a1	SRS11923448	-	M	M	84.50	9.15	USA: Alaska, Seward Peninsula	modern	N	Lan et al. (2022)
BB034	*Ursus arctos*	NorthAmerica	*	3a1	SRS11923449	-	M	M	83.53	8.47	USA: Alaska, North Slope	modern	N	Lan et al. (2022)
BB037	*Ursus arctos*	NorthAmerica	*	3b	SRS11923450	-	M	M	84.66	9.21	USA: Alaska, North Slope	modern	N	Lan et al. (2022)
BB049	*Ursus arctos*	NorthAmerica	*	3a1	SRS11923451	-	F	F	83.20	9.17	USA: Alaska, North Slope	modern	N	Lan et al. (2022)
BB059	*Ursus arctos*	NorthAmerica	*	3a1	SRS11923452	-	F	F	82.93	8.85	USA: Alaska, North Slope	modern	N	Lan et al. (2022)
Chi1	*Ursus arctos*	NorthAmerica	*	2a	SRS778691	-	F	F	80.02	6.85	Chichagof island, AK, USA	modern	N	Cahill et al. (2015)
Chi2	*Ursus arctos*	NorthAmerica	*	2a	SRS779820	-	F	F	81.26	7.51	Chichagof island, AK, USA	modern	N	Cahill et al. (2015)
CON001	*Ursus arctos*	NorthAmerica	*	4	SRS11923454	-	NA	F	83.11	9.04	USA: Yellowstone National Park	modern	N	Lan et al. (2022)
Den	*Ursus arctos*	NorthAmerica	-	3a1	SRS412587	-	F	F	85.90	17.24	Denali, Alaska, USA	modern	N	Cahill et al. (2013)
EB027	*Ursus arctos*	NorthAmerica	*	3b	SRS11923453	-	F	F	82.98	9.32	USA: Alaska, Anchorage	modern	N	Lan et al. (2022)
GP01	*Ursus arctos*	NorthAmerica	-	4	SRS459930	-	NA	F	88.65	18.55	Glacier Park, Montana	modern	Y	Liu et al. (2014)
GRZ	*Ursus arctos*	NorthAmerica	-	3a1	SRS347022	-	F	F	89.07	28.21	Kenai, AK, USA	modern	Y	Miller et al. (2012)
WB039	*Ursus arctos*	NorthAmerica	*	3a1	SRS11923455	-	M	M	83.39	8.72	USA: Alaska, Douglas river	modern	N	Lan et al. (2022)
GT_1	*Ursus arctos horribilis*	NorthAmerica	*	3b	SRS3717847	-	M	M	90.37	35.19	Toronto zoo (from somewhere of Alaska), USA	modern	N	Taylor et al. (2018)
GS136	taxa *ingressus*	Cave bear	-	-	ERS2582834	-	NA	NA	59.47	-	Austria, Gamssulzen Cave	ancient	Y	Barlow et al. (2018)
HV74	taxa *kudarensis*	Cave bear	-	-	ERS2582836	-	NA	NA	77.41	-	Armenia, Hovk	ancient	Y	Barlow et al. (2018)
APB	*Ursus maritimus*	Ancient_Polar	-	2b	SRS347019	-	M	NA	89.58	-	Poolepynten, Svalbard	ancient	Y	Lan et al. (2022)
Bruno	*Ursus maritimus*	Ancient_Polar	-	2b	SRS8777210	-	F	NA	91.59	-	USA: northern Alaska (Beaufort Sea coast)	ancient	Y	Wang et al. (2022)
PB10	*Ursus maritimus*	Polar bear	-	2b	SRS346999	-	M	M	88.74	13.82	Spitsbergen, Svalbard	modern	Y	Miller et al. (2012)
PB105	*Ursus maritimus*	Polar bear	-	2b	SRS463541	-	F	F	88.77	29.36	West Greenland, Aasiaat, Disko West	modern	Y	Liu et al. (2014), Benazzo et al. (2017)
PB11	*Ursus maritimus*	Polar bear	*	2b	SRS347000	-	M	M	85.23	7.48	Spitsbergen, Svalbard	modern	N	Miller et al. (2012)
PB12	*Ursus maritimus*	Polar bear	-	2b	SRS463526	-	F	F	88.71	16.58	West Greenland, Iskanten Hvalsund, Qaanaq	modern	Y	Liu et al. (2014), Benazzo et al. (2017)
PB28	*Ursus maritimus*	Polar bear	-	2b	SRS463480	-	F	F	89.21	29.76	East Greenland, Uunartoq, Ittorqortoormiut	modern	Y	Liu et al. (2014), Benazzo et al. (2017)
PB3	*Ursus maritimus*	Polar bear	-	2b	SRS346992	-	F	F	87.98	16.30	Svalbard, Spitsbergen	modern	Y	Miller et al. (2012), Benazzo et al. (2017)
PB68	*Ursus maritimus*	Polar bear	-	2b	SRS463506	-	F	F	88.73	29.54	West Greenland, Ud for Anoritooq, Qaanaq	modern	Y	Liu et al. (2014), Benazzo et al. (2017)
PB7a	*Ursus maritimus*	Polar bear	-	2b	SRS463487	-	F	F	88.66	27.93	East Greenland, Ittorqortoormiut	modern	Y	Liu et al. (2014), Benazzo et al. (2017)
PB9	*Ursus maritimus*	Polar bear	-	2b	SRS346998	-	M	M	88.46	13.55	Spitsbergen, Svalbard	modern	Y	Miller et al. (2012)
E_VD_1838	taxa *spelaeus*	Cave bear	-	-	ERS2582835	-	NA	NA	80.70	-	Spain, Eiros	ancient	Y	Barlow et al. (2018)
WK01	taxa *eremus*	Cave bear	-	-	ERS2582833	-	NA	NA	84.94	-	Austria, Windischkopf	ancient	Y	Barlow et al. (2018)
Asiatic_black_bear	*Ursus thibetanus*	Out group	-	-	ERS781634	-	F	F	85.47	10.57	Zoo Madrid, Spain	modern	N	Kumar et al. (2017)
Honshu	*Ursus thibetanus*	Out group	*	-	DRS159244	-	NA	M	90.27	55.11	Japan, Tokushima	modern	N	-

The "species" label of the Cave bear was followed by Barlow et al. (2018) and Barlow et al. (2021). Red letters means the sex detected by sex test based on the depth of the X chromosome and the Y chromosome. Samples with grey markers are samples applied whole-genome resequencing in this study.

Table 22. The mitochodria DNA sequences data used in this study.

NCBI Accession Number	Species
AF303110	*Ursus arctos*
AP012562	*Ursus arctos*
AP012563	*Ursus arctos*
AP012564	*Ursus arctos*
AP012565	*Ursus arctos*
AP012566	*Ursus arctos*
AP012567	*Ursus arctos*
AP012568	*Ursus arctos*
AP012569	*Ursus arctos*
AP012571	*Ursus arctos*
AP012572	*Ursus arctos*
AP012574	*Ursus arctos*
AP012576	*Ursus arctos*
AP012577	*Ursus arctos*
AP012580	*Ursus arctos*
AP012584	*Ursus arctos*
AP012585	*Ursus arctos*
AP012586	*Ursus arctos*
AP012588	*Ursus arctos*
AP012589	*Ursus arctos*
AP012590	*Ursus arctos*
AP012591	*Ursus arctos*
AP012592	*Ursus arctos*
AP012593	*Ursus arctos*
EU497665	*Ursus arctos*
GU573486	*Ursus arctos*
GU573487	*Ursus arctos*
GU573489	*Ursus arctos*
GU573491	*Ursus arctos*
HQ685911	*Ursus arctos*
HQ685927	*Ursus arctos*
HQ685942	*Ursus arctos*
HQ685957	*Ursus arctos*
HQ685964	*Ursus arctos*
JX196367	*Ursus arctos*
JX196368	*Ursus arctos*
JX196369	*Ursus arctos*
KX641319	*Ursus arctos*
KX641322	*Ursus arctos*
KX641323	*Ursus arctos*
KX641325	*Ursus arctos*
KX641326	*Ursus arctos*
KX641327	*Ursus arctos*
KX641328	*Ursus arctos*
KX641336	*Ursus arctos*
MG066702	*Ursus arctos*
MG066703	*Ursus arctos*
MG066705	*Ursus arctos*
KF437625	*Ursus deningeri*
AP012594	*Ursus maritimus*
AP012595	*Ursus maritimus*
AP012596	*Ursus maritimus*
AP012597	*Ursus maritimus*
GU573485	*Ursus maritimus*
GU573488	*Ursus maritimus*
GU573490	*Ursus maritimus*
JX196370	*Ursus maritimus*
JX196371	*Ursus maritimus*
JX196372	*Ursus maritimus*
JX196373	*Ursus maritimus*
JX196374	*Ursus maritimus*
JX196375	*Ursus maritimus*
JX196376	*Ursus maritimus*
JX196377	*Ursus maritimus*
JX196378	*Ursus maritimus*
JX196379	*Ursus maritimus*
JX196380	*Ursus maritimus*
JX196381	*Ursus maritimus*
JX196382	*Ursus maritimus*
JX196383	*Ursus maritimus*
JX196384	*Ursus maritimus*
JX196385	*Ursus maritimus*
JX196386	*Ursus maritimus*
JX196387	*Ursus maritimus*
JX196388	*Ursus maritimus*
JX196389	*Ursus maritimus*
JX196391	*Ursus maritimus*
JX196392	*Ursus maritimus*
NC003428	*Ursus maritimus*
EU327344	*Ursus spelaeus*
NC011112	*Ursus spelaeus*

Table 23. Values for the *f*4 (Outgroup, Polar bear; X, Kazakhstan(U13M)) statistic based on the dataset included ancient samples.

Outgroup	Polar bear	X	Kazakhstan(U13M)	f4	Zscore	ABBA	BABA	N
American	APB	ancient_JBB_32K	CAsia_U13M	-0.007116	-17.549	1915	3419	211299
American	APB	ancient_Kunashir1	CAsia_U13M	-0.002912	-8.943	3348	4152	275883
American	APB	ancient_Leitrim_4	CAsia_U13M	-0.005312	-21.191	7615	11391	710855
American	APB	ancient_Leitrim_5	CAsia_U13M	-0.007986	-27.385	5047	9054	501878
American	APB	ancient_Uap	CAsia_U13M	-0.004163	-26.874	34749	47687	3107524
American	APB	CAsia_235	CAsia_U13M	-0.001193	-8.504	43514	47761	3559355
American	APB	CAsia_U05M	CAsia_U13M	-0.000545	-3.606	44253	46192	3559355
American	APB	CAsia_U40	CAsia_U13M	-0.000804	-5.436	44403	47266	3559355
American	APB	CAsia_U76	CAsia_U13M	-0.001019	-6.132	44392	48018	3559355
American	APB	EAsia_AA1	CAsia_U13M	-0.001143	-7.27	44540	48608	3559355
American	APB	EAsia_ETF1	CAsia_U13M	-0.001574	-10.087	44560	50163	3559355
American	APB	EAsia_U34	CAsia_U13M	-0.000962	-6.62	44642	48065	3559355
American	APB	Europe_191Y	CAsia_U13M	-0.001186	-7.779	43212	47433	3559355
American	APB	Europe_ALP1	CAsia_U13M	-0.00064	-4.396	44281	46559	3559355
American	APB	Europe_APN2	CAsia_U13M	-0.000537	-3.529	44568	46479	3559355
American	APB	Europe_OFS01	CAsia_U13M	-0.000752	-5.114	44018	46696	3559355
American	APB	Europe_RF01	CAsia_U13M	-0.000477	-3.261	44767	46465	3559355
American	APB	Europe_SJS01	CAsia_U13M	-0.000827	-5.505	44146	47091	3559355
American	APB	Europe_SLK1	CAsia_U13M	-0.000545	-3.474	44716	46655	3559355
American	APB	Europe_SPA1	CAsia_U13M	-0.000444	-2.935	44508	46088	3559355
American	APB	Europe_Swe	CAsia_U13M	-0.001815	-11.464	42197	48658	3559355
American	APB	Hokkaido_2231	CAsia_U13M	-0.001722	-10.63	44153	50282	3559355
American	APB	Hokkaido_421	CAsia_U13M	-0.001621	-10.214	44616	50387	3559355
American	APB	Hokkaido_5010	CAsia_U13M	-0.001531	-9.38	44612	50062	3559355
American	APB	Hokkaido_5046	CAsia_U13M	-0.001563	-9.361	44623	50185	3559355
American	APB	Hokkaido_518	CAsia_U13M	-0.001536	-9.278	44542	50008	3559355
American	APB	Hokkaido_819	CAsia_U13M	-0.001732	-10.328	44304	50470	3559355
American	APB	NAmerica_ABC01	CAsia_U13M	-0.005088	-19.526	41615	59724	3559355
American	APB	NAmerica_ABC02	CAsia_U13M	-0.00535	-20.998	41499	60543	3559355
American	APB	NAmerica_ABC03	CAsia_U13M	-0.005767	-22.229	40946	61474	3559355
American	APB	NAmerica_ABC04	CAsia_U13M	-0.005158	-20.462	41745	60102	3559355
American	APB	NAmerica_ABC05	CAsia_U13M	-0.005235	-17.815	41697	60329	3559355
American	APB	NAmerica_ABC06	CAsia_U13M	-0.004108	-17.35	42530	57151	3559355
American	APB	NAmerica_ABC1	CAsia_U13M	-0.003862	-14.937	43350	57097	3559355
American	APB	NAmerica_ABC2	CAsia_U13M	-0.00493	-18.735	42030	59578	3559355
American	APB	NAmerica_Adm1	CAsia_U13M	-0.00412	-16.849	42846	57511	3559355
American	APB	NAmerica_BB020	CAsia_U13M	-0.002696	-14.617	42904	52500	3559355
American	APB	NAmerica_BB034	CAsia_U13M	-0.002812	-13.697	43123	53132	3559355
American	APB	NAmerica_BB037	CAsia_U13M	-0.003078	-16.748	42640	53595	3559355
American	APB	NAmerica_BB049	CAsia_U13M	-0.00293	-15.032	43212	53640	3559355
American	APB	NAmerica_BB059	CAsia_U13M	-0.002914	-14.822	43090	53462	3559355
American	APB	NAmerica_Chi1	CAsia_U13M	-0.006069	-20.098	40469	62070	3559355
American	APB	NAmerica_Chi2	CAsia_U13M	-0.006298	-24.121	40058	62474	3559355
American	APB	NAmerica_CON001	CAsia_U13M	-0.003049	-14.31	44828	55680	3559355
American	APB	NAmerica_Den	CAsia_U13M	-0.002678	-13.807	43132	52662	3559355
American	APB	NAmerica_EB027	CAsia_U13M	-0.002543	-13.716	43525	52575	3559355
American	APB	NAmerica_GP01	CAsia_U13M	-0.002967	-13.48	44963	55524	3559355
American	APB	NAmerica_GRZ	CAsia_U13M	-0.002398	-12.06	43490	52024	3559355
American	APB	NAmerica_GT_1	CAsia_U13M	-0.003564	-15.951	43389	56074	3559355
American	APB	NAmerica_WB039	CAsia_U13M	-0.002455	-13.927	42953	51690	3559355
American	APB	WAsia_Ge	CAsia_U13M	-0.000018	-0.133	45392	45457	3559355
American	APB	WAsia_U12M	CAsia_U13M	0.000193	1.317	45449	44764	3559355
American	APB	WAsia_U47M	CAsia_U13M	0.000067	0.469	45697	45457	3559355
Asiatic	APB	ancient_JBB_32K	CAsia_U13M	-0.007214	-18.224	1977	3502	211299
Asiatic	APB	ancient_Kunashir1	CAsia_U13M	-0.003062	-8.995	3441	4286	275883
Asiatic	APB	ancient_Leitrim_4	CAsia_U13M	-0.005521	-22.965	7786	11710	710855
Asiatic	APB	ancient_Leitrim_5	CAsia_U13M	-0.008025	-29.131	5139	9167	501878
Asiatic	APB	ancient_Uap	CAsia_U13M	-0.00432	-28.346	35488	48912	3107524
Asiatic	APB	CAsia_235	CAsia_U13M	-0.001281	-9.624	44352	48913	3559355
Asiatic	APB	CAsia_U05M	CAsia_U13M	-0.000633	-4.266	45164	47418	3559355
Asiatic	APB	CAsia_U40	CAsia_U13M	-0.000875	-6.013	45440	48556	3559355
Asiatic	APB	CAsia_U76	CAsia_U13M	-0.001116	-7.064	45354	49325	3559355
Asiatic	APB	EAsia_AA1	CAsia_U13M	-0.001224	-8.192	45578	49936	3559355

Asiatic	APB	EAsia_ETF1	CAsia_U13M	-0.001683	-10.57	45579	51570	3559355
Asiatic	APB	EAsia_U34	CAsia_U13M	-0.001128	-8.219	45441	49456	3559355
Asiatic	APB	Europe_191Y	CAsia_U13M	-0.001207	-8.497	44412	48709	3559355
Asiatic	APB	Europe_ALP1	CAsia_U13M	-0.000648	-4.795	45363	47668	3559355
Asiatic	APB	Europe_APN2	CAsia_U13M	-0.000479	-3.201	45938	47641	3559355
Asiatic	APB	Europe_OFS01	CAsia_U13M	-0.000759	-5.12	45156	47857	3559355
Asiatic	APB	Europe_RF01	CAsia_U13M	-0.000461	-3.347	45846	47488	3559355
Asiatic	APB	Europe_SJS01	CAsia_U13M	-0.000952	-6.565	44844	48232	3559355
Asiatic	APB	Europe_SLK1	CAsia_U13M	-0.000617	-4.311	45684	47881	3559355
Asiatic	APB	Europe_SPA1	CAsia_U13M	-0.000539	-4.065	45375	47292	3559355
Asiatic	APB	Europe_Swe	CAsia_U13M	-0.001886	-12.293	43271	49984	3559355
Asiatic	APB	Hokkaido_2231	CAsia_U13M	-0.001836	-11.188	45166	51702	3559355
Asiatic	APB	Hokkaido_421	CAsia_U13M	-0.001709	-10.802	45744	51826	3559355
Asiatic	APB	Hokkaido_5010	CAsia_U13M	-0.001633	-9.822	45622	51433	3559355
Asiatic	APB	Hokkaido_5046	CAsia_U13M	-0.001679	-9.959	45592	51568	3559355
Asiatic	APB	Hokkaido_518	CAsia_U13M	-0.001667	-10.026	45462	51396	3559355
Asiatic	APB	Hokkaido_819	CAsia_U13M	-0.001805	-11.184	45372	51796	3559355
Asiatic	APB	NAmerica_ABC01	CAsia_U13M	-0.00549	-22.174	41672	61213	3559355
Asiatic	APB	NAmerica_ABC02	CAsia_U13M	-0.005816	-22.804	41471	62173	3559355
Asiatic	APB	NAmerica_ABC03	CAsia_U13M	-0.006108	-23.812	41046	62786	3559355
Asiatic	APB	NAmerica_ABC04	CAsia_U13M	-0.005568	-22.92	41711	61529	3559355
Asiatic	APB	NAmerica_ABC05	CAsia_U13M	-0.005576	-21.337	41776	61622	3559355
Asiatic	APB	NAmerica_ABC06	CAsia_U13M	-0.004546	-20.384	42484	58665	3559355
Asiatic	APB	NAmerica_ABC1	CAsia_U13M	-0.004429	-18.861	42900	58666	3559355
Asiatic	APB	NAmerica_ABC2	CAsia_U13M	-0.005321	-21.643	42123	61064	3559355
Asiatic	APB	NAmerica_Adm1	CAsia_U13M	-0.004656	-19.926	42532	59105	3559355
Asiatic	APB	NAmerica_BB020	CAsia_U13M	-0.003137	-18.564	43064	54229	3559355
Asiatic	APB	NAmerica_BB034	CAsia_U13M	-0.003148	-16.753	43383	54590	3559355
Asiatic	APB	NAmerica_BB037	CAsia_U13M	-0.003538	-19.981	42748	55341	3559355
Asiatic	APB	NAmerica_BB049	CAsia_U13M	-0.003264	-17.936	43529	55147	3559355
Asiatic	APB	NAmerica_BB059	CAsia_U13M	-0.003321	-18.099	43234	55054	3559355
Asiatic	APB	NAmerica_Chi1	CAsia_U13M	-0.006403	-23.771	40572	63363	3559355
Asiatic	APB	NAmerica_Chi2	CAsia_U13M	-0.006628	-25.473	40328	63920	3559355
Asiatic	APB	NAmerica_CON001	CAsia_U13M	-0.00382	-19.707	43956	57551	3559355
Asiatic	APB	NAmerica_Den	CAsia_U13M	-0.003029	-16.741	43441	54223	3559355
Asiatic	APB	NAmerica_EB027	CAsia_U13M	-0.002951	-16.738	43602	54107	3559355
Asiatic	APB	NAmerica_GP01	CAsia_U13M	-0.003738	-18.825	44062	57368	3559355
Asiatic	APB	NAmerica_GRZ	CAsia_U13M	-0.002776	-15.421	43767	53647	3559355
Asiatic	APB	NAmerica_GT_1	CAsia_U13M	-0.00398	-18.721	43358	57526	3559355
Asiatic	APB	NAmerica_WB039	CAsia_U13M	-0.0027	-16.273	43361	52971	3559355
Asiatic	APB	WAsia_Ge	CAsia_U13M	-0.000123	-0.934	46369	46807	3559355
Asiatic	APB	WAsia_U12M	CAsia_U13M	0.000128	0.835	46487	46032	3559355
Asiatic	APB	WAsia_U47M	CAsia_U13M	-0.000018	-0.124	46713	46775	3559355
American	Bruno	ancient_JBB_32K	CAsia_U13M	-0.007048	-17.607	1924	3413	211343
American	Bruno	ancient_Kunashir1	CAsia_U13M	-0.002963	-9.285	3364	4181	275944
American	Bruno	ancient_Leitrim_4	CAsia_U13M	-0.005234	-20.608	7656	11377	711001
American	Bruno	ancient_Leitrim_5	CAsia_U13M	-0.008097	-28.34	5046	9111	501994
American	Bruno	ancient_Uap	CAsia_U13M	-0.004252	-27.294	34741	47956	3108241
American	Bruno	CAsia_235	CAsia_U13M	-0.001258	-8.868	43556	48033	3560194
American	Bruno	CAsia_U05M	CAsia_U13M	-0.00061	-4.013	44250	46422	3560194
American	Bruno	CAsia_U40	CAsia_U13M	-0.000789	-5.27	44450	47258	3560194
American	Bruno	CAsia_U76	CAsia_U13M	-0.001068	-6.356	44395	48197	3560194
American	Bruno	EAsia_AA1	CAsia_U13M	-0.001221	-7.68	44485	48831	3560194
American	Bruno	EAsia_ETF1	CAsia_U13M	-0.001646	-10.74	44559	50420	3560194
American	Bruno	EAsia_U34	CAsia_U13M	-0.000994	-6.646	44697	48234	3560194
American	Bruno	Europe_191Y	CAsia_U13M	-0.001245	-8.101	43164	47596	3560194
American	Bruno	Europe_ALP1	CAsia_U13M	-0.000731	-5.095	44245	46847	3560194
American	Bruno	Europe_APN2	CAsia_U13M	-0.000558	-3.68	44625	46612	3560194
American	Bruno	Europe_OFS01	CAsia_U13M	-0.000802	-5.351	44073	46928	3560194
American	Bruno	Europe_RF01	CAsia_U13M	-0.000511	-3.459	44818	46636	3560194
American	Bruno	Europe_SJS01	CAsia_U13M	-0.000857	-5.773	44246	47297	3560194
American	Bruno	Europe_SLK1	CAsia_U13M	-0.000562	-3.629	44838	46838	3560194
American	Bruno	Europe_SPA1	CAsia_U13M	-0.00051	-3.357	44561	46378	3560194
American	Bruno	Europe_Swe	CAsia_U13M	-0.001863	-11.838	42249	48882	3560194
American	Bruno	Hokkaido_2231	CAsia_U13M	-0.00177	-10.788	44215	50517	3560194

American	Bruno	Hokkaido_421	CAsia_U13M	-0.001693	-10.649	44607	50633	3560194
American	Bruno	Hokkaido_5010	CAsia_U13M	-0.001582	-9.609	44651	50281	3560194
American	Bruno	Hokkaido_5046	CAsia_U13M	-0.001636	-9.797	44585	50412	3560194
American	Bruno	Hokkaido_518	CAsia_U13M	-0.001608	-9.684	44545	50269	3560194
American	Bruno	Hokkaido_819	CAsia_U13M	-0.001804	-10.855	44305	50728	3560194
American	Bruno	NAmerica_ABC01	CAsia_U13M	-0.005253	-19.97	41536	60238	3560194
American	Bruno	NAmerica_ABC02	CAsia_U13M	-0.005504	-21.156	41485	61081	3560194
American	Bruno	NAmerica_ABC03	CAsia_U13M	-0.005967	-22.729	40884	62129	3560194
American	Bruno	NAmerica_ABC04	CAsia_U13M	-0.005321	-20.81	41703	60646	3560194
American	Bruno	NAmerica_ABC05	CAsia_U13M	-0.005389	-17.998	41654	60841	3560194
American	Bruno	NAmerica_ABC06	CAsia_U13M	-0.004275	-17.72	42431	57652	3560194
American	Bruno	NAmerica_ABC1	CAsia_U13M	-0.004031	-15.45	43269	57619	3560194
American	Bruno	NAmerica_ABC2	CAsia_U13M	-0.005101	-19.049	41967	60129	3560194
American	Bruno	NAmerica_Adm1	CAsia_U13M	-0.004298	-17.427	42695	57996	3560194
American	Bruno	NAmerica_BB020	CAsia_U13M	-0.002775	-14.633	42950	52830	3560194
American	Bruno	NAmerica_BB034	CAsia_U13M	-0.002894	-13.816	43158	53461	3560194
American	Bruno	NAmerica_BB037	CAsia_U13M	-0.003196	-17.341	42648	54026	3560194
American	Bruno	NAmerica_BB049	CAsia_U13M	-0.003043	-15.355	43184	54018	3560194
American	Bruno	NAmerica_BB059	CAsia_U13M	-0.003018	-14.976	43081	53827	3560194
American	Bruno	NAmerica_Chi1	CAsia_U13M	-0.006211	-20.21	40424	62537	3560194
American	Bruno	NAmerica_Chi2	CAsia_U13M	-0.006464	-24.088	39977	62989	3560194
American	Bruno	NAmerica_CON001	CAsia_U13M	-0.003201	-14.601	44762	56157	3560194
American	Bruno	NAmerica_Den	CAsia_U13M	-0.002801	-14.337	43126	53096	3560194
American	Bruno	NAmerica_EB027	CAsia_U13M	-0.002653	-14.212	43548	52993	3560194
American	Bruno	NAmerica_GP01	CAsia_U13M	-0.003134	-13.999	44886	56045	3560194
American	Bruno	NAmerica_GRZ	CAsia_U13M	-0.00252	-12.79	43445	52416	3560194
American	Bruno	NAmerica_GT_1	CAsia_U13M	-0.003685	-16.355	43394	56514	3560194
American	Bruno	NAmerica_WB039	CAsia_U13M	-0.002552	-14.517	42952	52037	3560194
American	Bruno	WAsia_Ge	CAsia_U13M	-0.000088	-0.643	45388	45702	3560194
American	Bruno	WAsia_U12M	CAsia_U13M	0.000159	1.081	45530	44964	3560194
American	Bruno	WAsia_U47M	CAsia_U13M	0.000048	0.33	45740	45570	3560194
Asiatic	Bruno	ancient_JBB_32K	CAsia_U13M	-0.007146	-18.183	1970	3481	211343
Asiatic	Bruno	ancient_Kunashir1	CAsia_U13M	-0.003113	-9.425	3440	4298	275944
Asiatic	Bruno	ancient_Leitrim_4	CAsia_U13M	-0.005443	-22.68	7841	11711	711001
Asiatic	Bruno	ancient_Leitrim_5	CAsia_U13M	-0.008136	-29.761	5141	9225	501994
Asiatic	Bruno	ancient_Uap	CAsia_U13M	-0.004407	-28.873	35408	49104	3108241
Asiatic	Bruno	CAsia_235	CAsia_U13M	-0.001345	-10.009	44322	49110	3560194
Asiatic	Bruno	CAsia_U05M	CAsia_U13M	-0.000698	-4.665	45080	47563	3560194
Asiatic	Bruno	CAsia_U40	CAsia_U13M	-0.000858	-5.866	45398	48454	3560194
Asiatic	Bruno	CAsia_U76	CAsia_U13M	-0.001164	-7.241	45330	49474	3560194
Asiatic	Bruno	EAsia_AA1	CAsia_U13M	-0.001302	-8.626	45502	50138	3560194
Asiatic	Bruno	EAsia_ETF1	CAsia_U13M	-0.001754	-11.282	45475	51721	3560194
Asiatic	Bruno	EAsia_U34	CAsia_U13M	-0.001159	-8.221	45464	49591	3560194
Asiatic	Bruno	Europe_191Y	CAsia_U13M	-0.001265	-8.742	44333	48838	3560194
Asiatic	Bruno	Europe_ALP1	CAsia_U13M	-0.000739	-5.504	45248	47880	3560194
Asiatic	Bruno	Europe_APN2	CAsia_U13M	-0.000499	-3.314	45957	47733	3560194
Asiatic	Bruno	Europe_OFS01	CAsia_U13M	-0.000809	-5.314	45190	48068	3560194
Asiatic	Bruno	Europe_RF01	CAsia_U13M	-0.000495	-3.544	45830	47594	3560194
Asiatic	Bruno	Europe_SJS01	CAsia_U13M	-0.000982	-6.86	44882	48377	3560194
Asiatic	Bruno	Europe_SLK1	CAsia_U13M	-0.000634	-4.449	45737	47995	3560194
Asiatic	Bruno	Europe_SPA1	CAsia_U13M	-0.000606	-4.526	45384	47543	3560194
Asiatic	Bruno	Europe_Swe	CAsia_U13M	-0.001934	-12.676	43238	50126	3560194
Asiatic	Bruno	Hokkaido_2231	CAsia_U13M	-0.001884	-11.328	45142	51850	3560194
Asiatic	Bruno	Hokkaido_421	CAsia_U13M	-0.00178	-11.269	45683	52020	3560194
Asiatic	Bruno	Hokkaido_5010	CAsia_U13M	-0.001682	-10.004	45598	51587	3560194
Asiatic	Bruno	Hokkaido_5046	CAsia_U13M	-0.001752	-10.331	45500	51737	3560194
Asiatic	Bruno	Hokkaido_518	CAsia_U13M	-0.001738	-10.382	45390	51579	3560194
Asiatic	Bruno	Hokkaido_819	CAsia_U13M	-0.001876	-11.689	45304	51982	3560194
Asiatic	Bruno	NAmerica_ABC01	CAsia_U13M	-0.005657	-22.515	41519	61659	3560194
Asiatic	Bruno	NAmerica_ABC02	CAsia_U13M	-0.005971	-22.908	41368	62626	3560194
Asiatic	Bruno	NAmerica_ABC03	CAsia_U13M	-0.006309	-24.186	40910	63371	3560194
Asiatic	Bruno	NAmerica_ABC04	CAsia_U13M	-0.005732	-23.094	41602	62009	3560194
Asiatic	Bruno	NAmerica_ABC05	CAsia_U13M	-0.005732	-21.457	41666	62072	3560194
Asiatic	Bruno	NAmerica_ABC06	CAsia_U13M	-0.004714	-20.525	42312	59097	3560194
Asiatic	Bruno	NAmerica_ABC1	CAsia_U13M	-0.004598	-19.282	42756	59124	3560194

Asiatic	Bruno	NAmerica_ABC2	CAsia_U13M	-0.005494	-21.884	41968	61529	3560194
Asiatic	Bruno	NAmerica_Adm1	CAsia_U13M	-0.004834	-20.407	42330	59540	3560194
Asiatic	Bruno	NAmerica_BB020	CAsia_U13M	-0.003216	-18.443	43073	54523	3560194
Asiatic	Bruno	NAmerica_BB034	CAsia_U13M	-0.003231	-16.8	43375	54877	3560194
Asiatic	Bruno	NAmerica_BB037	CAsia_U13M	-0.003657	-20.519	42665	55683	3560194
Asiatic	Bruno	NAmerica_BB049	CAsia_U13M	-0.003378	-18.28	43433	55460	3560194
Asiatic	Bruno	NAmerica_BB059	CAsia_U13M	-0.003426	-18.155	43183	55380	3560194
Asiatic	Bruno	NAmerica_Chi1	CAsia_U13M	-0.006547	-23.818	40467	63776	3560194
Asiatic	Bruno	NAmerica_Chi2	CAsia_U13M	-0.006795	-25.468	40179	64372	3560194
Asiatic	Bruno	NAmerica_CON001	CAsia_U13M	-0.003972	-20.013	43825	57966	3560194
Asiatic	Bruno	NAmerica_Den	CAsia_U13M	-0.003154	-17.189	43349	54576	3560194
Asiatic	Bruno	NAmerica_EB027	CAsia_U13M	-0.003062	-17.037	43575	54474	3560194
Asiatic	Bruno	NAmerica_GP01	CAsia_U13M	-0.003905	-19.359	43931	57835	3560194
Asiatic	Bruno	NAmerica_GRZ	CAsia_U13M	-0.002898	-16.211	43641	53960	3560194
Asiatic	Bruno	NAmerica_GT_1	CAsia_U13M	-0.004102	-18.999	43311	57913	3560194
Asiatic	Bruno	NAmerica_WB039	CAsia_U13M	-0.002798	-16.785	43308	53268	3560194
Asiatic	Bruno	WAsia_Ge	CAsia_U13M	-0.000192	-1.463	46321	47005	3560194
Asiatic	Bruno	WAsia_U12M	CAsia_U13M	0.000094	0.609	46464	46128	3560194
Asiatic	Bruno	WAsia_U47M	CAsia_U13M	-0.000038	-0.263	46681	46814	3560194
American	Polar	ancient_JBB_32K	CAsia_U13M	-0.006919	-18.316	1938	3400	211345
American	Polar	ancient_Kunashir1	CAsia_U13M	-0.002991	-9.56	3367	4192	275944
American	Polar	ancient_Leitrim_4	CAsia_U13M	-0.005483	-22.149	7659	11557	711003
American	Polar	ancient_Leitrim_5	CAsia_U13M	-0.008439	-28.931	5036	9272	501995
American	Polar	ancient_Uap	CAsia_U13M	-0.00443	-28.554	34602	48372	3108265
American	Polar	CAsia_235	CAsia_U13M	-0.001251	-8.859	43547	48000	3560255
American	Polar	CAsia_U05M	CAsia_U13M	-0.000603	-4.012	44251	46396	3560255
American	Polar	CAsia_U40	CAsia_U13M	-0.000785	-5.345	44414	47208	3560255
American	Polar	CAsia_U76	CAsia_U13M	-0.001088	-6.602	44353	48228	3560255
American	Polar	EAsia_AA1	CAsia_U13M	-0.001217	-7.71	44480	48815	3560255
American	Polar	EAsia_ETF1	CAsia_U13M	-0.001603	-10.502	44606	50315	3560255
American	Polar	EAsia_U34	CAsia_U13M	-0.000973	-6.583	44729	48193	3560255
American	Polar	Europe_191Y	CAsia_U13M	-0.001265	-8.266	43164	47668	3560255
American	Polar	Europe_ALP1	CAsia_U13M	-0.00073	-5.098	44236	46834	3560255
American	Polar	Europe_APN2	CAsia_U13M	-0.000547	-3.648	44686	46635	3560255
American	Polar	Europe_OFS01	CAsia_U13M	-0.000797	-5.37	44056	46895	3560255
American	Polar	Europe_RF01	CAsia_U13M	-0.000546	-3.772	44750	46695	3560255
American	Polar	Europe_SJS01	CAsia_U13M	-0.000871	-5.849	44173	47276	3560255
American	Polar	Europe_SLK1	CAsia_U13M	-0.000564	-3.635	44797	46805	3560255
American	Polar	Europe_SPA1	CAsia_U13M	-0.000477	-3.205	44592	46289	3560255
American	Polar	Europe_Swe	CAsia_U13M	-0.001893	-12.071	42186	48927	3560255
American	Polar	Hokkaido_2231	CAsia_U13M	-0.001744	-10.866	44220	50428	3560255
American	Polar	Hokkaido_421	CAsia_U13M	-0.001664	-10.674	44624	50549	3560255
American	Polar	Hokkaido_5010	CAsia_U13M	-0.001566	-9.56	44674	50249	3560255
American	Polar	Hokkaido_5046	CAsia_U13M	-0.001603	-9.807	44635	50341	3560255
American	Polar	Hokkaido_518	CAsia_U13M	-0.001561	-9.512	44603	50159	3560255
American	Polar	Hokkaido_819	CAsia_U13M	-0.001755	-10.666	44387	50635	3560255
American	Polar	NAmerica_ABC01	CAsia_U13M	-0.005295	-20.076	41547	60398	3560255
American	Polar	NAmerica_ABC02	CAsia_U13M	-0.005546	-21.273	41457	61201	3560255
American	Polar	NAmerica_ABC03	CAsia_U13M	-0.005996	-22.705	40887	62234	3560255
American	Polar	NAmerica_ABC04	CAsia_U13M	-0.00536	-20.907	41713	60796	3560255
American	Polar	NAmerica_ABC05	CAsia_U13M	-0.005439	-18.153	41656	61021	3560255
American	Polar	NAmerica_ABC06	CAsia_U13M	-0.004272	-17.822	42490	57701	3560255
American	Polar	NAmerica_ABC1	CAsia_U13M	-0.004009	-15.316	43307	57580	3560255
American	Polar	NAmerica_ABC2	CAsia_U13M	-0.005132	-19.321	41982	60252	3560255
American	Polar	NAmerica_Adm1	CAsia_U13M	-0.004264	-17.423	42784	57964	3560255
American	Polar	NAmerica_BB020	CAsia_U13M	-0.002773	-14.837	42951	52824	3560255
American	Polar	NAmerica_BB034	CAsia_U13M	-0.002887	-13.893	43193	53471	3560255
American	Polar	NAmerica_BB037	CAsia_U13M	-0.00318	-17.221	42694	54016	3560255
American	Polar	NAmerica_BB049	CAsia_U13M	-0.003043	-15.564	43192	54027	3560255
American	Polar	NAmerica_BB059	CAsia_U13M	-0.003029	-15.24	43054	53837	3560255
American	Polar	NAmerica_Chi1	CAsia_U13M	-0.006291	-20.42	40404	62803	3560255
American	Polar	NAmerica_Chi2	CAsia_U13M	-0.00655	-24.454	39931	63250	3560255
American	Polar	NAmerica_CON001	CAsia_U13M	-0.003186	-14.632	44799	56143	3560255
American	Polar	NAmerica_Den	CAsia_U13M	-0.002763	-14.12	43188	53024	3560255
American	Polar	NAmerica_EB027	CAsia_U13M	-0.002644	-14.259	43569	52982	3560255

American	Polar	NAmerica_GP01	CAsia_U13M	-0.003105	-13.959	44924	55979	3560255
American	Polar	NAmerica_GRZ	CAsia_U13M	-0.002476	-12.498	43510	52324	3560255
American	Polar	NAmerica_GT_1	CAsia_U13M	-0.003707	-16.603	43385	56582	3560255
American	Polar	NAmerica_WB039	CAsia_U13M	-0.002569	-14.695	42978	52123	3560255
American	Polar	WAsia_Ge	CAsia_U13M	-0.000082	-0.596	45395	45689	3560255
American	Polar	WAsia_U12M	CAsia_U13M	0.000136	0.929	45462	44977	3560255
American	Polar	WAsia_U47M	CAsia_U13M	0.000045	0.313	45740	45579	3560255
Asiatic	Polar	ancient_JBB_32K	CAsia_U13M	-0.007017	-18.765	1986	3469	211345
Asiatic	Polar	ancient_Kunashir1	CAsia_U13M	-0.003141	-9.758	3453	4320	275944
Asiatic	Polar	ancient_Leitrim_4	CAsia_U13M	-0.005691	-24.035	7820	11867	711003
Asiatic	Polar	ancient_Leitrim_5	CAsia_U13M	-0.008478	-30.279	5133	9389	501995
Asiatic	Polar	ancient_Uap	CAsia_U13M	-0.004585	-30.135	35299	49551	3108265
Asiatic	Polar	CAsia_235	CAsia_U13M	-0.001338	-10.026	44344	49107	3560255
Asiatic	Polar	CAsia_U05M	CAsia_U13M	-0.00069	-4.73	45129	47587	3560255
Asiatic	Polar	CAsia_U40	CAsia_U13M	-0.000855	-5.957	45427	48470	3560255
Asiatic	Polar	CAsia_U76	CAsia_U13M	-0.001184	-7.531	45301	49517	3560255
Asiatic	Polar	EAsia_AA1	CAsia_U13M	-0.001299	-8.737	45523	50148	3560255
Asiatic	Polar	EAsia_ETF1	CAsia_U13M	-0.001712	-11.057	45579	51673	3560255
Asiatic	Polar	EAsia_U34	CAsia_U13M	-0.001139	-8.235	45498	49552	3560255
Asiatic	Polar	Europe_191Y	CAsia_U13M	-0.001285	-9.104	44327	48901	3560255
Asiatic	Polar	Europe_ALP1	CAsia_U13M	-0.000738	-5.53	45278	47905	3560255
Asiatic	Polar	Europe_APN2	CAsia_U13M	-0.000488	-3.279	46025	47762	3560255
Asiatic	Polar	Europe_OFS01	CAsia_U13M	-0.000804	-5.394	45168	48031	3560255
Asiatic	Polar	Europe_RF01	CAsia_U13M	-0.000531	-3.863	45776	47667	3560255
Asiatic	Polar	Europe_SJS01	CAsia_U13M	-0.000996	-6.947	44837	48384	3560255
Asiatic	Polar	Europe_SLK1	CAsia_U13M	-0.000636	-4.499	45723	47987	3560255
Asiatic	Polar	Europe_SPA1	CAsia_U13M	-0.000572	-4.389	45420	47458	3560255
Asiatic	Polar	Europe_Swe	CAsia_U13M	-0.001964	-12.94	43208	50202	3560255
Asiatic	Polar	Hokkaido_2231	CAsia_U13M	-0.001858	-11.511	45209	51823	3560255
Asiatic	Polar	Hokkaido_421	CAsia_U13M	-0.001752	-11.309	45752	51988	3560255
Asiatic	Polar	Hokkaido_5010	CAsia_U13M	-0.001667	-9.963	45680	51613	3560255
Asiatic	Polar	Hokkaido_5046	CAsia_U13M	-0.001718	-10.429	45590	51708	3560255
Asiatic	Polar	Hokkaido_518	CAsia_U13M	-0.001691	-10.294	45505	51525	3560255
Asiatic	Polar	Hokkaido_819	CAsia_U13M	-0.001827	-11.563	45427	51930	3560255
Asiatic	Polar	NAmerica_ABC01	CAsia_U13M	-0.005699	-22.647	41545	61833	3560255
Asiatic	Polar	NAmerica_ABC02	CAsia_U13M	-0.006013	-23.08	41351	62757	3560255
Asiatic	Polar	NAmerica_ABC03	CAsia_U13M	-0.006338	-24.198	40924	63487	3560255
Asiatic	Polar	NAmerica_ABC04	CAsia_U13M	-0.005771	-23.252	41597	62144	3560255
Asiatic	Polar	NAmerica_ABC05	CAsia_U13M	-0.005782	-21.66	41671	62255	3560255
Asiatic	Polar	NAmerica_ABC06	CAsia_U13M	-0.004711	-20.77	42399	59171	3560255
Asiatic	Polar	NAmerica_ABC1	CAsia_U13M	-0.004576	-19.195	42814	59106	3560255
Asiatic	Polar	NAmerica_ABC2	CAsia_U13M	-0.005524	-22.147	41994	61661	3560255
Asiatic	Polar	NAmerica_Adm1	CAsia_U13M	-0.0048	-20.526	42428	59517	3560255
Asiatic	Polar	NAmerica_BB020	CAsia_U13M	-0.003214	-18.581	43087	54530	3560255
Asiatic	Polar	NAmerica_BB034	CAsia_U13M	-0.003223	-16.909	43407	54884	3560255
Asiatic	Polar	NAmerica_BB037	CAsia_U13M	-0.00364	-20.371	42747	55708	3560255
Asiatic	Polar	NAmerica_BB049	CAsia_U13M	-0.003379	-18.499	43468	55497	3560255
Asiatic	Polar	NAmerica_BB059	CAsia_U13M	-0.003436	-18.394	43180	55414	3560255
Asiatic	Polar	NAmerica_Chi1	CAsia_U13M	-0.006627	-24.071	40443	64036	3560255
Asiatic	Polar	NAmerica_Chi2	CAsia_U13M	-0.006881	-25.863	40148	64647	3560255
Asiatic	Polar	NAmerica_CON001	CAsia_U13M	-0.003957	-19.981	43878	57967	3560255
Asiatic	Polar	NAmerica_Den	CAsia_U13M	-0.003116	-17.039	43427	54519	3560255
Asiatic	Polar	NAmerica_EB027	CAsia_U13M	-0.003052	-17.119	43597	54464	3560255
Asiatic	Polar	NAmerica_GP01	CAsia_U13M	-0.003876	-19.196	43988	57788	3560255
Asiatic	Polar	NAmerica_GRZ	CAsia_U13M	-0.002854	-15.852	43753	53915	3560255
Asiatic	Polar	NAmerica_GT_1	CAsia_U13M	-0.004123	-19.265	43325	58005	3560255
Asiatic	Polar	NAmerica_WB039	CAsia_U13M	-0.002815	-16.928	43348	53369	3560255
Asiatic	Polar	WAsia_Ge	CAsia_U13M	-0.000187	-1.423	46330	46994	3560255
Asiatic	Polar	WAsia_U12M	CAsia_U13M	0.000072	0.467	46452	46196	3560255
Asiatic	Polar	WAsia_U47M	CAsia_U13M	-0.00004	-0.281	46708	46851	3560255

Table 24. Values for the *f*4 (Outgroup, Polar bear; X, Kazakhstan(U13M)) statistic based on only modern samples dataset.

Outgroup	Polar bear	X	Kazakhstan(U13M)	f4	Zscore	ABBA	BABA	N
American	Polar	CAsia_235	CAsia_U13M	-0.001111	-9.944	284902	314154	26334978
American	Polar	CAsia_U05M	CAsia_U13M	-0.000598	-5.073	291146	306892	26334978
American	Polar	CAsia_U40	CAsia_U13M	-0.000704	-6.061	294051	312603	26334978
American	Polar	CAsia_U76	CAsia_U13M	-0.000983	-7.643	290278	316154	26334978
American	Polar	EAsia_AA1	CAsia_U13M	-0.001172	-9.42	290192	321057	26334978
American	Polar	EAsia_ETF1	CAsia_U13M	-0.001534	-12.352	290204	330604	26334978
American	Polar	EAsia_U34	CAsia_U13M	-0.000908	-8.066	292158	316057	26334978
American	Polar	Europe_191Y	CAsia_U13M	-0.00114	-9.506	282978	312991	26334978
American	Polar	Europe_ALP1	CAsia_U13M	-0.000719	-6.373	289527	308456	26334978
American	Polar	Europe_APN2	CAsia_U13M	-0.000531	-4.545	292223	306194	26334978
American	Polar	Europe_OFS01	CAsia_U13M	-0.000701	-5.96	289713	308171	26334978
American	Polar	Europe_RF01	CAsia_U13M	-0.000543	-4.913	291930	306238	26334978
American	Polar	Europe_SJS01	CAsia_U13M	-0.000826	-7.254	288428	310174	26334978
American	Polar	Europe_SLK1	CAsia_U13M	-0.000597	-4.842	292556	308284	26334978
American	Polar	Europe_SPA1	CAsia_U13M	-0.000502	-4.204	292101	305330	26334978
American	Polar	Europe_Swe	CAsia_U13M	-0.001688	-14.098	276409	320856	26334978
American	Polar	Hokkaido_2231	CAsia_U13M	-0.00159	-12.346	288630	330507	26334978
American	Polar	Hokkaido_421	CAsia_U13M	-0.001509	-12.063	291516	331243	26334978
American	Polar	Hokkaido_5010	CAsia_U13M	-0.001439	-11.008	291177	329065	26334978
American	Polar	Hokkaido_5046	CAsia_U13M	-0.001489	-11.472	291250	330465	26334978
American	Polar	Hokkaido_518	CAsia_U13M	-0.001482	-11.129	290592	329626	26334978
American	Polar	Hokkaido_819	CAsia_U13M	-0.001564	-12.022	290929	332116	26334978
American	Polar	NAmerica_ABC01	CAsia_U13M	-0.004636	-21.123	272152	394238	26334978
American	Polar	NAmerica_ABC02	CAsia_U13M	-0.00489	-21.939	270861	399643	26334978
American	Polar	NAmerica_ABC03	CAsia_U13M	-0.00524	-23.017	267783	405766	26334978
American	Polar	NAmerica_ABC04	CAsia_U13M	-0.004704	-21.104	272977	396849	26334978
American	Polar	NAmerica_ABC05	CAsia_U13M	-0.004788	-18.566	272428	398529	26334978
American	Polar	NAmerica_ABC06	CAsia_U13M	-0.003773	-18.257	278117	377483	26334978
American	Polar	NAmerica_ABC1	CAsia_U13M	-0.003543	-15.968	282314	375628	26334978
American	Polar	NAmerica_ABC2	CAsia_U13M	-0.004581	-20.041	273997	394628	26334978
American	Polar	NAmerica_Adm1	CAsia_U13M	-0.003737	-18.251	279807	378210	26334978
American	Polar	NAmerica_BB020	CAsia_U13M	-0.00255	-17.205	280627	347785	26334978
American	Polar	NAmerica_BB034	CAsia_U13M	-0.002631	-15.559	281768	351058	26334978
American	Polar	NAmerica_BB037	CAsia_U13M	-0.002875	-19.069	278414	354125	26334978
American	Polar	NAmerica_BB049	CAsia_U13M	-0.002695	-16.706	281624	352599	26334978
American	Polar	NAmerica_BB059	CAsia_U13M	-0.002716	-16.768	280712	352244	26334978
American	Polar	NAmerica_Chi1	CAsia_U13M	-0.005527	-20.781	264123	409670	26334978
American	Polar	NAmerica_Chi2	CAsia_U13M	-0.005756	-25.09	261458	413053	26334978
American	Polar	NAmerica_CON001	CAsia_U13M	-0.002857	-15.505	292229	367469	26334978
American	Polar	NAmerica_Den	CAsia_U13M	-0.002475	-15.344	281276	346448	26334978
American	Polar	NAmerica_EB027	CAsia_U13M	-0.002403	-15.532	284114	347402	26334978
American	Polar	NAmerica_GP01	CAsia_U13M	-0.002791	-14.931	293035	366525	26334978
American	Polar	NAmerica_GRZ	CAsia_U13M	-0.002225	-13.625	284437	343027	26334978
American	Polar	NAmerica_GT_1	CAsia_U13M	-0.003289	-17.555	282751	369367	26334978
American	Polar	NAmerica_WB039	CAsia_U13M	-0.002337	-16.923	279771	341316	26334978
American	Polar	WAsia_Ge	CAsia_U13M	-0.000139	-1.313	296879	300545	26334978
American	Polar	WAsia_U12M	CAsia_U13M	0.00006	0.542	299167	297592	26334978
American	Polar	WAsia_U47M	CAsia_U13M	0.000004	0.037	301509	301397	26334978
Asiatic	Polar	CAsia_235	CAsia_U13M	-0.001184	-11.275	289062	320231	26334978
Asiatic	Polar	CAsia_U05M	CAsia_U13M	-0.000644	-5.632	296513	313483	26334978
Asiatic	Polar	CAsia_U40	CAsia_U13M	-0.000713	-6.394	300670	319447	26334978
Asiatic	Polar	CAsia_U76	CAsia_U13M	-0.001068	-8.811	295039	323174	26334978
Asiatic	Polar	EAsia_AA1	CAsia_U13M	-0.001247	-10.696	295201	328034	26334978
Asiatic	Polar	EAsia_ETF1	CAsia_U13M	-0.001595	-12.833	295862	337862	26334978
Asiatic	Polar	EAsia_U34	CAsia_U13M	-0.001013	-9.214	296579	323244	26334978
Asiatic	Polar	Europe_191Y	CAsia_U13M	-0.001169	-10.6	289087	319872	26334978
Asiatic	Polar	Europe_ALP1	CAsia_U13M	-0.000705	-6.405	295621	314185	26334978

Asiatic	Polar	Europe_APN2	CAsia_U13M	-0.000489	-4.201	299421	312304	26334978
Asiatic	Polar	Europe_OFS01	CAsia_U13M	-0.000711	-6.087	295651	314372	26334978
Asiatic	Polar	Europe_RF01	CAsia_U13M	-0.000558	-5.252	297313	312015	26334978
Asiatic	Polar	Europe_SJS01	CAsia_U13M	-0.000901	-8.102	292486	316213	26334978
Asiatic	Polar	Europe_SLK1	CAsia_U13M	-0.00061	-5.479	298046	314098	26334978
Asiatic	Polar	Europe_SPA1	CAsia_U13M	-0.000599	-5.678	296121	311902	26334978
Asiatic	Polar	Europe_Swe	CAsia_U13M	-0.001741	-14.331	281810	327664	26334978
Asiatic	Polar	Hokkaido_2231	CAsia_U13M	-0.00168	-13.227	294009	338259	26334978
Asiatic	Polar	Hokkaido_421	CAsia_U13M	-0.00158	-12.902	297282	338897	26334978
Asiatic	Polar	Hokkaido_5010	CAsia_U13M	-0.001509	-11.639	296956	336687	26334978
Asiatic	Polar	Hokkaido_5046	CAsia_U13M	-0.001577	-12.228	296504	338044	26334978
Asiatic	Polar	Hokkaido_518	CAsia_U13M	-0.001592	-12.242	295243	337158	26334978
Asiatic	Polar	Hokkaido_819	CAsia_U13M	-0.001627	-13.093	296427	339281	26334978
Asiatic	Polar	NAmerica_ABC01	CAsia_U13M	-0.004997	-23.429	271191	402790	26334978
Asiatic	Polar	NAmerica_ABC02	CAsia_U13M	-0.005269	-23.849	269707	408463	26334978
Asiatic	Polar	NAmerica_ABC03	CAsia_U13M	-0.005518	-24.141	267836	413151	26334978
Asiatic	Polar	NAmerica_ABC04	CAsia_U13M	-0.00505	-23.002	271847	404829	26334978
Asiatic	Polar	NAmerica_ABC05	CAsia_U13M	-0.005092	-22.082	271766	405858	26334978
Asiatic	Polar	NAmerica_ABC06	CAsia_U13M	-0.004144	-20.985	276906	386038	26334978
Asiatic	Polar	NAmerica_ABC1	CAsia_U13M	-0.003985	-19.68	279001	383959	26334978
Asiatic	Polar	NAmerica_ABC2	CAsia_U13M	-0.004902	-22.738	273400	402502	26334978
Asiatic	Polar	NAmerica_Adm1	CAsia_U13M	-0.004161	-20.841	277444	387029	26334978
Asiatic	Polar	NAmerica_BB020	CAsia_U13M	-0.002876	-20.532	280626	356364	26334978
Asiatic	Polar	NAmerica_BB034	CAsia_U13M	-0.002951	-18.788	281223	358944	26334978
Asiatic	Polar	NAmerica_BB037	CAsia_U13M	-0.003235	-21.977	278388	363588	26334978
Asiatic	Polar	NAmerica_BB049	CAsia_U13M	-0.002992	-19.485	281783	360588	26334978
Asiatic	Polar	NAmerica_BB059	CAsia_U13M	-0.003045	-19.817	280598	360793	26334978
Asiatic	Polar	NAmerica_Chi1	CAsia_U13M	-0.005841	-24.475	263407	417233	26334978
Asiatic	Polar	NAmerica_Chi2	CAsia_U13M	-0.00604	-25.875	261932	420991	26334978
Asiatic	Polar	NAmerica_CON001	CAsia_U13M	-0.003492	-20.353	285928	377891	26334978
Asiatic	Polar	NAmerica_Den	CAsia_U13M	-0.002738	-17.326	282951	355057	26334978
Asiatic	Polar	NAmerica_EB027	CAsia_U13M	-0.002711	-17.741	284059	355461	26334978
Asiatic	Polar	NAmerica_GP01	CAsia_U13M	-0.003413	-19.733	286521	376405	26334978
Asiatic	Polar	NAmerica_GRZ	CAsia_U13M	-0.002519	-16.301	285404	351740	26334978
Asiatic	Polar	NAmerica_GT_1	CAsia_U13M	-0.003574	-19.97	282444	376565	26334978
Asiatic	Polar	NAmerica_WB039	CAsia_U13M	-0.002536	-18.933	282063	348836	26334978
Asiatic	Polar	WAsia_Ge	CAsia_U13M	-0.000217	-2.17	301905	307616	26334978
Asiatic	Polar	WAsia_U12M	CAsia_U13M	0.000025	0.223	304366	303704	26334978

Table 25. Values for the *f*4 (Outgroup, Cave bear; X, modern Polar bear) statistic based on the dataset included ancient samples.

Outgroup	Cave bear	X	modern Polar bear	f4	Zscore	ABBA	BABA	N
American	Cave_E_VD_1838	ancient_JBB_32K	Polar	0.00058	1.976	1889	1773	199545
American	Cave_E_VD_1838	ancient_Kunashir1	Polar	0.001291	3.75	3371	3035	260046
American	Cave_E_VD_1838	ancient_Leitrim_4	Polar	0.000871	4.802	7792	7213	665567
American	Cave_E_VD_1838	ancient_Leitrim_5	Polar	0.000933	4.011	5132	4692	471587
American	Cave_E_VD_1838	ancient_Uap	Polar	0.000792	6.116	34534	32203	2945115
American	Cave_E_VD_1838	CAsia_235	Polar	0.001315	9.93	45221	40806	3358874
American	Cave_E_VD_1838	CAsia_U05M	Polar	0.001376	9.799	46001	41380	3358874
American	Cave_E_VD_1838	CAsia_U13M	Polar	0.000895	6.15	46226	43220	3358874
American	Cave_E_VD_1838	CAsia_U40	Polar	0.001434	10.113	45969	41152	3358874
American	Cave_E_VD_1838	CAsia_U76	Polar	0.001359	9.531	45468	40903	3358874
American	Cave_E_VD_1838	EAsia_AA1	Polar	0.001431	10.345	45404	40597	3358874
American	Cave_E_VD_1838	EAsia_ETF1	Polar	0.001429	10.009	45140	40340	3358874
American	Cave_E_VD_1838	EAsia_U34	Polar	0.001409	10.434	45584	40850	3358874
American	Cave_E_VD_1838	Europe_191Y	Polar	0.000963	7.12	44705	41470	3358874
American	Cave_E_VD_1838	Europe_ALP1	Polar	0.000979	6.819	45322	42033	3358874
American	Cave_E_VD_1838	Europe_APN2	Polar	0.001084	7.224	45854	42213	3358874
American	Cave_E_VD_1838	Europe_OFS01	Polar	0.00111	7.822	45416	41687	3358874
American	Cave_E_VD_1838	Europe_RF01	Polar	0.001077	7.963	45652	42035	3358874
American	Cave_E_VD_1838	Europe_SJS01	Polar	0.001125	7.946	45349	41571	3358874
American	Cave_E_VD_1838	Europe_SLK1	Polar	0.001076	7.66	45719	42104	3358874
American	Cave_E_VD_1838	Europe_SPA1	Polar	0.001073	7.247	45664	42058	3358874
American	Cave_E_VD_1838	Europe_Swe	Polar	0.001092	8.087	44060	40393	3358874
American	Cave_E_VD_1838	Hokkaido_2231	Polar	0.001429	10.48	45035	40235	3358874
American	Cave_E_VD_1838	Hokkaido_421	Polar	0.001413	10.218	45070	40323	3358874
American	Cave_E_VD_1838	Hokkaido_5010	Polar	0.001406	10.082	45209	40487	3358874
American	Cave_E_VD_1838	Hokkaido_5046	Polar	0.001425	10.046	45238	40451	3358874
American	Cave_E_VD_1838	Hokkaido_518	Polar	0.001439	10.421	45288	40453	3358874
American	Cave_E_VD_1838	Hokkaido_819	Polar	0.001352	9.612	44926	40384	3358874
American	Cave_E_VD_1838	NAmerica_ABC01	Polar	0.001455	10.473	42104	37218	3358874
American	Cave_E_VD_1838	NAmerica_ABC02	Polar	0.001514	11.225	42006	36919	3358874
American	Cave_E_VD_1838	NAmerica_ABC03	Polar	0.001417	10.787	41501	36743	3358874
American	Cave_E_VD_1838	NAmerica_ABC04	Polar	0.001503	11.246	41990	36944	3358874
American	Cave_E_VD_1838	NAmerica_ABC05	Polar	0.001528	10.075	42110	36978	3358874
American	Cave_E_VD_1838	NAmerica_ABC06	Polar	0.001554	10.919	43120	37899	3358874
American	Cave_E_VD_1838	NAmerica_ABC1	Polar	0.001636	10.962	43546	38050	3358874
American	Cave_E_VD_1838	NAmerica_ABC2	Polar	0.001531	10.385	42482	37339	3358874
American	Cave_E_VD_1838	NAmerica_Adm1	Polar	0.001592	11.401	43184	37836	3358874
American	Cave_E_VD_1838	NAmerica_BB020	Polar	0.001575	11.039	44269	38977	3358874
American	Cave_E_VD_1838	NAmerica_BB034	Polar	0.001543	10.977	44151	38967	3358874
American	Cave_E_VD_1838	NAmerica_BB037	Polar	0.001618	11.911	43961	38527	3358874
American	Cave_E_VD_1838	NAmerica_BB049	Polar	0.001527	10.877	43975	38846	3358874
American	Cave_E_VD_1838	NAmerica_BB059	Polar	0.00161	11.964	44081	38674	3358874
American	Cave_E_VD_1838	NAmerica_Chi1	Polar	0.001497	10.074	41147	36118	3358874
American	Cave_E_VD_1838	NAmerica_Chi2	Polar	0.001422	11.027	40766	35990	3358874
American	Cave_E_VD_1838	NAmerica_CON001	Polar	0.001992	12.823	44522	37831	3358874
American	Cave_E_VD_1838	NAmerica_Den	Polar	0.001613	11.67	44294	38876	3358874
American	Cave_E_VD_1838	NAmerica_EB027	Polar	0.001597	10.888	44389	39024	3358874
American	Cave_E_VD_1838	NAmerica_GP01	Polar	0.002037	12.734	44862	38021	3358874
American	Cave_E_VD_1838	NAmerica_GRZ	Polar	0.001562	11.648	44493	39245	3358874
American	Cave_E_VD_1838	NAmerica_GT_1	Polar	0.001568	11.328	43494	38227	3358874
American	Cave_E_VD_1838	NAmerica_WB039	Polar	0.001291	9.406	44049	39714	3358874
American	Cave_E_VD_1838	WAsia_Ge	Polar	0.000772	5.307	45589	42995	3358874
American	Cave_E_VD_1838	WAsia_U12M	Polar	0.000675	4.221	45944	43675	3358874
American	Cave_E_VD_1838	WAsia_U47M	Polar	0.000891	6.297	46081	43090	3358874
American	Cave_GS136	ancient_JBB_32K	Polar	0.000023	0.069	1321	1318	149687
American	Cave_GS136	ancient_Kunashir1	Polar	0.000171	0.445	2341	2308	194733
American	Cave_GS136	ancient_Leitrim_4	Polar	-0.000373	-1.663	5658	5856	529149
American	Cave_GS136	ancient_Leitrim_5	Polar	0	-0.002	3750	3750	371386
American	Cave_GS136	ancient_Uap	Polar	0.000089	0.643	22575	22393	2041677
American	Cave_GS136	CAsia_235	Polar	0.000493	3.39	30283	29124	2351196
American	Cave_GS136	CAsia_U05M	Polar	0.000519	3.584	30670	29450	2351196

American	Cave_GS136	CAsia_U13M	Polar	-0.00004	-0.26	30946	31039	2351196
American	Cave_GS136	CAsia_U40	Polar	0.00062	4.278	30725	29266	2351196
American	Cave_GS136	CAsia_U76	Polar	0.000467	3.074	30424	29326	2351196
American	Cave_GS136	EAsia_AA1	Polar	0.000531	3.696	30313	29065	2351196
American	Cave_GS136	EAsia_ETF1	Polar	0.000505	3.201	30106	28918	2351196
American	Cave_GS136	EAsia_U34	Polar	0.000526	3.672	30520	29283	2351196
American	Cave_GS136	Europe_191Y	Polar	0.000116	0.806	29991	29718	2351196
American	Cave_GS136	Europe_ALP1	Polar	0.000109	0.701	30351	30096	2351196
American	Cave_GS136	Europe_APN2	Polar	0.000271	1.753	30728	30092	2351196
American	Cave_GS136	Europe_OFS01	Polar	0.000254	1.723	30451	29853	2351196
American	Cave_GS136	Europe_RF01	Polar	0.000159	1.075	30516	30141	2351196
American	Cave_GS136	Europe_SJS01	Polar	0.00018	1.246	30249	29826	2351196
American	Cave_GS136	Europe_SLK1	Polar	0.000176	1.151	30514	30101	2351196
American	Cave_GS136	Europe_SPA1	Polar	0.000212	1.36	30553	30055	2351196
American	Cave_GS136	Europe_Swe	Polar	0.000231	1.557	29477	28935	2351196
American	Cave_GS136	Hokkaido_2231	Polar	0.000539	3.638	30121	28853	2351196
American	Cave_GS136	Hokkaido_421	Polar	0.000521	3.512	30111	28886	2351196
American	Cave_GS136	Hokkaido_5010	Polar	0.000489	3.304	30171	29020	2351196
American	Cave_GS136	Hokkaido_5046	Polar	0.000507	3.366	30153	28961	2351196
American	Cave_GS136	Hokkaido_518	Polar	0.000534	3.605	30197	28940	2351196
American	Cave_GS136	Hokkaido_819	Polar	0.000395	2.609	29941	29013	2351196
American	Cave_GS136	NAmerica_ABC01	Polar	0.000657	4.695	28214	26670	2351196
American	Cave_GS136	NAmerica_ABC02	Polar	0.000691	5.071	28125	26500	2351196
American	Cave_GS136	NAmerica_ABC03	Polar	0.000628	4.606	27846	26371	2351196
American	Cave_GS136	NAmerica_ABC04	Polar	0.000685	4.824	28176	26565	2351196
American	Cave_GS136	NAmerica_ABC05	Polar	0.000743	4.708	28273	26526	2351196
American	Cave_GS136	NAmerica_ABC06	Polar	0.000738	4.673	28936	27202	2351196
American	Cave_GS136	NAmerica_ABC1	Polar	0.000811	4.889	29248	27340	2351196
American	Cave_GS136	NAmerica_ABC2	Polar	0.000756	4.969	28452	26675	2351196
American	Cave_GS136	NAmerica_Adm1	Polar	0.00072	4.736	28969	27277	2351196
American	Cave_GS136	NAmerica_BB020	Polar	0.000698	4.697	29610	27968	2351196
American	Cave_GS136	NAmerica_BB034	Polar	0.000688	4.469	29565	27946	2351196
American	Cave_GS136	NAmerica_BB037	Polar	0.000731	4.983	29388	27668	2351196
American	Cave_GS136	NAmerica_BB049	Polar	0.000658	4.363	29421	27873	2351196
American	Cave_GS136	NAmerica_BB059	Polar	0.000728	4.943	29414	27703	2351196
American	Cave_GS136	NAmerica_Chi1	Polar	0.000747	4.802	27651	25895	2351196
American	Cave_GS136	NAmerica_Chi2	Polar	0.00071	5.443	27426	25756	2351196
American	Cave_GS136	NAmerica_CON001	Polar	0.00119	7.532	29848	27051	2351196
American	Cave_GS136	NAmerica_Den	Polar	0.000746	5.022	29854	28100	2351196
American	Cave_GS136	NAmerica_EB027	Polar	0.000785	5.218	29831	27985	2351196
American	Cave_GS136	NAmerica_GP01	Polar	0.00123	7.429	30084	27191	2351196
American	Cave_GS136	NAmerica_GRZ	Polar	0.000749	5.025	29947	28186	2351196
American	Cave_GS136	NAmerica_GT_1	Polar	0.00077	5.439	29227	27417	2351196
American	Cave_GS136	NAmerica_WB039	Polar	0.000364	2.487	29419	28562	2351196
American	Cave_GS136	WAsia_Ge	Polar	-0.00013	-0.841	30543	30848	2351196
American	Cave_GS136	WAsia_U12M	Polar	-0.0002	-1.216	30688	31158	2351196
American	Cave_GS136	WAsia_U47M	Polar	-0.000027	-0.184	30775	30838	2351196
American	Cave_HV74	ancient_JBB_32K	Polar	-0.000035	-0.107	1816	1823	196124
American	Cave_HV74	ancient_Kunashir1	Polar	0.000107	0.295	3131	3104	255150
American	Cave_HV74	ancient_Leitrim_4	Polar	-0.000216	-1.122	7220	7362	656613
American	Cave_HV74	ancient_Leitrim_5	Polar	-0.000327	-1.426	4733	4885	463966
American	Cave_HV74	ancient_Uap	Polar	-0.000373	-2.783	31962	33040	2885842
American	Cave_HV74	CAsia_235	Polar	0.000057	0.41	42031	41842	3291135
American	Cave_HV74	CAsia_U05M	Polar	0.000217	1.554	42769	42056	3291135
American	**Cave_HV74**	**CAsia_U13M**	**Polar**	**-0.000453**	**-3.047**	**42928**	**44418**	**3291135**
American	Cave_HV74	CAsia_U40	Polar	0.000296	2.039	42812	41836	3291135
American	Cave_HV74	CAsia_U76	Polar	0.000209	1.431	42280	41593	3291135
American	Cave_HV74	EAsia_AA1	Polar	0.000171	1.213	42192	41629	3291135
American	Cave_HV74	EAsia_ETF1	Polar	0.00026	1.811	41998	41141	3291135
American	Cave_HV74	EAsia_U34	Polar	0.000208	1.507	42553	41870	3291135
American	Cave_HV74	Europe_191Y	Polar	-0.000319	-2.253	41408	42459	3291135
American	Cave_HV74	Europe_ALP1	Polar	-0.000282	-1.872	42094	43022	3291135
American	Cave_HV74	Europe_APN2	Polar	-0.000225	-1.445	42613	43354	3291135

American	Cave_HV74	Europe_OFS01	Polar	-0.000134	-0.953	42254	42695	3291135
American	Cave_HV74	Europe_RF01	Polar	-0.000213	-1.508	42446	43146	3291135
American	Cave_HV74	Europe_SJS01	Polar	-0.000097	-0.668	42228	42548	3291135
American	Cave_HV74	Europe_SLK1	Polar	-0.000224	-1.518	42485	43221	3291135
American	Cave_HV74	Europe_SPA1	Polar	-0.000122	-0.794	42543	42945	3291135
American	Cave_HV74	Europe_Swe	Polar	-0.000142	-1.061	40877	41345	3291135
American	Cave_HV74	Hokkaido_2231	Polar	0.000262	1.917	41861	41000	3291135
American	Cave_HV74	Hokkaido_421	Polar	0.000178	1.24	41894	41308	3291135
American	Cave_HV74	Hokkaido_5010	Polar	0.000217	1.523	42101	41386	3291135
American	Cave_HV74	Hokkaido_5046	Polar	0.000222	1.546	42032	41301	3291135
American	Cave_HV74	Hokkaido_518	Polar	0.000231	1.588	42109	41349	3291135
American	Cave_HV74	Hokkaido_819	Polar	0.000174	1.211	41835	41264	3291135
American	Cave_HV74	NAmerica_ABC01	Polar	0.000351	2.487	39254	38098	3291135
American	Cave_HV74	NAmerica_ABC02	Polar	0.000379	2.775	39072	37824	3291135
American	Cave_HV74	NAmerica_ABC03	Polar	0.000338	2.539	38675	37562	3291135
American	Cave_HV74	NAmerica_ABC04	Polar	0.000362	2.61	39146	37956	3291135
American	Cave_HV74	NAmerica_ABC05	Polar	0.0004	2.661	39208	37892	3291135
American	Cave_HV74	NAmerica_ABC06	Polar	0.000455	3.182	40273	38776	3291135
American	Cave_HV74	NAmerica_ABC1	Polar	0.000512	3.383	40625	38939	3291135
American	Cave_HV74	NAmerica_ABC2	Polar	0.000431	2.8	39587	38169	3291135
American	Cave_HV74	NAmerica_Adm1	Polar	0.000487	3.416	40332	38729	3291135
American	Cave_HV74	NAmerica_BB020	Polar	0.000404	2.814	41211	39882	3291135
American	Cave_HV74	NAmerica_BB034	Polar	0.0004	2.711	41085	39768	3291135
American	Cave_HV74	NAmerica_BB037	Polar	0.000466	3.393	40857	39325	3291135
American	Cave_HV74	NAmerica_BB049	Polar	0.000353	2.424	40892	39731	3291135
American	Cave_HV74	NAmerica_BB059	Polar	0.000491	3.508	41069	39453	3291135
American	Cave_HV74	NAmerica_Chi1	Polar	0.000405	2.752	38295	36962	3291135
American	Cave_HV74	NAmerica_Chi2	Polar	0.000298	2.253	37942	36961	3291135
American	Cave_HV74	NAmerica_CON001	Polar	0.000815	5.247	41524	38842	3291135
American	Cave_HV74	NAmerica_Den	Polar	0.000448	3.189	41331	39857	3291135
American	Cave_HV74	NAmerica_EB027	Polar	0.000384	2.638	41284	40020	3291135
American	Cave_HV74	NAmerica_GP01	Polar	0.000907	5.899	41933	38949	3291135
American	Cave_HV74	NAmerica_GRZ	Polar	0.00041	2.995	41534	40187	3291135
American	Cave_HV74	NAmerica_GT_1	Polar	0.000398	2.909	40531	39222	3291135
American	Cave_HV74	NAmerica_WB039	Polar	0.000213	1.521	41200	40500	3291135
American	**Cave_HV74**	**WAsia_Ge**	**Polar**	**-0.000595**	**-3.837**	**42293**	**44251**	**3291135**
American	**Cave_HV74**	**WAsia_U12M**	**Polar**	**-0.000732**	**-4.38**	**42575**	**44985**	**3291135**
American	**Cave_HV74**	**WAsia_U47M**	**Polar**	**-0.000473**	**-3.193**	**42741**	**44299**	**3291135**
American	Cave_WK01	ancient_JBB_32K	Polar	0.000501	1.633	1965	1862	206437
American	Cave_WK01	ancient_Kunashir1	Polar	0.000734	2.184	3438	3240	269140
American	Cave_WK01	ancient_Leitrim_4	Polar	0.000374	2.038	7956	7697	691919
American	Cave_WK01	ancient_Leitrim_5	Polar	0.000667	3.01	5354	5028	488924
American	Cave_WK01	ancient_Uap	Polar	0.000357	2.685	35383	34299	3036972
American	Cave_WK01	CAsia_235	Polar	0.000911	6.678	46605	43445	3469189
American	Cave_WK01	CAsia_U05M	Polar	0.000911	6.522	47176	44014	3469189
American	Cave_WK01	CAsia_U13M	Polar	0.000388	2.581	47498	46151	3469189
American	Cave_WK01	CAsia_U40	Polar	0.000973	6.823	47149	43772	3469189
American	Cave_WK01	CAsia_U76	Polar	0.000936	6.475	46726	43480	3469189
American	Cave_WK01	EAsia_AA1	Polar	0.000989	7.147	46674	43242	3469189
American	Cave_WK01	EAsia_ETF1	Polar	0.001006	6.934	46445	42953	3469189
American	Cave_WK01	EAsia_U34	Polar	0.000967	7.04	46934	43579	3469189
American	Cave_WK01	Europe_191Y	Polar	0.000495	3.489	45972	44256	3469189
American	Cave_WK01	Europe_ALP1	Polar	0.00051	3.453	46629	44860	3469189
American	Cave_WK01	Europe_APN2	Polar	0.000598	4.018	47157	45082	3469189
American	Cave_WK01	Europe_OFS01	Polar	0.000612	4.265	46640	44517	3469189
American	Cave_WK01	Europe_RF01	Polar	0.000624	4.602	46951	44787	3469189
American	Cave_WK01	Europe_SJS01	Polar	0.000669	4.623	46581	44259	3469189
American	Cave_WK01	Europe_SLK1	Polar	0.000649	4.446	47068	44817	3469189
American	Cave_WK01	Europe_SPA1	Polar	0.000607	4.023	46954	44847	3469189
American	Cave_WK01	Europe_Swe	Polar	0.000598	4.335	45253	43180	3469189
American	Cave_WK01	Hokkaido_2231	Polar	0.000981	7.166	46288	42885	3469189
American	Cave_WK01	Hokkaido_421	Polar	0.000997	6.964	46381	42924	3469189
American	Cave_WK01	Hokkaido_5010	Polar	0.000979	6.867	46528	43130	3469189

American	Cave_WK01	Hokkaido_5046	Polar	0.001007	6.978	46520	43024	3469189
American	Cave_WK01	Hokkaido_518	Polar	0.001007	7.098	46587	43095	3469189
American	Cave_WK01	Hokkaido_819	Polar	0.000905	6.269	46143	43004	3469189
American	Cave_WK01	NAmerica_ABC01	Polar	0.001031	7.359	43253	39677	3469189
American	Cave_WK01	NAmerica_ABC02	Polar	0.00108	7.944	43110	39363	3469189
American	Cave_WK01	NAmerica_ABC03	Polar	0.000993	7.424	42622	39177	3469189
American	Cave_WK01	NAmerica_ABC04	Polar	0.001081	7.918	43199	39448	3469189
American	Cave_WK01	NAmerica_ABC05	Polar	0.001129	7.338	43299	39382	3469189
American	Cave_WK01	NAmerica_ABC06	Polar	0.001161	8.079	44379	40350	3469189
American	Cave_WK01	NAmerica_ABC1	Polar	0.001218	7.95	44813	40589	3469189
American	Cave_WK01	NAmerica_ABC2	Polar	0.001118	7.481	43664	39785	3469189
American	Cave_WK01	NAmerica_Adm1	Polar	0.00117	8.215	44432	40374	3469189
American	Cave_WK01	NAmerica_BB020	Polar	0.001143	7.754	45527	41563	3469189
American	Cave_WK01	NAmerica_BB034	Polar	0.001115	7.626	45358	41491	3469189
American	Cave_WK01	NAmerica_BB037	Polar	0.00115	8.498	45183	41195	3469189
American	Cave_WK01	NAmerica_BB049	Polar	0.001093	7.658	45221	41431	3469189
American	Cave_WK01	NAmerica_BB059	Polar	0.00117	8.491	45327	41268	3469189
American	Cave_WK01	NAmerica_Chi1	Polar	0.00111	7.345	42305	38452	3469189
American	Cave_WK01	NAmerica_Chi2	Polar	0.000992	7.392	41887	38446	3469189
American	Cave_WK01	NAmerica_CON001	Polar	0.001571	10.196	45803	40354	3469189
American	Cave_WK01	NAmerica_Den	Polar	0.001176	8.281	45599	41520	3469189
American	Cave_WK01	NAmerica_EB027	Polar	0.001171	7.861	45668	41604	3469189
American	Cave_WK01	NAmerica_GP01	Polar	0.001595	10.177	46066	40531	3469189
American	Cave_WK01	NAmerica_GRZ	Polar	0.001111	7.959	45766	41912	3469189
American	Cave_WK01	NAmerica_GT_1	Polar	0.001117	7.865	44727	40852	3469189
American	Cave_WK01	NAmerica_WB039	Polar	0.000857	6.115	45323	42350	3469189
American	Cave_WK01	WAsia_Ge	Polar	0.000306	2.024	46933	45870	3469189
American	Cave_WK01	WAsia_U12M	Polar	0.000203	1.259	47201	46496	3469189
American	Cave_WK01	WAsia_U47M	Polar	0.000417	2.833	47320	45875	3469189
Asiatic	Cave_E_VD_1838	ancient_JBB_32K	Polar	0.001007	3.347	1970	1769	199545
Asiatic	Cave_E_VD_1838	ancient_Kunashir1	Polar	0.002182	7.372	3521	2953	260046
Asiatic	Cave_E_VD_1838	ancient_Leitrim_4	Polar	0.001414	7.797	8166	7225	665567
Asiatic	Cave_E_VD_1838	ancient_Leitrim_5	Polar	0.001399	6.796	5370	4710	471587
Asiatic	Cave_E_VD_1838	ancient_Uap	Polar	0.001367	11.549	36068	32042	2945115
Asiatic	Cave_E_VD_1838	CAsia_235	Polar	0.002009	16.789	47326	40580	3358874
Asiatic	Cave_E_VD_1838	CAsia_U05M	Polar	0.002073	16.225	48253	41291	3358874
Asiatic	Cave_E_VD_1838	CAsia_U13M	Polar	0.001649	12.765	48487	42948	3358874
Asiatic	Cave_E_VD_1838	CAsia_U40	Polar	0.00215	16.809	48245	41023	3358874
Asiatic	Cave_E_VD_1838	CAsia_U76	Polar	0.002029	15.919	47510	40693	3358874
Asiatic	Cave_E_VD_1838	EAsia_AA1	Polar	0.002139	17.83	47536	40352	3358874
Asiatic	Cave_E_VD_1838	EAsia_ETF1	Polar	0.002089	16.359	47138	40120	3358874
Asiatic	Cave_E_VD_1838	EAsia_U34	Polar	0.002033	16.828	47550	40723	3358874
Asiatic	Cave_E_VD_1838	Europe_191Y	Polar	0.001735	13.981	46988	41159	3358874
Asiatic	Cave_E_VD_1838	Europe_ALP1	Polar	0.001766	13.89	47663	41732	3358874
Asiatic	Cave_E_VD_1838	Europe_APN2	Polar	0.001917	15.081	48096	41657	3358874
Asiatic	Cave_E_VD_1838	Europe_OFS01	Polar	0.001887	14.487	47691	41353	3358874
Asiatic	Cave_E_VD_1838	Europe_RF01	Polar	0.001874	14.574	48018	41724	3358874
Asiatic	Cave_E_VD_1838	Europe_SJS01	Polar	0.00177	13.895	47311	41365	3358874
Asiatic	Cave_E_VD_1838	Europe_SLK1	Polar	0.001789	14.48	47812	41803	3358874
Asiatic	Cave_E_VD_1838	Europe_SPA1	Polar	0.001761	13.693	47842	41926	3358874
Asiatic	Cave_E_VD_1838	Europe_Swe	Polar	0.001806	14.326	46146	40078	3358874
Asiatic	Cave_E_VD_1838	Hokkaido_2231	Polar	0.002093	17.1	47007	39977	3358874
Asiatic	Cave_E_VD_1838	Hokkaido_421	Polar	0.0021	17.02	47125	40072	3358874
Asiatic	Cave_E_VD_1838	Hokkaido_5010	Polar	0.002076	16.08	47190	40217	3358874
Asiatic	Cave_E_VD_1838	Hokkaido_5046	Polar	0.002087	17.051	47196	40188	3358874
Asiatic	Cave_E_VD_1838	Hokkaido_518	Polar	0.002077	16.894	47175	40199	3358874
Asiatic	Cave_E_VD_1838	Hokkaido_819	Polar	0.002049	16.416	46964	40083	3358874
Asiatic	Cave_E_VD_1838	NAmerica_ABC01	Polar	0.001847	15.857	43159	36956	3358874
Asiatic	Cave_E_VD_1838	NAmerica_ABC02	Polar	0.001847	15.964	43074	36870	3358874
Asiatic	Cave_E_VD_1838	NAmerica_ABC03	Polar	0.001878	16.337	42796	36488	3358874
Asiatic	Cave_E_VD_1838	NAmerica_ABC04	Polar	0.001879	16.563	43194	36883	3358874
Asiatic	Cave_E_VD_1838	NAmerica_ABC05	Polar	0.001972	16.366	43328	36704	3358874
Asiatic	Cave_E_VD_1838	NAmerica_ABC06	Polar	0.0019	15.359	44154	37774	3358874

Asiatic	Cave_E_VD_1838	NAmerica_ABC1	Polar	0.001855	15.155	44361	38129	3358874
Asiatic	Cave_E_VD_1838	NAmerica_ABC2	Polar	0.001932	16.464	43608	37119	3358874
Asiatic	Cave_E_VD_1838	NAmerica_Adm1	Polar	0.001842	15.948	44010	37824	3358874
Asiatic	Cave_E_VD_1838	NAmerica_BB020	Polar	0.001923	16.515	45425	38967	3358874
Asiatic	Cave_E_VD_1838	NAmerica_BB034	Polar	0.001978	15.494	45414	38770	3358874
Asiatic	Cave_E_VD_1838	NAmerica_BB037	Polar	0.001945	16.291	45142	38609	3358874
Asiatic	Cave_E_VD_1838	NAmerica_BB049	Polar	0.001983	16.691	45390	38729	3358874
Asiatic	Cave_E_VD_1838	NAmerica_BB059	Polar	0.001987	16.769	45367	38693	3358874
Asiatic	Cave_E_VD_1838	NAmerica_Chi1	Polar	0.001948	16.557	42375	35833	3358874
Asiatic	Cave_E_VD_1838	NAmerica_Chi2	Polar	0.001871	15.761	41990	35706	3358874
Asiatic	Cave_E_VD_1838	NAmerica_CON001	Polar	0.002018	16.526	44750	37972	3358874
Asiatic	Cave_E_VD_1838	NAmerica_Den	Polar	0.002058	17.875	45771	38859	3358874
Asiatic	Cave_E_VD_1838	NAmerica_EB027	Polar	0.001977	16.12	45648	39007	3358874
Asiatic	Cave_E_VD_1838	NAmerica_GP01	Polar	0.002053	16.142	44991	38096	3358874
Asiatic	Cave_E_VD_1838	NAmerica_GRZ	Polar	0.001978	16.414	45964	39319	3358874
Asiatic	Cave_E_VD_1838	NAmerica_GT_1	Polar	0.00196	16.184	44802	38218	3358874
Asiatic	Cave_E_VD_1838	NAmerica_WB039	Polar	0.001807	15.271	45618	39550	3358874
Asiatic	Cave_E_VD_1838	WAsia_Ge	Polar	0.001451	11.837	47796	42922	3358874
Asiatic	Cave_E_VD_1838	WAsia_U12M	Polar	0.00139	10.563	48076	43408	3358874
Asiatic	Cave_E_VD_1838	WAsia_U47M	Polar	0.001586	12.173	48257	42929	3358874
Asiatic	Cave_GS136	ancient_JBB_32K	Polar	0.000623	1.802	1403	1310	149687
Asiatic	Cave_GS136	ancient_Kunashir1	Polar	0.001392	4.058	2503	2232	194733
Asiatic	Cave_GS136	ancient_Leitrim_4	Polar	0.000297	1.381	6041	5883	529149
Asiatic	Cave_GS136	ancient_Leitrim_5	Polar	0.000567	2.42	3918	3707	371386
Asiatic	Cave_GS136	ancient_Uap	Polar	0.000784	6.343	23689	22088	2041677
Asiatic	Cave_GS136	CAsia_235	Polar	0.00122	9.292	31694	28826	2351196
Asiatic	Cave_GS136	CAsia_U05M	Polar	0.001273	9.743	32246	29254	2351196
Asiatic	Cave_GS136	CAsia_U13M	Polar	0.000773	5.494	32563	30746	2351196
Asiatic	Cave_GS136	CAsia_U40	Polar	0.001388	10.726	32316	29052	2351196
Asiatic	Cave_GS136	CAsia_U76	Polar	0.00118	8.53	31858	29084	2351196
Asiatic	Cave_GS136	EAsia_AA1	Polar	0.001305	9.91	31812	28743	2351196
Asiatic	Cave_GS136	EAsia_ETF1	Polar	0.00123	8.969	31517	28626	2351196
Asiatic	Cave_GS136	EAsia_U34	Polar	0.001201	9.206	31881	29057	2351196
Asiatic	Cave_GS136	Europe_191Y	Polar	0.000928	6.979	31530	29350	2351196
Asiatic	Cave_GS136	Europe_ALP1	Polar	0.000953	6.978	31942	29701	2351196
Asiatic	Cave_GS136	Europe_APN2	Polar	0.00115	8.694	32320	29615	2351196
Asiatic	Cave_GS136	Europe_OFS01	Polar	0.001059	7.847	31912	29423	2351196
Asiatic	Cave_GS136	Europe_RF01	Polar	0.00105	7.706	32200	29732	2351196
Asiatic	Cave_GS136	Europe_SJS01	Polar	0.000903	6.84	31587	29465	2351196
Asiatic	Cave_GS136	Europe_SLK1	Polar	0.000974	7.123	32069	29779	2351196
Asiatic	Cave_GS136	Europe_SPA1	Polar	0.001009	7.161	32116	29744	2351196
Asiatic	Cave_GS136	Europe_Swe	Polar	0.001006	7.43	30844	28478	2351196
Asiatic	Cave_GS136	Hokkaido_2231	Polar	0.001315	9.699	31548	28456	2351196
Asiatic	Cave_GS136	Hokkaido_421	Polar	0.001276	9.664	31484	28483	2351196
Asiatic	Cave_GS136	Hokkaido_5010	Polar	0.001236	9.01	31577	28671	2351196
Asiatic	Cave_GS136	Hokkaido_5046	Polar	0.00125	9.488	31500	28561	2351196
Asiatic	Cave_GS136	Hokkaido_518	Polar	0.001264	9.489	31526	28555	2351196
Asiatic	Cave_GS136	Hokkaido_819	Polar	0.001156	8.6	31321	28603	2351196
Asiatic	Cave_GS136	NAmerica_ABC01	Polar	0.001057	8.878	28950	26464	2351196
Asiatic	Cave_GS136	NAmerica_ABC02	Polar	0.001029	8.701	28836	26415	2351196
Asiatic	Cave_GS136	NAmerica_ABC03	Polar	0.001102	9.261	28720	26129	2351196
Asiatic	Cave_GS136	NAmerica_ABC04	Polar	0.001079	8.75	28997	26461	2351196
Asiatic	Cave_GS136	NAmerica_ABC05	Polar	0.001158	9.16	29088	26366	2351196
Asiatic	Cave_GS136	NAmerica_ABC06	Polar	0.001142	8.745	29697	27012	2351196
Asiatic	Cave_GS136	NAmerica_ABC1	Polar	0.001079	8.23	29836	27299	2351196
Asiatic	Cave_GS136	NAmerica_ABC2	Polar	0.001197	9.72	29249	26436	2351196
Asiatic	Cave_GS136	NAmerica_Adm1	Polar	0.001019	7.872	29578	27182	2351196
Asiatic	Cave_GS136	NAmerica_BB020	Polar	0.001129	9.016	30489	27835	2351196
Asiatic	Cave_GS136	NAmerica_BB034	Polar	0.001169	8.622	30465	27715	2351196
Asiatic	Cave_GS136	NAmerica_BB037	Polar	0.001111	8.971	30177	27564	2351196
Asiatic	Cave_GS136	NAmerica_BB049	Polar	0.001156	9.006	30414	27696	2351196
Asiatic	Cave_GS136	NAmerica_BB059	Polar	0.00118	9.454	30365	27592	2351196
Asiatic	Cave_GS136	NAmerica_Chi1	Polar	0.001176	9.36	28471	25706	2351196

Asiatic	Cave_GS136	NAmerica_Chi2	Polar	0.001148	9.682	28219	25519	2351196
Asiatic	Cave_GS136	NAmerica_CON001	Polar	0.001219	9.579	29924	27058	2351196
Asiatic	Cave_GS136	NAmerica_Den	Polar	0.001269	10.436	30837	27854	2351196
Asiatic	Cave_GS136	NAmerica_EB027	Polar	0.001241	9.832	30692	27774	2351196
Asiatic	Cave_GS136	NAmerica_GP01	Polar	0.001235	9.312	30137	27233	2351196
Asiatic	Cave_GS136	NAmerica_GRZ	Polar	0.001203	9.324	30934	28106	2351196
Asiatic	Cave_GS136	NAmerica_GT_1	Polar	0.001163	9.448	30101	27366	2351196
Asiatic	Cave_GS136	NAmerica_WB039	Polar	0.000947	7.392	30495	28267	2351196
Asiatic	Cave_GS136	WAsia_Ge	Polar	0.000642	4.83	32165	30656	2351196
Asiatic	Cave_GS136	WAsia_U12M	Polar	0.000565	3.949	32218	30890	2351196
Asiatic	Cave_GS136	WAsia_U47M	Polar	0.000751	5.494	32326	30561	2351196
Asiatic	Cave_HV74	ancient_JBB_32K	Polar	0.000346	1.123	1898	1830	196124
Asiatic	Cave_HV74	ancient_Kunashir1	Polar	0.001039	3.161	3285	3020	255150
Asiatic	Cave_HV74	ancient_Leitrim_4	Polar	0.000372	1.925	7639	7395	656613
Asiatic	Cave_HV74	ancient_Leitrim_5	Polar	0.000273	1.287	4955	4828	463966
Asiatic	Cave_HV74	ancient_Uap	Polar	0.000248	2.14	33483	32767	2885842
Asiatic	Cave_HV74	CAsia_235	Polar	0.000778	6.335	44203	41643	3291135
Asiatic	Cave_HV74	CAsia_U05M	Polar	0.000951	7.65	45161	42032	3291135
Asiatic	Cave_HV74	CAsia_U13M	Polar	0.000366	2.782	45349	44144	3291135
Asiatic	Cave_HV74	CAsia_U40	Polar	0.001043	8.349	45177	41746	3291135
Asiatic	Cave_HV74	CAsia_U76	Polar	0.000924	7.654	44495	41456	3291135
Asiatic	Cave_HV74	EAsia_AA1	Polar	0.000909	7.623	44395	41404	3291135
Asiatic	Cave_HV74	EAsia_ETF1	Polar	0.000973	7.535	44158	40955	3291135
Asiatic	Cave_HV74	EAsia_U34	Polar	0.000833	6.818	44580	41839	3291135
Asiatic	Cave_HV74	Europe_191Y	Polar	0.000475	3.811	43797	42235	3291135
Asiatic	Cave_HV74	Europe_ALP1	Polar	0.000517	3.943	44510	42809	3291135
Asiatic	Cave_HV74	Europe_APN2	Polar	0.000644	5.079	44902	42781	3291135
Asiatic	Cave_HV74	Europe_OFS01	Polar	0.000651	5.158	44534	42392	3291135
Asiatic	Cave_HV74	Europe_RF01	Polar	0.000624	4.848	44888	42834	3291135
Asiatic	Cave_HV74	Europe_SJS01	Polar	0.000563	4.389	44231	42376	3291135
Asiatic	Cave_HV74	Europe_SLK1	Polar	0.00051	4.058	44601	42921	3291135
Asiatic	Cave_HV74	Europe_SPA1	Polar	0.000588	4.619	44740	42805	3291135
Asiatic	Cave_HV74	Europe_Swe	Polar	0.000589	4.71	42970	41032	3291135
Asiatic	Cave_HV74	Hokkaido_2231	Polar	0.000951	8.193	43963	40832	3291135
Asiatic	Cave_HV74	Hokkaido_421	Polar	0.000903	7.447	44045	41073	3291135
Asiatic	Cave_HV74	Hokkaido_5010	Polar	0.000921	7.334	44210	41178	3291135
Asiatic	Cave_HV74	Hokkaido_5046	Polar	0.000915	7.806	44117	41107	3291135
Asiatic	Cave_HV74	Hokkaido_518	Polar	0.000897	7.382	44119	41167	3291135
Asiatic	Cave_HV74	Hokkaido_819	Polar	0.000909	7.5	44000	41008	3291135
Asiatic	Cave_HV74	NAmerica_ABC01	Polar	0.000761	6.49	40480	37975	3291135
Asiatic	Cave_HV74	NAmerica_ABC02	Polar	0.000706	6.3	40227	37902	3291135
Asiatic	Cave_HV74	NAmerica_ABC03	Polar	0.000791	6.893	40098	37495	3291135
Asiatic	Cave_HV74	NAmerica_ABC04	Polar	0.000756	6.513	40438	37950	3291135
Asiatic	Cave_HV74	NAmerica_ABC05	Polar	0.000857	7.334	40514	37693	3291135
Asiatic	Cave_HV74	NAmerica_ABC06	Polar	0.000808	6.857	41444	38784	3291135
Asiatic	Cave_HV74	NAmerica_ABC1	Polar	0.000739	6.163	41505	39073	3291135
Asiatic	Cave_HV74	NAmerica_ABC2	Polar	0.000835	6.964	40854	38107	3291135
Asiatic	Cave_HV74	NAmerica_Adm1	Polar	0.000747	6.458	41296	38838	3291135
Asiatic	Cave_HV74	NAmerica_BB020	Polar	0.000794	6.903	42505	39892	3291135
Asiatic	Cave_HV74	NAmerica_BB034	Polar	0.000858	6.863	42486	39662	3291135
Asiatic	Cave_HV74	NAmerica_BB037	Polar	0.000804	6.927	42153	39508	3291135
Asiatic	Cave_HV74	NAmerica_BB049	Polar	0.000817	7.03	42376	39688	3291135
Asiatic	Cave_HV74	NAmerica_BB059	Polar	0.000888	7.692	42422	39500	3291135
Asiatic	Cave_HV74	NAmerica_Chi1	Polar	0.000865	7.588	39597	36750	3291135
Asiatic	Cave_HV74	NAmerica_Chi2	Polar	0.000772	6.539	39251	36711	3291135
Asiatic	Cave_HV74	NAmerica_CON001	Polar	0.000827	6.854	41848	39127	3291135
Asiatic	Cave_HV74	NAmerica_Den	Polar	0.000891	7.818	42767	39835	3291135
Asiatic	Cave_HV74	NAmerica_EB027	Polar	0.000799	6.572	42637	40009	3291135
Asiatic	Cave_HV74	NAmerica_GP01	Polar	0.000928	7.535	42218	39164	3291135
Asiatic	Cave_HV74	NAmerica_GRZ	Polar	0.000846	7.077	42996	40213	3291135
Asiatic	Cave_HV74	NAmerica_GT_1	Polar	0.000795	6.871	41823	39207	3291135
Asiatic	Cave_HV74	NAmerica_WB039	Polar	0.000777	6.647	42894	40337	3291135
Asiatic	Cave_HV74	WAsia_Ge	Polar	0.000133	1.041	44640	44202	3291135

Asiatic	Cave_HV74	WAsia_U12M	Polar	0.000016	0.114	44769	44718	3291135
Asiatic	Cave_HV74	WAsia_U47M	Polar	0.000254	1.92	44999	44164	3291135
Asiatic	Cave_WK01	ancient_JBB_32K	Polar	0.000909	3.16	2044	1857	206437
Asiatic	Cave_WK01	ancient_Kunashir1	Polar	0.001705	5.61	3626	3167	269140
Asiatic	Cave_WK01	ancient_Leitrim_4	Polar	0.000975	5.164	8424	7750	691919
Asiatic	Cave_WK01	ancient_Leitrim_5	Polar	0.001181	5.792	5604	5026	488924
Asiatic	Cave_WK01	ancient_Uap	Polar	0.000973	8.505	36993	34038	3036972
Asiatic	Cave_WK01	CAsia_235	Polar	0.001629	13.678	48878	43226	3469189
Asiatic	Cave_WK01	CAsia_U05M	Polar	0.001638	13.104	49650	43968	3469189
Asiatic	Cave_WK01	CAsia_U13M	Polar	0.001193	9.168	49983	45842	3469189
Asiatic	Cave_WK01	CAsia_U40	Polar	0.001721	13.672	49619	43649	3469189
Asiatic	Cave_WK01	CAsia_U76	Polar	0.00165	13.29	49011	43285	3469189
Asiatic	Cave_WK01	EAsia_AA1	Polar	0.00172	14.487	49003	43036	3469189
Asiatic	Cave_WK01	EAsia_ETF1	Polar	0.001701	13.385	48565	42663	3469189
Asiatic	Cave_WK01	EAsia_U34	Polar	0.001614	13.149	49078	43481	3469189
Asiatic	Cave_WK01	Europe_191Y	Polar	0.001281	10.415	48410	43968	3469189
Asiatic	Cave_WK01	Europe_ALP1	Polar	0.001314	10.466	49152	44592	3469189
Asiatic	Cave_WK01	Europe_APN2	Polar	0.00145	11.874	49608	44576	3469189
Asiatic	Cave_WK01	Europe_OFS01	Polar	0.001412	11.013	49046	44146	3469189
Asiatic	Cave_WK01	Europe_RF01	Polar	0.001457	11.824	49539	44485	3469189
Asiatic	Cave_WK01	Europe_SJS01	Polar	0.001344	10.711	48697	44033	3469189
Asiatic	Cave_WK01	Europe_SLK1	Polar	0.001382	11.206	49386	44591	3469189
Asiatic	Cave_WK01	Europe_SPA1	Polar	0.001321	10.452	49305	44724	3469189
Asiatic	Cave_WK01	Europe_Swe	Polar	0.00133	10.65	47491	42878	3469189
Asiatic	Cave_WK01	Hokkaido_2231	Polar	0.001677	14.12	48448	42631	3469189
Asiatic	Cave_WK01	Hokkaido_421	Polar	0.00172	13.876	48602	42634	3469189
Asiatic	Cave_WK01	Hokkaido_5010	Polar	0.001693	13.485	48677	42803	3469189
Asiatic	Cave_WK01	Hokkaido_5046	Polar	0.001697	13.869	48631	42745	3469189
Asiatic	Cave_WK01	Hokkaido_518	Polar	0.001669	13.74	48642	42852	3469189
Asiatic	Cave_WK01	Hokkaido_819	Polar	0.001639	13.166	48374	42687	3469189
Asiatic	Cave_WK01	NAmerica_ABC01	Polar	0.001441	12.553	44529	39531	3469189
Asiatic	Cave_WK01	NAmerica_ABC02	Polar	0.001429	12.338	44350	39392	3469189
Asiatic	Cave_WK01	NAmerica_ABC03	Polar	0.001451	12.641	44070	39035	3469189
Asiatic	Cave_WK01	NAmerica_ABC04	Polar	0.001482	12.819	44559	39418	3469189
Asiatic	Cave_WK01	NAmerica_ABC05	Polar	0.001596	13.197	44702	39166	3469189
Asiatic	Cave_WK01	NAmerica_ABC06	Polar	0.001523	12.501	45521	40237	3469189
Asiatic	Cave_WK01	NAmerica_ABC1	Polar	0.00146	12.082	45742	40677	3469189
Asiatic	Cave_WK01	NAmerica_ABC2	Polar	0.001545	13.277	44984	39623	3469189
Asiatic	Cave_WK01	NAmerica_Adm1	Polar	0.001443	12.383	45370	40364	3469189
Asiatic	Cave_WK01	NAmerica_BB020	Polar	0.001517	13.257	46876	41613	3469189
Asiatic	Cave_WK01	NAmerica_BB034	Polar	0.001591	12.582	46804	41285	3469189
Asiatic	Cave_WK01	NAmerica_BB037	Polar	0.001501	12.867	46476	41267	3469189
Asiatic	Cave_WK01	NAmerica_BB049	Polar	0.001559	13.405	46818	41411	3469189
Asiatic	Cave_WK01	NAmerica_BB059	Polar	0.001568	13.339	46794	41353	3469189
Asiatic	Cave_WK01	NAmerica_Chi1	Polar	0.001583	13.255	43708	38216	3469189
Asiatic	Cave_WK01	NAmerica_Chi2	Polar	0.001466	12.504	43223	38138	3469189
Asiatic	Cave_WK01	NAmerica_CON001	Polar	0.001607	13.741	46112	40538	3469189
Asiatic	Cave_WK01	NAmerica_Den	Polar	0.001626	14.246	47168	41527	3469189
Asiatic	Cave_WK01	NAmerica_EB027	Polar	0.001577	12.983	47116	41644	3469189
Asiatic	Cave_WK01	NAmerica_GP01	Polar	0.00164	13.487	46366	40678	3469189
Asiatic	Cave_WK01	NAmerica_GRZ	Polar	0.001537	13.064	47360	42029	3469189
Asiatic	Cave_WK01	NAmerica_GT_1	Polar	0.001526	12.761	46121	40828	3469189
Asiatic	Cave_WK01	NAmerica_WB039	Polar	0.001417	11.941	47058	42142	3469189
Asiatic	Cave_WK01	WAsia_Ge	Polar	0.001003	7.941	49335	45855	3469189
Asiatic	Cave_WK01	WAsia_U12M	Polar	0.000945	7.136	49564	46285	3469189
Asiatic	Cave_WK01	WAsia_U47M	Polar	0.001131	8.639	49694	45771	3469189

The rows in bold font indicate significant gene flow (|Z score| > 3) between the Cave bear and X.

Table 26. The admixture proportion from the polar bear estimated by f_4 ratio.

Outgroup	Polar bear	X	α	1-α	std.err	Z
American	APB	ancient_JBB_32K	0.762711	0.237289	0.020689	36.865
American	APB	ancient_Kunashir1	0.843646	0.156354	0.01758	47.988
American	APB	ancient_Leitrim_4	0.886241	0.113759	0.011083	79.966
American	APB	ancient_Leitrim_5	0.859591	0.140409	0.014205	60.511
American	APB	ancient_Uap	0.871244	0.128756	0.008439	103.239
American	APB	CAsia_235	0.98916	0.01084	0.009055	109.235
American	APB	CAsia_U05M	1 >	< 0	0.015021	66.661
American	APB	Casia_U40	0.982922	0.017078	0.014679	66.963
American	APB	Casia_U76	0.949135	0.050865	0.009798	96.87
American	APB	EAsia_AA1	0.938696	0.061304	0.009216	101.853
American	APB	EAsia_ETF1	0.901527	0.098473	0.009864	91.399
American	APB	Easia_U34	0.948421	0.051579	0.008774	108.101
American	APB	Europe_191Y	0.990546	0.009454	0.008005	123.733
American	APB	Europe_ALP1	0.999739	0.000261	0.008111	123.263
American	APB	Europe_APN2	0.98626	0.01374	0.008507	115.941
American	APB	Europe_OFS01	0.996924	0.003076	0.008957	111.299
American	APB	Europe_RF01	0.988265	0.011735	0.008419	117.388
American	APB	Europe_SJS01	0.986526	0.013474	0.008879	111.112
American	APB	Europe_SLK1	0.978084	0.021916	0.008222	118.954
American	APB	Europe_SPA1	0.995488	0.004512	0.008604	115.697
American	APB	Europe_Swe	0.980565	0.019435	0.00894	109.681
American	APB	Hokkaido_2231	0.908291	0.091709	0.009466	95.949
American	APB	Hokkaido_421	0.892924	0.107076	0.009714	91.921
American	APB	Hokkaido_5010	0.898962	0.101038	0.009456	95.07
American	APB	Hokkaido_5046	0.897545	0.102455	0.009569	93.794
American	APB	Hokkaido_518	0.903705	0.096295	0.009039	99.979
American	APB	Hokkaido_819	0.900437	0.099563	0.009513	94.654
American	APB	NAmerica_ABC01	0.843131	0.156869	0.010712	78.709
American	APB	NAmerica_ABC02	0.831327	0.168673	0.010944	75.965
American	APB	NAmerica_ABC03	0.83326	0.16674	0.010396	80.153
American	APB	NAmerica_ABC04	0.835206	0.164794	0.010424	80.121
American	APB	NAmerica_ABC05	0.83511	0.16489	0.011839	70.54
American	APB	NAmerica_ABC06	0.856065	0.143935	0.010573	80.965
American	APB	NAmerica_ABC1	0.843041	0.156959	0.011266	74.832
American	APB	NAmerica_ABC2	0.835811	0.164189	0.01182	70.709
American	APB	NAmerica_Adm1	0.848504	0.151496	0.010357	81.929
American	APB	NAmerica_BB020	0.907055	0.092945	0.009888	91.736
American	APB	NAmerica_BB034	0.895938	0.104062	0.010538	85.016
American	APB	NAmerica_BB037	0.893421	0.106579	0.009867	90.545
American	APB	NAmerica_BB049	0.890676	0.109324	0.011566	77.009
American	APB	NAmerica_BB059	0.890651	0.109349	0.010535	84.546
American	APB	NAmerica_Chi1	0.823571	0.176429	0.011805	69.763
American	APB	NAmerica_Chi2	0.825882	0.174118	0.009794	84.329
American	APB	NAmerica_CON001	0.800811	0.199189	0.011673	68.603
American	APB	NAmerica_Den	0.908435	0.091565	0.009737	93.299
American	APB	NAmerica_EB027	0.89825	0.10175	0.009991	89.908
American	APB	NAmerica_GP01	0.807404	0.192596	0.012451	64.845
American	APB	NAmerica_GRZ	0.913119	0.086881	0.009735	93.799
American	APB	NAmerica_GT_1	0.85843	0.14157	0.009832	87.311

American	APB	NAmerica_WB039	0.932315	0.067685	0.009701	96.101
Asiatic	APB	ancient_JBB_32K	0.77182	0.22818	0.022499	34.305
Asiatic	APB	ancient_Kunashir1	0.840665	0.159335	0.018707	44.939
Asiatic	APB	ancient_Leitrim_4	0.889421	0.110579	0.011668	76.227
Asiatic	APB	ancient_Leitrim_5	0.855556	0.144444	0.014888	57.465
Asiatic	APB	ancient_Uap	0.868881	0.131119	0.008762	99.163
Asiatic	APB	CAsia_235	0.988925	0.011075	0.009394	105.276
Asiatic	APB	CAsia_U05M	1 >	< 0	0.015695	63.818
Asiatic	APB	Casia_U40	0.981379	0.018621	0.01465	66.988
Asiatic	APB	Casia_U76	0.947847	0.052153	0.010163	93.268
Asiatic	APB	EAsia_AA1	0.936031	0.063969	0.009483	98.701
Asiatic	APB	EAsia_ETF1	0.899042	0.100958	0.009696	92.721
Asiatic	APB	Easia_U34	0.95136	0.04864	0.009176	103.681
Asiatic	APB	Europe_191Y	0.986253	0.013747	0.008521	115.748
Asiatic	APB	Europe_ALP1	0.994987	0.005013	0.008369	118.893
Asiatic	APB	Europe_APN2	0.976921	0.023079	0.008549	114.275
Asiatic	APB	Europe_OFS01	0.99198	0.00802	0.009518	104.226
Asiatic	APB	Europe_RF01	0.981623	0.018377	0.008777	111.846
Asiatic	APB	Europe_SJS01	0.988417	0.011583	0.009274	106.584
Asiatic	APB	Europe_SLK1	0.976445	0.023555	0.008615	113.348
Asiatic	APB	Europe_SPA1	0.995916	0.004084	0.009289	107.21
Asiatic	APB	Europe_Swe	0.978932	0.021068	0.009322	105.008
Asiatic	APB	Hokkaido_2231	0.906415	0.093585	0.009694	93.5
Asiatic	APB	Hokkaido_421	0.88878	0.11122	0.009915	89.639
Asiatic	APB	Hokkaido_5010	0.895901	0.104099	0.009703	92.328
Asiatic	APB	Hokkaido_5046	0.895334	0.104666	0.009878	90.638
Asiatic	APB	Hokkaido_518	0.902687	0.097313	0.009354	96.498
Asiatic	APB	Hokkaido_819	0.89565	0.10435	0.009702	92.319
Asiatic	APB	NAmerica_ABC01	0.856329	0.143671	0.009981	85.793
Asiatic	APB	NAmerica_ABC02	0.847954	0.152046	0.010207	83.073
Asiatic	APB	NAmerica_ABC03	0.84226	0.15774	0.010264	82.062
Asiatic	APB	NAmerica_ABC04	0.848574	0.151426	0.009927	85.485
Asiatic	APB	NAmerica_ABC05	0.844218	0.155782	0.010511	80.319
Asiatic	APB	NAmerica_ABC06	0.871991	0.128009	0.010124	86.132
Asiatic	APB	NAmerica_ABC1	0.866356	0.133644	0.010159	85.281
Asiatic	APB	NAmerica_ABC2	0.848029	0.151971	0.010851	78.153
Asiatic	APB	NAmerica_Adm1	0.870152	0.129848	0.009883	88.045
Asiatic	APB	NAmerica_BB020	0.925162	0.074838	0.009746	94.924
Asiatic	APB	NAmerica_BB034	0.907205	0.092795	0.009739	93.15
Asiatic	APB	NAmerica_BB037	0.912185	0.087815	0.009957	91.614
Asiatic	APB	NAmerica_BB049	0.90161	0.09839	0.010129	89.01
Asiatic	APB	NAmerica_BB059	0.906049	0.093951	0.009998	90.623
Asiatic	APB	NAmerica_Chi1	0.831818	0.168182	0.010564	78.74
Asiatic	APB	NAmerica_Chi2	0.833961	0.166039	0.009883	84.383
Asiatic	APB	NAmerica_CON001	0.834928	0.165072	0.010254	81.424
Asiatic	APB	NAmerica_Den	0.921139	0.078861	0.009825	93.758
Asiatic	APB	NAmerica_EB027	0.914043	0.085957	0.009628	94.931
Asiatic	APB	NAmerica_GP01	0.841806	0.158194	0.010485	80.29
Asiatic	APB	NAmerica_GRZ	0.927645	0.072355	0.009578	96.847
Asiatic	APB	NAmerica_GT_1	0.873124	0.126876	0.009599	90.962
Asiatic	APB	NAmerica_WB039	0.939431	0.060569	0.010053	93.447

American	Bruno	ancient_JBB_32K	0.759368	0.240632	0.020872	36.382
American	Bruno	ancient_Kunashir1	0.841155	0.158845	0.017837	47.157
American	Bruno	ancient_Leitrim_4	0.883419	0.116581	0.011408	77.436
American	Bruno	ancient_Leitrim_5	0.856201	0.143799	0.014539	58.892
American	Bruno	ancient_Uap	0.86876	0.13124	0.008615	100.842
American	Bruno	CAsia_235	0.988933	0.011067	0.009215	107.322
American	Bruno	CAsia_U05M	1 >	< 0	0.015286	65.509
American	Bruno	Casia_U40	0.982652	0.017348	0.01494	65.774
American	Bruno	Casia_U76	0.948199	0.051801	0.009971	95.094
American	Bruno	EAsia_AA1	0.937604	0.062396	0.009385	99.909
American	Bruno	EAsia_ETF1	0.899823	0.100177	0.010059	89.452
American	Bruno	Easia_U34	0.947491	0.052509	0.008936	106.029
American	Bruno	Europe_191Y	0.990363	0.009637	0.008148	121.542
American	Bruno	Europe_ALP1	0.999679	0.000321	0.008255	121.104
American	Bruno	Europe_APN2	0.986085	0.013915	0.008668	113.765
American	Bruno	Europe_OFS01	0.996835	0.003165	0.009117	109.336
American	Bruno	Europe_RF01	0.987998	0.012002	0.008574	115.226
American	Bruno	Europe_SJS01	0.986299	0.013701	0.009034	109.18
American	Bruno	Europe_SLK1	0.977629	0.022371	0.008365	116.865
American	Bruno	Europe_SPA1	0.995445	0.004555	0.008757	113.672
American	Bruno	Europe_Swe	0.980184	0.019816	0.0091	107.707
American	Bruno	Hokkaido_2231	0.906737	0.093263	0.009655	93.917
American	Bruno	Hokkaido_421	0.891006	0.108994	0.009901	89.995
American	Bruno	Hokkaido_5010	0.897205	0.102795	0.009653	92.948
American	Bruno	Hokkaido_5046	0.895744	0.104256	0.009755	91.828
American	Bruno	Hokkaido_518	0.901971	0.098029	0.009207	97.961
American	Bruno	Hokkaido_819	0.898675	0.101325	0.009689	92.756
American	Bruno	NAmerica_ABC01	0.840256	0.159744	0.010932	76.864
American	Bruno	NAmerica_ABC02	0.828234	0.171766	0.011141	74.339
American	Bruno	NAmerica_ABC03	0.830177	0.169823	0.010596	78.348
American	Bruno	NAmerica_ABC04	0.832206	0.167794	0.010649	78.145
American	Bruno	NAmerica_ABC05	0.832083	0.167917	0.012091	68.82
American	Bruno	NAmerica_ABC06	0.853436	0.146564	0.010774	79.214
American	Bruno	NAmerica_ABC1	0.840179	0.159821	0.011488	73.138
American	Bruno	NAmerica_ABC2	0.832764	0.167236	0.012038	69.176
American	Bruno	NAmerica_Adm1	0.845781	0.154219	0.010541	80.238
American	Bruno	NAmerica_BB020	0.905248	0.094752	0.010093	89.692
American	Bruno	NAmerica_BB034	0.894033	0.105967	0.010756	83.119
American	Bruno	NAmerica_BB037	0.891419	0.108581	0.010053	88.673
American	Bruno	NAmerica_BB049	0.888626	0.111374	0.011799	75.311
American	Bruno	NAmerica_BB059	0.888575	0.111425	0.010756	82.616
American	Bruno	NAmerica_Chi1	0.820325	0.179675	0.012061	68.015
American	Bruno	NAmerica_Chi2	0.822711	0.177289	0.010007	82.214
American	Bruno	NAmerica_CON001	0.797163	0.202837	0.011936	66.786
American	Bruno	NAmerica_Den	0.90672	0.09328	0.009934	91.279
American	Bruno	NAmerica_EB027	0.896329	0.103671	0.010167	88.159
American	Bruno	NAmerica_GP01	0.803911	0.196089	0.01271	63.248
American	Bruno	NAmerica_GRZ	0.911537	0.088463	0.009928	91.813
American	Bruno	NAmerica_GT_1	0.85584	0.14416	0.010022	85.398
American	Bruno	NAmerica_WB039	0.931008	0.068992	0.009875	94.275
Asiatic	Bruno	ancient_JBB_32K	0.766821	0.233179	0.022993	33.35

Asiatic	Bruno	ancient_Kunashir1	0.837548	0.162452	0.019014	44.049
Asiatic	Bruno	ancient_Leitrim_4	0.886007	0.113993	0.012036	73.613
Asiatic	Bruno	ancient_Leitrim_5	0.851502	0.148498	0.015304	55.641
Asiatic	Bruno	ancient_Uap	0.865858	0.134142	0.008961	96.626
Asiatic	Bruno	CAsia_235	0.988605	0.011395	0.009598	102.997
Asiatic	Bruno	CAsia_U05M	1 >	< 0	0.016026	62.499
Asiatic	Bruno	Casia_U40	0.980956	0.019044	0.014959	65.575
Asiatic	Bruno	Casia_U76	0.946649	0.053351	0.01038	91.202
Asiatic	Bruno	EAsia_AA1	0.934694	0.065306	0.009686	96.5
Asiatic	Bruno	EAsia_ETF1	0.896923	0.103077	0.009907	90.532
Asiatic	Bruno	Easia_U34	0.950292	0.049708	0.00938	101.314
Asiatic	Bruno	Europe_191Y	0.985883	0.014117	0.008704	113.272
Asiatic	Bruno	Europe_ALP1	0.994879	0.005121	0.008546	116.417
Asiatic	Bruno	Europe_APN2	0.976442	0.023558	0.008742	111.701
Asiatic	Bruno	Europe_OFS01	0.991805	0.008195	0.009726	101.971
Asiatic	Bruno	Europe_RF01	0.981216	0.018784	0.008975	109.332
Asiatic	Bruno	Europe_SJS01	0.988201	0.011799	0.009466	104.396
Asiatic	Bruno	Europe_SLK1	0.975881	0.024119	0.008796	110.944
Asiatic	Bruno	Europe_SPA1	0.995957	0.004043	0.009488	104.975
Asiatic	Bruno	Europe_Swe	0.978481	0.021519	0.009527	102.706
Asiatic	Bruno	Hokkaido_2231	0.904494	0.095506	0.009918	91.194
Asiatic	Bruno	Hokkaido_421	0.886395	0.113605	0.010133	87.476
Asiatic	Bruno	Hokkaido_5010	0.893717	0.106283	0.009937	89.941
Asiatic	Bruno	Hokkaido_5046	0.893116	0.106884	0.010107	88.368
Asiatic	Bruno	Hokkaido_518	0.900562	0.099438	0.009566	94.145
Asiatic	Bruno	Hokkaido_819	0.893424	0.106576	0.009918	90.084
Asiatic	Bruno	NAmerica_ABC01	0.853293	0.146707	0.010203	83.634
Asiatic	Bruno	NAmerica_ABC02	0.844708	0.155292	0.01041	81.144
Asiatic	Bruno	NAmerica_ABC03	0.838891	0.161109	0.010507	79.843
Asiatic	Bruno	NAmerica_ABC04	0.845343	0.154657	0.010152	83.266
Asiatic	Bruno	NAmerica_ABC05	0.840916	0.159084	0.010735	78.334
Asiatic	Bruno	NAmerica_ABC06	0.869265	0.130735	0.010328	84.166
Asiatic	Bruno	NAmerica_ABC1	0.863451	0.136549	0.010361	83.333
Asiatic	Bruno	NAmerica_ABC2	0.84479	0.15521	0.011082	76.23
Asiatic	Bruno	NAmerica_Adm1	0.867391	0.132609	0.010082	86.037
Asiatic	Bruno	NAmerica_BB020	0.923459	0.076541	0.00998	92.532
Asiatic	Bruno	NAmerica_BB034	0.905206	0.094794	0.009958	90.899
Asiatic	Bruno	NAmerica_BB037	0.910252	0.089748	0.010177	89.444
Asiatic	Bruno	NAmerica_BB049	0.899481	0.100519	0.010374	86.708
Asiatic	Bruno	NAmerica_BB059	0.903979	0.096021	0.010242	88.262
Asiatic	Bruno	NAmerica_Chi1	0.82823	0.17177	0.010793	76.739
Asiatic	Bruno	NAmerica_Chi2	0.83045	0.16955	0.010111	82.135
Asiatic	Bruno	NAmerica_CON001	0.83137	0.16863	0.010464	79.447
Asiatic	Bruno	NAmerica_Den	0.919472	0.080528	0.010048	91.512
Asiatic	Bruno	NAmerica_EB027	0.912123	0.087877	0.009835	92.742
Asiatic	Bruno	NAmerica_GP01	0.838403	0.161597	0.010691	78.42
Asiatic	Bruno	NAmerica_GRZ	0.926125	0.073875	0.009792	94.577
Asiatic	Bruno	NAmerica_GT_1	0.870367	0.129633	0.009823	88.608
Asiatic	Bruno	NAmerica_WB039	0.938116	0.061884	0.010271	91.334
American	Polar	ancient_JBB_32K	0.756359	0.243641	0.021099	35.848
American	Polar	ancient_Kunashir1	0.840461	0.159539	0.017959	46.798

American	Polar	ancient_Leitrim_4	0.883419	0.116581	0.011397	77.511
American	Polar	ancient_Leitrim_5	0.85579	0.14421	0.014575	58.716
American	Polar	ancient_Uap	0.868154	0.131846	0.008615	100.771
American	Polar	CAsia_235	0.988912	0.011088	0.009245	106.966
American	Polar	CAsia_U05M	1 >	< 0	0.015338	65.29
American	Polar	Casia_U40	0.982615	0.017385	0.014987	65.563
American	Polar	Casia_U76	0.948039	0.051961	0.010004	94.763
American	Polar	EAsia_AA1	0.937415	0.062585	0.009404	99.687
American	Polar	EAsia_ETF1	0.899477	0.100523	0.01007	89.321
American	Polar	Easia_U34	0.947327	0.052673	0.008961	105.721
American	Polar	Europe_191Y	0.990362	0.009638	0.008176	121.124
American	Polar	Europe_ALP1	0.999704	0.000296	0.008284	120.685
American	Polar	Europe_APN2	0.986047	0.013953	0.008697	113.383
American	Polar	Europe_OFS01	0.996835	0.003165	0.009148	108.973
American	Polar	Europe_RF01	0.98797	0.01203	0.008601	114.865
American	Polar	Europe_SJS01	0.986265	0.013735	0.009062	108.835
American	Polar	Europe_SLK1	0.977578	0.022422	0.008392	116.49
American	Polar	Europe_SPA1	0.995442	0.004558	0.008786	113.295
American	Polar	Europe_Swe	0.980134	0.019866	0.009127	107.393
American	Polar	Hokkaido_2231	0.90642	0.09358	0.009672	93.717
American	Polar	Hokkaido_421	0.89064	0.10936	0.009912	89.856
American	Polar	Hokkaido_5010	0.896871	0.103129	0.009655	92.889
American	Polar	Hokkaido_5046	0.89541	0.10459	0.009761	91.731
American	Polar	Hokkaido_518	0.901659	0.098341	0.009219	97.803
American	Polar	Hokkaido_819	0.898347	0.101653	0.009705	92.564
American	Polar	NAmerica_ABC01	0.83974	0.16026	0.010923	76.877
American	Polar	NAmerica_ABC02	0.827675	0.172325	0.01115	74.232
American	Polar	NAmerica_ABC03	0.82965	0.17035	0.010604	78.242
American	Polar	NAmerica_ABC04	0.831655	0.168345	0.010643	78.144
American	Polar	NAmerica_ABC05	0.831536	0.168464	0.012098	68.731
American	Polar	NAmerica_ABC06	0.852975	0.147025	0.010791	79.045
American	Polar	NAmerica_ABC1	0.839673	0.160327	0.011495	73.045
American	Polar	NAmerica_ABC2	0.832237	0.167763	0.012046	69.088
American	Polar	NAmerica_Adm1	0.845285	0.154715	0.010551	80.113
American	Polar	NAmerica_BB020	0.904955	0.095045	0.010112	89.49
American	Polar	NAmerica_BB034	0.893703	0.106297	0.010772	82.962
American	Polar	NAmerica_BB037	0.891075	0.108925	0.010056	88.607
American	Polar	NAmerica_BB049	0.888265	0.111735	0.011824	75.127
American	Polar	NAmerica_BB059	0.888215	0.111785	0.010785	82.354
American	Polar	NAmerica_Chi1	0.819739	0.180261	0.012064	67.952
American	Polar	NAmerica_Chi2	0.822146	0.177854	0.010001	82.206
American	Polar	NAmerica_CON001	0.796494	0.203506	0.011921	66.813
American	Polar	NAmerica_Den	0.906405	0.093595	0.009933	91.249
American	Polar	NAmerica_EB027	0.896028	0.103972	0.01019	87.929
American	Polar	NAmerica_GP01	0.803226	0.196774	0.012708	63.205
American	Polar	NAmerica_GRZ	0.911246	0.088754	0.009955	91.534
American	Polar	NAmerica_GT_1	0.855352	0.144648	0.010039	85.204
American	Polar	NAmerica_WB039	0.93079	0.06921	0.0099	94.018
Asiatic	Polar	ancient_JBB_32K	0.763769	0.236231	0.023223	32.888
Asiatic	Polar	ancient_Kunashir1	0.836471	0.163529	0.019207	43.551
Asiatic	Polar	ancient_Leitrim_4	0.886012	0.113988	0.012027	73.671

Asiatic	Polar	ancient_Leitrim_5	0.850778	0.149222	0.015367	55.365
Asiatic	Polar	ancient_Uap	0.864989	0.135011	0.008993	96.186
Asiatic	Polar	CAsia_235	0.988563	0.011437	0.009647	102.469
Asiatic	Polar	CAsia_U05M	1 >	< 0	0.01611	62.177
Asiatic	Polar	Casia_U40	0.980889	0.019111	0.015035	65.239
Asiatic	Polar	Casia_U76	0.946367	0.053633	0.010431	90.728
Asiatic	Polar	EAsia_AA1	0.934381	0.065619	0.009726	96.07
Asiatic	Polar	EAsia_ETF1	0.896387	0.103613	0.009945	90.135
Asiatic	Polar	Easia_U34	0.950049	0.049951	0.009421	100.847
Asiatic	Polar	Europe_191Y	0.98582	0.01418	0.008747	112.702
Asiatic	Polar	Europe_ALP1	0.994861	0.005139	0.008589	115.832
Asiatic	Polar	Europe_APN2	0.976328	0.023672	0.008781	111.181
Asiatic	Polar	Europe_OFS01	0.991771	0.008229	0.009774	101.465
Asiatic	Polar	Europe_RF01	0.981122	0.018878	0.009015	108.836
Asiatic	Polar	Europe_SJS01	0.988152	0.011848	0.009513	103.873
Asiatic	Polar	Europe_SLK1	0.975761	0.024239	0.008838	110.399
Asiatic	Polar	Europe_SPA1	0.995928	0.004072	0.009536	104.444
Asiatic	Polar	Europe_Swe	0.97837	0.02163	0.00957	102.228
Asiatic	Polar	Hokkaido_2231	0.904	0.096	0.009954	90.819
Asiatic	Polar	Hokkaido_421	0.885822	0.114178	0.01016	87.186
Asiatic	Polar	Hokkaido_5010	0.89318	0.10682	0.009955	89.721
Asiatic	Polar	Hokkaido_5046	0.892587	0.107413	0.010147	87.97
Asiatic	Polar	Hokkaido_518	0.900066	0.099934	0.009596	93.796
Asiatic	Polar	Hokkaido_819	0.892896	0.107104	0.009951	89.729
Asiatic	Polar	NAmerica_ABC01	0.852569	0.147431	0.010231	83.334
Asiatic	Polar	NAmerica_ABC02	0.843941	0.156059	0.010442	80.823
Asiatic	Polar	NAmerica_ABC03	0.838103	0.161897	0.010537	79.54
Asiatic	Polar	NAmerica_ABC04	0.844584	0.155416	0.010187	82.906
Asiatic	Polar	NAmerica_ABC05	0.840112	0.159888	0.010775	77.971
Asiatic	Polar	NAmerica_ABC06	0.868601	0.131399	0.01037	83.759
Asiatic	Polar	NAmerica_ABC1	0.862799	0.137201	0.010408	82.901
Asiatic	Polar	NAmerica_ABC2	0.844018	0.155982	0.011113	75.949
Asiatic	Polar	NAmerica_Adm1	0.866731	0.133269	0.010123	85.617
Asiatic	Polar	NAmerica_BB020	0.923093	0.076907	0.010014	92.184
Asiatic	Polar	NAmerica_BB034	0.904747	0.095253	0.00999	90.57
Asiatic	Polar	NAmerica_BB037	0.909809	0.090191	0.010202	89.177
Asiatic	Polar	NAmerica_BB049	0.89898	0.10102	0.010409	86.366
Asiatic	Polar	NAmerica_BB059	0.903496	0.096504	0.010276	87.924
Asiatic	Polar	NAmerica_Chi1	0.827361	0.172639	0.010829	76.4
Asiatic	Polar	NAmerica_Chi2	0.829614	0.170386	0.010123	81.951
Asiatic	Polar	NAmerica_CON001	0.83052	0.16948	0.010465	79.358
Asiatic	Polar	NAmerica_Den	0.919058	0.080942	0.01007	91.264
Asiatic	Polar	NAmerica_EB027	0.911713	0.088287	0.009876	92.317
Asiatic	Polar	NAmerica_GP01	0.837567	0.162433	0.010716	78.158
Asiatic	Polar	NAmerica_GRZ	0.925751	0.074249	0.009832	94.162
Asiatic	Polar	NAmerica_GT_1	0.869708	0.130292	0.009849	88.301
Asiatic	Polar	NAmerica_WB039	0.937812	0.062188	0.010312	90.942

Table 27. The admixture proportion from the cave bear estimated by f_4 ratio.

Outgroup	Cave bear bear	X	α	1-α	std.err	Z
American	Cave_E_VD_1838	ancient_JBB_32K	1 >	< 0	0.011031	99.467
American	Cave_E_VD_1838	ancient_Kunashir1	0.950802	0.049198	0.009841	96.618
American	Cave_E_VD_1838	ancient_Leitrim_4	1 >	< 0	0.007969	131.967
American	Cave_E_VD_1838	ancient_Leitrim_5	1 >	< 0	0.010925	105.998
American	Cave_E_VD_1838	ancient_Uap	1 >	< 0	0.005388	188.053
American	Cave_E_VD_1838	CAsia_235	0.898291	0.101709	0.005174	173.615
American	Cave_E_VD_1838	CAsia_U05M	0.874062	0.125938	0.005833	149.859
American	Cave_E_VD_1838	CAsia_U13M	0.853732	0.146268	0.006354	134.359
American	Cave_E_VD_1838	Casia_U40	0.880187	0.119813	0.005752	153.014
American	Cave_E_VD_1838	Casia_U76	0.892283	0.107717	0.005561	160.443
American	Cave_E_VD_1838	EAsia_AA1	0.897296	0.102704	0.005119	175.285
American	Cave_E_VD_1838	EAsia_ETF1	0.910116	0.089884	0.005539	164.299
American	Cave_E_VD_1838	Easia_U34	0.888894	0.111106	0.005026	176.856
American	Cave_E_VD_1838	Europe_191Y	0.899861	0.100139	0.005508	163.376
American	Cave_E_VD_1838	Europe_ALP1	0.880174	0.119826	0.005627	156.416
American	Cave_E_VD_1838	Europe_APN2	0.872455	0.127545	0.00573	152.25
American	Cave_E_VD_1838	Europe_OFS01	0.881646	0.118354	0.005489	160.63
American	Cave_E_VD_1838	Europe_RF01	0.873286	0.126714	0.0052	167.939
American	Cave_E_VD_1838	Europe_SJS01	0.884332	0.115668	0.005475	161.533
American	Cave_E_VD_1838	Europe_SLK1	0.874213	0.125787	0.005616	155.67
American	Cave_E_VD_1838	Europe_SPA1	0.870845	0.129155	0.005571	156.305
American	Cave_E_VD_1838	Europe_Swe	0.921441	0.078559	0.005455	168.924
American	Cave_E_VD_1838	Hokkaido_2231	0.915049	0.084951	0.005239	174.647
American	Cave_E_VD_1838	Hokkaido_421	0.912144	0.087856	0.005124	178.012
American	Cave_E_VD_1838	Hokkaido_5010	0.909039	0.090961	0.005419	167.752
American	Cave_E_VD_1838	Hokkaido_5046	0.910096	0.089904	0.00553	164.585
American	Cave_E_VD_1838	Hokkaido_518	0.907918	0.092082	0.005459	166.321
American	Cave_E_VD_1838	Hokkaido_819	0.915565	0.084435	0.00534	171.443
American	Cave_E_VD_1838	WAsia_Ge	0.85644	0.14356	0.005579	153.517
American	Cave_E_VD_1838	WAsia_U12M	0.848114	0.151886	0.005638	150.422
American	Cave_E_VD_1838	WAsia_U47M	0.851547	0.148453	0.005798	146.876
Asiatic	Cave_E_VD_1838	ancient_JBB_32K	1 >	< 0	0.010601	102.469
Asiatic	Cave_E_VD_1838	ancient_Kunashir1	0.946427	0.053573	0.009782	96.754
Asiatic	Cave_E_VD_1838	ancient_Leitrim_4	1 >	< 0	0.007606	136.471
Asiatic	Cave_E_VD_1838	ancient_Leitrim_5	1 >	< 0	0.009553	119.031
Asiatic	Cave_E_VD_1838	ancient_Uap	1 >	< 0	0.004957	202.462
Asiatic	Cave_E_VD_1838	CAsia_235	0.888061	0.111939	0.005213	170.366
Asiatic	Cave_E_VD_1838	CAsia_U05M	0.864228	0.135772	0.005872	147.17
Asiatic	Cave_E_VD_1838	CAsia_U13M	0.842228	0.157772	0.006174	136.405
Asiatic	Cave_E_VD_1838	Casia_U40	0.869529	0.130471	0.005837	148.968
Asiatic	Cave_E_VD_1838	Casia_U76	0.883041	0.116959	0.005412	163.175
Asiatic	Cave_E_VD_1838	EAsia_AA1	0.886581	0.113419	0.005126	172.953
Asiatic	Cave_E_VD_1838	EAsia_ETF1	0.900887	0.099113	0.005491	164.06
Asiatic	Cave_E_VD_1838	Easia_U34	0.88147	0.11853	0.004965	177.538
Asiatic	Cave_E_VD_1838	Europe_191Y	0.886704	0.113296	0.005399	164.232
Asiatic	Cave_E_VD_1838	Europe_ALP1	0.866904	0.133096	0.005551	156.173
Asiatic	Cave_E_VD_1838	Europe_APN2	0.857626	0.142374	0.005845	146.716
Asiatic	Cave_E_VD_1838	Europe_OFS01	0.868702	0.131298	0.005701	152.364

Asiatic	Cave_E_VD_1838	Europe_RF01	0.859775	0.140225	0.005365	160.266
Asiatic	Cave_E_VD_1838	Europe_SJS01	0.876188	0.123812	0.005469	160.224
Asiatic	Cave_E_VD_1838	Europe_SLK1	0.863778	0.136222	0.00564	153.159
Asiatic	Cave_E_VD_1838	Europe_SPA1	0.86142	0.13858	0.005496	156.75
Asiatic	Cave_E_VD_1838	Europe_Swe	0.909967	0.090033	0.00527	172.685
Asiatic	Cave_E_VD_1838	Hokkaido_2231	0.905575	0.094425	0.005227	173.261
Asiatic	Cave_E_VD_1838	Hokkaido_421	0.901903	0.098097	0.005107	176.585
Asiatic	Cave_E_VD_1838	Hokkaido_5010	0.899452	0.100548	0.005413	166.167
Asiatic	Cave_E_VD_1838	Hokkaido_5046	0.900817	0.099183	0.0054	166.809
Asiatic	Cave_E_VD_1838	Hokkaido_518	0.899571	0.100429	0.00549	163.86
Asiatic	Cave_E_VD_1838	Hokkaido_819	0.904883	0.095117	0.005126	176.521
Asiatic	Cave_E_VD_1838	WAsia_Ge	0.847661	0.152339	0.00545	155.539
Asiatic	Cave_E_VD_1838	WAsia_U12M	0.838177	0.161823	0.006091	137.612
Asiatic	Cave_E_VD_1838	WAsia_U47M	0.842243	0.157757	0.005778	145.755
American	Cave_GS136	ancient_JBB_32K	1 >	< 0	0.011625	95.684
American	Cave_GS136	ancient_Kunashir1	0.972253	0.027747	0.010069	96.556
American	Cave_GS136	ancient_Leitrim_4	1 >	< 0	0.007702	138.342
American	Cave_GS136	ancient_Leitrim_5	1 >	< 0	0.010448	112.954
American	Cave_GS136	ancient_Uap	1 >	< 0	0.005326	193.794
American	Cave_GS136	CAsia_235	0.908748	0.091252	0.004953	183.487
American	Cave_GS136	CAsia_U05M	0.888816	0.111184	0.005651	157.276
American	Cave_GS136	CAsia_U13M	0.863997	0.136003	0.006014	143.67
American	Cave_GS136	Casia_U40	0.893261	0.106739	0.005577	160.155
American	Cave_GS136	Casia_U76	0.900519	0.099481	0.005195	173.33
American	Cave_GS136	EAsia_AA1	0.906294	0.093706	0.004943	183.331
American	Cave_GS136	EAsia_ETF1	0.922241	0.077759	0.005162	178.655
American	Cave_GS136	Easia_U34	0.899008	0.100992	0.004779	188.116
American	Cave_GS136	Europe_191Y	0.905675	0.094325	0.005024	180.267
American	Cave_GS136	Europe_ALP1	0.889842	0.110158	0.005241	169.78
American	Cave_GS136	Europe_APN2	0.881964	0.118036	0.005256	167.793
American	Cave_GS136	Europe_OFS01	0.892106	0.107894	0.005158	172.944
American	Cave_GS136	Europe_RF01	0.885151	0.114849	0.004855	182.333
American	Cave_GS136	Europe_SJS01	0.895171	0.104829	0.005299	168.94
American	Cave_GS136	Europe_SLK1	0.884231	0.115769	0.005171	171.013
American	Cave_GS136	Europe_SPA1	0.878883	0.121117	0.005392	162.996
American	Cave_GS136	Europe_Swe	0.928146	0.071854	0.005084	182.566
American	Cave_GS136	Hokkaido_2231	0.924636	0.075364	0.005052	183.033
American	Cave_GS136	Hokkaido_421	0.922913	0.077087	0.005	184.593
American	Cave_GS136	Hokkaido_5010	0.919585	0.080415	0.005181	177.483
American	Cave_GS136	Hokkaido_5046	0.921875	0.078125	0.005176	178.107
American	Cave_GS136	Hokkaido_518	0.919912	0.080088	0.004938	186.311
American	Cave_GS136	Hokkaido_819	0.925554	0.074446	0.005016	184.518
American	Cave_GS136	WAsia_Ge	0.86576	0.13424	0.005338	162.176
American	Cave_GS136	WAsia_U12M	0.863764	0.136236	0.005379	160.59
American	Cave_GS136	WAsia_U47M	0.866049	0.133951	0.005609	154.395
Asiatic	Cave_GS136	ancient_JBB_32K	1 >	< 0	0.01174	93.652
Asiatic	Cave_GS136	ancient_Kunashir1	0.957178	0.042822	0.00941	101.714
Asiatic	Cave_GS136	ancient_Leitrim_4	1 >	< 0	0.007143	146.726
Asiatic	Cave_GS136	ancient_Leitrim_5	1 >	< 0	0.009039	128.5
Asiatic	Cave_GS136	ancient_Uap	1 >	< 0	0.00495	205.97

Asiatic	Cave_GS136	CAsia_235	0.899413	0.100587	0.004968	181.028
Asiatic	Cave_GS136	CAsia_U05M	0.879051	0.120949	0.005555	158.232
Asiatic	Cave_GS136	CAsia_U13M	0.85282	0.14718	0.006122	139.296
Asiatic	Cave_GS136	Casia_U40	0.882893	0.117107	0.005594	157.823
Asiatic	Cave_GS136	Casia_U76	0.891854	0.108146	0.005113	174.423
Asiatic	Cave_GS136	EAsia_AA1	0.895374	0.104626	0.004947	180.983
Asiatic	Cave_GS136	EAsia_ETF1	0.912637	0.087363	0.005222	174.767
Asiatic	Cave_GS136	Easia_U34	0.891691	0.108309	0.004788	186.238
Asiatic	Cave_GS136	Europe_191Y	0.893494	0.106506	0.00511	174.858
Asiatic	Cave_GS136	Europe_ALP1	0.876905	0.123095	0.005339	164.258
Asiatic	Cave_GS136	Europe_APN2	0.868018	0.131982	0.005438	159.62
Asiatic	Cave_GS136	Europe_OFS01	0.88051	0.11949	0.005289	166.488
Asiatic	Cave_GS136	Europe_RF01	0.870746	0.129254	0.005067	171.839
Asiatic	Cave_GS136	Europe_SJS01	0.886315	0.113685	0.005239	169.177
Asiatic	Cave_GS136	Europe_SLK1	0.873042	0.126958	0.005281	165.329
Asiatic	Cave_GS136	Europe_SPA1	0.867867	0.132133	0.005346	162.325
Asiatic	Cave_GS136	Europe_Swe	0.916639	0.083361	0.004914	186.523
Asiatic	Cave_GS136	Hokkaido_2231	0.913214	0.086786	0.005109	178.763
Asiatic	Cave_GS136	Hokkaido_421	0.912229	0.087771	0.00503	181.358
Asiatic	Cave_GS136	Hokkaido_5010	0.909305	0.090695	0.005395	168.536
Asiatic	Cave_GS136	Hokkaido_5046	0.911663	0.088337	0.005272	172.91
Asiatic	Cave_GS136	Hokkaido_518	0.910217	0.089783	0.005181	175.695
Asiatic	Cave_GS136	Hokkaido_819	0.914609	0.085391	0.005106	179.13
Asiatic	Cave_GS136	WAsia_Ge	0.855954	0.144046	0.005147	166.306
Asiatic	Cave_GS136	WAsia_U12M	0.854243	0.145757	0.005718	149.393
Asiatic	Cave_GS136	WAsia_U47M	0.856012	0.143988	0.005589	153.162
American	Cave_HV74	ancient_JBB_32K	1 >	< 0	0.010214	106.145
American	Cave_HV74	ancient_Kunashir1	0.953129	0.046871	0.009178	103.855
American	Cave_HV74	ancient_Leitrim_4	1 >	< 0	0.007129	147.333
American	Cave_HV74	ancient_Leitrim_5	1 >	< 0	0.010014	114.981
American	Cave_HV74	ancient_Uap	1 >	< 0	0.005029	201.623
American	Cave_HV74	CAsia_235	0.907327	0.092673	0.00475	191.026
American	Cave_HV74	CAsia_U05M	0.885292	0.114708	0.005381	164.517
American	Cave_HV74	CAsia_U13M	0.866267	0.133733	0.005852	148.029
American	Cave_HV74	Casia_U40	0.891232	0.108768	0.00528	168.806
American	Cave_HV74	Casia_U76	0.901626	0.098374	0.005119	176.117
American	Cave_HV74	EAsia_AA1	0.90572	0.09428	0.004658	194.424
American	Cave_HV74	EAsia_ETF1	0.919027	0.080973	0.00509	180.553
American	Cave_HV74	Easia_U34	0.89764	0.10236	0.004713	190.466
American	Cave_HV74	Europe_191Y	0.907591	0.092409	0.005046	179.853
American	Cave_HV74	Europe_ALP1	0.889607	0.110393	0.005182	171.674
American	Cave_HV74	Europe_APN2	0.884676	0.115324	0.005268	167.923
American	Cave_HV74	Europe_OFS01	0.891758	0.108242	0.005085	175.375
American	Cave_HV74	Europe_RF01	0.883466	0.116534	0.004798	184.134
American	Cave_HV74	Europe_SJS01	0.894063	0.105937	0.005055	176.879
American	Cave_HV74	Europe_SLK1	0.885003	0.114997	0.005173	171.074
American	Cave_HV74	Europe_SPA1	0.880739	0.119261	0.005137	171.454
American	Cave_HV74	Europe_Swe	0.92765	0.07235	0.005042	183.968
American	Cave_HV74	Hokkaido_2231	0.922651	0.077349	0.004873	189.323
American	Cave_HV74	Hokkaido_421	0.920378	0.079622	0.004722	194.931

American	Cave_HV74	Hokkaido_5010	0.916671	0.083329	0.004999	183.358
American	Cave_HV74	Hokkaido_5046	0.917504	0.082496	0.00511	179.567
American	Cave_HV74	Hokkaido_518	0.916594	0.083406	0.005094	179.949
American	Cave_HV74	Hokkaido_819	0.922331	0.077669	0.004941	186.65
American	Cave_HV74	WAsia_Ge	0.868672	0.131328	0.005094	170.536
American	Cave_HV74	WAsia_U12M	0.86186	0.13814	0.005198	165.813
American	Cave_HV74	WAsia_U47M	0.864429	0.135571	0.005255	164.491
Asiatic	Cave_HV74	ancient_JBB_32K	1 >	< 0	0.010083	106.737
Asiatic	Cave_HV74	ancient_Kunashir1	0.948058	0.051942	0.009175	103.326
Asiatic	Cave_HV74	ancient_Leitrim_4	1 >	< 0	0.006851	151.403
Asiatic	Cave_HV74	ancient_Leitrim_5	1 >	< 0	0.008903	127.184
Asiatic	Cave_HV74	ancient_Uap	1 >	< 0	0.004578	219.428
Asiatic	Cave_HV74	CAsia_235	0.897562	0.102438	0.004779	187.799
Asiatic	Cave_HV74	CAsia_U05M	0.875508	0.124492	0.005265	166.292
Asiatic	Cave_HV74	CAsia_U13M	0.854045	0.145955	0.005684	150.244
Asiatic	Cave_HV74	Casia_U40	0.880929	0.119071	0.005237	168.213
Asiatic	Cave_HV74	Casia_U76	0.892158	0.107842	0.004999	178.466
Asiatic	Cave_HV74	EAsia_AA1	0.895413	0.104587	0.004653	192.458
Asiatic	Cave_HV74	EAsia_ETF1	0.909287	0.090713	0.005034	180.633
Asiatic	Cave_HV74	Easia_U34	0.891247	0.108753	0.004576	194.744
Asiatic	Cave_HV74	Europe_191Y	0.895356	0.104644	0.004928	181.67
Asiatic	Cave_HV74	Europe_ALP1	0.877576	0.122424	0.005038	174.198
Asiatic	Cave_HV74	Europe_APN2	0.870384	0.129616	0.005345	162.845
Asiatic	Cave_HV74	Europe_OFS01	0.880162	0.119838	0.005289	166.4
Asiatic	Cave_HV74	Europe_RF01	0.870295	0.129705	0.00491	177.234
Asiatic	Cave_HV74	Europe_SJS01	0.88656	0.11344	0.005076	174.658
Asiatic	Cave_HV74	Europe_SLK1	0.875229	0.124771	0.005167	169.391
Asiatic	Cave_HV74	Europe_SPA1	0.871847	0.128153	0.005017	173.779
Asiatic	Cave_HV74	Europe_Swe	0.917122	0.082878	0.00489	187.543
Asiatic	Cave_HV74	Hokkaido_2231	0.913599	0.086401	0.004769	191.58
Asiatic	Cave_HV74	Hokkaido_421	0.910191	0.089809	0.004648	195.806
Asiatic	Cave_HV74	Hokkaido_5010	0.907257	0.092743	0.004972	182.46
Asiatic	Cave_HV74	Hokkaido_5046	0.908467	0.091533	0.004993	181.934
Asiatic	Cave_HV74	Hokkaido_518	0.908461	0.091539	0.005024	180.816
Asiatic	Cave_HV74	Hokkaido_819	0.911753	0.088247	0.004712	193.516
Asiatic	Cave_HV74	WAsia_Ge	0.859446	0.140554	0.004976	172.733
Asiatic	Cave_HV74	WAsia_U12M	0.852094	0.147906	0.005651	150.783
Asiatic	Cave_HV74	WAsia_U47M	0.855307	0.144693	0.005279	162.019
American	Cave_WK01	ancient_JBB_32K	1 >	< 0	0.010634	103.123
American	Cave_WK01	ancient_Kunashir1	0.955001	0.044999	0.009333	102.32
American	Cave_WK01	ancient_Leitrim_4	1 >	< 0	0.007657	137.609
American	Cave_WK01	ancient_Leitrim_5	1 >	< 0	0.010379	111.565
American	Cave_WK01	ancient_Uap	1 >	< 0	0.005165	196.565
American	Cave_WK01	CAsia_235	0.901165	0.098835	0.005025	179.334
American	Cave_WK01	CAsia_U05M	0.879054	0.120946	0.005613	156.616
American	Cave_WK01	CAsia_U13M	0.857128	0.142872	0.006113	140.218
American	Cave_WK01	Casia_U40	0.884976	0.115024	0.005528	160.102
American	Cave_WK01	Casia_U76	0.89625	0.10375	0.005352	167.473
American	Cave_WK01	EAsia_AA1	0.900633	0.099367	0.004898	183.888
American	Cave_WK01	EAsia_ETF1	0.913816	0.086184	0.005309	172.127

American	Cave_WK01	Easia_U34	0.89199	0.10801	0.004804	185.666
American	Cave_WK01	Europe_191Y	0.902046	0.097954	0.005291	170.486
American	Cave_WK01	Europe_ALP1	0.883033	0.116967	0.005431	162.597
American	Cave_WK01	Europe_APN2	0.876345	0.123655	0.005503	159.245
American	Cave_WK01	Europe_OFS01	0.885882	0.114118	0.005277	167.867
American	Cave_WK01	Europe_RF01	0.877087	0.122913	0.005026	174.52
American	Cave_WK01	Europe_SJS01	0.887854	0.112146	0.00532	166.896
American	Cave_WK01	Europe_SLK1	0.877322	0.122678	0.005419	161.911
American	Cave_WK01	Europe_SPA1	0.873903	0.126097	0.005443	160.557
American	Cave_WK01	Europe_Swe	0.923893	0.076107	0.005303	174.233
American	Cave_WK01	Hokkaido_2231	0.918389	0.081611	0.005062	181.427
American	Cave_WK01	Hokkaido_421	0.915506	0.084494	0.004903	186.73
American	Cave_WK01	Hokkaido_5010	0.912131	0.087869	0.005227	174.499
American	Cave_WK01	Hokkaido_5046	0.913196	0.086804	0.005302	172.222
American	Cave_WK01	Hokkaido_518	0.911372	0.088628	0.005308	171.691
American	Cave_WK01	Hokkaido_819	0.918689	0.081311	0.005113	179.664
American	Cave_WK01	WAsia_Ge	0.860086	0.139914	0.005383	159.773
American	Cave_WK01	WAsia_U12M	0.853226	0.146774	0.005504	155.023
American	Cave_WK01	WAsia_U47M	0.855933	0.144067	0.005541	154.468
Asiatic	Cave_WK01	ancient_JBB_32K	1 >	< 0	0.010257	106.014
Asiatic	Cave_WK01	ancient_Kunashir1	0.949713	0.050287	0.009223	102.973
Asiatic	Cave_WK01	ancient_Leitrim_4	1 >	< 0	0.007309	142.224
Asiatic	Cave_WK01	ancient_Leitrim_5	1 >	< 0	0.009166	124.298
Asiatic	Cave_WK01	ancient_Uap	1 >	< 0	0.004781	210.254
Asiatic	Cave_WK01	CAsia_235	0.891392	0.108608	0.005031	177.176
Asiatic	Cave_WK01	CAsia_U05M	0.869463	0.130537	0.005571	156.065
Asiatic	Cave_WK01	CAsia_U13M	0.845256	0.154744	0.005977	141.417
Asiatic	Cave_WK01	Casia_U40	0.874533	0.125467	0.005588	156.497
Asiatic	Cave_WK01	Casia_U76	0.886726	0.113274	0.005227	169.629
Asiatic	Cave_WK01	EAsia_AA1	0.890448	0.109552	0.004912	181.277
Asiatic	Cave_WK01	EAsia_ETF1	0.904611	0.095389	0.005349	169.127
Asiatic	Cave_WK01	Easia_U34	0.88494	0.11506	0.004744	186.521
Asiatic	Cave_WK01	Europe_191Y	0.889896	0.110104	0.005199	171.176
Asiatic	Cave_WK01	Europe_ALP1	0.870637	0.129363	0.005325	163.515
Asiatic	Cave_WK01	Europe_APN2	0.862412	0.137588	0.005601	153.969
Asiatic	Cave_WK01	Europe_OFS01	0.873568	0.126432	0.005515	158.405
Asiatic	Cave_WK01	Europe_RF01	0.863815	0.136185	0.005158	167.476
Asiatic	Cave_WK01	Europe_SJS01	0.879894	0.120106	0.005349	164.489
Asiatic	Cave_WK01	Europe_SLK1	0.86754	0.13246	0.005442	159.405
Asiatic	Cave_WK01	Europe_SPA1	0.8649	0.1351	0.005356	161.47
Asiatic	Cave_WK01	Europe_Swe	0.913176	0.086824	0.005132	177.948
Asiatic	Cave_WK01	Hokkaido_2231	0.909053	0.090947	0.005033	180.623
Asiatic	Cave_WK01	Hokkaido_421	0.905251	0.094749	0.004891	185.073
Asiatic	Cave_WK01	Hokkaido_5010	0.90229	0.09771	0.005233	172.426
Asiatic	Cave_WK01	Hokkaido_5046	0.904195	0.095805	0.005225	173.04
Asiatic	Cave_WK01	Hokkaido_518	0.903351	0.096649	0.005311	170.099
Asiatic	Cave_WK01	Hokkaido_819	0.907994	0.092006	0.00492	184.535
Asiatic	Cave_WK01	WAsia_Ge	0.85195	0.14805	0.005263	161.868
Asiatic	Cave_WK01	WAsia_U12M	0.843648	0.156352	0.005926	142.366
Asiatic	Cave_WK01	WAsia_U47M	0.847272	0.152728	0.005593	151.479

Table 28. All results to evaluate the relative habitat suitable models pf the Polar bear.

rm	fc	tune.args	auc.train	cbi.train	auc.diff.avg	auc.diff.sd	auc.val.avg	auc.val.sd	cbi.val.avg	cbi.val.sd	or.10p.avg	or.10p.sd	or.mtp.avg	or.mtp.sd	AICc	delta.AICc	w.AIC	ncoef
0.5	LQH	rm.0.5_fc.LQH	0.9897304	NA	0.00207735	0.00155434	0.9883894	0.00188489	NA	NA	0.11445783	0.03208948	0.00487805	0.01090765	10936.26	57.04194	4.11E-13	110
1	LQH	rm.1_fc.LQH	0.9882409	NA	0.00176815	0.00126845	0.9871807	0.00163268	NA	NA	0.11204819	0.0318646	0.00243902	0.00545382	10879.22	0	1.00E+00	67
1.5	LQH	rm.1.5_fc.LQH	0.9869886	NA	0.00167581	0.00114982	0.9859376	0.0015497	NA	NA	0.10957978	0.02150453	0.00243902	0.00545382	10918.31	39.0935	3.24E-09	60
2.5	LQH	rm.2.5_fc.LQH	0.9854175	NA	0.00147657	0.0007997	0.9844932	0.00135858	NA	NA	0.10467235	0.01426825	0.00243902	0.00545382	10990.11	110.89601	8.30E-25	54
3	LQH	rm.3_fc.LQH	0.9850095	NA	0.00147387	0.0007334	0.9839629	0.00131688	NA	NA	0.10464296	0.01111546	0.00243902	0.00545382	11011.94	132.72396	1.51E-29	51
2	LQH	rm.2_fc.LQH	0.9861243	NA	0.00157645	0.00097198	0.9850537	0.00139113	NA	NA	0.10226271	0.02244629	0.00243902	0.00545382	10934.71	55.49388	8.91E-13	49
1.5	LQ	rm.1.5_fc.LQ	0.9651431	NA	0.00560805	0.00412109	0.9634669	0.00683187	NA	NA	0.09976491	0.02008125	0.0072583	0.01079285	11460.42	581.20217	6.22E-127	10
0.5	LQ	rm.0.5_fc.LQ	0.9675647	NA	0.00554414	0.00409253	0.9655609	0.00691517	NA	NA	0.10464296	0.02537867	0.0072583	0.01079285	11347.92	468.70671	1.67E-102	9
1	LQ	rm.1_fc.LQ	0.9666511	NA	0.00546584	0.00415427	0.964823	0.00676817	NA	NA	0.10464296	0.03068418	0.0072583	0.01079285	11400.83	521.61574	5.40E-114	9
2	LQ	rm.2_fc.LQ	0.964835	NA	0.00527366	0.0038827	0.9630841	0.00622729	NA	NA	0.09976491	0.02008125	0.0072583	0.01079285	11484.13	604.90825	4.42E-132	9
2.5	LQ	rm.2.5_fc.LQ	0.9644691	NA	0.00487885	0.00365654	0.9629196	0.00574428	NA	NA	0.10708199	0.02921848	0.0072583	0.01079285	11507.21	627.99502	4.29E-137	8
3	LQ	rm.3_fc.LQ	0.9640002	NA	0.00449506	0.00343177	0.962634	0.00521954	NA	NA	0.10464296	0.02386873	0.0072583	0.01079285	11533.82	654.60493	7.15E-143	8
0.5	L	rm.0.5_fc.L	0.9473314	NA	0.00469931	0.00328715	0.9463719	0.00551262	NA	NA	0.10461358	0.02033576	0.00240964	0.00538812	12322.05	1442.82953	4.937959e-3	7
1	L	rm.1_fc.L	0.9476477	NA	0.00415891	0.00335486	0.946804	0.00490066	NA	NA	0.09976491	0.01813549	0.00240964	0.00538812	12324.38	1445.16052	1.539500e-3	7
1.5	L	rm.1.5_fc.L	0.9475725	NA	0.0037427	0.00332894	0.9468317	0.00441207	NA	NA	0.0997943	0.02362213	0.00243902	0.00545382	12328.87	1449.64851	1.632395e-3	7
2	L	rm.2_fc.L	0.947229	NA	0.00340221	0.00318907	0.9465458	0.00395997	NA	NA	0.10470173	0.0320224	0.00243902	0.00545382	12335.09	1455.87655	7.251432e-3	7
2.5	L	rm.2.5_fc.L	0.9466343	NA	0.00310354	0.00324665	0.9462682	0.00383888	NA	NA	0.10714076	0.03295448	0.00243902	0.00545382	12337.06	1457.8409	2.715634e-3	5
3	L	rm.3_fc.L	0.9462516	NA	0.00310522	0.00304893	0.9460664	0.00374281	NA	NA	0.09738466	0.01956295	0.00243902	0.00545382	12339.84	1460.62694	6.743566e-3	5

Table 29. Contributions of each environment variance in the best model.

variance	contribution(%)
bio_8	43.1949
bio_9	24.0979
bio_7	12.6638
bio_19	7.638
bio_18	6.924
bio_17	2.9907
bio_15	2.4907